Part A, Volume 1, No. 8, August 1963

Journal of Polymer Science

Part A: General Papers

Editorial Board: R. M. Fuoss • J. J. Hermans • H. Mark • H. W. Melville • C. G. Overberger • G. Smets

Contents

RAFFAELE SABIA and F. R. EIRICH: Viscoelastic Behavior of Plasticized Polyvinyl Chloride at Large Deformations. I. Stress Relaxation 2497

RAFFAELE SABIA and F. R. EIRICH: Viscoelastic Behavior of Plasticized Polyvinyl Chloride at Large Deformations. II. Creep 2511

TOD W. CAMPBELL and RICHARD N. MCDONALD: Polymeric Derivatives of 3,3-Bis(aminomethyl)-Oxetane and of Exoxysuccinyl Chloride 2525

S. M. MILLER, M. W. SPINDLER, and R. L. VALE: Use of Dimaleimides as Accelerators for the Radiation-Induced Vulcanization of Hydrocarbon Polymers. Part II. Synthetic Rubbers and Saturated Polymers 2537

W. G. LLOYD: The Influence of Transition Metal Salts in Polyglycol Autoxidations 2551

R. M. BARRER, J. A. BARRIE, and M. G. ROGERS: Heterogeneous Membranes: Diffusion in Filled Rubber 2565

WAYNE E. SMITH AND RALPH G. ZELMER: An Interpretation of Ethylene Polymerization with Alkyl-Promoted Transition-Metal Catalysts 2587

J. SCHMORAK and M. LEWIN: The Chemical and Physicochemical Properties of Wheat Starch Mildly Oxidized with Alkaline Sodium Hypochlorite 2601

S. KRIMM, V. L. FOLT, J. J. SHIPMAN, and A. R. BERENS: Infrared Spectra and Assignments for Polyvinyl Chloride and Deuterated Analogs 2621

continued inside

Published by INTERSCIENCE PUBLISHERS a division of John Wiley & Sons, Inc.

Journal of Polymer Science **Part A: General Papers**

Editorial Board:

R. M. Fuoss • J. J. Hermans • H. Mark • H. W. Melville • C. G. Overberger • G. Smets

Advisory Board:

T. Alfrey, Jr.	P. Debye	W. Kuhn	G. V. Schulz
W. O. Baker	F. Eirich	M. Magat	H. M. Spurlin
H. Benoit	P. J. Flory	C. S. Marvel	A. J. Staverman
C. J. Bevington	J. Furukawa	G. Natta	J. K. Stille
J. W. Breitenbach	G. Gee	S. Okamura	W. H. Stockmayer
A. M. Bueche	A. Katchalsky	A. Peterlin	M. Szwarc
C. W. Bunn	A. Keller	C. C. Price	A. V. Tobolsky
G. M. Burnett	G. M. Kline	Ch. Sadron	K. Ueberreiter
F. S. Dainton	O. Kratky	N. G. Gaylord, Book Review Editor	

Contents (continued), Volume 1, No. 8

SAMUEL H. MARON and THOMAS T. CHIU: Study of Entanglement of Polymers in Solution by Viscosity Measurements. II. Polymethyl Methacrylate in Various Solvents 2651

G. J. HOWARD: Turbidimetric Titration of Nylon 66 2667

MAURICE MORTON and WILLIAM E. GIBBS: The Emulsion Polymerization of 2,3-Dimethylbutadiene-1,3 2679

MASAKAZU INOUE: Studies on Crystallization of High Polymers by Differential Thermal Analysis 2697

F. H. OWENS and F. E. ZIMMERMAN: Photochlorination of Poly(methyl Methacrylate) in Aqueous Suspension 2711

C. M. HUGGINS, L. E. ST. PIERRE, and A. M. BUECHE: Further NMR Studies of Polydimethylsiloxanes: Effects of Radiation-Induced Crosslinking 2731

C. V. STEPHENSON and W. S. WILCOX: Ultraviolet Irradiation of Plastics. IV. Further Studies of Environmental Effects on Films and Fibers 2741

The Journal of Polymer Science is published in three sections as follows: Part A, General Papers, monthly; Part B, Polymer Letters, monthly; Part C, Polymer Symposia, irregular.

Published semi-monthly by Interscience Publishers, a Division of John Wiley & Sons, Inc., covering one volume annually. Publication Office at 20th and Northampton Sts., Easton, Pa. Executive, Editorial, and Circulation Offices at 605 Third Avenue, New York 16, N. Y. Second-class postage paid at Easton, Pa. Subscription price, $154.00 per volume (including Part B: Polymer Letters; and Part C: Polymer Symposia). Foreign postage $3.50 per volume (including Parts B and C).

Copyright © 1963, by John Wiley & Sons, Inc. *Printed in U.S.A.*

JOURNAL OF POLYMER SCIENCE: PART A VOL. 1, PP. 2497–2510 (1963)

Viscoelastic Behavior of Plasticized Polyvinyl Chloride at Large Deformations. I. Stress Relaxation*

RAFFAELE SABIA† and F. R. EIRICH, *Department of Chemistry, and Institute of Polymer Chemistry, Polytechnic Institute of Brooklyn, Brooklyn, New York*

Synopsis

Two vinyl chloride polymers with intrinsic viscosities of 0.65 and 1.17 were compounded with four plasticizers. Stress relaxation data were obtained at three temperatures and analyzed by a step function of seven parameters in Maxwell representation. The relaxation times were nearly independent of plasticizer type, plasticizer content, molecular weight, and temperature. The moduli were found to decrease with increasing plasticizer content and/or temperature, the equilibrium moduli being directly dependent on the molecular weight while the delayed moduli were more dependent on plasticizer type. The molecular weight dependence of the equilibrium moduli can be attributed to a participation of the individual chains in several crystalline areas which act as crosslinking points.

Introduction

Polyvinyl chloride (PVC) has a glass transition temperature of 90°C.;[1] at approximately 125°C. there is a transition to rubberlike elasticity,[2] while near 200°C. it will flow under its own weight and does not maintain elastic strain.[2,3] To reduce brittleness and improve processability, it is usually copolymerized with 5% vinyl acetate. Plasticizers are used to lower the glass transition temperature.

Current theories of plasticizer action are incapable of explaining the phenomena of plasticization in all their aspects.[4,5] Whatever the mechanism, plasticizers act by reducing intermolecular forces, whereby the chemical nature of the plasticizer determines its compatibility and efficiency. Qualitatively, plasticizers shift the modulus-temperature curve to lower temperatures. As the temperature and/or plasticizer content rise, the short-time compliance increases, and the delayed elasticity decreases.[6,7] At 90% plasticizer content and −30°C. the behavior of PVC is that of an

* This work comprises a portion of a thesis presented by Raffaele Sabia in partial fulfillment of the requirem nts for the degree of Doctor of Philosophy at the Graduate School of the Polytechnic Institute of Brooklyn.

† Present address: W. R. Grace and Co., Polymer Chemicals Division, Clifton, New Jersey.

ideal rubber.[3] The presence of a three-dimensional network has been made probable by the results of different experimental techniques.[8,9]

Except for plasticizer evaluation, few attempts have been made to describe the mechanical properties in terms of known parameters.[10,11] A detailed investigation of the whole range of PVC deformation is still wanted.

Experimental

Two specially prepared vinyl chloride polymers with intrinsic viscosities of 0.65 and 1.17, and number-average molecular weights estimated at 43,000 and 81,000, were supplied by the Monsanto Chemical Company. Plasticizers and stabilizers were commercial products.

The formulations used are listed in Table I. They were dry mixed and then milled at 250–265°F. for 6 min. to a gauge of 35 mils. Individual sheets were run and placed in a press between two plates with side shims across the running direction of the calendar marks allowing for $^1/_2$ in. flow-out at 60–70 tons pressure and heated to 360–365°F. At this point the sheets were cooled as rapidly as possible to room temperature while still under pressure.

TABLE I
Formulation of Unfilled Samples

Material	Parts used, g.		
Resin	100	100	100
Plasticizer	20	40	60
Mark XI[a]	6	6	6
Mark XX[a]	3	3	3

[a] Stabilizers, Argus Chem. Co.

The following abbreviations will be used in this paper: tricresyl phosphate, TCP; dioctyl adipate, DOA; diphenyl phthalate, DPP; arochlor 1254, ARO. A sample, for example, identified as TCP-40-80000 contains 40 parts of plasticizer and 100 parts of the resin of 80,000 molecular weight.

All samples, cut in the usual dumbbell form, were conditioned at the temperature of the experiment for 1 hr. At 50 and 75°C., the samples showed no change in length; on annealing unstrained specimens at 125°C., a negative set of 1–2% was recorded which could be due to loss of plasticizer. It can then be assumed that the samples were reasonably free from frozen-in strains. Inspection between crossed nicols showed this assumption to be essentially correct.

The stress relaxation apparatus has been described elsewhere.[12] The samples were stretched within 1 sec. to predetermined lengths and the first readings recorded within 10 sec., followed by others, at increasing intervals, for 90 min. The strains, $\Delta L/L_0$, measured between bench marks in the gage region, corresponded to 0.125, 0.201, 0.295, and 0.383.

Results

The stress relaxation curves (Fig. 1) shows a very rapid drop in stress for the first minute, followed by a less steep decay for the next 60 min. A very slow further drop in stress continues, and no sign of a real equilibrium can be seen even after two weeks. From the absence of true flow shown during creep, we must conclude, however, that an equilibrium must finally be reached.[13]

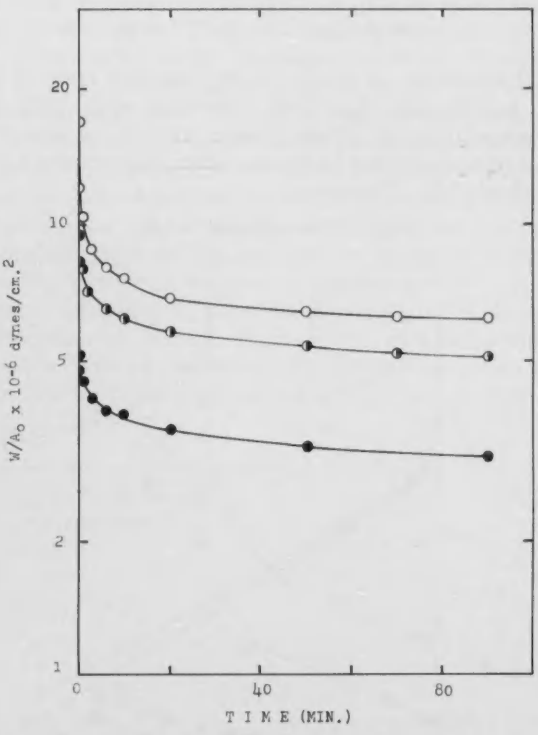

Fig. 1. Typical relaxation curve at 50°C., strain = 0.201: (○) TCP-20-80000; (◑) TCP-40-80000; (●) TCP-60-80000.

A quantitative representation of stress relaxation and strain recovery is possible with a model consisting of three Maxwell elements and one spring, all in parallel.

$$G(t) = G_e + G_1e^{-t/\tau_1} + G_2e^{-t/\tau_2} + G_3e^{-t/\tau_3} \quad (1)$$

where G_i and τ_i represent the shear moduli and relaxation times respectively, and t the time.

Guth et al.[14] have shown that the time dependence of large deformations ($\lambda = 1 + \Delta L/L_0 = 1 + \gamma$) can be written as the product

$$S(\lambda,t) = F(\lambda)G(t) \tag{2}$$

In linear extensions, assuming constant volume, one uses the relation

$$G = E/3 = (S/3)/F(\lambda) \tag{3}$$

where E is Young's modulus (as λ approaches 1) and S is the stress.

Equation (1) then becomes

$$S(t) = S_e + S_1e^{-t/\tau_1} + S_2e^{-t/\tau_2} + S_3e^{-t/\tau_3} \tag{4}$$

The value of τ_3 is high, as shown by the long-time creep of plasticized PVC[7] and by the fact that PVC plasticized with 35% TCP still shows relaxation after 6×10^5 sec., even at 60°C.[8] In view of this, the experimental time was limited to 90 min. where, on assuming $\tau_3 = 10^5$ sec., S_3 has relaxed only 5%. Therefore,

$$S_3e^{-t/\tau_3} \approx \text{constant} = S_3 \tag{5}$$

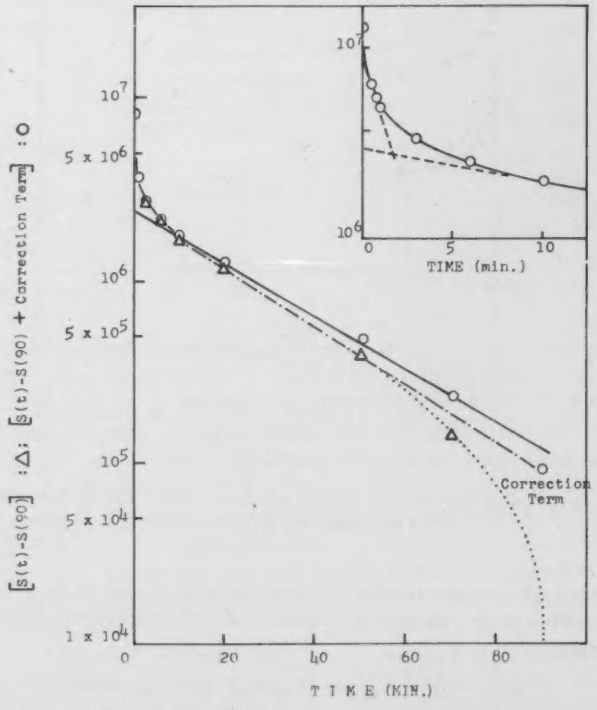

Fig. 2. Typical stress relaxation analysis: (△) $S(t) - S(90)$; (○) $S(t) - S(90)$ + correction term. The mid-point mark on the ordinate of the insert is $S \times 10^6$.

At the same time, S_1e^{-t/τ_1} after 1 min., is very small and can be neglected. Consequently, the reading at 90 min. can be reduced to

$$S(90) = (S_e + S_3) + S_2e^{-5400/\tau_2} \tag{6}$$

On substituting, we get

$$S(t) - S(90) + S_2e^{-5400/\tau_2} = S_2e^{-t/\tau_2} \tag{7}$$

for times greater than approximately 10^2 sec.

$S(t)$ and $S(90)$ are obtained experimentally. On assuming that S_2e^{-5400/τ_2} is small compared to $[S(t) - S(90)]$, we may neglect it at first and plot the ln $[S(t) - S(90)]$ versus time. A straight line drawn through the early points (10–50 min.) will give an intercept at the 90-min. reading. This intercept is taken to be S_2e^{-5400/τ_2} and is added to the difference between $S(t)$ and $S(90)$ and replotted. The resulting intercept at $t = 0$ is S_2, while the slope is τ_2. This procedure, as shown in Figure 2, was adopted to eliminate a great deal of arbitrariness in determing slopes and intercepts. It will be noticed how, by the addition of the correction term, the 70-min. reading is brought up to the line and that the value of S_2 (intercept) is essentially unaffected, while τ_2 changes to a moderate extent.

At very short times (Fig. 1), there is a sharp drop in the curve indicative of the shorter relaxation time τ_1. From a survey of many curves it appears that this section could be characterized by a single relaxation time of 110 sec. This is shown by drawing a tangent to the curves as illustrated in the

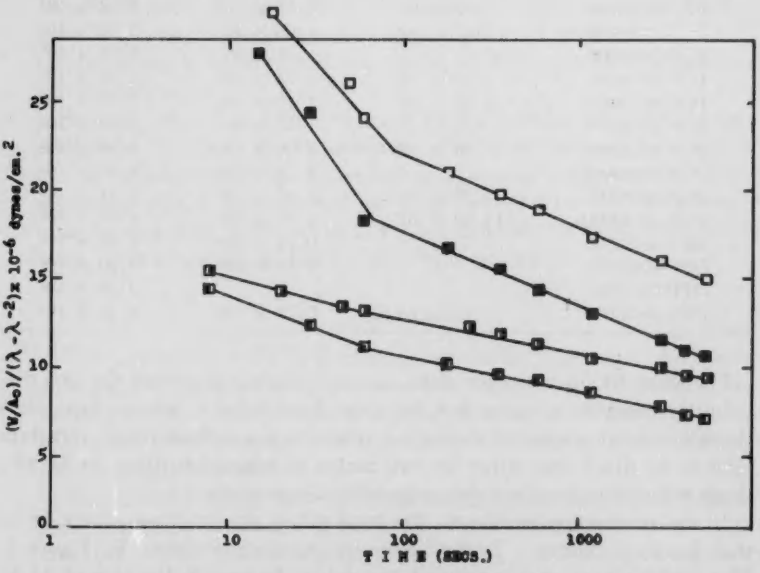

Fig. 3. Modulus vs. time: (□) DOA-20-80000, 50°C.; (■) DOA-20-40000, 50°C.; (□■) DOA-20-80000, 75°C.; (■□) DOA-20-40000, 75°C.

insert of Figure 2. The difference between the new intercept and S_2 is termed S_1.

If, on the other hand, we were to assume a continuous distribution of relaxation times, the generalized Maxwell equation[15]

$$E(t) - E_e = H(\tau)e^{-t/\tau} \ln \tau \tag{8}$$

or its first-order approximation

$$H(\tau) = -dE(t)/d \ln t \tag{9}$$

has to be used. In Figure 3, some of our data appears as the plot of E versus ln t. It will be seen that most of the slope of each curve is approximately constant and thus indicates a "box" distribution for $H(\tau)$,[16] characterized by three parameters which define the height (E_0), and the range (τ_1 and τ_2) of the box.

Of these parameters, E_0 can be determined from our data as the slope of the E–ln t plot and, since it is independent of strain, average values are reported in Table II. We cannot determine τ_1 and τ_2 for lack of data.

TABLE II
E_0 Values of the Box Distribution

	E_0, dynes/cm.^{2}		
	32°C.	50°C.	75°C.
TCP-60-80000	1.12×10^6	0.62×10^6	3.58×10^5
TCP-40-80000	2.92×10^6	1.06×10^6	5.52×10^5
TCP-20-80000		1.49×10^6	8.76×10^5
TCP-60-40000	1.40×10^6	0.73×10^6	3.67×10^5
TCP-40-40000	2.92×10^6	1.10×10^6	5.67×10^5
TCP-20-40000		1.52×10^6	8.31×10^5
DOA-40-80000	2.66×10^6	1.06×10^6	4.98×10^5
DOA-20-80000		1.79×10^6	8.37×10^5
DOA-40-40000	3.29×10^6	1.16×10^6	4.21×10^5
DOA-20-40000	11.80×10^6	1.81×10^6	8.09×10^5
DPP-60-80000		0.72×10^6	4.15×10^5
DPP-40-80000		0.84×10^6	4.90×10^5
DPP-60-40000			3.58×10^5
DPP-40-40000		0.78×10^6	5.43×10^5

For short times, a steeper slope appears which will extend the box distribution towards a higher box for very short times. Since a box refers though to a succession of relaxation times over a certain range, our data seem to be fitted best either by two ranges of relaxation times, or by two single relaxation times in a step approximation as above.

In the recovery experiments, the total strain observed was taken to be that between clamps. Typical recovery curves are shown in Figure 4. The experimental error is appreciable, as can be seen in the case of TCP-20-80000, where no instantaneous recovery was found.

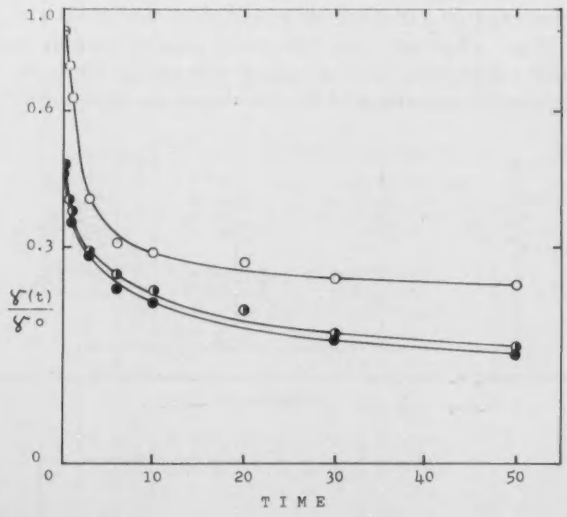

Fig. 4. Typical recovery curves, 50°C.: (○) TCP-20-80000; (◑) TCP-40-80000; (●) TCP-60-80000.

From the 1-min. readings at 50°C., i.e., almost instantaneous recovery, DOA-20 shows a greater recovery than TCP-20. The samples containing 40 and 60 parts of plasticizer showed a greater recovery, respectively, but were too close to be able to distinguish between plasticizers. At 75°C. the bunching is tighter, and one would need an apparatus of greater resolving power.

Samples relaxed at 75°C. were left at the experimental temperature an additional $2^1/_2$ hr. The deformation after this time was less than 0.2% for all samples made up of the higher molecular weight resin. The low molecular weight resin showed the same behavior for the two lowest constant strains used, but a set of 2–3% occurred at the two highest deformations. On annealing to 125°C., this set disappeared.

Discussion

The results show PVC to exhibit essentially four steps of viscoelastic deformation (neglecting others of minor significance) responsible for an initially fast and then slowing relaxation, and for a first fast and then slow recovery. PVC possesses also true elasticity as shown by indefinite stress retention and lack of flow.

The material can be characterized in Maxwell representation by seven parameters, as shown in Figure 5, i.e., three delayed elasticities and one Hookean. The latter is evident, in particular, by the almost instantaneous recovery of approximately 50% of the strain at the end of the relaxation experiments. The third delayed mechanism was found to be negligible

for measurements on our time scale and was combined with the non-relaxing spring. Thus, only five of the seven parameters were evaluated.

The stress values were plotted against the rubber strain, $\lambda - \lambda^{-2} = F(\lambda)$. The moduli, determined from the slopes, are reported in Table III.

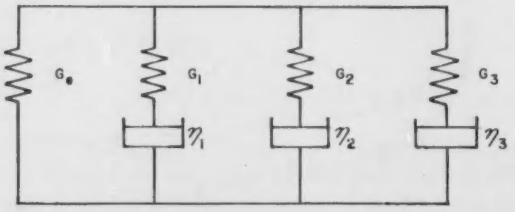

Fig. 5. Seven-parameter viscoelastic model, Maxwell representation, expressing observed behavior.

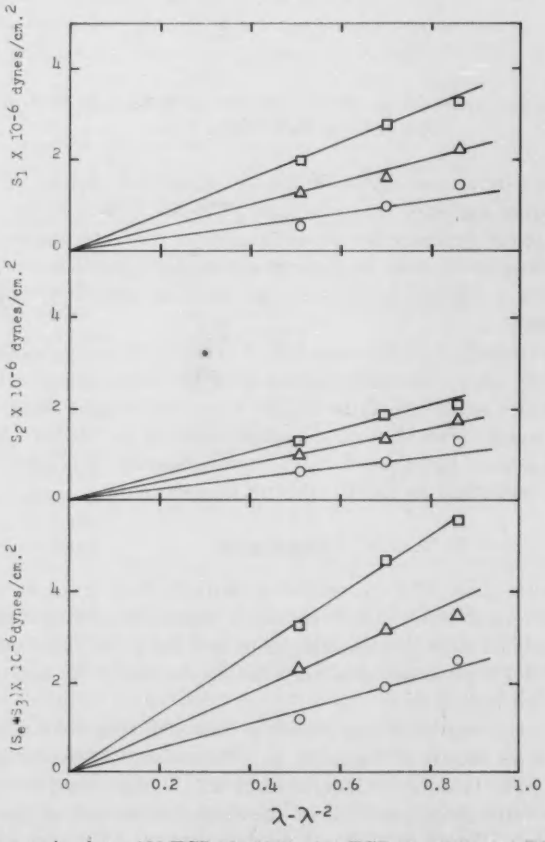

Fig. 6. Stress-strain plots: (O) TCP-20-40000; (△) TCP-40-40000; (□) TCP-60-40000.

TABLE III
Moduli from Stress Relaxation

	Moduli, dynes/cm.² [a]								
	32°C.			50°C.			75°C.		
	$S_1/F(\lambda)$	$S_2/F(\lambda)$	$S_3/F(\lambda)$ [b]	$S_1/F(\lambda)$	$S_2/F(\lambda)$	$S_3/F(\lambda)$	$S_1/F(\lambda)$	$S_2/F(\lambda)$	$S_3/F(\lambda)$
TCP-60-80000	5.09×10^6	3.88×10^6	1.27×10^7	2.46×10^6	1.98×10^6	5.64×10^6	1.56×10^6	1.17×10^6	3.56×10^6
TCP-40-80000	1.86×10^7	8.88×10^6	2.05×10^7	5.80×10^6	3.09×10^6	9.19×10^6	2.76×10^6	1.78×10^6	6.80×10^6
TCP-20-80000				1.15×10^7	4.01×10^6	1.16×10^7	4.44×10^6	2.58×10^6	9.70×10^6
TCP-60-40000	6.01×10^6	5.09×10^6	1.39×10^7	3.58×10^6	2.55×10^6	5.35×10^6	1.37×10^6	1.21×10^6	2.68×10^6
TCP-40-40000		8.78×10^6	2.29×10^7	6.01×10^6	3.60×10^6	7.85×10^6	2.54×10^6	1.96×10^6	4.41×10^6
TCP-20-40000				8.31×10^6	3.92×10^6	8.62×10^6	3.84×10^6	2.54×10^6	6.40×10^6
DOA-40-80000		7.89×10^6	2.48×10^7	5.72×10^6	3.72×10^6	9.40×10^6	2.43×10^6	1.52×10^6	5.93×10^6
DOA-20-80000				1.04×10^7	5.66×10^6	1.38×10^7	3.68×10^6	2.74×10^6	9.21×10^6
DOA-40-40000		1.16×10^7	2.84×10^7	5.35×10^6	3.92×10^6	7.01×10^6	2.74×10^6	1.45×10^6	3.92×10^6
DOA-20-40000		3.50×10^7	5.64×10^7	8.82×10^6	5.88×10^6	1.06×10^7	3.27×10^6	2.64×10^6	6.40×10^6
DPP-60-80000				4.07×10^6	1.48×10^6	6.07×10^6	1.90×10^6	1.37×10^6	4.70×10^6
DPP-40-80000				4.50×10^6	2.58×10^6	7.52×10^6	2.13×10^6	1.74×10^6	5.66×10^6
DPP-60-40000							1.96×10^6	1.15×10^6	2.33×10^6
DPP-40-40000				3.46×10^6	1.27×10^6	5.09×10^6	2.94×10^6	1.80×10^6	3.66×10^6

[a] $F(\lambda) = \lambda - \lambda^{-2}$
[b] Actually $(S_3 + S_e)/F(\lambda)$

TABLE IV
Stress Relaxation Time τ_2

	τ_2, sec.		
	32°C.	50°C.	75°C.
TCP-60-80000	1680	1770	1825
TCP-40-80000	1740	1770	1910
TCP-20-80000		1820	1800
TCP-60-40000	1630	1500	1800
TCP-40-40000	1740	1550	1846
TCP-20-40000		1635	1750
DOA-40-80000	1730	1760	1800
DOA-20-80000		1800	1800
DOA-40-40000	1740	1520	1736
DOA-20-40000	1590	1600	1640
DPP-60-80000		1825	1800
DPP-40-80000		1825	1910
DPP-60-40000			1800
DPP-40-40000		1540	1800

Representative stress–strain plots with reasonable straight lines drawn through the origin are shown in Figure 6. Since τ_2 is independent of strain, average values are reported in Table IV. As noted in the previous section, τ_1 is assumed to remain constant at 110 sec.

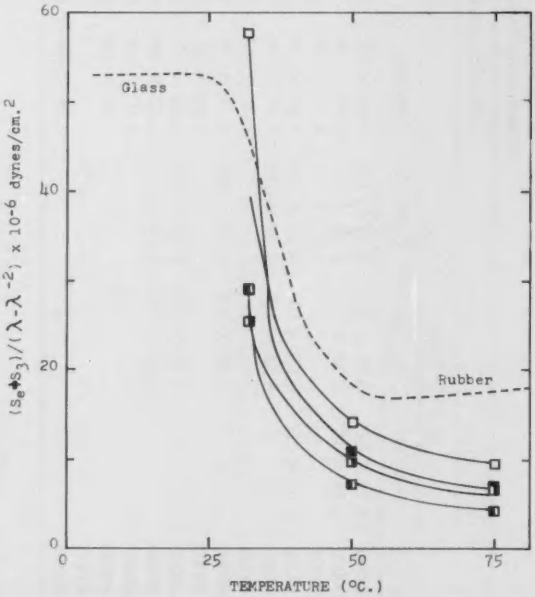

Fig. 7. "Equilibrium" modulus as a function of temperature: (□) DOA-20-80000; (◨) DOA-40-80000; (■) DOA-20-40000; (◧) DOA-40-40000; (--) idealized transition of amorphous polymer.

It is interesting to analyze the various effects of plasticizers on the parameters of PVC, although we are limited by the fact that we do not possess a zero line in the form of unplasticized PVC. First, some moduli are plotted in Figures 7 and 8 against temperature and plasticizer content. By comparing these plots to the familiar idealized modulus–temperature curve, it is seen that we are in the region just before the onset of true rubber elasticity (held at 75°C. after releasing the stress the samples would recover

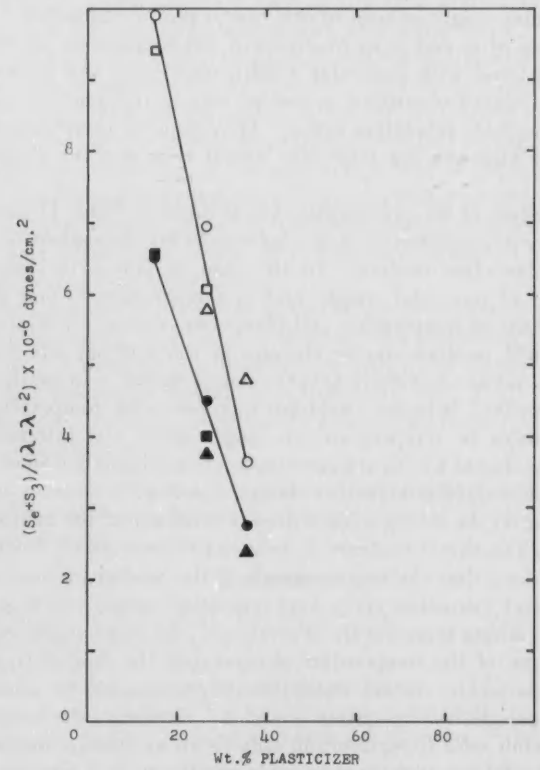

Fig. 8. "Equilibrium" modulus vs. plasticizer content, 75°C.: (○) TCP-80000; (●) TCP-40000; (□) DOA-80000; (■) DOA-40000; (△) DPP-80000; (▲) DPP-40000.

completely within less than 3 hr.). Remembering that in an ideal rubber the restoring force and the observed moduli are entirely due to entropy changes, and that changes in moduli with either temperature, density (high elongations), or plasticizer are due to implicit changes in the internal energy, it can be seen from Figures 7 and 8 that for the temperatures and plasticizers considered, the amount is more important than the nature of the plasticizer. Both effects are strongly influenced by molecular weight. Except

for the molecular weight effect, these statements are seen further to be true for the delayed as well as for the equilibrium modulus.

The theory of rubber elasticity treats equilibrium phenomena and gives the modulus as being inversely proportional to the molecular weight. For crosslinked resins, the molecular weight has to be replaced by that between crosslinks. We are dealing here certainly with the latter case. Since longer chain molecules can participate in more "crystallite" regions than shorter ones and there are fewer free chain ends, an increase in modulus with molecular weight as seen in this case is not unreasonable.

The values of τ_2 and τ_1 as functions of temperature do not follow any pronounced trend with molecular weight, plasticizer, and plasticizer content. The delayed viscosities, η_1 and η_2, may be obtained by multiplying the moduli with the relaxation times. They show no appreciable difference between the high and low molecular weight resin and the plasticizer employed.

The E_0 values of the box distribution as listed in Table II show that E_0 is essentially independent of molecular weight but dependent on temperature and plasticizer content. In the case of polyisobutylene, E_0 was independent of molecular weight and of temperature.[16] Our data show that the effects of temperature and plasticizer content are equivalent and that both will produce similar changes in the internal structure. This deduction is not new but it was never so clearly shown. In another parallel, once "rubberlike" behavior (modulus increases with temperature) is obtained, changes in temperature no longer affect the internal energy;[3] this suggests that at a critical concentration the polymer becomes saturated with plasticizer and has no further binding capacity.[17]

Reflecting on the strong temperature dependence of the moduli, even of $(S_e + S_3)/F(\lambda)$, this is contrary to behavior of true elastic moduli. It is, therefore, likely that the measurements of the moduli include, implicitly, extremely stiff viscosities (very long relaxation times) which reveal their nature by a strong temperature dependence. In other words, for a better representation of the temperature dependence, the moduli G_1 and G_2 of the seven-parameter model should be supplemented by shunting viscosities in parallel to the springs 1 and 2. Similarly, the so-called equilibrium moduli refer to equilibrium only as an approximation, since PVC continues to deform slightly even after months so that the third delayed mechanism, G_3, which we combined with G_2, cannot be neglected if very long-term experiments are considered.

In conclusion, PVC, with a glass transition temperature of about 90°C., is a tough, leathery, material for the next approximately 50 degrees, i.e., up to 130°C. when softening to a weak rubber occurs. This extended leathery range is most likely due to strong interchain forces of the polar molecules and the presence of a network, or skeleton, of semicrystalline areas. When the glass point is depressed to, or below, room temperature by increasing amount of plasticizer, the leathery range shifts also to lower temperatures. It is the mechanical behavior at large deformations in this,

the "useful," range and the relative action of four plasticizers of different nature which can be summarized as follows.

The theory of delayed elastic, or viscoelastic, bodies was found useful in representing the deformation cycles performed which were preponderantly of the reversible type. In particular, a step function of seven parameters was found suitable. Of these, the equilibrium modulus, the relaxation time of the first and the intermediate mechanism could be derived from the relaxation data by Maxwell representation.

The relaxation times obtained were nearly independent of plasticizer type, plasticizer content, molecular weight, and temperature. This is not too surprising since, under our conditions, both the moduli and the internal viscosities decrease with increasing plasticizer content and/or temperature. The equilibrium moduli were found to be directly dependent on molecular weight, while the delayed moduli were more dependent on plasticizer type. The temperature dependence of the moduli is typical of the leathery range between T_g and true rubber behavior. The molecular weight dependence of the equilibrium moduli, in conjunction with the elastic behavior, can be attributed to a participation of the individual chains in several "crystalline" areas which act as crosslinking points.

Assuming a box distribution, the E_0 values are independent of molecular weight and plasticizer type, while changing with plasticizer content and temperature. Comparison of these results with those on polyisobutylene indicates that changes in internal structure occur with plasticizer content and temperature. It further suggests the equivalence of changes in temperature and plasticizer content.

We wish to express our gratitude to Congoleum Nairn Co. for financial support, and for the preparation of the samples; to the Monsanto Chemical Company for the donation of experimental resins.

References

1. Buchdahl, R., in F. R. Eirich, Ed., *Rheology, Theory and Application*, Vol. II, Academic Press, New York, 1958, Chap. 4.
2. Ito, K., *J. Polymer Sci.*, **27**, 419 (1958).
3. Walter, A. T., *J. Polymer Sci.*, **13**, 207 (1954).
4. Stuchlik, P., *Ind. Plastiques Mod. (Paris)*, **3**, No. 9, 39 (1951).
5. Doolittle, A. K., *The Technology of Solvents and Plasticizers*, Wiley, New York, 1954.
6. Leaderman, H., *Ind. Eng. Chem.*, **35**, 374 (1943).
7. Aiken, W., T. Alfrey, Jr.. A. Janssen, and H. Mark, *J. Polymer Sci.*, **2**, 178 (1947).
8. Alfrey, T., Jr., N. Wiederhorn, R. S. Stein, and A. V. Tobolsky, *Ind. Eng. Chem.*, **41**, 701 (1948).
9. Alfrey, T., Jr., N. Wiederhorn, R. S. Stein, and A. V. Tobolsky, *J. Colloid Sci.*, **4**, 211 (1949).
10. Buchdahl, R., and L. E. Nielsen, *J. Appl. Phys.*, **22**, 1344 (1951).
11. Dyson, A., *J. Polymer Sci.*, **7**, 147 (1951).
12. Andrews, R. D., N. Hofman-Bang, and A. V. Tobolsky, *J. Polymer Sci.*, **3**, 669 (1947).
13. Sabia, R., and F. R. Eirich, *J. Polymer Sci.*, **A1**, 2511 (1963).

14. Guth, E., P. E. Wack, and R. L. Anthony, *J. Appl. Phys.*, **17**, 347 (1946).
15. Schwarzl, F., and A. J. Staverman, *Physics*, **18**, 791 (1952).
16. Andrews, R. D., and A. V. Tobolsky, *J. Polymer Sci.*, **7**, 225 (1951).
17. Würstlin, F., *Kunststoff-Tech. Kunststoff-Anwend.*, **11**, 269 (1941).

Résumé

On a mélangé deux polymères du chlorure vinylique, ayant des viscosités intrinsèques de 0,65 et de 1,17, avec quatre plastifiants. Des connées de tension de rélaxation sont obtenues à trois températures différentes et analysées par une fonction progressive à sept paramètres dans la représentation de Maxwell. Les temps de rélaxation étaient presque indépendants du type de plastifiant, de la quantité de plastifiant, du poids moléculaire et de la température. On constatait que les modules diminuaient avec une augmentation de la quantité de plastifiant et/ou de la température, les modules d'équilibre étant directement dépendant du poids moléculaire, tandis que les modules différés dépendiaient plus du type de plastifiant. La variation des modules d'équilibre avec le poids moléculaire, peut être attributée à la participation des chaînes individuelles dans plusieurs régions cristallines qui servent de lieux de pontage.

Zusammenfassung

Zwei Vinylchloridpolymeren mit Viskositätszahlen von 0,65 und 1,17 wurden vier Weichmacher zugesetzt. Spannungsrelaxationsdaten wurden bei drei Temperaturen erhalten und mit einer siebenparametrigen Stufenfunktion in der Darstellung nach Maxwell analysiert. Die Relaxationszeit war von Weichmachertyp, Weichmachergehalt, Molekulargewicht und Temperatur nahezu unabhängig. Der Modul nahm mitzunehmendem Weichmachergehalt und Temperatur ab. Der Gleichgewichtsmodul war vom Molekulargewicht direkt abhängig, während der Modul bei Verzögerung mehr vom Weichmachertyp abhing. Die Molekulargewichtsabhängigkeit des Gleichgewichtsmoduls kann auf eine Beteiligung individueller Ketten an mehreren kristallinen Bereichen, die als Vernetzungsstellen wirken, zurückgeführt werden.

Received April 23, 1962

JOURNAL OF POLYMER SCIENCE: PART A VOL. 1, PP. 2511–2523 (1963)

Viscoelastic Behavior of Plasticized Polyvinyl Chloride at Large Deformations. II. Creep*

RAFFAELE SABIA† and F. R. EIRICH, *Department of Chemistry, Polytechnic Institute of Brooklyn, Brooklyn, New York*

Synopsis

Plasticized polyvinyl chloride has been found to undergo a permanent deformation when strained past 100%. At the same strains, internal energy effects become pronounced as reflected in the stress-strain curves. Plasticizer efficiency has been evaluated in several respects, namely rubber-like behavior, recovery, glass transition, set, and stress-strain at break. While no single plasticizer stands out, the following sequence has been established with respect to the first four aspects listed above: DOA $\geqslant$ TCP > DPP $\geqslant$ ARO.

INTRODUCTION

In Part I of this series of papers on the viscoelastic behavior of polyvinyl chloride (PVC) at large deformations, stress relaxation techniques were used to study the influence of molecular weight, temperature, plasticizer type, and plasticizer content.[1]

The viscoelastic relaxation was characterized by a seven parameter Maxwell model. The relaxation times were nearly independent of the above four factors. The moduli were found to decrease with increasing plasticizer content and/or temperature, the equilibrium moduli being directly dependent upon the molecular weight, while the delayed moduli depended upon plasticizer type. The molecular weight dependence of the equilibrium moduli was attributed to a participation of the individual chains in several crystalline areas which act as crosslinking points.

In this study, creep techniques were used to study the viscoelastic behavior at large deformations up to break. Special attention was directed toward an evaluation of plasticizer efficiency.

A study of the stress relaxation of the samples used here was carried out simultaneously by R. Katzenstein[2] and showed these materials to behave closely to the samples utilized in Part I. The results reported here may, therefore, be compared with those from the relaxation study of Part I.

* This work comprises a portion of a thesis presented by Raffaele Sabia in partial fulfillment of the requirements for the degree of Doctor of Philosophy. We wish to express our gratitude to Congoleum Nairn Co. for financial support and for the preparation of the samples.

† Present address: W. R. Grace and Co., Polymer Chemicals Division, Clifton, New Jersey.

EXPERIMENTAL

A batch of commercial Bakelite resin QYSQ was used in this study. Plasticizers and stabilizers were the same as reported in Part I,[1] and were commercial products; similarly, the formulations, the mixing procedure, and the other steps were identical with those described previously.

The creep instrument used was like that described by Aiken et al.[3] except for windows which allowed the direct observation of the samples. In the volume studies, a stretch apparatus allowed us to elongate the sample to a given amount and to keep it that way while elongation, width, and thickness were measured by means of a cathetometer, a caliper, and a micrometer respectively. This procedure was shown by Smith[4] to give satisfactory results when compared to dilatometric methods.

In creep under constant load, the strain was measured from one minute onwards. Since the samples underwent at first rapid elongations, the strain was measured by following a bench mark on the lower clamp with a cathetometer. At the end of the experiment, the sample was unloaded but no provisions were made to remove the bottom clamp.

Recovery was measured for 30–60 min. at the temperature of the experiment. As in our stress relaxation work,[1] all samples were annealed at 125 ± 2°C. for one hour and bench marks, in the gage area of the dumbell shaped samples, were used to determine the degree of recovery.

As in Part I, the following abbreviations will be used for the plasticizers: tricresyl phosphate (TCP); dioctyl adipate (DOA); diphenyl phthalate (DPP); and arochlor 1254 (ARO).

A sample, for example, identified as TCP-40 contains 40 parts of the plasticizer TCP and 100 parts of the resin QYSQ.

RESULTS

At high plasticizer content and/or high temperatures, PVC shows a large short time compliance and a small long time creep.[3,5] Plotting the Cauchy strain ($\Delta L/L_0$) vs. log time, the delayed strain increases slowly and almost linearly, see Figure 1, so that at 50 and 75°C. the 400 min. reading is approximately 90% of the 1500 min., and 86% of the 4600 min. reading. For practical reasons, the creep time was limited to 1500 min.

Some of the data were plotted in Figure 2 according to the theory of rubber elasticity as

$$W/A_0 = kT\,(\lambda - \lambda^{-2}) \tag{1}$$

where $\lambda = 1 + \Delta L/L_0$, W is the load, A_0 the original cross sectional area and k the Boltzmann constant. It can be seen that TCP-60 at 50°C. could be considered a true rubber but for the time dependence. At lower plasticizer contents, reasonable extrapolation of the data indicates that W/A_0 is proportional to $(\lambda - \lambda^{-2})$ at small strains. All plasticized samples become more "rubber-like" at 75°C.

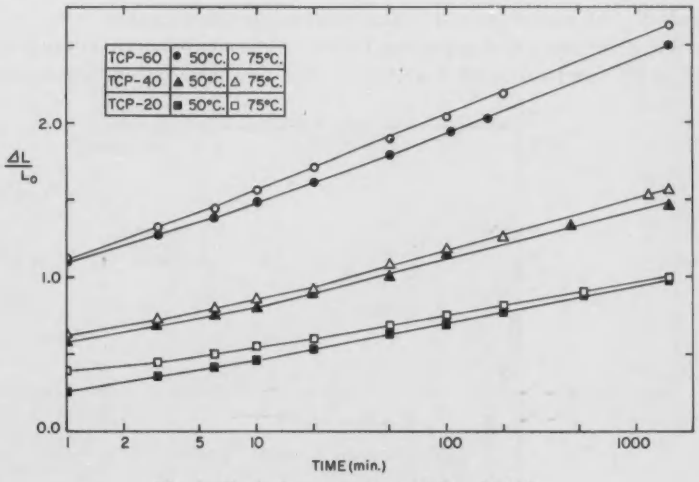

Fig. 1. Typical creep curves at 50 and 75°C.

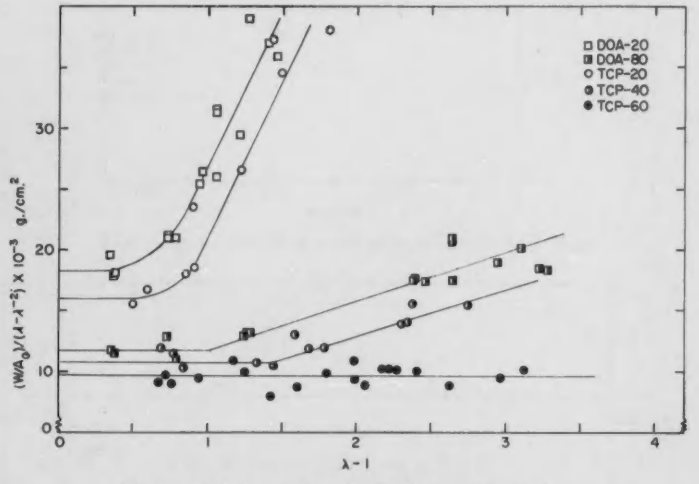

Fig. 2. Modulus at 400 min. vs. deformation, 50°C.

The compliance, J, may be approximated as[6]

$$J(t) = J_1 (1 - e^{-t}/\tau_1) \tag{2}$$

Differentiating

$$d[J(t)]/dt = J_1/\tau_1 e^{-t/\tau_1} \tag{3}$$

In Figure 3 we plotted three creep curves according to the logarithmic form eq. (3). The 400th minute readings are in the region of zero slope in

Figure 2. All curves have the same retardation times (slopes = 1.9×10^3 and 8.0×10^4 secs.) and approximately the same compliances (intercepts = 5.66×10^{-5} and 1.6×10^{-5} cm.^{2}/g.). The first retardation time is of the

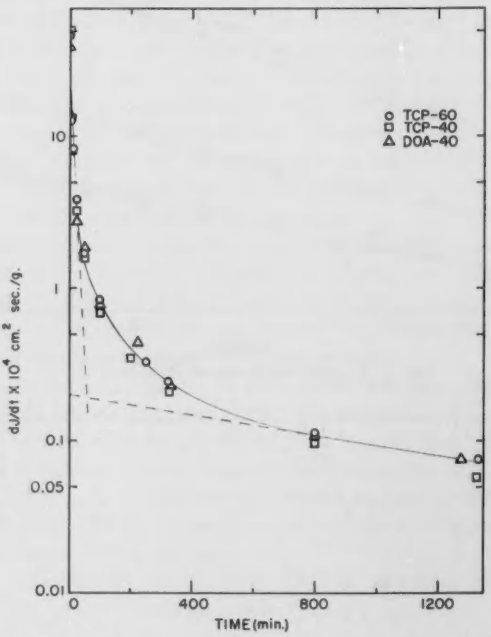

Fig. 3. The change in compliance with time vs. time, 50°C.

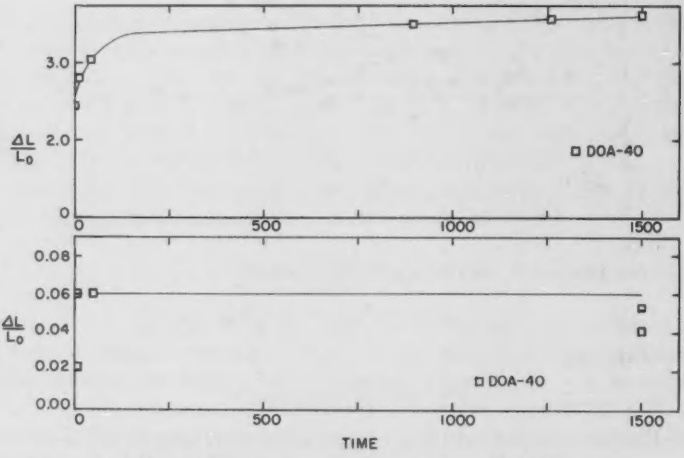

Fig. 4. Creep and set under constant load, 50°C.

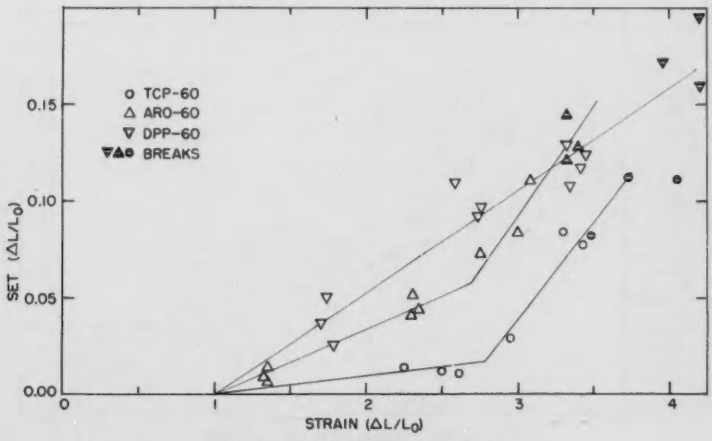

Fig. 5. Set vs. final strain, 50°C.

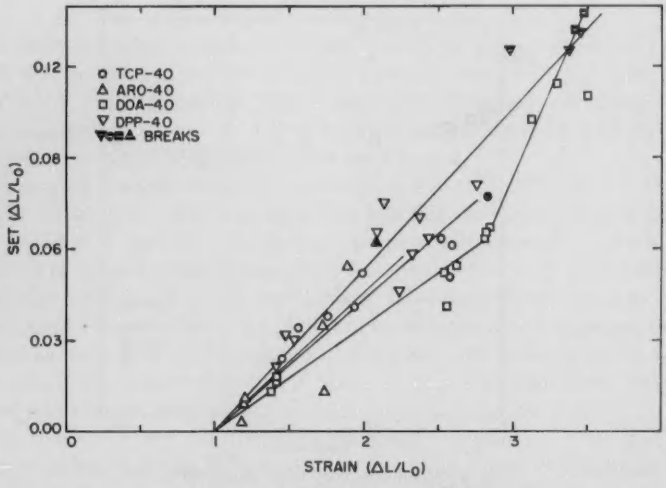

Fig. 6. Set vs. final strain, 50°C.

same order as τ_2 of the relaxation study, while the second is of the same order as τ_3 which was neglected in the relaxation study.[1]

Figure 4 shows the creep of DOA-40 at 50°C. under a constant load and at high extensions ($\Delta L/L_0$ 260%), and the corresponding permanent set after annealing at 125°C. for 60 min. The set shown in Figure 4 is continuously increasing, but at an ever decreasing rate and therefore is not due to true flow.

The set shown by two different plasticizer systems exhibits entirely different dependences on the stress when the set is plotted against the deforma-

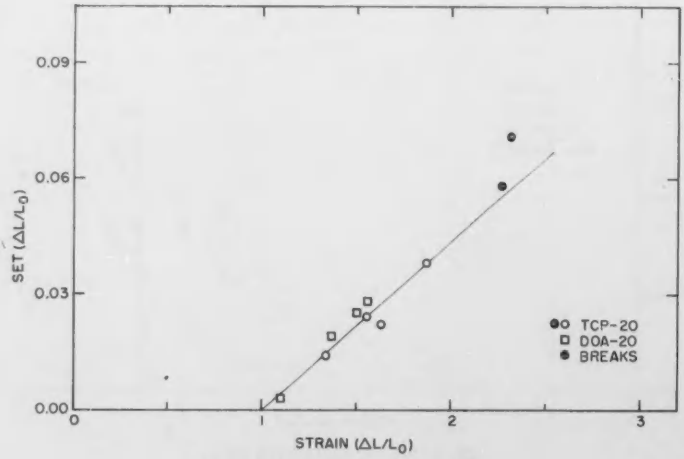

Fig. 7. Set vs. final strain, 50°C.

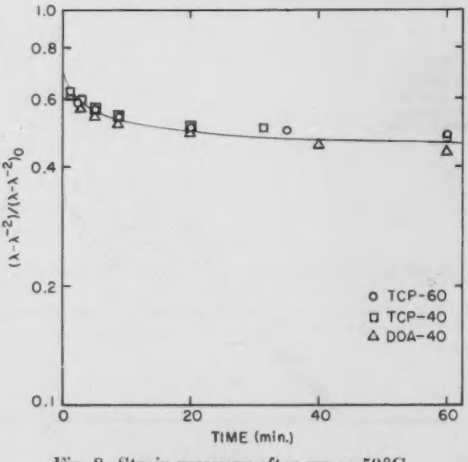

Fig. 8. Strain recovery after creep, 50°C.

tion at 1500 min. The results are seen in Figures 5, 6, and 7. In all cases, the data at "small" strains are omitted because there the permanent set is zero within experimental error. Reasonable extrapolation of the "set" gives an intercept on the abscissa which seems to be a constant for our polymer. This "set-free" intercept corresponds roughly to 100% deformation and agrees with Rider, Summer, and Myers[7] who reported a set smaller than the experimental error for deformations of 100%. Even at 75°C. the intercept remained essentially the same but all curves had nearly identical slopes. The set at break increased with strain. The slower the rate of straining, the higher the strain and set at break.

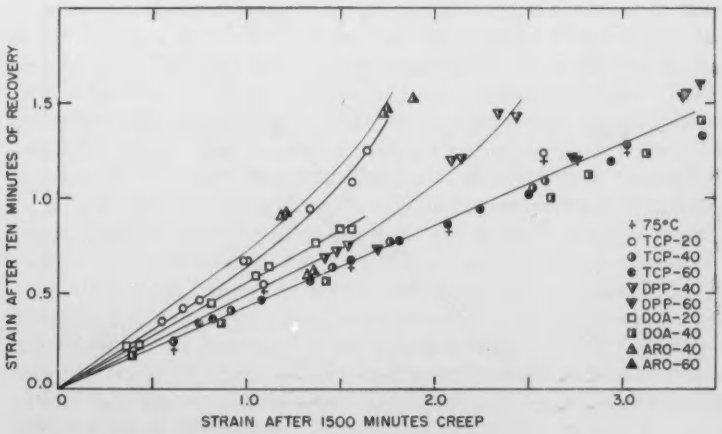

Fig. 9. Percent creep recovery after 10 min. at 50 and 75°C.

On the other hand, samples stretched quickly to a given strain $\Delta L/L_0$ of 370% and released after 0.3–125 min. show (on recovery) the same sets. If the latter were due to flow, they would have to increase with creep time. The conclusion of absence of flow was mentioned before in view of the ever decreasing creep rate and growth of set see Figure 4.

Concerning the type of failure, no necking occurred at 50 and 75°C. but samples broke either by forming cracks starting on the surface, or in the interior, of the material which then propagated perpendicularly to the direction of stress.[8] Sometimes minutes elapsed between the appearance of a crack and the break. (By comparison, filled samples broke in seconds, sometimes by shattering.) At high strains, opaque spots appeared in the unfilled samples and breaks seemed to originate sometimes from the spots. With time, the number of opaque spots increased so that some samples turned white before break.

The creep recovery for the samples whose compliances were given in Figure 3 follows essentially one curve as shown in Figure 8 indicating that the same retardation times are involved. In Figure 9 the strain after 10 min. of recovery has been plotted vs. the strain after 1500 min. of creep. The data at 50 and 75°C. are included in order to facilitate comparison.

At room temperature, TCP-20 necked immediately and soon afterwards shattered. DPP-40 also necked immediately but, at the completion of the necking process, the volume was found to have remained constant indicating that no appreciable orientation or recrystallization occurred. DOA-20, TCP-40, and ARO-40 showed no necking.

At high strains, DOA-20 and TCP-40 showed a definite increase in volume. If an elastic paralleliped is deformed at constant volume V then

$$\lambda_1\lambda_2\lambda_3 = V/V_0 = 1 \tag{4}$$

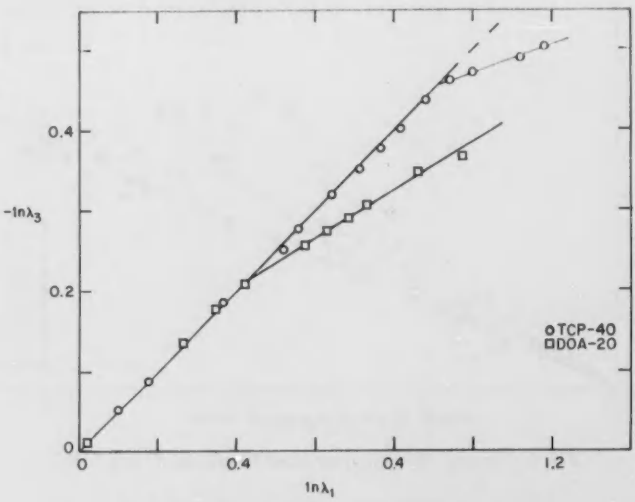

Fig. 10. Variation in thickness and length during extension.

where the subscripts 1, 2, and 3 correspond to the length, width, and thickness respectively. Since in tension $\lambda_2 = \lambda_3$

$$\log\lambda_2/\log\lambda_1 = -1/2 \tag{5}$$

The data are plotted as shown in Figure 10, it will be seen that sudden departures from the slopes of $1/2$ occur. Three sets of readings taken along the length of the samples definitely exclude necking. All increases in volume were accompanied by a whitening of the samples which was completed by the time the new constant slope was obtained. TCP-60, DOA-40, and ARO-40 specimens either turned white just before the break occurred or the slope was much less pronounced. In the creep experiments at 50°C., the above samples turned white just before break occurred. No whitening was observed at 75°C.

DOA samples (annealed for 10 min. at various temperatures up to 147°C., quenched to room temperature for 10 min., and then strained) showed an increase in the critical strain for the onset of volume increase and also an increase for the secondary slope of Figure 10 with increasing annealing temperature. This may be explained in terms of crystallites, as will be done below. It is further pertinent that a large number of cracks were visible in the body of the samples after release from strain.

DISCUSSION

The shapes of the creep curves are nearly independent of temperature, nature of the plasticizer, and plasticizer content in agreement with the relaxation data.[1] The first order approximation to the creep function[6]

requires a plot of the compliance (in the absence of flow) vs. ln time. A rather constant value of the slopes for times greater than one minute may be seen. On the other hand, if the creep function is expressed in terms of Voigt elements eq. (2), we can see in Figure 3 that from the 1–1500 min. point two Voigt elements are acting, in agreement with the analysis of the relaxation data. The retardation times obtained in these cases are independent of plasticizer and plasticizer content. The first of these times, τ_2, is now found to be equivalent to τ_2 of the relaxation study, while the second corresponds to τ_3 which was neglected before. Another retardation time, τ_1, acts over times of the order of less than one minute, too short to be noted during the creep experiments and, therefore, concealed in the measurement of J_e. In other words, seven parameters are again necessary under our conditions to describe the mechanical behavior of PVC in creep by a step function. Of these, G_e, τ_1, and τ_2 express themselves conveniently within the range of the relaxation studies, while J_e, τ_2, and τ_3 can be derived readily from the creep work.

Expressing the modulus according to the theory of rubber elasticity, eq. (1), it is seen that TCP-60 at 50°C. could be considered a true rubber but for the time dependence. As the plasticizer content decreases, internal energy changes become more pronounced at lower strains (as shown by the increase in the modulus in Figure 2) and limits the linear viscoelastic behavior. The moduli range from 1 to 2 $\times$ 10^4 g./cm.^{2} and increase with decreasing plasticizer content.

The principal finding with respect to the permanent deformation, or "set," is that it occurs only after a minimum deformation. Further, the set varies with plasticizer, plasticizer content, and temperature. It has been suggested[3] that long time creep behavior is due to two different processes. Creep takes place first by the elongation of the amorphous regions between "crystallites"* which act as points of crosslinking until a critical elongation is attained at which the stress becomes equal to the yield stress of the weakest crystallites. At this point, a secondary creep process sets in and the crystallites, in the order of their strength, begin to deform in cold-flow. As a result, the sample is no longer in elastic equilibrium. This picture was supplemented by the observation that samples which were allowed to recover gave a higher compliance when they were strained again immediately after recovery.

Accepting this, it follows that, as soon as any deformation of the crystallites occurs, permanent set must be observed. In the plot of moduli vs. rubber strain according to the theory of rubber elasticity, Figure 3, the modulus increases rapidly after a strain of approximately 100% has been reached. In view of this coincidence between the values of strain which will produce set and those giving rise to deviations from linear viscoelastic behavior, one is tempted to assume that there is a functional relationship

* The question of the crystallinity of PVC is not unambiguously settled. The "crystallites" are obviously of very low order, and represent presumably areas of aligned chains, for which lately the term "paracrystalline" has been applied.[9]

between these observations. We believe this to be the case in that internal energy changes begin to make themselves felt in extension when segment rotation has led to such extended chain configurations that the stress reaches the yield value of crosslinking crystallites. In other words, our finding of a lower limit of set and a simultaneous sharp increase in internal energy confirms the views of Aiken et al.[3], and the set is to be interpreted as a minor chain alignment and/or recrystallization in the direction of relieving the stress. Apart from this, the crystalline skeleton of PVC behaves like a nonplastic solid and breaks by rupture at a strain which depends on the plasticizer but is not much dependent on temperature. This suggests that the same number of chains per unit area are broken every time and that break occurs within the crystals whenever the latter become subject to a critical stress at the end of the cold flow. When this stress will be reached depends on the overall modulus of the sample so that the elongations are found to be smaller in the poorer, and larger in the better plasticized samples. Further, the larger the deformation before the critical stress is reached, the more extensive will be the alignment of chains and, thus, crystal growth and set.

The most important finding with respect to plasticizer emerging from this investigation is that plasticizer efficiency may vary greatly from case to case according to which performance is considered. A plasticizer classification according to facilitation of strain recovery may not agree with one based on lowering the modulus or one permitting large deformations without break.

In the literature, the plasticizer efficiencies of DPP and TCP have been determined, according to the method of Clash and Berg[10] by varying plasticizer content until an apparent modulus of 1800 lbs./sq. in. at 25°C. is obtained in five seconds. In this test, less TCP was required.[11] According to Ghersa,[12] from the relative lowering of T_g, DOA is more efficient than TCP. Similarly, DOA and TCP have been evaluated by varying plasticizer content until a tensile modulus of 1000 psi was obtained at 75% elongation and 23°C. on a tensile machine with constant rate of loading at 15000 psi per minute and again less DOA was required.[13]

From our observations, plasticizer effects have to be classified as follows, depending on whether plasticizer is beneficial for:

(*a*) reducing the set per given deformation;
(*b*) reducing moduli and internal viscosity, i.e., lowering of the glass transition temperature;
(*c*) increasing the range of the linear stress-strain relation;
(*d*) raising the stress and elongation at break;
(*e*) enhancing strain recovery; and
(*f*) assisting in the wetting of the filler.

If plasticizer efficiency is expressed by increased deformation accompanied by the same or reduced set, then the data show the following sequence:

60 parts of plasticizer: TCP > ARO > DPP

40 parts of plasticizer: DOA > TCP > ARO > DPP

20 parts of plasticizer: DOA ≳ TCP

As to moduli, their initial values from the stress-strain curves in creep follow the order ARO > DOA > TCP > DPP which is found in stress relaxation.[2] From Figure 3, the retardation time for linear viscoelastic behavior is seen to be independent of plasticizer and of plasticizer content and the same sequence may be assumed for the internal viscosities.

Regarding the part played by internal energy changes, the moduli at large deformation follow the sequence ARO > DPP > DOA > TCP. The rubber-like behavior, as reflected by the degree of curvature in the plot of the moduli in Figure 2, gives: TCP = DOA > DPP > ARO.

Crystalline polymers exhibit the phenomenon of cold-drawing as shown by necking. In the case of PVC, with a largely amorphous component and a "crystalline" skeleton, cold flow can be observed readily only below the glass temperature, from which an effectiveness of plasticizer to decrease T_g can be deduced. From the volume changes with extension at room temperature coinciding with the absence or presence of necking, we may list here the following sequence: DOA > TCP = ARO > DPP. We did not have a composition which would distinguish TCP from ARO.

Whenever the samples underwent cold flow, cracks appeared. It is tempting to associate these cracks with the opaqueness mentioned above but, since the sample is white by the time the constant slope of Figure 10 is changed, it must be assumed either that all cracks have been formed by this time, or that there is an additional process responsible for the whitening, e.g. a critical plasticizer separation or formation of large density fluctuations of PVC and plasticizer. The increase in volume with further strain must be due to a growth of these fluctuations to become cracks. This latter increase in volume must not be confused with the permanent set, since the former will disappear on annealing.

Plasticizer efficiency may be manifested also by modifying the stresses and strains at break. In the former case, the sequence ARO > DPP > DOA > TCP is obtained, while if we allow large strains at break we find the order: DOA > DPP > TCP ≳ ARO.

Recovery is primarily governed by the concentration and nature of the plasticizer. From the amount of recovery after 10 min. we obtained: DOA > TCP > DPP ≳ ARO. The efficiency with respect to filler wetting will be discussed in a later paper, Part III.

In this discussion we have listed the sequences in such a way that the first plasticizer induced most of the desired property. By consulting these orders, it is seen that not one plasticizer is best in all cases. Using the set, recovery, rubber-like behavior and relative lowering of T_g, the following sequence emerges: DOA > TCP > DPP ≳ ARO.

In conclusion, of the theories for large deformations, the stress-strain measure of the theory of rubber-like elasticity was found to allow convenient representation of the data. It affords a clear delineation of where the restoring force is purely entropic in nature and where internal energy effects begin to be felt. This occurs at about 100% elongation and this threshold is not very sensitive to plasticizer content or even temperature, except for TCP additions of more than 40%. Internal energy changes are due to volume changes which can indeed be observed at higher deformations for the poorly plasticized samples. At 100% elongation the volume changes are not in evidence and the situation is best understood by assuming that they are too small and pertain only to the crystalline network. It is the latter which can sustain only 100% elongation and then begins to recrystallize as cold flow, and to reorganize so as to permit elongations up to 400%. Then the limit of the new extensibility is reached: the network and with it the samples break characteristically by a brittle fracture and at almost constant stress.

It follows that the set can be interpreted as the extent of cold flow of the crystalline skeleton. The fact that the set is nonrecoverable shows that a phase change or transformation must have taken place; the existence of a critical strain for its onset indicates that the crystalline areas must possess the nature of a network. The problem remains how a rearrangement of the network which leads to a 30% permanent elongation only, can allow a temporary 3–4 fold overall extension.

The main result concerning plasticizer efficiency lies in the recognition that it is an inadmissible oversimplification to speak of "a" plasticizer effect. Rather, there are as many effects as one chooses types of resin performance. In retrospect it appears quite obvious that the intricate interactions between the chain molecules and an imbibed liquid will have quite different effects on such arbitrarily selected functions as modulus, critical extension, spontaneous recovery or the prevalence of the entropic restoring force. Similarly, it is clear that placing the plasticizers in order regarding one such function will not necessarily arrange them in the same order regarding another function. The best plasticizer will present a suitable compromise, but unfortunately, none has been found as yet which gives a really good performance concerning fast spontaneous recovery of deformation. The structure and behavior of the plasticizers used here do not allow any extrapolation to one that would render a better service. Only at temperatures sufficiently above the glass point does the internal viscosity drop to a value that allows quick restoration of the molecular random state. With present day plasticizers one has to go to such high percentages (80% and up) that the resin becomes too soft.

References

1. Sabia, R., and F. R. Eirich, *J. Polymer Sci.*, **A1**, 2497 (1963).
2. Katzenstein, R., Master's Thesis, Poly. Inst. of Brooklyn, 1958.
3. Aiken, W., T. Alfrey, Jr., A. Janssen, and H. Mark, *J. Polymer Sci.*, **2**, 178 (1947).
4. Smith, T. L., *Trans. Soc. Rheol.*, **3**, 113 (1959).
5. Leaderman, H., *Ind. Eng. Chem.*, **35**, 374 (1943).
6. Staverman, A. J., and F. Schwarzal, in H. A. Stuart, ed., *Die Physik der Hochpolymern, Vol. IV*, Springer-Verlag, Berlin, 1956, Chapter 1.
7. Rider, D. K., J. K. Summer, and R. J. Myers, *Ind. Eng. Chem.*, **41**, 709 (1949).
8. Regel, V. R., and Yu. M. Nedoshivin, *Zhur. Tekh. Fiz.*, **23**, 1333 (1953).
9. Hosemann, R., *Z. Angew. Phys.*, **128**, 1, 465 (1956).
10. Clash, R. F., and R. M. Berg, *Ind. Eng. Chem.*, **34**, 1218 (1942).
11. Lawerence, R. R., and E. B. McIntyre, *Ind. Eng. Chem.*, **41**, 689 (1949).
12. Ghersa, P., *Modern Plastics*, **36**, 135 (1958).
13. Doolittle, A. K., *The Technology of Solvents and Plasticizers*, Wiley, New York, 1954.

Résumé

On a trouvé que le chlorure de polyvinyle plastifié subit une déformation permanente quand il est étiré plus que 100%. Dans ces conditions de tension les effets de l'énergie interne deviennent prononcés, ce qui est révélé par les courbes force-tension. L'efficacité des plastifiants a été déterminée sous différents aspects, entr'autres le comportement caoutchouteux, la récupération, la transition vitreuse et la relation force-tension à la rupture. Bien qu'aucun plastifiant ne soit spéc ialement remarquable, on a pu établir la séquence suivante pour les quatre premières propriétés de la liste précédente: DOA > TCP > DPP > ARO.

Zusammenfassung

Weichgemachtes Polyvinylchlorid erleidet bei Beanspruchung über 100% eine permanente Deformation. Bei der gleichen Beanspruchung treten, wie man an den Spannungs-Dehnungskurven erkennen kann, die Einflüsse der inneren Energie in den Vordergrund. Die Weichmacherwirksamkeit wurde in verschiedener Hinsicht, nämlich für kautschykariges Verhalten, Rückfederung, Glasumwandlung, bleibende Verformung und Spanning-Dehnung beim Bruch bestimmt. Kein Weichmacher zeigt ein abweichendes Verhalten; in bezug auf due vier erstgenannten Kriterien besteht folgende Reihenfolge: DOA ≥ TCP > DPP ≥ ARO.

Received May 11, 1962

JOURNAL OF POLYMER SCIENCE: PART A VOL. 1, PP. 2525–2535 (1963)

Polymeric Derivatives of 3,3-Bis(aminomethyl)-Oxetane and of Exoxysuccinyl Chloride

TOD W. CAMPBELL* and RICHARD N. McDONALD,† *Pioneering Research Division, Textile Fibers Department, E. I. du Pont de Nemours & Company, Inc., Experimental Station, Wilmington, Delaware*

Synopsis

Two monomers, bis(aminomethyl)oxetane (I) and epoxysuccinyl chloride (II)

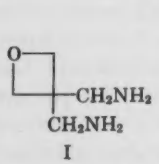

I

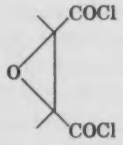

II

have been prepared and converted to condensation polymers, structurally similar to the epoxides. Both monomers were stable and easy to handle. The polymers crosslinked to insoluble, infusible products.

Condensation polymers, such as polyamides, polyureas, and polyurethanes, which can be fabricated in the usual way into films and fibers and then crosslinked by a relatively simple technique such as the application of heat or treatment with a chemical reagent[1] are not common. Since it is known that compounds containing the oxetane ring[2] or the epoxide group[3] are easily polymerized, it should be possible to design monomers containing these groups which will give high molecular weight condensation polymers with mechanical properties suitable for films and fibers, which could be crosslinked after fabrication. (The usual epoxy resins ordinarily do not have the tensile properties needed for film and fiber formation.) Two such monomers, bis(aminomethyl)oxetane (I) and *cis*- and *trans*-epoxysuccinyl chloride (II and III), were chosen for study.

* To whom inquiries should be addressed.

† Present address: Department of Chemistry, Kansas State University, Manhattan, Kansas.

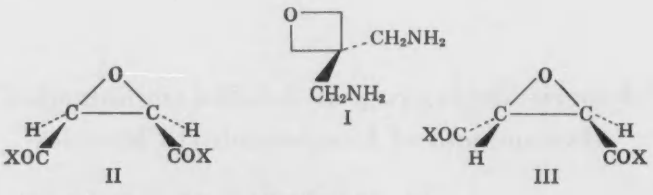

where (IIa, IIIa) X = OH or (IIb, IIIb) X = Cl.

Preparation and Characterization of Monomers

Synthesis of the diamine (I) presented no problem.[4]

Three monomeric derivatives were prepared as models of polymeric structures. They were the dibenzamide (IV), 3,3-bis(phenylureidomethyl)oxetane (V), and 3,3-bis(phenylthioureidomethyl)oxetane (VI). Some properties of these substances are noted below.

Lossen[5] has described the preparation of *trans*-epoxy-succinyl chloride (IIb). No mention was made of this compound being unstable, although it contains both acid chloride and epoxide groups. (Lossen dehydrohalogenated chloro- or bromomalic acid with base and converted the resulting *trans*-epoxysuccinic acid to the acid chloride with phosphorus pentachloride. No yields were given.) To verify the proposed structure, Lossen converted I with ammonia to the diamide, identical with that prepared from the free acid via the dimethyl ester. The silver salt of *trans*-epoxysuccinic acid was prepared and treated with methyl iodide to yield the dimethyl ester. The preparation of the *cis* isomer, *cis*-epoxysuccinyl chloride (IIIb), and certain of its derivatives, has been described more recently.[6]

Epoxides and oxetanes are known to react violently with acid chlorides:[4]

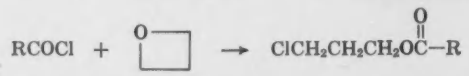

It is therefore not inconceivable that the compound assigned the structure of epoxysuccinyl chloride could actually be, for example, VII.

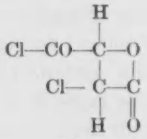

VII

Compound VII, if it existed, would in all likelihood revert to derivatives of II and III on hydrolysis or amination. It was decided to reinvestigate the preparation of these intermediates and to use modern methods to establish their structure definitely.

Compounds IIa and IIIa have recently been prepared by Payne and Williams[7] by the hydrogen peroxide epoxidation of maleic and fumeric acid, respectively, catalyzed by sodium tungstate.

Both acids, IIa and IIIa, were isolated as the disodium salts, converted to the barium salts, and the free acids generated by neutralization with sulfuric acid. The yields of IIa and IIIa were good. It was not necessary to recrystallize IIa, since all of the material was readily soluble in cold water. (It was found by Payne and Williams[7] that a small amount of fumaric acid was in the product and could be readily separated from Ia due to the insolubility of fumaric acid in cold water.) The acids were converted to their corresponding acid chlorides with phosphorus pentachloride.

Confirmation of structure IIIb, considered to apply to IIb as well, was obtained as follows: (*1*) IIIb was hydrolyzed to acid IIIa, (*2*) the NMR spectrum showed only one type of hydrogen, either CH or CH_2, (*3*) a Rast molecular weight showed it to be monomeric, (*4*) the infrared spectrum showed only one type of carbonyl, that of an acid chloride, and is consistent with the structure, (*5*) the elemental analysis, and (*6*) conversion to derivatives and polymerization to high molecular weight polymers, all agree with the proposed structures.

The unexpected stability of IIb and IIIb can be rationalized. The carbon atoms of the epoxide ring, attached to electron-withdrawing acid chloride groups, carry a $\delta+$ charge. This charge can then be transferred to the epoxide oxygen by induction. Another explanation might involve the direct overlap of the π-electron cloud of the carbonyl with the p-electrons of the epoxide oxygen. In both cases, the p-electron density of the epoxide oxygen would be less than that of a simple epoxide. If we assume that the mechanism of the reaction of acid chlorides with epoxides is attack of the p-electrons of the epoxide oxygen on the carbonyl, as in VIII, then IIb and IIIb

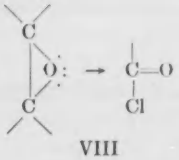

VIII

owe their stability to the lower availability of such p-electrons.

Preparation of Polymers

The sensitive nature of the monomers precludes their use in melt polymerization systems. However, it was found possible to prepare polymers by low temperature techniques.[8,9]

The diamine (I) was converted to polyamides, by use of adipoyl chloride, sebacoyl chloride, and terephthaloyl chloride. A polyurea was prepared from tolylene diisocyanate, and a polyurethane from ethylene bischloroformate. In general, these polymers were very water-sensitive; in fact, the polymer from adipoyl chloride was water-soluble. The terephthalamide was converted by hot water from a moderately tough film to a plastic gum.

The dilute solution viscosities of these polymers were all much higher in formic acid than in *m*-cresol, and the specific viscosity over concentration curve had a sharp upward slope which became more pronounced as the concentration decreased.[10,11] Some typical data are shown in the Experimental Part.

All polymers prepared from this diamine showed a strong tendency to crosslink (become insoluble), either on standing or on heating. Polymers were, in general, difficult to obtain uncrosslinked. When a sample was obtained which was soluble in formic acid, it generally became insoluble on standing; the exception noted was the terephthalamide. This polymer dissolved in formic acid to give viscous solutions of 25–30% polymer, which were cast at room temperature to give a clear, tough film which could be redissolved in formic acid. A film was cut into strips and heated at 100°C. After about 45 min., the film formed a gel in formic acid. After 1 hr., it was completely insoluble and remained so throughout a 24-hr. cycle.

Crosslinking must have involved cleavage of the oxetane ring, so a sample of film was heated at 100°C. and the infrared spectrum was checked at hourly intervals. Insolubilization occurred as above. However, no visible change occurred in the spectrum. This implied that if the oxetane ring was involved in this crosslinking phase, it involved only a very small percentage of these rings, at least at this temperature. (The oxetane ring has a characteristic band in the range of 10.2 μ.)[3,12] Therefore, at 100°C., the crosslinks were probably produced by reaction of a few random trimethylene oxide rings with reactive endgroups, which were, of course, present in relatively low concentration:

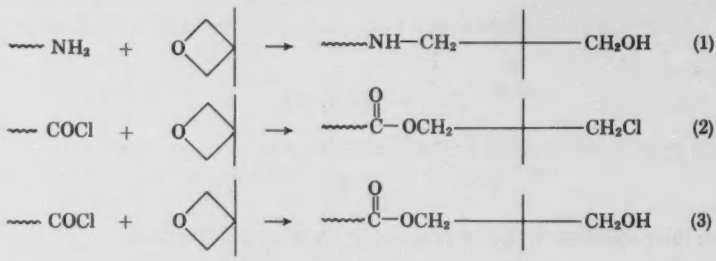

At higher temperatures, the more numerous but less reactive amide groups entered into the reaction and produced a detectable decrease of trimethylene oxide rings.

Trans-epoxysuccinyl chloride (IIIb) was polymerized[8] with *trans*-2,5-dimethylpiperazine, bis(4-aminocyclohexyl)methane, hexamethylenediamine, and decamethylenediamine. Inherent viscosities could be obtained only on the polymers of the latter two diamines. (Inherent viscosity = ln η_{rel}, where concentration is 0.5% in the solvent at 25°C.) However, both of these became insoluble on standing. A copolymer of III and adipyl chloride (1/1) with decamethylenediamine gave a clear, tough film when

dry-cast from a tetrachloroethane–phenol mixture. However, heating of this film at 250°C. for two minutes did not effect insolubilization.

In all of the homopolymers of IIIb, rapid insolubilization of the polymer was noted. Since the acid chloride was melted and weighed out as a liquid, it was possible that IIIb was changing in the molten state. To check this, a sample of Ib was heated on the steam bath and the liquid sampled at various intervals of time. There was no detectable difference in the infrared spectra of freshly distilled acid chloride and the various samples which were heated up to 24 hr. This demonstrates the remarkable stability of these epoxysuccinyl chlorides.

Experimental

All melting points were determined on a Köfler hot stage and boiling points were not corrected.

Bis(aminoethyl)oxetane. The free diamine was prepared by treating the dihydrochloride with saturated potassium carbonate solution.[4] It boiled at 75.5°C./0.5 mm.

ANAL. Calcd. for $C_8H_{12}ON_2$: C, 51.64%; H, 10.41%. Found: C, 51.46, 51.49%; H, 10.20, 10.31%.

The dihydrobromide melted with decomposition at 237–240°.

ANAL. Calcd. for $C_8H_{18}ON_2BR_2$: C, 21.60%; H, 5.38%; Br, 57.6%; Found: C, 21.84, 22.17%; H, 5.50, 5.65%; Br, 58.3, 58.9%.

3,3-Bis(benzamidomethyl)oxetane (IV). The diamine was dibenzoylated by a Schotten-Baumann procedure.[4] The product melted at 168–169°C.

3,3-Bis(phenylthioureidomethyl)oxetane (VI). This compound was prepared from phenyl isothiocyanate, and the diamine and melted at 164–165°C.[4]

3,3-Bis(phenylureidomethyl)oxetane (V). Phenylisocyanate (3.17 g.) in 25 ml. of dimethylformamide was added to bis(aminomethyl)oxetane (1.55 g.) in 15 ml. of dimethylformamide. The mixture became warm and was cooled with an ice bath. Next day, the solution was poured on ice to give a gummy precipitate which became friable after working with a stirring rod. The solid was filtered, washed with water, and dried in a vacuum. The crystalline product melted at 196–197°C., but was not analytically pure. It was recrystallized from absolute ethanol to give clumps of short rods, m.p. 202°C.

ANAL. Calcd. for $C_{19}H_{22}O_3N_4$: C, 64.39%; H, 6.25%. Found: C, 64.54, 64.32%; H, 6.44, 6.38%.

Effect of Heat on 3,3-Bis(benzamidomethyl)oxetane (IV). Several small samples of this compound were heated at 180° in a vacuum. Samples were removed and the intensity of the infrared band at 10.3 μ was determined at intervals. After 24 hr., the intensity had decreased to 65% of the initial value, indicating disappearance of the trimethylene oxide ring. The

infrared spectrum of IV was quite similar to that of the polyamide based on terephthalic acid.

3,3-Bis(phenylureidomethyl)oxetane (V). Samples of this material were studied as above. After 24 hr. at 100°C., the infrared spectrum had altered completely. The band at 10.28 μ shifted to 10.13 μ, and a new band appeared at 13.57μ. The melting point of this compound (V) determined between crossed Polaroids on a hot stage was sharp at 202°C. However, the melt crystallized partially on cooling to give a crystalline phase embedded in an amorphous, glasslike substance. On reheating, this crystalline phase melted at 250–255°C. This, coupled with the spectral data quoted above, indicated strongly that a relatively straight-forward chemical change had taken place. However, the fact that the new phase had an infrared band at 10.13 μ made it impossible to decide whether the change involved the trimethylene oxide ring.

About 500 mg. of bis(phenylureidomethyl)oxetane was maintained in a test tube at 200°C. under a nitrogen blanket, for about 1 hr. A few droplets of liquid collected near the top of the test tube; these were removed by a micropipet and identified as aniline (odor; insoluble in water, soluble in dilute HCl; diazotized, gave azo dye with alkaline phenol). The residue was sublimed in a high vacuum; the crystalline sublimate melted at 265–270°C. with a phase change at ca. 250°C. A redetermination of the melting point, with one block preheated to 250°C., gave a melting point of 274°C. (dec.); again, a phase change was noted at about 255°C.

ANAL. Found: C, 57.85%; H, 7.22%; N, 17.76%.

3,3-Bis(phenylthioureidomethyl)oxetane (VI). No significant changes were detected in the infrared spectrum of this compound after heating at 100 and at 200°C. as above.

***cis* and *trans*-Epoxysuccinic Acids.** These diacids were prepared as described by Payne and Williams[7] in yields of 70 and 60%, respectively.

***cis*-Epoxysuccinyl Chloride.** A mixture of 40.0 g. (0.30 mole) of the *cis*-epoxy acid and 137.4 g. (0.66 mole) of phosphorus pentachloride was heated in an oil bath maintained at 80–85°C. till all of the solid dissolved (ca. 3 hr.). The by-product, phosphorus oxychloride, was distilled at 42 mm. The pressure was then reduced to 14 mm. and a small intermediate fraction collected, b.p. 81.5–8.35°C. The desired product (40.5 g., 80%) boiled over the range of 103.5–105°C. at 14 mm. This material solidified on cooling to room temperature, m.p. 38–41° (Lit.:[6] b.p. 95°C./13 mm., 104–108°C./25 mm.; m.p. 36–41°C.).

ANAL. Calcd. for $C_4H_2O_3Cl_2$: C, 28.43%; H, 1.20%; Cl, 41.97%. Found: C, 28.22, 28.26%; H, 1.11, 1.15%; Cl, 41.7, 41.4, 41.1%.

***trans*-Epoxysuccinyl Chloride.** This was made exactly as the *cis* compound. The product (42.0 g., 83%) boiled at 102–104°C./40 mm. This material crystallized on cooling to give plates, m.p. 50–52°C., (Lit.:[5] m.p. 53°C.) which could be recrystallized from petroleum ether.

ANAL. Calcd. for $C_4H_2O_5Cl_2$: C, 28.4%; H, 1.20%; Cl, 41.9%; M.W., 170.0. Found: C, 28.22%; H, 1.11%; Cl, 41.7%; M.W. (Rast) 187.3, 189.5.

The NMR spectrum showed only one type of hydrogen, either CH or CH_2. The infrared showed only one type of carbonyl (that of an acid chloride) and is consistent with the structure.

Preparation of Polymers

Preliminary Experiments on Preparation of Polyamides from Bis(aminomethyl)oxetane. The preparation of the polyamide of terephthalic acid was carried out in a water–methylene chloride system. Terephthaloyl chloride (0.98 g.) was dissolved in 100 ml. of anhydrous methylene chloride, and poured with vigorous stirring into a solution of 0.91 g. diamine dihydrochloride in water (150 ml.) containing excess base. The polymer, a swollen, sticky mass, was separated and dried. It was found to be soluble in chloroform–methanol, formic acid (98%), and in *m*-cresol. The inherent viscosity (formic acid) was 0.97. Films cast from formic acid were clear and hard, and moderately tough. The polymer could not be melted; soluble film heated at about 100°C. could no longer be dissolved in formic acid.

Polyamides were made from sebacoyl chloride and from adipoyl chloride. These latter polyamides appeared to be very water-sensitive. Samples which were soluble when freshly prepared became insoluble on standing.

Copolymers. Several attempts to prepare copolymers from mixtures of hexamethylenediamine with bis(aminoethyl)oxetane and sebacoyl

TABLE I
Polymerizations of Bis(aminomethyl)oxetane in Solution

Diacid chloride	Solvent	η_{inh} Formic acid	η_{inh} Cresol	Remarks
Sebacoyl	$CHCl_3$	2.82	0.62	Anomalous viscosity behavior is typical of these polyamides.
Adipoyl	$CHCl_3$	1.04	0.33	Film cast from water as solvent. Heated overnight at 120°C., no longer soluble.
Terephthaloyl	$CHCl_3$	1.95	0.72	Film cast from formic acid insolublized by heating at 100°C. overnight
Terephthaloyl	$CHCl_3$	0.80	—	$[\eta] = 1.35$ (formic).
Sebacoyl	100 $CHCl_3$ + 75 hexane	Insol.	Insol.	Polymer when first prepared was soluble in formic acid. After standing, became insoluble.
Adipoyl	100 $CHCl_3$ + Hexane	0.73	—	Tacky, water-sensitive polymer.
Terephthaloyl	$CHCl_3$	1.03	0.43	$[\eta] = 0.35$ (cresol) $[\eta] = 4.0$ (formic acid)

chloride in two-phase systems were unsuccessful. The only product isolated was the 6–10 homopolymer, m.p. 224°C.

Preparation of Polymers in Solution. The most useful method for preparing polymers of the diamine was by polymerization in chloroform.[9] The polymers and copolymers prepared in this manner are listed in Table I.

Preparation and Properties of the Polyterephthalamide of Bis(aminomethyl)oxetane. A solution of 2.37 g. of bis(aminomethyl) oxetane and 4.6 g. of redistilled triethylamine was dissolved in 50 ml. of washed and dried chloroform and added to a solution of 4.14 g. of terephthaloyl chloride in 150 ml. of chloroform in a high speed mixer. The polymer precipitated at once as a curdy, swollen mass, which could be redissolved by the addition of a little methanol. The precipitated polymer was filtered, washed with ethanol, then water, then dried. The polymer melt temperature (PMT)[13] was 300°C., the yield, about 90%, $\eta_{inh} = 1.96$ (formic acid).

A solution of the terephthalamide in formic acid was cast on a glass plate to give a clear, fairly tough film. This film was very sensitive to water. It became rubbery and very weak and could be balled up, rather like chewing gum when soaked for a few moments in water; on the other hand, it became quite brittle when absolutely dry. A portion of this film was heated at 100°C. overnight. It was then completely insoluble in formic acid and cresol, but was still quite water sensitive, although more form-stable. Crosslinked film treated with hot water became quite pliable, but was not like chewing gum in that it could not be balled up or badly stretched out of shape. Crosslinked film was also much tougher when wet, though still brittle when dry.

A sample of the terephthalamide ($\eta_{inh} = 0.78$ in 98% formic acid) was cast into a film with a 0.005-in. doctor knife, formic acid being used as solvent. This film, after drying at room temperature, was removed from the plate and cut into strips weighing about 0.10–0.15 g. These were heated at 100°C. (vacuum oven) for varying periods of time. After the

TABLE II
Change in Characteristic Properties of Bis(aminomethyl)oxetane Polyterephthalmide of Film at 100°C.[a]

Time at 100°C., hr.	η_{inh} (formic acid)	Solubility in formic acid
0	0.78	Easily soluble
0.25	0.67	Easily soluble
0.50	1.05	Easily soluble
0.75	0.89	Incompletely soluble; gel formation
1.0	—	Insoluble; swollen
1.5	—	Insoluble
24	—	Insoluble

[a] No detectable change in infrared after any of the treatments.

heating cycles, the properties of the samples were determined as indicated in Table II.

Other strips were drawn on the hot pin 3× at 100°C. to give highly oriented birefringent, but complete noncrystalline (x-ray) products. These oriented strips were insolubilized at 140°C. as above, without losing their orientation. Infrared showed about 35% of trimethylene oxide rings.

Anomalous Viscosity Relationships of Solutions of the Terephthalamide. All polymers based on bis(aminomethyl)oxetane which were studied during this work showed unusual viscosity behavior. Thus, the inherent viscosities determined in formic acid were much higher than those in *m*-cresol. Furthermore, the intrinsic viscosity curves showed strong upward curvature, after the manner of polyelectrolytes. These differences may be seen more clearly by examination of the data in Table III. This effect is noticeable even in copolymers.

TABLE III
Viscosity Relationships

Viscosity	Bis(aminomethyl)-oxetane terephthalamide	Coterephthalamide of bis(aminomethyl)-oxetane 2,5-dimethyl-piperazine (10/90)	Terephthalamide of 2,5-dimethyl-piperazine
η_{inh} (*m*-cresol)	0.72	2.31	1.96
η_{inh} (formic acid)	1.96[a]	1.71	1.03
η_{intr} (formic acid)	2.60	2.30	1.08

[a] At 0.5% the value of η_{inh} (formic acid) does not change with time.

Polyurethane from Bis(aminomethyl)oxetane and Ethylene Bischloroformate. A solution of 2.82 g. of the diamine in 50 ml. of water containing 7 g. of potassium carbonate was added to a vigorously agitated solution of 4.54 g. of ethylene bischloroformate in 100 ml. of pure chloroform plus 50 ml. of pure hexane. The polymer separated as a rubbery lamp which became hard and tough on removing residual solvent. The yield was 3.7 g., the inherent viscosity 0.41 in *m*-cresol.

The infrared spectrum showed a band at 10.25 μ. A polymer sample was heated at 100°C. for 24 hr., then at 120°C. for 24 hr. There was no detectable change in the spectrum. However, the polymer was no longer soluble.

Polyurea from Bis(aminomethyl)oxetane and Toluene 2,4-Diisocyanate. Solutions of the diamine (2.18 g.) and the diisocyanate (3.05 g.) were prepared in 15 cc. portions of DMF. On mixing the two solutions, an exothermic reaction was noted, and the viscosity of the solution increased. The solution was poured into water, and the polymer (η_{inh} = 0.2 in DMF) filtered and dried.

Some polymer was dissolved in formic acid and cast to a film. A portion of the film was heated 24 hr. at 120°C. The unheated polymer had a band

at 10.55 μ which disappeared on heating. The heated product had a new band at 9.5 μ.

Polymers of *trans*-Epoxysuccinyl Chloride (IIIb). The polymer with *trans*-2,5-dimethylpiperazine was prepared by interfacial polymerization[8] with methylene chloride as the organic phase. The solid polymer obtained was very water-sensitive and on isolation formed a gummy mass.

The polymer with bis(4-aminocyclohexyl)methane (mixture of isomers) was prepared by interfacial polymerization[8] with methylene chloride as the organic phase. Most of the polymer was insoluble, but some could be dissolved in dimethyl sulfoxide. A film dry-cast from this solvent was very weak. The polymer had a polymer melt temperature of 400°C., with browning starting at 260°C.

The polymer with hexamethylenediamine was prepared by interfacial polymerization[8] with methylene chloride as the organic phase. The polymer was obtained in 57% yield, η_{inh} 0.76 (5% lithium chloride–dimethylformamide). A film dry-cast from this solvent mixture was brittle, which may have been due to cross-linking at the drying temperature (120°C.). The polymer became insoluble on standing on the shelf.

The polymer with decamethylenediamine was prepared by interfacial polymerization[8] with methylene chloride as the organic phase. The polymer had η_{inh} 0.63 (hexamethylphosphoramide) and became insoluble on standing on the shelf.

Copolymer of IIb and Adipyl Chloride (1/1) with Decamethylenediamine. This was prepared by interfacial polymerization[8] with methylene chloride as the organic phase. The resulting polymer had η_{inh} 0.66 (tetrachloroethane-phenol), polymer melt temperature ca. 400°C. A film from the solvent mixture was tough and slightly opaque. Heating of this film at 250°C. for 2 min. did not effect insolubilization.

Polymers of the *cis*-acid were not prepared.

References

1. See, for example, T. L. Cairns, H. D. Foster, A. W. Larchar, A. K. Schneider, and R. S. Schrieber, *J. Am. Chem. Soc.*, **71**, 651 (1949); A. J. Hall, *Silk J. Rayon World*, **23**, 30 (1947); R. Muller et al., *Angew. Chem.*, **64**, 523 (1952).

2. Farthing, A. C., and W. J. Reynolds, *J. Polymer Sci.*, **12**, 503 (1954); A. C. Farthing, *J. Chem. Soc.*, **1955**, 3648; H. K. Boardman, paper presented at Delaware Section American Chemical Society Symposium, February 18, 1956.

3. Hill, F. N., F. E. Bailey, and J. T. Fitzpatrick, *Ind. Eng. Chem.*, **50**, 5 (1958); H. Staudinger and H. Lohmann, *Ann. Chem.*, **505**, 41 (1933); W. R. Sorenson and T. W. Campbell, *Preparative Methods of Polymer Chemistry*, Interscience New York, 1961.

4. Campbell, T. W., *J. Org. Chem.*, **22**, 1029 (1957).

5. Lossen, W. C., *Ann.*, **348**, 299 (1906).

6. Schopf, C., and W. Arnold, *Chem. Ber.*, **558**, 109 (1947); J. A. King, V. Hofmann, and F. H. McMillan, *J. Org. Chem.*, **16**, 1100 (1951).

7. Payne, G. B., and P. H. Williams, *J. Org. Chem.*, **24**, 54 (1959).

8. Wittbecker, E. L., and P. W. Morgan, *J. Polymer Sci.*, **40**, 289 (1959); R. G. Beaman, P. W. Morgan, C. R. Koller, E. L. Wittbecker, and E. E. Magat, *ibid.*, **40**, 329 (1959).

9. Morgan, P. W., and S. L. Kwolek, *J. Polymer Sci.*, **A1**, 1147 (1963).
10. Schaefgen, J. R., and C. F. Trivisonno, *J. Am. Chem. Soc.*, **73**, 4580 (1951).
11. Schaefgen, J. R., and C. F. Trivisonno, *J. Am. Chem. Soc.*, **74**, 2715 (1952).
12. Barrow, G. M., and S. Searles, *J. Am. Chem. Soc.*, **75**, 1175 (1953).
13. R. G. Beaman and F. B. Cramer, *J. Polymer Sci.*, **21**, 223 (1956).

Résumé

On a préparé deux monomères, le bis(aminométhyl)oxétane (I) et le chlorure d'époxysuccinyle (II) (v. le résumé anglais) on les a transformés en polycondensats dont la structure est similaire à celle des époxydes. Les deux monomères sont stables et faciles à manier. Les polymères sont des produits pontés, insolubles et infusibles.

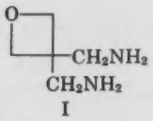

I

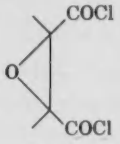

II

Zusammenfassung

Zwei Monomere, Bis-(aminomethyl)-oxetan (I) und Epoxysuccinylchlorid (II) (siehe englische Zusammenfassung) wurden dargestellt und in Kondensationspolymere mit ähnlicher Struktur wie Epoxyharze umgewandelt. Beide Monomere erwiesen sich als stabil und leicht zu verarbeiten. Die Polymeren vernetzten zu unlöslichen, unschmelzbaren Produkten.

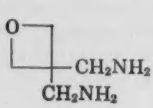

I

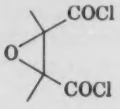

II

Received March 16, 1962
Revised April 30, 1962

JOURNAL OF POLYMER SCIENCE: PART A VOL. 1, PP. 2537–2549 (1963)

Use of Dimaleimides as Accelerators for the Radiation-Induced Vulcanization of Hydrocarbon Polymers. Part II. Synthetic Rubbers and Saturated Polymers

S. M. MILLER, M. W. SPINDLER, and R. L. VALE, *United Kingdom Atomic Energy Authority, Isotope Research Division, Wantage Research Laboratory (A.E.R.E.), Wantage, Berks, England*

Synopsis

The effect of *m*-phenylenedimaleimide on the rate of cross linking of synthetic rubbers, polyvinyl acetate, polyvinyl chloride, polyethylene, and other polymers, under the action of ionizing radiation is described. The dose reduction factor for equivalent degrees of crosslinking obtained with and without the maleimide varies from 10 to 25 for the synthetic rubber. Further evidence is given to show that maleimides sensitize the vulcanization of unsaturated polymers, principally by copolymerization, and certain saturated polymers containing labile atoms, by a transfer mechanism.

INTRODUCTION

In a previous publication[1] the use of dimaleimides as accelerators for the radiation-induced vulcanization of natural rubber has been described. It was found that the aromatic compound, *m*-phenylenedimaleimide, was the most effective accelerator and two chain mechanisms of crosslinking were considered. It has now been found that *N*-phenylmaleimide is even more effective in crosslinking certain polymers, and a study of both mono- and dimaleimides has provided further information about the mode of crosslinking. It is clear that crosslinking initiated by radiation may occur by copolymerization between the unsaturated units in a diene polymer and the carbon–carbon double bond of either a monomaleimide or dimaleimide, or alternatively by a hydrogen transfer process in the case of certain saturated polymers when dimaleimides are used. The experiments with synthetic rubbers were designed to extend the range of application of the maleimides, whereas the saturated polymers were chosen to give information about the cross linking mechanism.

EXPERIMENTAL

1. Radiation Sources

A 500-curie source of Co^{60} in a concrete shield as described by Dove, Murray, and Roberts[2] was used for the γ-irradiation, giving a dose rate of 1.3×10^5 rads/hr. in the position used.

A 4 M.e.v. linear accelerator delivering a pulsed beam of electrons at a frequency of 600 pulses/sec. with a pulse duration of 2.5 μsec. and therefore the peak dose rates are 600 times the mean values quoted.

The energy deposition in the samples was determined by means of the ferrous sulfate dosimeter for γ irradiation using $G_{Fe^{3+}} = 15.6$, and by water calorimetry for electron irradiation. A correction was made for the relative electron densities of ferrous sulfate solution and polymers.

2. Materials

The natural rubber was a pale crepe given by the Natural Rubber Producers Research Association. It was masticated on a mill until it was completely benzene-soluble. The *cis*-1,4-polyisoprene was obtained from Shell Chemical Company and the *cis*-1,4-polybutadiene and SBR (butadiene–styrene copolymer) from Phillips Petroleum Company. The polybutadiene is a commercial rubber containing 95.5% *cis* component and 0.5% of a phenolic antioxidant. The SBR Philiprene 1502 contains between 4.75 and 7.0% of a mixed fatty rosin acid and approximately 1.25% of antioxidant. The polychloroprene was obtained from Dunlop Rubber Company and is a commercial product graded W.R.T.

The polyisobutylenes were obtained through the Sherman Chemical Company and the medium viscosity polydimethylsiloxane (MS 200 silicone oil) from Midland Silicones. The polyvinyl chloride was a pure polymer (Geon 101) supplied by British Geon Ltd. The polyvinyl acetate was prepared by the photopolymerization of pure monomer and had a viscosity-average molecular weight of 320,000. The polyethylene was an antioxidant-free material given by I.C.I. Ltd. and had an $\bar{M}_w = 513{,}000$ and $M_n = 26{,}000$.

All the synthetic rubbers were purified by acetone extraction in the dark in a Soxhlet apparatus and under an atmosphere of nitrogen for 48 hr. The extraction was facilitated by cutting the rubbers into small pieces, volume about 0.5 cm.^{3}. Following extraction, certain of the rubbers gelled easily on heating and, therefore, all the rubbers were dried *in vacuo* at room temperature for periods of 1 to 4 weeks in the dark. Purified polychloroprene gelled under these conditions and had to be used in the non-extracted state. The purified rubbers were stored *in vacuo* in the dark until required. The saturated polymers were used without further purification.

Analar reagent benzene was dried over sodium wire for use in swelling measurements.

TABLE I

Compound	Melting point, °C.	Structure
m-Phenylenedimaleimide	202	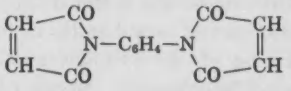
N-phenylmaleimide	90.5	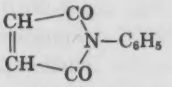

Maleimides (Table I) were synthesized by the method described by Searle.[3] Greatly improved yields were obtained by purifying the amines by recrystallization before attempting the condensation with maleic anhydride. The C^{14}-labeled *m*-phenylenedimaleimide had an activity of 1.5 μc./g.

3. Preparation of Samples for Irradiation

Solutions of the purified polymers were prepared by dissolving 1 g. of the polymer in 75 ml. of benzene in the case of synthetic rubbers and polyvinyl acetate. For polyethylene it was necessary to reflux the polymer with benzene to obtain a clear solution, and for polyvinyl chloride tetrahydrofuran was used as the solvent. The maleimides were added to the benzene solution by dissolving a known weight in a small volume of acetone and mixing the two solutions. The mixed solutions were freeze-dried and the dry rubber was evacuated at $<10^{-4}$ mm. Hg for two days at room temperature. The samples were then rolled into a tight ball and transferred to a cylindrical Pyrex glass tube of 15–16 mm. diameter and sealed under vacuum.

The polyisobutylene and silicone, which were oils at room temperature, were mixed with the powdered maleimide by stirring at high speed. This produced a suspension of solid particles of additive in the oil.

4. Irradiation Procedure

For γ-irradiation, samples were kept at a standard distance from the source tube by fixing the glass tubes containing the polymers in a Terry spring clip and securing the lower end of the tubes in a circular plate containing holes. During electron irradiation the mean dose rate varied from 3×10^5 to 5×10^7 rads/min., and sample tubes were cooled continuously during the irradiation by passing a stream of cold water over them.

5. Determination of Swelling Index and Gel Fraction

The swelling indices and gel fractions of irradiated rubber samples were determined by swelling in benzene for 48 hr. at 25°C. The gel fractions of the polyethylene powders were determined by refluxing in a Soxhlet

extractor with toluene for 48 hr. About 0.5 g. of polymer was placed in a glass cylinder, the ends of which were sealed with sintered glass No. 3. The sample was inserted through a side arm which projected upwards and also served as a handle to lower the cylinder into the extractor. After drying of the cylinder and contents, the weight of insoluble polymer could be obtained. In order to measure a swelling index on a polyethylene sample it was necessary to press the freeze-dried powder in a hydraulic press at 120°C. to make a thin disk which could be handled in the same manner as the irradiated rubbers. The polyvinyl acetate freeze-dried powder could be readily rolled into a firm ball which was rigid during the swelling measurements.

To determine the concentration of crosslinks in the irradiated rubber samples, the volume fractions V_r of polymer in the swollen gels were calculated from the swelling indices I by the expression $V_r = 1/(I\rho_r + 1)$. The molecular weights M_c of chains between adjacent crosslink points on a given chain were then obtained from the Flory-Rehner[4] equation:

$$-\ln (1 - V_r) - V_r - \mu V_r^2 = V\rho_r M_c^{-1}[V_r^{1/3} - (V_r/2)]$$

where ρ_r is the density of rubber, μ is the solvent–polymer interaction coefficient, and V is the molar volume of solvent.

Values of $\mu = 0.42$ and 0.37 were used for natural rubber and SBR, respectively, and a value of 0.40 was taken for polybutadiene and neoprene. Since this equation can only be used with reliability in the range of swelling indices of 2–10, in those polymer solvent systems where very high doses were required to produce such a crosslink density comparisons were made between swelling indices or gel fractions rather than the absolute values of crosslinks.

For all the rubber systems studied, gel contents were at least 95% for doses of 10^6 rads, so that there is little error in disregarding the few crosslinks in the sol fraction and indices are a reliable measure of the degree of crosslinking. However, for polymers, such as polyvinyl acetate and polyethylene, in which the ratio of scission to crosslinking is high, very high doses are required to obtain gel fractions above 95%, and the gel fraction, usually possessing a very high swelling index, must be used as a measure of the extent of reaction. The anomaly that may arise is that samples of the same gel content may not necessarily possess the same concentration of cross links and to avoid this, the dose for gelation R_G has been measured. At the gelation point there is, on the average, one crosslinked unit per weight-average molecule, and the efficiency of crosslinking may therefore be calculated from the expression:

$$G_x = 0.48 \times 10^6/R_G\bar{M}_w$$

where G_x is the number of crosslinks formed per 100 electron volts of energy absorbed and $\bar{M}_w$ is the weight-average molecular weight of the initial polymer before irradiation. The dose for gelation is expressed in megarads.

6. Determination of Activity of Polymers Containing Labeled Dimaleimide

Approximately 30-mg. samples were combusted in a stream of oxygen and the resulting CO_2 trapped in liquid oxygen and used to fill a gas counter containing a little CS_2, giving a total pressure of 10 cm. Hg. The activity was determined in the conventional manner with a 1009A scaler. The activities were expressed as counts/min. for a standard filling after correcting for paralysis time and background. The method of calculating the crosslink densities from the active counts has been given in the previous paper.[1]

RESULTS

It is convenient to divide the hydrocarbon polymers into two groups, namely, those containing unsaturated units in the main chain and those which are fully saturated. The first group respond strongly to the sensitizing action of maleimides, whereas only certain members of the second group show any response at all.

1. Unsaturated Rubbers

The rubbers studied in this group can all be crosslinked in the pure state by ionizing radiation, and the rate of crosslinking at constant dose rate is increased by the addition of *m*-phenylenedimaleimide (Fig. 1). Table II shows the approximate G_x values for crosslinking at room temperature in the presence of 5% by weight of dimaleimide, determined by the slope of the plots in Figure 1 to avoid the induction period found in certain rubbers. As the cross linking reaction is dose rate-dependent, a rate intensity exponent of 0.55 being found for natural rubber,[1] the values are not the optimum values and higher values would be found at lower dose rates. An error is to be expected owing to uncertainty in the choice of

TABLE II
G_x Crosslinking Values for Various Rubbers at a Dose Rate Co^{60} $\gamma = 1.6 \times 10^5$ rad/hr.

Rubber	G_x, Crosslinks formed/100 e.v. absorbed		
	No additive	5% *m*-phenylene-dimaleimide	6.28% *N*-phenyl-maleimide
Natural rubber (pale crepe)	1.8	46	70
cis-1,4-Polyisoprene	0.9	19	
cis-1,4-Polybutadiene	5.8	38	
SBR (Philiprene 1502)	3.8	52	
Polychloroprene[a]	9.6	56	

[a] Not purified.

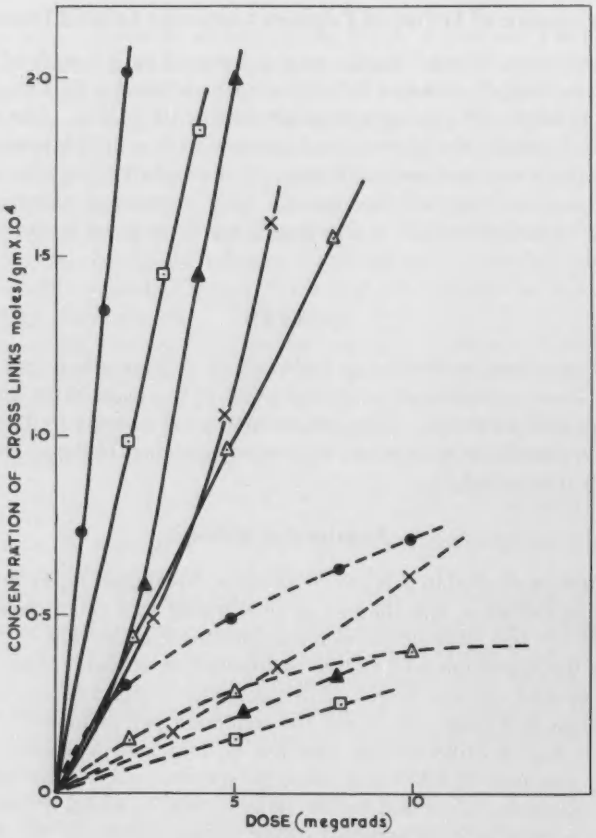

Fig. 1. Yield of crosslinks in various rubbers on γ-irradiation at a dose rate of 1.3 $\times$ 10^5 rad/hr. (—) in the presence of 5% of *m*-phenylene dimaleimide and (--) with no additive: (●) neoprene; (□) natural rubber; (△) SBR (Philiprene 1502); (×) *cis*-1,4-polybutadiene; (▲) *cis*-1,4-polyisoprene.

μ values, but this does not invalidate the comparison between the polymers with and without additive.

No data are available for the use of *N*-phenylmaleimide with these rubbers but its action will be analogous to that with natural rubber which is included in the table to assist in the discussion of the reaction mechanism.

2. Saturated Polymers

Polydimethylsiloxane. There was no improvement in the extent of crosslinking by the addition of 5–10% of *m*-phenylenedimaleimide.

Polyisobutylene. Two rubbers, one a very high molecular weight sample, and the other a viscous oil, were irradiated with electrons at dose rates

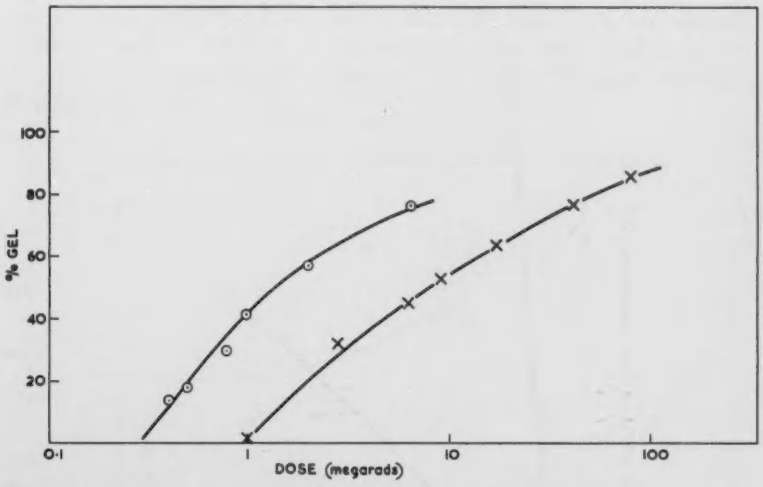

Fig. 2. Gel fraction curves for polyethylene powder at a dose rate of 10^6 rad/min.: (⊙) 5% *m*-phenylenedimaleimide; (×) no additive.

from 10^6 rad/min. to 2.5×10^7 rad/min. to total doses of 2.5 and 5.0 Mrads. No gel fraction was found with or without the use of dimaleimide. Similarly, irradiation with γ-rays at 1.25×10^5 rad/hr. at doses of 2.5 and 10 Mrads produced no gel fraction.

Polyvinyl Chloride. Irradiation of films of pure polyvinyl chloride with γ-rays (dose rate 1.03×10^5 rad/hr.) at doses from 10^6 to 4×10^7 rads gave gel contents ranging from 0.38 to 0.6%, whereas with 5% *m*-phenylenedimaleimide in the film the gels increased from 0.83 to 6.8%.

Polyethylene. The dose required for gelation R_G for a sample of pure polyethylene was 10^6 rad ($G_x = 1.8$) and was independent of dose rate. In the presence of 5% of *m*-phenylenedimaleimide R_G was reduced to 2.5×10^5 rad ($G_x = 7.2$). The gel fraction curve is shown in Figure 2 for powder samples. When pressed sheets were used, the hot pressing resulted in a retardation, and no sensitizing action of the dimaleimide was observed.

The contribution of the dimaleimide to the crosslinking process may be judged from Figure 3, which shows the crosslinks determined from swelling measurements compared with those determined with the use of labeled dimaleimide, assuming that each dimaleimide molecule present forms a crosslink, as in the case of natural rubber.[1]

A comparison was made of the infrared absorptions of films of polyethylene after irradiation. Irradiated samples were extracted with boiling toluene to remove the sol fraction and uncombined dimaleimide. The ratio of the absorptions at 830 cm.$^{-1}$ (RCH=CHR) to that at 1508 cm.$^{-1}$ (—CO—N—CO—) characteristic of the imide linkage, showed that about 40% of the unsaturated units in the combined dimaleimide had not reacted. The initial *trans* vinylene unsaturation at 965 cm.$^{-1}$ showed a slight fall in

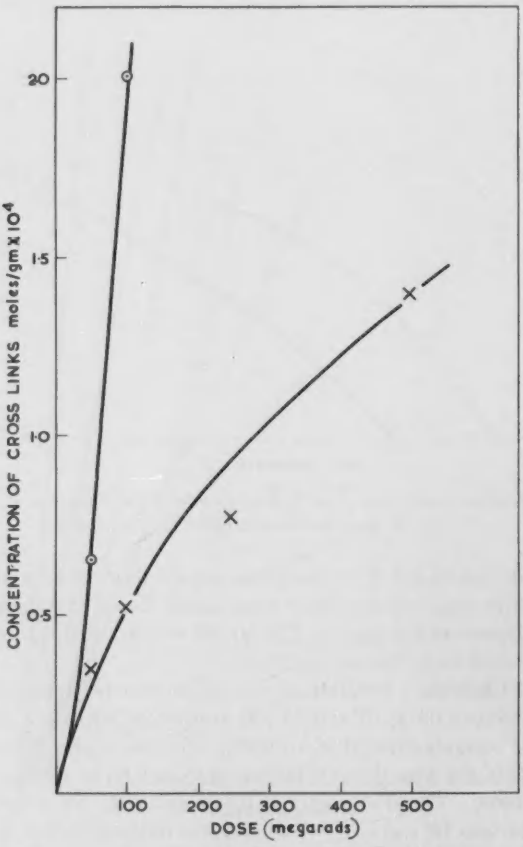

Fig. 3. Yield of crosslinks in polyethylene containing 5% *m*-phenylenedimaleimide: (⊙) determined from swelling in toluene; (×) calculated from C^{14} maleimide.

the additive sample up to 2 Mrads and then rose at the rate characteristic of a pure sample of polyethylene on irradiation.

Polyvinyl Acetate. The effects of *m*-phenylenedimaleimide are more pronounced on the extent of crosslinking of polyvinyl acetate than any other saturated polymer examined. The dose for gelation R_G is decreased by a factor of 50 from 10^7 rad to 5×10^5 rad at a dose rate of 10^6 rad/min. The gel fraction at a given dose appears to be dose rate-dependent for both additive and control samples (Fig. 4), and it is believed that this is due to a trace of oxygen remaining in the polymer. The dose rate effect is the reverse to that to be expected from a bimolecular chain process, e.g., as found with natural rubber–maleimide mixtures,[1] since the higher the dose rate the lower the dose required for gelation. The gel fraction curve and the

crosslinks determined from the use of labeled dimaleimide are shown in Figures 5 and 6. Addition of *N*-phenylmaleimide (10%) was found to retard the crosslinking reaction, giving a rate slightly less than that for pure polyvinyl acetate.

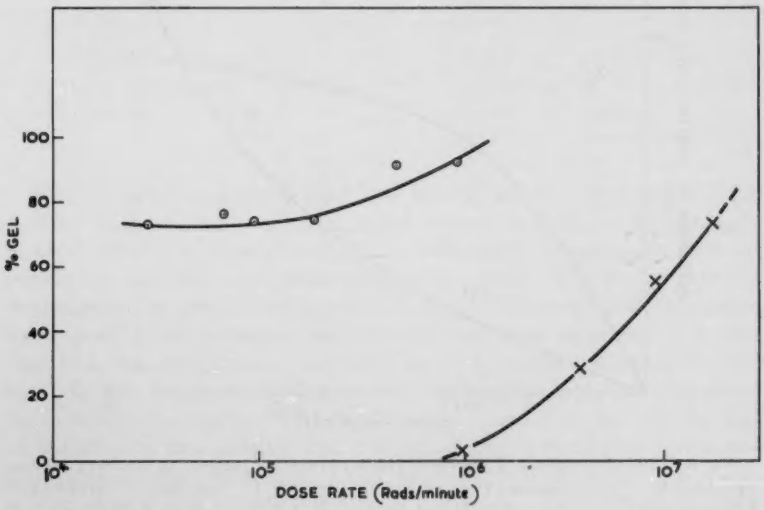

Fig. 4. Effect of dose rate on the gel fraction of polyvinyl acetate at a total of dose 10 rad: (⊙) 5% *m*-phenylenedimaleimide; (×) no additive.

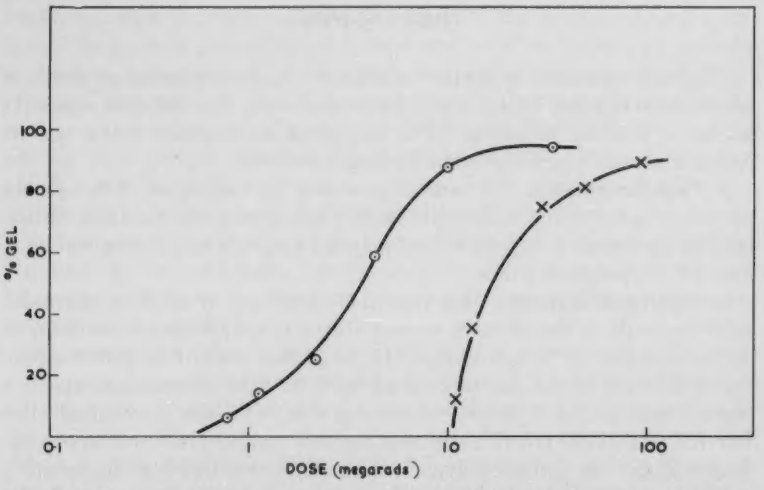

Fig. 5. Gel fraction curve for polyvinyl acetate at dose rate of 10^6 rad/min.: (⊙) 5% *m*-phenylenedimaleimide (×) no additive.

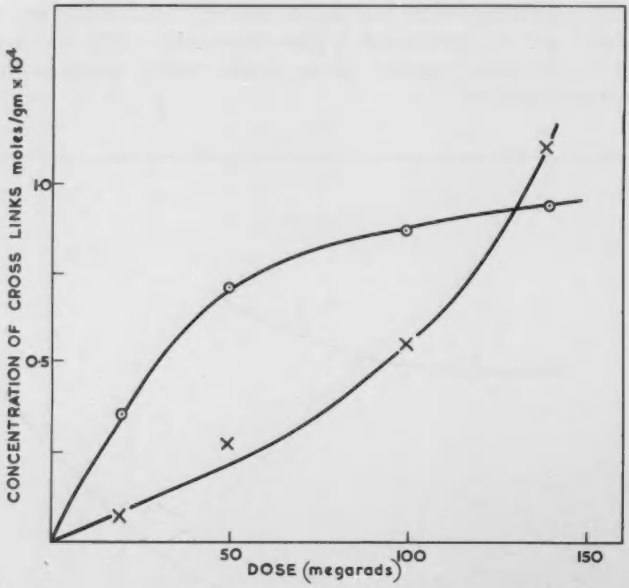

Fig. 6. Yield of crosslinks in irradiated polyvinyl acetate containing 5% *m*-phenylenedimaleimide: (×) determined from swelling in benzene; (⊙) calculated from combined C^{14} maleimide.

DISCUSSION

Emphasis was made in the previous paper[1] on the two apparent modes of acceleration of crosslinking of natural rubber using dimaleimides under the action of ionizing radiation. The two processes outlined below are referred to as copolymerization and hydrogen transfer.

a. Copolymerization. A radical produced by radiolysis of the parent polymer reacts with a maleimide double bond, and the resulting radical adds to the double bond of a second polymer molecule and this continues to give a 1:1 copolymerization.

b. Hydrogen Transfer. The radical (I) produced by addition of a maleimide molecule to the primary radical abstracts a hydrogen atom from an adjacent chain. The new radical (II) may then either add to the second ethylenic bond in the case of a dimaleimide or with a monomaleimide to a second molecule of additive. Assuming that with the dimaleimide this internal addition is possible and that the new radical (III) abstracts a hydrogen atom from another polymer chain, then a crosslink is produced and a radical center is propagated. With a monomaleimide, the overall result would be a series of attached pendant maleimide units but no crosslinks.

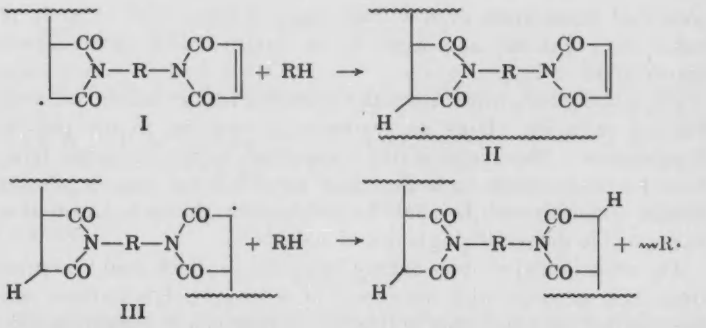

The significant discovery since the first paper was prepared is that *N*-phenylmaleimide is even more powerful than *m*-phenylenedimaleimide in accelerating the radiation-induced crosslinking of unsaturated rubbers, despite the fact that *N*-ethylmaleimide is very poor. This proves that the predominant reaction in the case of unsaturated polymers must be copolymerization, since hydrogen transfer would not lead to crosslinks in the case of a monomaleimide. However, since polyvinyl acetate and polyvinyl chloride are crosslinked more readily in the presence of *m*-phenylenedimaleimide, this suggests that the hydrogen transfer mechanism can also be operative in special cases, and it is interesting to recall that the monomaleimide, *N*-phenylmaleimide, not only fails to accelerate the crosslinking of polyvinyl acetate but retards it slightly. Furthermore, looking at Figure 6 it can be seen that the proportion of bound radioactive dimaleimide is higher than the number of crosslinks. This indicates that some molecules, add to the primary radical, abstract from a neighboring chain, but then the new radical fails to add to the second ethylenic unit in the dimaleimide molecule, but instead adds to a free maleimide molecule so that an attached unit is obtained which does not contribute to the crosslink network. It is well known[6] that the hydrogen atoms on the acetate groups of polyvinyl acetate are labile, and these probably form the site for the hydrogen transfer. Similarly the chlorine atoms of polyvinyl chloride may be abstracted to give a proportion of dimaleimide crosslinks. The failure of *N*-phenylmaleimide to sensitize the crosslinking of polyvinyl acetate shows that when the sensitizing molecule does not contain a second ethylenic group, hydrogen transfer simply leads to attached additive molecules, and therefore crosslinking is not increased in a saturated system using a monomaleimide.

By comparison, the transfer mechanism does not operate with polyethylene and the initial improvement in the dose for gelation may arise following the consumption of the initial small amount of unsaturation in the polymer. For example, the *trans* vinylene has been shown to fall until a dose of 2 Mrad and then it rises again at the normal rate and the dimaleimides become ineffective. Presumably the vinylene unsaturation produced on irradiation is unable to react with maleimide. The proportion of

combined dimaleimide even at high doses is quite small (Fig. 3), and it can be seen that only approximately one quarter of the crosslinks contain dimaleimide.

Polyisobutylene, which normally degrades readily under the action of ionizing radiation, shows no tendency to crosslink in the presence of dimalemides. This result is not unexpected, as the repeating unit contains no unsaturation or labile atoms suitable for a transfer mechanism. Similar comments can be made for polydimethylsiloxane, which also fails to respond to the sensitizing action of maleimides.

The unsaturated rubbers behave in a manner which might be predicted from their structure with the exception of *cis*-1,4-polybutadiene, which is less reactive than the other polymers. The aromatic content of the SBR rubber, which might have been expected to make the rubber radiation-resistant, is probably compensated by the reactive pendant vinyl groups in the molecule resulting from the 1,2 polymerization of a proportion of the butadiene units. Polychloroprene is reactive even in the absence of dimaleimide due to the high radical yield of the chlorinated molecule.

A suggestion was made[1] that the varying reactivities of the dimaleimides in natural rubber could be due to the solubility in the rubber. *N*-Phenylmaleimide is certainly more reactive than the dimaleimides and also more soluble, but this cannot be the entire explanation, as a series of phenylmaleimides substituted in the benzene ring have been prepared, some of which are more soluble but less reactive than the parent compound. The reactivity must be determined by a combination of factors including the ability to dissolve and diffuse in the solid rubber, the reactivity of the —C=C— double bond in the maleimide, and the influence by the aromatic ring. The aliphatic monomaleimides are such poor accelerators and, furthermore, the position of substituent groups in the substituted phenyl maleimides has a pronounced effect on the reactivity of the double bond. *N*-Benzylmaleimide is also a very poor accelerator.

It is instructive to look at sheets of crepe rubber containing *N*-phenylmaleimide which have been irradiated with increasing doses of radiation. At 1–2 Mrads the sheets appear blotchy and contain areas of high and low concentrations of additive. At 3–4 Mrads the sheets are just cloudy, whereas at 5 Mrad, they become quite clear and transparent, showing that the additive has reacted completely.

A study of the mechanical properties of maleimide-cured gum rubbers and black-loaded rubbers is now being made, and has already shown that tensile strengths above 4000 psi can be obtained at doses of 5 Mrads with elongation at break of 500% and these appear to represent a considerable improvement on straight radiation cures, using higher doses.

The authors wish to thank Dr. R. Roberts for all his interest in this work, Mr. M. R. H. Hill for assistance with some of the experiments, Mr. P. Fydelor for infrared measurements, and the companies mentioned in the text for their generosity in supplying rubber samples.

References

1. Miller, S. M., R. Roberts, and R. L. Vale, *J. Polymer Sci.*, **58**, 737 (1962).
2. Dove, D., G. S. Murray, and R. Roberts, Unesco Int. Conf. on Radiation, UNESCO/NS/RIC/19.
3. Searle, N. E., U. S. Pats. 2,444,536 (1948), 2,462,835 (1949).
4. Flory, P. J. and J. Rehner, *J. Chem. Phys.*, **11**, 512 (1943).
5. Zimm, B. H., and I. Myerson, *J. Am. Chem. Soc.*, **68**, 911 (1946).
6. Bevington, J. C., G. M. Guzman, and H. W. Melville, *Proc. Roy. Soc.* (*London*,, **A221**, 437 (1954).

Résumé

On décrit l'influence de la *m*-phènylène-dimaléimide sur la vitesse de pontage du caoutchouc synthétique, le l'acétate de polyvinyle, du polyéthylène et d'autres polymères sous l'action de radiations ionisantes. Le facteur de diminution d'intensité pour des degrés de pontage équivalents, d'une part en présence de maléimide et d'autre part sans maléimide, varie de 10 à 25 pour le cas des caoutchoucs synthétiques. En plus, on a mis en évidence que les maléimides influencement par un mécanisme de transfert la vulcanisation de polymères insaturés, principalement lors d'une copolymérisation, et certains polymères saturés qui ont des atomes labiles.

Zusammenfassung

Der Einfluss von *m*-Phenylendimaleinimid auf die Vernetzungsgeschwindigkeit von synthetischem Kautschuk, Polyvinylacetat, Polyvinylchlorid, Polyäthylen und anderen Polymeren unter der Einwirkung ionisierender Strahlung wird beschrieben. Der Dosisreduktionsfaktor für äquivalenten Vernetzungsgrad mit und ohne Maleinimid variiert bei synthetischem Kautschuk von 10 bis 25. Es wird gezeigt, dass Maleinimide die Vulkanisation von ungesättigten Polymeren hauptsächlich durch Copolymerisation und von gewissen gesättigten Polymeren mit labilen Atomen durch einen Übertragungsmechanismus sensibilisieren.

Received March 13, 1962
Revised May 1, 1962

JOURNAL OF POLYMER SCIENCE: PART A VOL. 1, PP. 2551–2563 (1923)

The Influence of Transition Metal Salts in Polyglycol Autoxidations

W. G. LLOYD,* *Polymer Research Laboratory, The Dow Chemical Company, Midland, Michigan*

Synopsis

The addition of small amounts of transition metal salts, e.g., $CuCl_2$, to low molecular weight polyoxyalkylenediols results in pronounced autoxidation inhibition. This is in contrast with McGary's findings that this same class of salts accelerates the autoxidative degradation of high molecular weight polyethylene glycols. Inhibition of diethylene glycol is shown to relate to catalyzed hydroperoxide decomposition. With polyoxyethylenediol of molecular weight 600 this inhibition with $CuCl_2$ is less pronounced, and with both polyoxyethylene diols and polyoxypropylene diols the inhibitory effect gives way to a net accelerating effect with increasing polymer molecular weight. The inhibitory effect is insensitive to increasing medium polarity and to changes in oxygen pressure, but is markedly sensitive to terminal group capping. Combinations of appropriate metal salts and organic antioxidants produce synergistic stabilization. The results may be explained by postulating a competition between the normal radical-generating reactions of hydroperoxides with transition metal ions and the formation of specific terminal-hydroperoxide complexes which decompose heterolytically.

INTRODUCTION

In a recent paper McGary[1] has reported the autoxidative degradation of high-molecular weight polyethylene glycols to be markedly accelerated by certain transition metal salts, such as $CuCl_2$. On the other hand, we have observed that $CuCl_2$ and several other salts markedly inhibit the autoxidation of diethylene glycol and of several other low molecular weight polyglycols. Since the chemical behavior of polymers is frequently adduced by analogy with that of small molecules of similar chemical composition, it is of interest to account for the sharply contrary effects observed between congeners of different molecular weights.

EXPERIMENTAL

Diethylene glycol dimethyl ether was obtained from the Ansul Chemical Company, Marinette, Wisconsin. Other glycols, polyglycols, and derivatives are recent production samples from the Dow Chemical Company used without further purification except as otherwise noted. Other chemicals are reagent grade.

* Present address: The Lummus Co., Newark, N. J.

Autoxidations were carried out under 1 atm. oxygen and with 0.100% of 2,2′-azobis(2-methylpropionitrile) (azo initiator) initially present, except as otherwise noted. Oxygen uptake runs at pressures of 1 atm. and runs below this were made using a recording manometric apparatus.[2] Dynamic autoxidations were carried out with a glass percolator assembly.[3] A standard ASTM bomb assembly[4] was used for autoxidations at greater than atmospheric pressure, the assembly being immersed in a silicone fluid bath to permit greater flexibility of temperature. Total acids were determined by the modified[3] method of Smith, Mitchell, and Billmeyer.[5] Peroxide was determined by the arsenite method.[6] Formaldehyde and water were determined by standard methods.

RESULTS

Diethylene Glycol

A doubly redistilled sample of diethylene glycol (2,2′-oxybisethanol), spectroscopically pure, was placed in the manometric oxidation apparatus at 75° under 1 atm. oxygen and with 0.100% azo initiator, smoothly under-

TABLE I

Effect of Metal Salts upon Oxygen Consumption Rates of Diethylene Glycol[a]

Glycol[b]	Temp., °C.	Salt added	Salt concn., moles $l.^{-1}$	Oxidation rate, mmoles $l.^{-1}$ $hr.^{-1}$	
				With salt	Control (no salt)
I	75.0	NaCl	0.0085	16.3	16. (av.)
I	75.0	NaBr	0.0038	16.5	"
I	75.0	$NiCl_2$	0.0051	5.9	"
I	75.0	$FeCl_2$	0.0054	0.7	"
I	75.0	$FeCl_3$	0.0054	0.2	"
I	75.0	$CoCl_2$	0.0051	0.4	"
I	75.0	$MnCl_2$	0.0055	0.1	"
I	75.0	$CuCl_2$	0.0047	0.1	"
I	90.0	$CuCl_2$	0.0010	1.0[c]	40. (av.)
I	90.0	$AlCl_3$	0.0037	44.	"
II	75.0	$CuCl_2$	0.0043	0.014[d]	1.55[c]
III	75.0	$Cu(na)_2$[f]	0.0008	0.07	7.1
IV	75.0	$CuCl_2$	0.0047	0.04	13.6
V	75.0	$CuCl_2$	0.0047	~0.0	12.7

[a] Under 1 atm. oxygen, 24 hr. runs with 0.100% 2,2′-azobis(2-methylpropionitrile) added, except as noted otherwise.

[b] Glycol samples are as follows: I—commercial production, II—same as above but without azo initiator added, III—center-cut of sample twice redistilled under prepurified nitrogen, IV—center-cut of anion-exchanged glycol, V—center-cut of cation-exchanged glycol.

[c] Steady-state rate after first three hours' oxidation.

[d] Average rate in 87.9-hr. run.

[e] Average rate in 55.5-hr. run.

[f] Copper naphthenate.

went autoxidation at a steady rate of 7.1×10^{-3} moles $l.^{-1}$ $hr.^{-1}$ A parallel autoxidation under conditions identical except for the addition of a trace amount of copper naphthenate (to give 0.0050% Cu) yielded an autoxidation rate of 7×10^{-5} moles $l.^{-1}$ $hr.^{-1}$. This inhibitory effect is consistently reproducible, and is observed also with the chlorides of copper, iron, cobalt, and manganese (Table I). Since the free autoxidation of this glycol under these conditions has been found to be independent of initiator concentration in the range 0.02–0.5%, and essentially independent of oxygen diffusion effects,[3] this constitutes a genuine inhibitory effect.

Chloride or nitrate salts of most other common metals exert no significant effect upon autoxidation rate under these conditions. Inactive cations, in

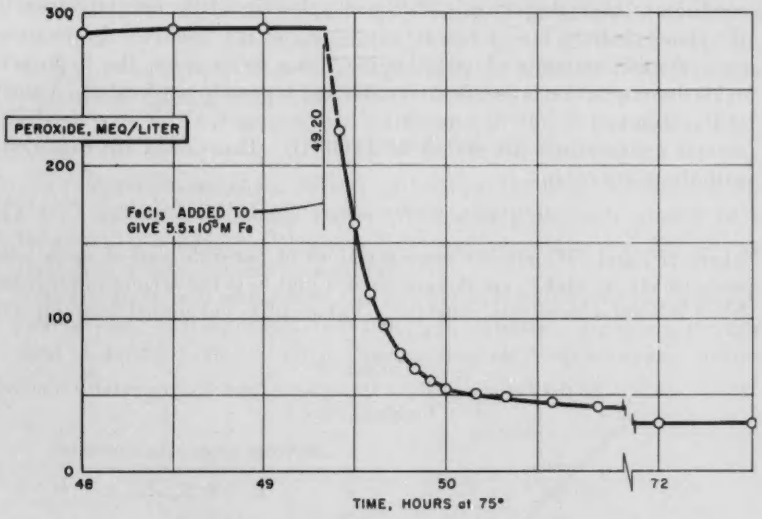

Fig. 1. Effect of Fe upon peroxide level of autoxidizing diethylene glycol.

addition to those shown in Table I, include K(I), Ag(I), Hg(I), Hg(II), Zn(II), Sn(II), Sn(IV), Cr(III), and Sb(III).

This inhibitory effect is also sharply influenced by the anionic portion of the salt. Bromides, iodides, nitrates, and perchlorates of the "active" metals are effective inhibitors, while such salts as $FeSO_4$ (cf. ref. 1), $Fe_2(SO_4)_3$, $Fe(NH_4)_2(SO_4)_2$, and ferric benzoate are completely inactive.

Going autoxidations of diethylene glycol are abruptly arrested by the addition of active metal salts. Redistilled diethylene glycol was subjected to autoxidation at 75° with 6.1×10^{-3} *M* azo initiator, and immediately attained a steady oxygen uptake rate of 12.3 mmoles $l.^{-1}$ $hr.^{-1}$ (stand. dev. ±0.13). After three hours of oxidation, a small volume of fresh glycol containing predissolved $FeCl_3$ was added to the system, to afford an overall concentration of 2.0×10^{-3} *M* Fe. The oxygen uptake curve im-

mediately flattened, with the post-addition oxidation rate for the following 20 hrs. at 0.19 mmoles $l.^{-1}$ $hr.^{-1}$ (stand. dev. ± 0.018).

A parallel autoxidation was carried out using a dynamic apparatus which facilitated periodic sampling.[3] After a steady-state peroxide level of about 290 meq. $l.^{-1}$ was attained, $FeCl_3$, predissolved in a small volume of glycol, was added to afford a concentration of 5.5×10^{-5} M Fe. The effect of this addition is shown in Figure 1. The peroxide concentration dropped rapidly and smoothly to a new steady-state level of about 32 meq. $l.^{-1}$. Further additions of $FeCl_3$ depressed the steady-state peroxide level to still lower concentrations.

The peroxide formed in diethylene glycol autoxidation is the α-hydroperoxide, $HOCH_2CH_2OCH(OOH)CH_2OH$ (I).[5] Under static nonoxidizing conditions, this hydroperoxide undergoes a slow first-order decomposition in the glycol medium, $k_1 = 4.8 \times 10^7 \exp(-18{,}700/RT)$ $sec.^{-1}$.[3] In the presence of small amounts of oxidation-inhibiting metal salts, the hydroperoxide decomposition is pseudo-first order and is greatly accelerated. Values of the observed overall decomposition rate constant, k', for several salts at several temperatures are shown in Table II. These data are consistent with the relationship

$$-d(P)/dt = k'(P) = k_1(P) + k_2(M)(P) \qquad (1)$$

where (P) and (M) are the concentrations of peroxide and of metal salt respectively, k' and k_1 are defined above, and k_2 is the second-order catalyzed decomposition rate constant. Values of k_2 calculated from eq. (1)

TABLE II
Rate Constants for the Decomposition of Diethylene Glycol Hydroperoxide Catalyzed by Metal Salts

Salt	Concn., mmoles $l.^{-1}$	T, °C.	Peroxide decay rate constants[a] k'	k_1	k_2
$FeCl_3$	0.227	0.	0.234	0.000053	1.0_3
"	0.250	27.	1.301	0.0012	5.2_5
"	0.0989	27.	0.516	0.0012	5.2_0
"	0.0367	27.	0.188	0.0012	5.0_6
"	0.0171	50.	0.170	0.011	9.2_5
"	0.198	75.	2.68_9	0.089	$13._1$
"	0.110_5	75.	1.445	0.089	$12._3$
$CuCl_2$	0.550	35.	0.0556	0.0022	0.097
"	0.550	55.	0.600	0.016	1.06
"	0.550	75.	2.94_8	0.089	5.2_0
"	0.550	94.	18.1_0	0.40	$32._2$
$CoCl_2$	0.137	75.	0.290	0.089	1.47
$MnCl_2$	0.473	75.	0.186	0.089	0.20
$ZnCl_2$	1.03	75.	0.104	0.089	0.01 (nil?)
$SnCl_4$	0.222	75.	0.09_4	0.089	0.02 (nil?)
$Fe_2(SO_4)_3$	0.095	75.	0.090	0.089	nil

[a] Rate constants in eq. (1); k' and k_1 in $sec.^{-1} \times 10^3$; k_2 in l. $mole^{-1}$ $sec.^{-1}$; k_1 values calculated from data of reference 3.

are listed in Table II. Those salts found to be effective inhibitors (Table I) are also effective peroxide decomposition catalysts. Several noninhibiting salts show no catalytic activity. The $FeCl_3$-catalyzed decomposition does not follow an Arrhenius relationship. The copper chloride catalyzed decomposition does, however, showing an apparent activation energy of 21.7 (±0.9) kcal. and a pre-exponential factor of 2.5×10^{14} l. mole^{-1} sec.$^{-1}$ This catalytic enhancement unexpectedly appears to be entirely contained within the frequency factor.

The catalyzed decomposition of the hydroperoxide I leads to the formation of HCHO (1 equiv.) and water (apparent yield is 1.9 equiv., stand. dev. ±0.19), with no increase in free acids. In the acidic environment of the autoxidized glycol, formaldehyde readily converts to the formal,[7,8] accounting for one of the equivalents of water. The catalyzed decomposition thus produces one equivalent of formaldehyde and about one equivalent of water, and appears to correlate with the inhibitory effects of these salts in autoxidizing diethylene glycol.

Polyglycol E-600

To illuminate the sharp differences between the above results and McGary's findings[1] with high polyoxyethylenediols, the autoxidation of an intermediate congener, Polyglycol E-600 (polyoxyethylenediol of average molecular weight 600) has been examined.

In the absence of metal salts, this polyglycol readily undergoes autoxidation at 70.6° in the presence of 0.100% azo initiator. Its rate is independent of diffusion effects,[2] but is directly dependent upon oxygen pressure

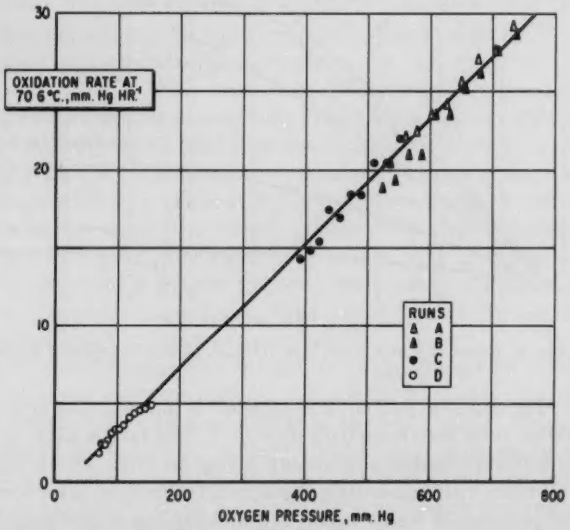

Fig. 2. Effect of oxygen pressure upon autoxidation rate of Polyglycol E-600.

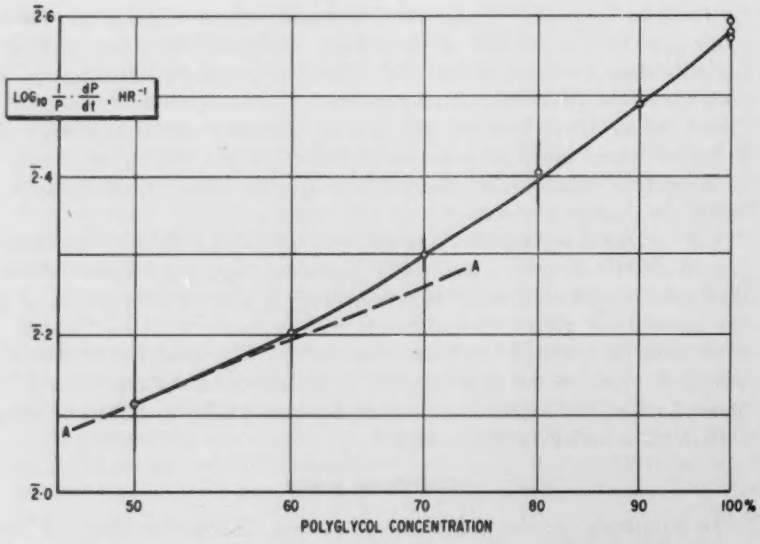

Fig. 3. Effect of water dilution upon autoxidation rate of Polyglycol E-600.

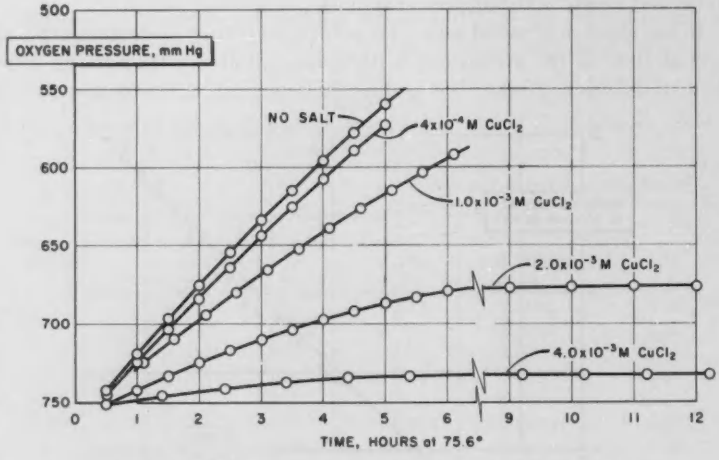

Fig. 4. Effect of $CuCl_2$ upon autoxidation rate of Polyglycol E-600.

(Fig. 2). Its rate like that of the diglycol[3] is independent of azo initiator concentration over the range 0.03–1.00%. (The rate is slightly depressed at higher initiator loadings, probably owing to cross termination.) The effect of dilution with water upon the autoxidation rate, after correcting for the partial pressure of water vapor, is nonlinear but rather moderate. The relationship between rate per oxygen pressure unit and concentration of

polyglycol in polyglycol-water systems is shown in Figure 3. At higher dilutions the slope of the log-log plot approaches unity (dashed line A—A), indicating first-order dependence of rate upon polyglycol concentration. The curvature in the 0–40% water range in Figure 3 may be entirely due to the depression of the dissolved oxygen concentration associated with the addition of water to the polyglycol. The peroxide level in Polyglycol E-600 autoxidizing at 70.6° quickly achieves a low steady-state concentration. Thus, like diethylene glycol, this polyglycol in the absence of inhibitors readily undergoes autoxidation by a short-KCL branching mechanism, the overall rate being proportional to oxygen pressure and (approximately) to polyglycol concentration.

The effect of addition of $CuCl_2$ to azo-initiated Polyglycol E-600 is shown in Figure 4. The autoxidation rate is appreciably retarded by 10^{-3} *M* $CuCl_2$, and is strongly inhibited by 4×10^{-3} *M* $CuCl_2$. This inhibition is, however, considerably less pronounced at lower salt concentrations than that observed with diethylene glycol (Table I).

Diagnostic Experiments

The usual role of a transition metal compound in autoxidations is that of an accelerator. The generally accepted mechanism of this acceleration is that of homolytic decomposition of the substrate hydroperoxide:[9-12]

$$ROOH + M^{n+} \rightarrow RO\cdot + HO^- + M^{(n+1)+} \quad (1)$$

$$ROOH + M^{(n+1)+} \rightarrow ROO\cdot + H^+ + M^{n+} \quad (2)$$

There is no reason to believe that reactions of this type do not occur in these autoxidations. Thus, for example, a qualitative test shows that the $FeCl_3$-catalyzed decomposition of diethylene glycol hydroperoxide at 26° initiates polymerization of acrylonitrile. However, for the case of these low molecular weight polyglycols, these homolytic reactions—which dominate in most other systems, including high molecular weight polyglycols—are overridden by some other inhibiting reaction(s). Three types of mechanism for this inhibitory effect may be considered: a general acid heterolysis of the hydroperoxides by these acidic salts, enhanced by the more highly polar media of low molecular weight polyglycols; chain-stopping of the carrier radicals by metal ions capable of readily undergoing one electron valence changes; and a specific hydroperoxide metal ion complex which decomposes to nonradical products. The following experiments were carried out to distinguish among these possibilities.

A series of autoxidations was carried out with Polyglycol E-600 water mixtures, all conditions being identical with those of the runs shown in Figure 3 except for the addition of 1.00×10^{-3} *M* $CuCl_2$. The ranges of rates are shown in Figure 5. Dilution with water appears to exert no unique effect upon the system Polyglycol E-600 $CuCl_2$ oxygen. This, together with the failure of such salts as $AlCl_3$ to inhibit diethylene glycol autoxidation (Table I), indicates that the concept of a general acid-cata-

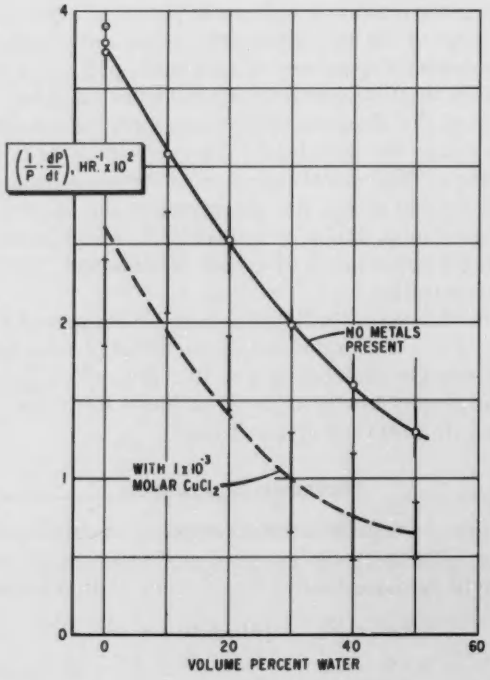

Fig. 5. Effect of dilution upon autoxidation rate of Polyglycol E-600.

lyzed hydroperoxide decay controlled by medium polarity, notwithstanding its applicability to some other systems,[13,14] does not explain the behavior of these systems.

The effect of polyglycol molecular weight upon the modification of autoxidation rate by several salts is summarized in Table III. The dominance of the inhibitory process is lost as the chain length of the polyoxyethylenediol increases. The same general pattern obtains with polyoxypropylenediols run under the same conditions. Thus, cobalt naphthenate (1×10^{-3} *M*) inhibits di-, tri-, and tetraoxypropylenediol, mildly retards Polyglycol P-400, and accelerates the autoxidation of Polyglycol P-750. Copper naphthenate inhibits Polyglycols P-250 and P-400, and with decreasing efficacy retards the higher homologs, Polyglycols P-750 and P-1200.

The effect of modification of terminal groups was investigated by comparing the rates of autoxidations of diethylene glycol, its monomethyl ether, and its dimethyl ether, with and without metal salts present. The results are summarized in Table IV. These data, like those of Table III, are subject to diffusion effects in the cases of oxidation acceleration. It is clear, however, that both salts inhibit the diol, that the copper salt inhibits 2-(2-methoxyethoxy)ethanol, and that both the iron and copper salts accelerate

TABLE III
Relative Rates of Oxidation of Polyoxyethylenediols[a]

Polyglycol	n[b]	Rate (with 10^{-3} M MCl_2)/Rate (with no salt)		
		M = Cu	M = Fe	M = Co
Diethylene	2	<0.004	0.007	0.012
Triethylene	3	<0.004[c]	0.5	1.1
E-200	4.1	<0.004[c]	1.2	—
E-400	8.7	0.5	—	—
E-600	13.	0.7	—	—

[a] At 75.6°, 1 atm. oxygen, 0.100% azo initiator.
[b] Average number of oxyethylene groups per molecule.
[c] Steady-state rate after initially faster autoxidation.

TABLE IV
Autoxidations of Diethylene Glycol Methyl Ethers[a]

Compound	Metal salt 1×10^{-3} M	Time for consumption of 0.1 mole oxygen per liter of substrate
CH_2CH_2OH / O / CH_2CH_2OH	nil	24. hr.
	$FeCl_3$	>100. "
	$CuCl_2$	>100. "
$CH_2CH_2OCH_3$ / O / CH_2CH_2OH	nil	4.5 "
	$FeCl_3$	6.1 "
	$CuCl_2$	> 24. "
$CH_2CH_2OCH_3$ / O / $CH_2CH_2OCH_3$	nil	2.7 "
	$FeCl_3$	2.2 "
	$CuCl_2$	1.8 "

[a] At 75.0°, 1 atm. oxygen, with 0.100% azo initiator.

the autoxidation of 2,2′-dimethoxydiethyl ether. One possible inference is that the crucial difference between low- and high-molecular weight polyglycols lies in the concentrations of terminal hydroxy groups.

Oxygen pressure has been shown to affect profoundly the overall rates of oxidation of polyglycols (Fig. 2, refs. 2, 3). If the effective metal ions inhibit primarily by stopping alkyl, alkoxy, or alkylperoxy radicals, variations in oxygen pressure might be expected to alter profoundly the effects of these metal ions. A series of initiated autoxidations with Polyglycol E-1450 (polyoxyethylenediol, average molecular weight 1450) at 75.6°, with and without 10^{-3} M $CoCl_2$, showed consistent mild acceleration by the salt at 0.2, 1.0, and 8.6 atm. oxygen. Similarly, increasing the oxygen pressure in the strongly inhibited diethylene glycol-$CuCl_2$ system to 8.6 atm. failed to alter perceptibly the powerful inhibition imparted by the $CuCl_2$. These tests, while not conclusive, fail to demonstrate the effects which might reasonably be expected if the mechanism were that of radical capture or radical deactivation by metal ion complexing.

A final series of autoxidations was carried out with Polyglycol 15–200 (a copolymer of ethylene and propylene oxides[15] of molecular weight about

2600), which has been the subject of a previous inhibition study.[2] At 126.1° under 1 atm. oxygen, this polyglycol readily undergoes autoxidation without initiation, and is not effectively inhibited by metal salts, though it is readily inhibited by suitable radical-trap antioxidants.[2] The effects of several combinations of metal salts with organic antioxidants are shown in Table V. The evidence of marked synergistic stabilization is to be expected from mixtures of peroxide decomposers and radical-traps[16–18] but would be hard to account for if the two additives were both operating by the same mechanism.

TABLE V
Synergistic Stabilization of Polyglycol 15-200[a]

Additive combination	Concentrations, Molar × 10^3		Induction period, hrs.
	Salt	Antioxidant	
$CuCl_2$ and Hydroquinone	nil	4.0	0.7
	0.5	2.0	31.
	1.0	nil	0.15
$CuCl_2$ and Phenyl 2-naphthylamine	nil	5.8	1.3
	0.5	2.9	62.
	1.0	nil	0.15
$CuCl_2$ and Phenothiazine	nil	0.62	1.5
	0.5	0.31	15.4
	1.0	nil	0.15
$MnCl_2$ and 2,6-Di-*tert*-butyl-4-methylphenol	nil	9.1	5.4
	2.0	4.55	10.7
	4.0	nil	0.1

[a] At 126.1°, 1 atm. oxygen, no initiator added.

DISCUSSION

Reducible salts such as $CuCl_2$ and $FeCl_3$ may terminate hydrocarbon radicals, i.e.,[9,18–21]

$$—R\cdot + M^nX_n \rightarrow —RX + M^{n-1}X_{n-1} \quad (8)$$

and there is at least a plausible circumstantial case for proposing similar termination or complex-deactivation reactions involving alkoxy and alkylperoxy radicals.[15,22–25] In the systems studied here, however, such mechanisms fail to account for the coincidental peroxide decomposition catalysis and for the effects of polyglycol chain length and of terminal group modifications and, most importantly, they are not consistent with the clear evidence of synergism with mixtures of effective metal salts and phenolic antioxidants. Radical termination by metal ions may occur in these systems, but its postulated occurrence is neither sufficient nor necessary to account for the experimental data.

Glycols are known to form coordination complexes with transition metal salts.[26,27] The strength of such complexes in bulk glycol media is indicated by the observed stoichiometry of the Cu(II)—ethylenediamine complex in diethylene glycol at room temperature, using Job's method[28] of continuous variation. EDA, which normally complexes to form the highly stable $Cu(EDA)_2^{++}$ species,[29,30] forms a well-defined 1:1 complex with $CuCl_2$ in this medium. Furthermore, there is a growing body of evidence that metal ion-hydroperoxide interactions, even where the metal ion is a pro-oxidant, involve the formation of an actual complex.[9,18,31-34]

In the light of the foregoing, the pattern of behavior of metal salts with polyglycols under oxidizing conditions may be interpreted in terms of specific complex formation. In polyglycol autoxidations the insensitivity to initiator concentrations, the rapid attainment of steady-state rates, the evident relationship between peroxide level (at a given temperature) and autoxidation rate, and the very sharp dependencies of induction periods upon antioxidant concentrations[2] all imply an overall kinetic pattern characterized by relatively slow propagation and strong kinetic chain branching. If it may be assumed that the driving force in these autoxidations is peroxide homolysis, then the present results may be explained by further assuming the facile formation of a chelate involving the metal ion and an α-hydroperoxide, a complex which would be strongly favored when this structure is adjacent to a terminal hydroxyl group. A complex with the function R—CH_2—O—CH(OOH)—CH_2—OH, for example, would serve to position the hydroxyl and hydroperoxide groups so as to facilitate heterolysis, e.g.:

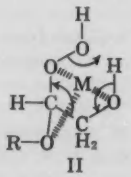

II

This interpretation is also consistent with the Cu(II)-catalyzed peroxide decomposition data (Table II), calculations from which indicate the catalytic enhancement to be contained within the pre-exponential factor. The discontinuity of inhibition with 10^{-3} M $CuCl_2$ between Polyglycols E-200 and E-400 (Table III) may also be explained, for these branching systems, within this framework. If f is the fraction of hydroperoxide decomposition that is homolytic, then an initial peroxide concentration, P, ultimately permits an amount of autoxidation equal to $P[2f\nu + (2f\nu)^2 + (2f\nu)^3 + \ldots]$, where ν is the average kinetic chain length. If $f\nu < 0.5$ this sum is finite and at steady-state a very low (inhibited) oxidation rate obtains. But as f increases to the point that $f\nu > 0.5$, this sum becomes infinite, and an overall rate of the order of (or greater than) that of the metal-free autoxidation is obtained. Semenov has analyzed similarly sharp transforma-

tions arising from slight changes in the relative contributions of branching and termination processes.[35]

If this argument is correct, then the competition between formation of terminal-group-involved complexes such as (II) and the "normal" metal ion-hydroperoxide homolytic reactions is statistically controlled by polyglycol chain length: lower polymers have more end groups and are liable to be inhibited by these transition metal salts, while high polymers have insignificant end-group concentrations and are always accelerated by the same salts.

The writer acknowledges with thanks the valuable assistance of Dr. M. C. Musolf, and of Mssrs. D. F. Wisniewski and R. G. Zimmerman, in obtaining much of the data.

References

1. McGary, C. W., Jr., *J. Polymer Sci.*, **46**, 51 (1960).
2. Lloyd, W. G., *J. Chem. Eng. Data*, **6**, 541 (1961).
3. Lloyd, W. G., *J. Am. Chem. Soc.*, **78**, 72 (1956).
4. ASTM Test D525-55, American Society for Testing Materials, *Standards*, Vol. VII, 1961, p. 266.
5. Smith, D. M., J. Mitchell, Jr., and A. M. Billmeyer, *Anal. Chem.*, **24**, 1847 (1952).
6. Siggia, S., *Quantitative Organic Analysis Via Functional Groups*, Wiley, New York, 1949, pp. 102 ff.
7. Noller, C. R., *Chemistry of Organic Compounds*, 2nd ed., Saunders, Philadelphia, 1957, pp. 203–4.
8. Mitchell, J., Jr., and D. M. Smith, *Aquametry*, Interscience, New York, 1948, pp. 120, 332.
9. Bawn, C. E. H., A. A. Pennington, and C. F. H. Tipper, *Discussions Faraday Soc.*, **10**, 282 (1951).
10. Bawn, C. E. H., *J. Oil Colour Chemists' Assoc.*, **36**, 443 (1953).
11. Kharasch, M. S., P. Pauson, and W. Nudenberg, *J. Org. Chem.*, **18**, 322 (1953).
12. Bateman, L., *Quart. Rev.*, **8**, 147 (1954).
13. Frank, C. E., *Chem. Rev.*, **46**, 155 (1950).
14. Kharasch, M. S., A. Fono, and W. Nudenberg, *J. Org. Chem.*, **16**, 113 (1951).
15. Horsley, L. H., and E. C. Britton, U. S. Patent 2,733,272 (January 1956), Dow Chemical Co.
16. Kennerly, G. W., and W. L. Patterson, Jr., *Ind. Eng. Chem.*, **48**, 1917 (1956).
17. Ingold, K. U., and I. E. Puddington, *ibid.*, **51**, 1319 (1959).
18. Ingold, K. U., *Chem. Rev.*, **61**, 563 (1961).
19. Kharasch, M. S., and A. Fono, *J. Org. Chem.*, **23**, 325 (1958); **24**, 606 (1959).
20. Bamford, C. H., A. D. Jenkins, and R. Johnston, *J. Polymer Sci.*, **29**, 355 (1958).
21. Hammond, G. S., and U. S. Nandi, *Effects of Ferric Chloride upon the Kinetics of Hydrocarbon Oxidation*, 137th Meeting, Am. Chem. Soc., April, 1960, *Abstracts*, 37R.
22. Kharasch, M. S., A. Fono, W. Nudenberg, and B. Bischof, *J. Org. Chem.*, **17**, 207 (1952).
23. Denisov, E. T., *Zh. Fiz. Khim.*, **32**, 1269 (1958); *Chem. Abs.*, **53**, 1904d (1959).
24. Kharasch, M. S., and A. Fono, *J. Org. Chem.*, **24**, 72 (1959).
25. Lawesson, S.-O., and C. Berglund, *Tetrahedron Letters*, No. 2, 4 (1960).
26. Grun, A., and E. Boedecker, *Ber.*, **43**, 1051 (1910).
27. Miyake, A., *Bull. Chem. Soc. (Japan)*, **32**, 1381 (1959).
28. Job, P., *Ann. Chim. (Paris) (10)*, **9**, 113 (1928).
29. Moeller, T., *Inorganic Chemistry*, Wiley, New York, 1952, p. 842.

30. Emeleus, H. J., and J. S. Anderson, Modern Aspects of Inorganic Chemistry, 3rd ed., Van Nostrand, New York, 1960, p. 234.
31. Freidin, B. G., *Zh. Prik. Khim.*, **30**, 768 (1957).
32. Chalk, A. J., and J. F. Smith, *Trans. Faraday Soc.*, **53**, 1214, 1235 (1957).
33. Kremer, M. L., *Nature*, **184**, 720 (1959).
34. Benson, D., and L. H. Sutcliffe, *Trans. Faraday Soc.*, **55**, 2107 (1959).
35. Semenov, N. N., *Chemical Kinetics and Chain Reactions*, Oxford University Press, London, 1935, pp. 45 ff.; *Some Problems in Chemical Kinetics and Reactivity*, Vol. II, Princeton University Press, Princeton, New Jersey, 1959, pp. 113 ff.

Résumé

L'addition de faibles quantités de sels de métaux de transition, p.ex. $CuCl_2$ à des polyoxyalkylènediols de bas poids moléculaire a comme effet une inhibition prononcée de l'autooxydation. Ceci fait contraste avec les découvertes de McGary suivant lesquelles la même classe de sels accélère la dégradation autooxydative de polyéthylène-glycols de haut poids moléculaire. On montre que l'inhibition due au diéthylène-glycol est liée à la décomposition catalytique d'hydroperoxydes. Avec du polyoxyéthylènediol de poids moléculaire 600 cette inhibition par $CuCl_2$ est moins prononcée, et avec le polyoxyéthylènediol et le polyoxypropyléne-diol, l'effet inhibiteur donne lieu à un net effet accélérateur avec une augmentation du poids moléculaire du polymère. Cet effet inhibiteur est insensible à une augmentation de la polarité du milieu et à des variations de la pression d'oxygène, mais il est forte sensible à l'égard des groupes terminaux. Des combinaisons de sels de métaux appropriés et d'antioxydants organiques produisent une stabilisation synergique. Les résultats peuvent être expliqués en postulant une compétition entre le réactions des hydroperoxydes qui fournissent un radical normal avec les ions de métaux transition et la formation de complexes spécifiques d'hydroperoxydes terminaux qui se décomposent de façon hétérolytique.

Zusammenfassung

Der Zusatz kleiner Mengen von Übergangsmetallsalzen, z.B. $CuCl_2$, zu niedermolekularen Polyoxyalkylendiolen führt zu einer ausgeprägten Verhinderung der Autoxydation. Das steht in Widerspruch zu dem Befund von McGary, dass die gleiche Klasse von Salzen den autoxydativen Abbau von hochmolekularen Polyäthylenglykolen beschleunigt. Die Inhibierung beim Diäthylenglykol zeigt eine Beziehung zur katalytischen Hydroperoxydzersetzung. Bei einem Polyoxyäthylendiol vom Molekulargewicht 600 ist die Inhibierung durch $CuCl_2$ weniger ausgeprägt und bei beiden, Polyoxyäthylenediolen und Polyoxypropylenediolen, fürht der Inhibierungseffekt schliesslich zu einer Beschleunigung mit steigendem Molekulargewicht des Polymeren. Der Inhibierungseffekt ist gegen eine Zunahme der Polarität des Mediums und gegen Änderungen im Sauerstoffdruck unempfindlich, zeigt aber merkliche Empfindlichkeit gegen eine Abdeckung der Endgruppe. Kombination geeigneter Metallsalze mit organischen Antioxydantien liefert synergistische Stabilisierung. Die Ergebnisse können durch die Annahme einer zur normalen Radikalbildungsreaktion zwischen Hydroperoxyden und Übergangsmetallionen kompetitiven, spezifischen Bildung von Komplexen mit endständigem Hydroperoxyd, die sich heterolytisch zersetzen, erklärt werden.

Received April 19, 1962

JOURNAL OF POLYMER SCIENCE: PART A VOL. 1, PP. 2565–2586 (1963)

Heterogeneous Membranes: Diffusion in Filled Rubber

R. M. BARRER, J. A. BARRIE, and M. G. ROGERS, *Physical Chemistry Laboratories, Chemistry Department, Imperial College, London, England*

Synopsis

The diffusion and solution of propane and of benzene has been studied over a range of temperatures in a series of heterogeneous membranes of natural rubber and zinc oxide filler. The volumes of filler were 0, 5, 10, 20, 30, and 40%. Evidence was obtained of the interaction between rubber and filler, and that some of the membranes involved three phases: polymer, filler, and open gaps between filler particles. No rigorous treatment of diffusion in heterogeneous media exists, but the model of two interdispersed phases was developed and discussed in relation to permeation rates and diffusion coefficients. Differences between steady state and time-lag diffusion coefficients were ascribed to different structure factors in steady and transient states of flow. Concentration dependences of the interdiffusion and intrinsic diffusion coefficients of benzene were measured. The influence of concentration dependence, filler, and structure factor was combined in one relationship relating the intrinsic diffusion coefficient in the filler rubber with that for diffusion in unfilled rubber, containing the same volume fraction of benzene. The resultant expression appears able to account qualitatively for some of the observed complex diffusion behavior.

INTRODUCTION

Barrer and Fergusson[1] observed that for the diffusion of benzene vapor at 50°C. in natural rubber and in partly crystalline polythene, the transient state diffusion coefficient was significantly less than that for the corresponding steady state of flow. This behavior might be expected with polymers below or just above their glass transition temperature, where the differences could arise from the presence of slow relaxation phenomena affecting the diffusion process. However, for a polymer well above its glass transition, such as natural rubber at 50°C., relaxation effects of this nature are not expected to be significant. Accordingly, alternative explanations for the diffusion behavior have been considered as, for example, a geometrical factor arising from the design of the diffusion cell.[2] It was concluded that the geometrical factor was not responsible for the observed differences in the diffusion coefficients.

The rubber investigated by Barrer and Fergusson contained a small amount of zinc oxide filler and also some protein and other impurities. In this paper the role of such filler particles in the diffusion process is investigated, particularly as regards any difference in transient and steady state

behavior which it may induce in the membrane. This work is complementary to a study conducted with filled silicone rubber[3] and serves to elucidate further the role of the filler particles in the solution and diffusion process.

Experimental

Samples

Natural rubber sheets, vulcanized by heating with 3% dicumyl peroxide for 45 min. at 140°C. and containing 0, 10, 20, 30, and 40 vol.-% of ZnO, were obtained from the Rubber and Plastics Research Association. An additional sample similar to that of Barrer and Fergusson was also supplied, the composition of which, in parts by weight, was smoked sheet 100, A32 accelerator 0.5, stearic acid 0.5, zinc oxide 3, sulfur 4. All samples prior to use were refluxed with acetone in a darkened Soxhlet apparatus for several hours and then thoroughly outgassed under high vacuum. Membrane thickness (~0.7 mm.) was determined for each sample from the mean of several readings taken with a micrometer screw gage. Research Grade samples of benzene and propane were supplied in sealed glass containers by the Chemical Research Laboratory, Teddington, and required no further purification.

Apparatus

The permeation and solubility apparatus was similar to that of a previous investigation.[2] With benzene as penetrant, both the ingoing and outgoing side of the permeation apparatus had to be modified. A constant ingoing pressure was maintained by thermostatting a few cubic centimeters of liquid benzene at the required temperature, and the vapor pressure obtained from Smith's equation.[4] To prevent condensation of the vapor, the glass tubing connecting the benzene reservoir to the diffusion cell was wound with electrically heated Nichrome wire. The closed capillary of the McLeod gage used to register the pressure on the outgoing side of the apparatus was also heated to prevent condensation and in addition to minimize departure from ideal-gas behavior. This was effected by placing around the capillary a Pyrex glass tube with a graded winding of Nichrome wire. The temperature was recorded on a thermometer placed inside the tube and was maintained around 100°C. The temperature gradient along the tube was less than 2%. To minimize temperature fluctuations the bulb of the gage was wound with asbestos cord and for high rates of flow it was also necessary to heat a small region at the top of the bulb with Nichrome wire, again to prevent condenstion of the benzene.

Solubility: Results and Discussion

Propane

Sorption isotherms were determined for the filled and unfilled rubbers at 40°C. and were linear over the pressure range investigated. The

Henry's law solubility coefficients σ (cm.^{3} at standard temperature and pressure (s.t.p.) per cm.^{3} of membrane per cm. Hg), obtained from the slopes of the isotherms are given in Table I.

TABLE I
Henry's Law Solubility Coefficients for Propane at 40°C.

ZnO, vol.-%	σ	ZnO, vol.-%	σ
0	0.0495	20	0.0430
5	0.0482	30	0.0422
10	0.0450	40	0.0415

Benzene

Figure 1 shows the benzene sorption isotherms for the different rubbers at 40°C. Henry's law solubility coefficients were estimated from the linear low pressure regions of the isotherms and are presented in Table II along with some values obtained in a similar manner at 30 and 50°C.

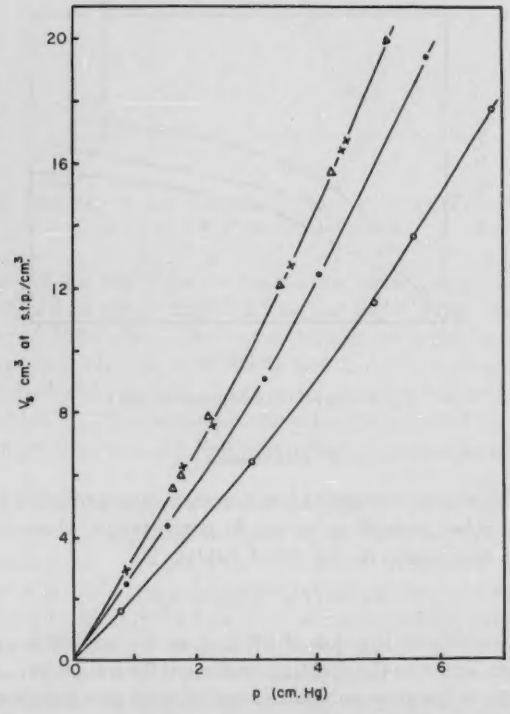

Fig. 1. Benzene sorption isotherms for filled rubbers at 40°C.: (×) unfilled rubber, (●) 10% ZnO, (△) sulfur cured, and (○) 40% ZnO.

TABLE II
Henry's Law Solubility Coefficients for Benzene

T, °C.	0% ZnO	10% ZnO	40% ZnO	Sulfur cured
30	5.00	4.15	—	4.72
40	3.22	2.83	2.00	3.26
50	2.32	1.95	—	2.27

ZnO Filler

The sorption isotherms for the hydrocarbons on the bulk filler were also determined. At 40°C. a Henry's law sorption coefficient of 0.0305 (cm.^{3} at s.t.p./cm.^{3} of filler per cm. Hg) was obtained for propane. Corresponding isotherms for benzene at 30, 40, and 50°C. were decidedly nonlinear and are shown in Figure 2. The BET surface area of the powder as calculated from a nitrogen sorption isotherm at liquid oxygen temperatures was 1.4 m.^{2}/g. This is a relatively small surface and is indicative of nonporous particles. Electron micrographs of the free powder showed that the particles were rodlike in shape.

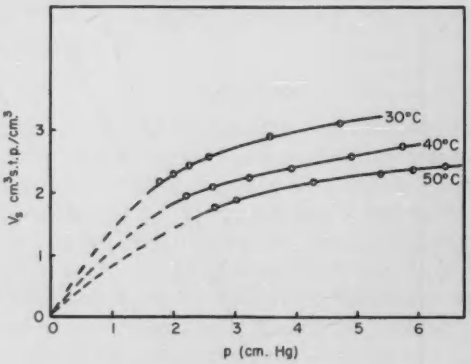

Fig. 2. Sorption of benzene on ZnO.

Discussion

If filled rubber to a first approximation may be regarded as composed of two phases, rubber and filler, which do not interact, then the solubility coefficient of the vapor in the filled rubber is[3]

$$\sigma = (1 - \lambda_f)\sigma_r + \lambda_f\sigma_f \qquad (1)$$

where λ_f is the volume fraction of filler, σ_r is the solubility coefficient for unfilled rubber, and σ_f is the sorption coefficient for bulk filler.

In Figure 3 the propane solubilities are plotted as a function of the volume fraction of zinc oxide. Also shown are the theoretical curves calculated from eq. (1) with $\sigma_r = 0.0495$ and $\sigma_f = 0$ and 0.0305, respectively.

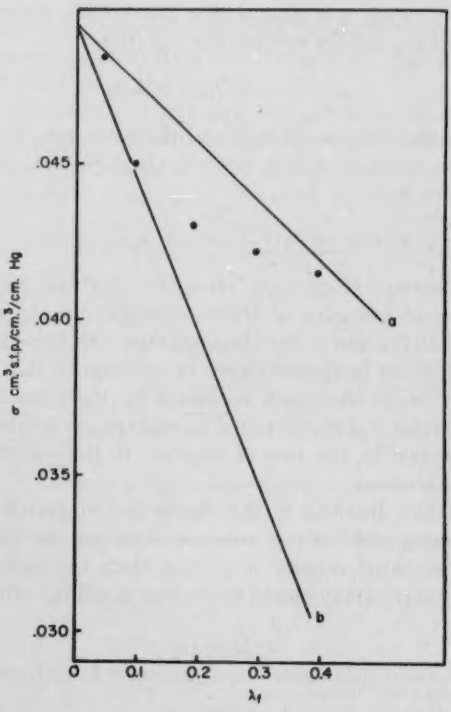

Fig. 3. Propane solubility vs. λ_f. Curve *a*, eq. (1); $\sigma_f = 0.0305$; curve *b*, eq. (1); $\sigma_f = 0$. (●) Experimental points.

At the higher volume fractions the results are more closely represented by curve *a* calculated on the assumption that the gas is sorbed independently by the rubber and the filler. Such a model is an oversimplification and in general the polymer may be expected to wet the filler surface and so compete with the gas for the surface. As a result the sorption coefficient for the filler in the rubber may be considerably less than its value for the free powder. This would lead to a straight line plot lying between curves *a* and *b* of Figure 3.

The falling off in the rate of decrease of solubility with filler content can be explained by a proportional increase in the filler surface available for sorption of penetrant. As the filler content of the rubber is increased, uniform dispersion of the individual filler particles is rendered more difficult, and at higher filler contents the formation of some particle conglomerates is likely. As a result gaps are created between some of the particles and the effect of these on the solution process will be twofold. First, gas may occupy the void volume so created and second, since the filler surface in the conglomerates will not be completely wetted by polymer, a proportionally larger fraction of the conglomerates is available for gas sorption.

One may consider the solubility σ in a three-phase system consisting of rubber, filler, and gas gaps in terms of the equation

$$\sigma = \lambda_r\sigma_r + \lambda_f\sigma_f + \lambda_g\sigma_g \tag{2}$$

where λ denotes the volume fraction and the subscripts r, f, and g denote the rubber, filler, and gas phases, respectively. Since $\lambda_r + \lambda_f + \lambda_g = 1$, eq. (2) can be written as

$$\sigma = \sigma_r + \lambda_f(\sigma_f - \sigma_r) + \lambda_g(\sigma_g - \sigma_r) \tag{3}$$

Here σ_g is the amount of gas (cm.^{3} at s.t.p.) at 1 cm. Hg contained per cubic centimeter of gas gaps at the temperature of the rubber sample. At 40°C., $\sigma_g = 0.0114$ and is less than σ_r so that the presence of gaps leads to a further reduction in the solubility in addition to that caused by the filler. However, σ_f is effectively increased by the formation of particle aggregates as a result of a proportional increase in the available free surface of filler. Consequently, the rate of decrease in the solubility falls off as the filler content is raised.

In Table III the densities of the sheets are compared with densities calculated assuming additivity of volumes of rubber and filler phases. In all cases the calculated density is greater than the experimental value indicating that gas gaps may indeed be present to a small extent.

TABLE III
Calculated and Experimental Densities for Filled Rubbers

ZnO, vol.-%	ρ, obs.	ρ, calc.
0	0.879	—
5	0.980	—
10	1.23	1.34
20	1.70	1.79
30	2.17	2.27
40	2.68	2.72

The benzene data are not so extensive in the range of filler contents investigated. From the data of Table II it is clear that there is little difference in solubility between the sulfur-cured and unfilled peroxide-cured rubbers. In Table IV percentage differences in the solubility, defined by $\Delta\sigma = [1 - (\sigma/\sigma_r)]100$, are presented for both benzene and propane.

TABLE IV
Percentage Difference in Solubility $\Delta\sigma$

	T, °C.	10% vol. ZnO	40% vol. ZnO	Sulfur cured
Benzene	30	17	—	5.6
Benzene	40	14.7	39.7	1.8
Benzene	50	15.9	—	2.2
Propane	40	9	16.1	—

The differences for benzene are considerably larger than for propane but perhaps not significantly so since the Henry's law region of the isotherm could not be determined as accurately.

These calculations do not take into account the possible presence of gas gaps in the filled rubber. From the experimental densities and the known amounts of filler and rubber in each sample an approximate estimate of λ_g, the volume fraction of gas gaps, was made for each rubber. Corrected

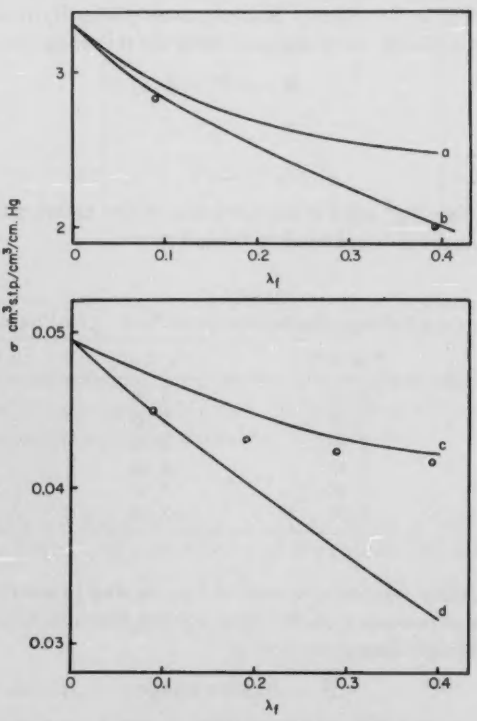

Fig. 4. Solubility vs. λ_f corrected for gas gaps, at 40°C. Curve *a*, benzene; eq. (1); $\sigma_f = 0.9$. Curve *b*, benzene; eq. (1); $\sigma_f = 0$. Curve *c*, propane; eq. (1); $\sigma_f = 0.0305$. Curve *d*, propane; eq. (1); $\sigma_f = 0$. (O) experimental points.

values of λ_f and λ_r were then obtained and used in conjunction with σ_r, σ_f, and σ_g to obtain reference lines of Figure 4. The effect of the gas gaps is to shift the reference lines toward the λ_f axis and in addition their curvature is increased. Thus even if σ_f remained constant over the range of filler content the presence of air gaps would result in curvature of the σ versus λ_f plot. The value of $\sigma_f = 0.9$ for benzene is only approximate since the sorption isotherms on the free ZnO powder were curved in the pressure range investigated.

Permeation

It is convenient to consider the benzene and propane results separately. The latter are more complete in the range of filler content investigated and are examined first.

Propane

The permeabilities $\bar{P}$ are given at 40°C. for the several membranes investigated in Table V. Steady and transient state diffusion coefficients D_S and D_L, respectively, were obtained from the relationships

$$D_S = \bar{P}/\sigma \tag{4}$$

and

$$D_L = l^2/6L \tag{5}$$

where L is the time lag[5] and l is the thickness of the membrane. Values of these coefficients are also included in Table V.

TABLE V
Permeabilities and Diffusion Coefficients (in cm.^{2} sec.$^{-1}$) for Propane at 40°C.

ZnO, %	$\bar{P} \times 10^8$	$D_S \times 10^7$	$D_L \times 10^7$
0	2.92	5.90	5.43
5	2.80	5.80	5.25
10	2.59	5.75	5.05
20	2.35	5.45	4.61
30	1.93	4.57	4.35
40	1.56	3.75	4.01

The permeability was independent of the ingoing pressure for all membranes, and its dependence on the filler volume fraction λ_f was well represented by the straight line

$$\bar{P} = \bar{P}_r(1 - 1.1\lambda_f) \tag{6}$$

where $\bar{P}_r$ denotes the permeability of the unfilled rubber. In Figure 5, D_S and D_L are plotted as functions of the filler volume fraction.

Diffusion Model for Filled Rubbers

For simplicity, transport is restricted to the rubber phase, the diffusion properties of which are assumed to be unaltered by the presence of filler. Further, for a comparison with the propane data, Henry's law sorption is considered to apply to both rubber and filler phases and the diffusion coefficient is constant. Then for transient state flow

$$\frac{\partial C}{\partial t} = \lambda_r k D_r \frac{\partial^2 C_r}{\partial x^2} = D_L \frac{\partial^2 C}{\partial x^2} \tag{7}$$

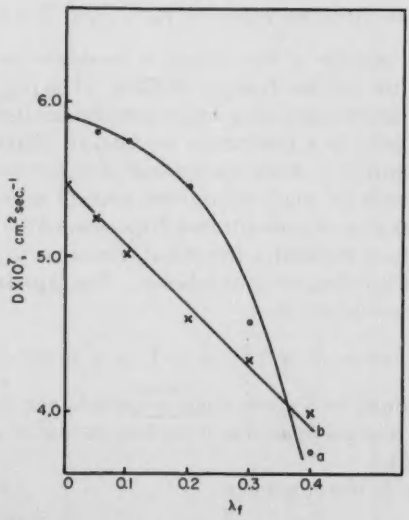

Fig. 5. Diffusion coefficient vs. λ_f for propane 40°C. (O) steady state diffusion coefficient D_S. (×) transient state diffusion coefficient D_L.

where D_r is the diffusion coefficient in the rubber phase, and κ is a structure factor to allow for, among other things, the increase in diffusion path length caused by the presence of filler particles. By definition

$$C = \lambda_r C_r + \lambda_f C_f$$

and for Henry's law sorption $C_f/C_r = \sigma_r/\sigma_f$, where σ_r and σ_f denote respectively the Henry's law solubilities of the rubber and filler phases. It follows that

$$D_L = \kappa D_r \frac{\lambda_r}{\lambda_r + \lambda_f(\sigma_f/\sigma_r)} \tag{8}$$

For steady state flow one may write:

$$J = -D_S \frac{\partial C}{\partial x} = -\lambda_r \kappa D_r \frac{\partial C_r}{\partial x} \tag{9}$$

and so one obtains the same expression for D_S as for D_L [eq. (8)], although only if the structure factor is the same for transient and steady states of flow.

For zero sorption ($\sigma_f = 0$),

$$D_S = D_L = \kappa D_r \tag{10}$$

Since $\bar{P}_r = D_r \sigma_r$ it can be shown that

$$\bar{P} = \lambda_r \kappa \bar{P}_r \tag{11}$$

irrespective of whether or not sorption occurs on the filler.

Dependence of the Structure Factor on the Volume Fraction of Filler λ_f

To further the analysis of the data it is necessary to consider the dependence of κ on the volume fraction of filler. The problem is analogous to the electrical conductance of a heterogeneous medium composed of a dispersion of particles in a continuous medium of different conductivity. Thus Maxwell[6] treated a dilute suspension of spheres while Fricke[7] extended his approach to cover oblate and prolate spheroids. Rayleigh[8] attempted to treat a more concentrated dispersion of particles. Meredith and Tobias[9] modified Rayleigh's treatment somewhat to obtain an expression for a close packed dispersion of spheres. The expressions for κ used in this investigation are listed below

$$\text{Fricke } (Y = 1.1): \quad \kappa = 1/[1 + (\lambda_f/Y)] \tag{12}$$

where Y is a constant for a given shape of particle and decreases from 2 to 1.10 as the shape changes from that of a sphere to that of an oblate spheroid with axial ratio of 4:1.

Rayleigh (cubic lattice of spheres):

$$\kappa = \frac{1}{\lambda_r}\left[1 - \frac{3\lambda_f}{2 + \lambda_f - 0.392\lambda_f^{10/3}}\right] \tag{13}$$

Rayleigh (cubic lattice of cylinders normal to flow direction):

$$\kappa = \frac{1}{\lambda_r}\left[1 - \frac{2\lambda_f}{2 + \lambda_f - 0.306\lambda_f^{4} - 0.0134\lambda_f^{8}}\right] \tag{14}$$

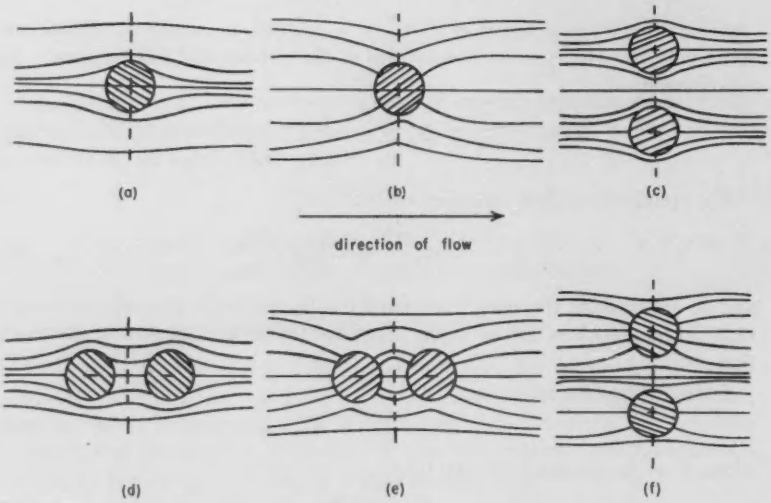

Fig. 6. Flow patterns for cylinders at right angles to flow: (*a*, *c*, *d*) Cylinders of zero conductivity. (*b*, *e*, *f*) Cylinders of infinite conductivity.

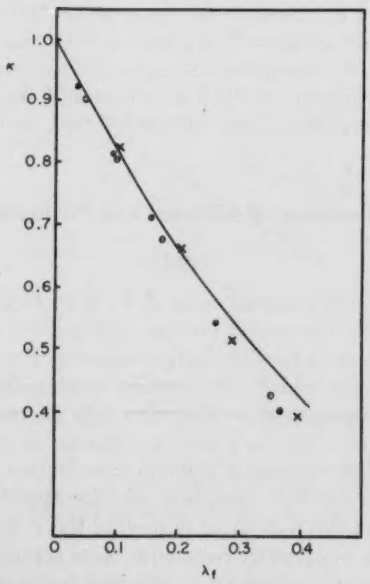

Fig. 7. Structure factor κ vs. λ_f. Full curve, from eq. (14). Results from electrical Teledeltos analog are: (O) cylinder radius = 0.825 cm. (random array); (●) cylinder radius = 0.825 cm. (regular array); and (×) cylinder radius = 2.12 cm. (random array).

Equations (13) and (14) include Runge's correction.[10] The complex pattern of flow in heterogeneous media may be illustrated by conductance analogs using Teledeltos paper,[2] which should correspond with Rayleigh's treatment for cylinders [eq. (14)]. Typical flow patterns are shown in Figure 6 around a section of a single cylinder with its axis at right angles to the direction of flow and having zero and infinite conductivity, respectively. A section of a nonconducting cylinder was represented by a circular hole in the paper while circular discs were painted on to the paper with silver emulsion to simulate sections of cylinders of infinite conductivity. It is observed that nonconducting cylinders exhibit a shadow effect. This is particularly noticeable for the two nonconducting cylinders in series, where the "dead-volume" between the cylinders is appreciable. Therefore, the structure factors for transient and steady state flow may be expected to differ, since the dead volume, although it contributes little to the steady state flow, must nevertheless be involved in the transient state. The more curved flow paths in the transient state imply a smaller structure factor in this state.

The conductance of a set of nonconducting cylinders arranged, both randomly and in regular fashion, at right angles to the direction of flow was also measured. The ratio of the conductance of the dispersion to that

of the original sheet is a measure of the structure factor κ for that dispersion. The results are compared in Figure 7 with the κ versus λ_f relation given by eq. (14), but the agreement is not particularly good. However, the data do not reveal any marked dependence of the structure factor on the type of array or, for a given volume fraction, on the diameter of the cylinders.

Discussion of Diffusion and Permeation

Propane

In Figure 8 the experimental ratio $\bar{P}/\bar{P}_r$ is plotted as a function of λ_f and compared with theoretical curves obtained by combining eq. (11) with eq. (12), (13), or (14). The experimental ratios are higher than the calculated values, for which two possible explanations are considered. First, electron micrographs of the ZnO filler indicate that the particle shape is rodlike. Now, eq. (14) considers a cubic array of cylinders normal to the flow direction whereas a random distribution will prevail in the filled rubber. The random dispersion may be approximated to by considering one-third of the rods to lie in each of the x, y, and z directions so that λ_f of eq. (14) is replaced by two-thirds of its actual value. With these values of κ satisfactory agreement is obtained between the observed and

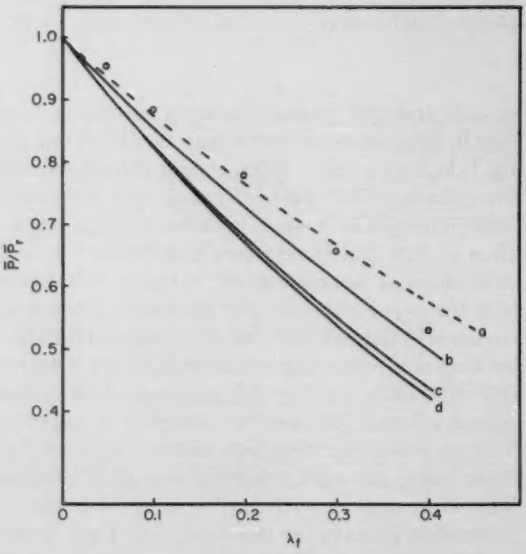

Fig. 8. $\bar{P}/\bar{P}_r$ vs. λ_f for propane at 40°C. Curve *a*, eq. (11) combined with eq. (14) modified for random dispersion. Curve *b*, eq. (11) combined with eq. (13). Curve *c* eq. (11) combined with eq. (12). Curve *d*, eq. (11) combined with eq. (14). (O) Experimental points.

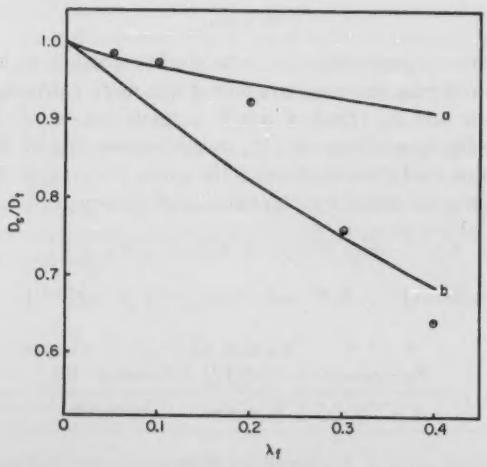

Fig. 9. D_S/D_r vs. λ_f for propane at 40°C. The full curves are obtained using eq. (14), modified for random dispersion and combined with eq. (10) (curve *a*) or eq. (8) (curve *b*). (O) Experimental points.

calculated $\bar{P}/\bar{P}_r$ ratios (curve *a*, Fig. 8). Second, the presence of gas gaps would also lead to abnormally high values of $\bar{P}$ and hence to values of κ larger than expected. The curvature in the plot of solubility versus λ_f is not reflected in that of $\bar{P}$ versus λ_f since eq. (11) is valid whether or not sorption occurs on the filler.

Since P versus λ_f is approximately linear it follows that a plot of D_S versus λ_f will reflect the curvature in the corresponding graph of solubility versus λ_f. On the other hand, D_L is linear in λ_f (Fig. 5). The data are again consistent with the presence of gas gaps within the medium. As noted earlier, κ will be less for transient than for steady state flow in systems where volume fractions of filler. But at higher volume fractions if gaps are present the time to establish steady state conditions will be shortened, so that relatively high values of D_L are obtained, and the curves of D_S and D_L versus λ_f cross (Fig. 5). In Figure 9 the ratio D_S/D_r is plotted as a function of λ_f and compared with ratios calculated from eqs. (8) and (10) with values of the structure factor calculated from eq. (14), modified for random dispersion. As the volume fraction of filler increases, the experimental ratios deviate rapidly from the zero sorption reference line toward that for immobile sorption. This is again consistent with the occurrence of gaps at high filler contents so that σ_f of eq. (8) is in effect a variable with filler content. At low volume fractions, with complete wetting of the filler particles by the rubber, σ_f will be small or zero while at higher volume fractions the value of σ_f will move toward that of the free powder.

This evidence of gaps is in line with that given earlier, based on observed and calculated densities of filled membranes (Table III).

Benzene

With benzene as penetrant the permeability coefficient was no longer independent of the ingoing pressure and it was more convenient to express the permeation rate J_A (cm.³ of liquid benzene/sec./cm.²) as a function of the volume fraction of benzene, λ_A, in the ingoing face of the membrane. For the different rubbers investigated the plots of J_A vs. λ_A at 30, 40, and 50°C. were well represented by a polynomial of the form

$$lJ_A = A\lambda_A + B\lambda_A^2 + C\lambda_A^3 + D\lambda_A^4 + \ldots \quad (15)$$

Values of the constants A, B, C, and D are given in Table VI.

TABLE VI
Constants A, B, C, and D of Equation (15)

T, °C.	$A \times 10^7$	$B \times 10^7$	$C \times 10^8$	$D \times 10^4$
		Unfilled Rubber		
50	7.516	9.50	—	4.26
40	4.462	8.50	—	2.07
30	2.420	—	3.00	1.20
		10% ZnO Filled Rubber		
50	7.48	0.25	—	7.5
40	5.56	1.00	—	1.9
30	3.05	—	16.0	—
		Sulfur-Cured Rubber		
50	5.622	13.0	—	8.37
40	3.400	8.0	—	4.00
30	2.300	—	—	1.04
		40% ZnO Filled Rubber		
40	3.375	0.20	0.349	—

Following Hartley and Crank[11] one has

$$(ldJ_A/d\lambda_A) = D_{AB} = D_A(1 - \lambda_A) \quad (16)$$

where D_{AB} and D_A are the interdiffusion and intrinsic diffusion coefficients, respectively. Equation (15) gives with eq. (16) the following expression for the intrinsic diffusion coefficient:

$$D_A(1 - \lambda_A) = A + 2B\lambda_A + 3C\lambda_A^2 + 4D\lambda_A^3 \quad (17)$$

Assuming diffusion to occur only in the rubber phase, one may write for the benzene flux in the filled rubber

$$J_A = -(1 - \lambda_f)(D_{AB})_r \frac{\partial(\lambda_A)_r}{\partial x} \quad (18)$$

$$= (1 \quad \lambda_f)\kappa(J_A)_r \quad (19)$$

where $(D_{AB})_r$ and $(\lambda_A)_r$ are respectively the diffusion coefficient in the rubber phase and the volume fraction of benzene with respect to the rubber phase. Equation 18 can now be used to calculate the J_A versus λ_A curves for the filled rubber assuming either zero or immobile sorption by the filler. Thus any particular point on the $(J_A)_r$ versus $(\lambda_A)_r$ curve for the unfilled rubber may be chosen. With the modified Rayleigh expression for a lattice of cylinders the quantity $\lambda_r\kappa(J_A)_r$ is calculated which in turn should equal J_A for the filled rubber with that value of λ_r. It only remains to convert $(\lambda_A)_r$ to the corresponding λ_A value referred to swollen filled rubber by means of the relationships

$$(\lambda_A)_r = V_A/(V_A + V_r) \tag{20}$$

$$\text{(zero sorption):}\quad \lambda_A = V_A/(V_A + V_r + V_f) \tag{21}$$

$$\text{(immobile sorption):}\quad \lambda_A = \frac{V_A + (V_A)_f}{(V_A)_f + V_A + V_r + V_f} \tag{22}$$

where V denotes the volume and the subscripts A, r, and f refer to benzene, rubber, and filler phases, respectively. Assuming additivity of volume, V_f and V_r are known from the composition of the filled rubber sheet and hence by fixing some value of $(\lambda_A)_r$ one obtains V_A. The value of $(\lambda_A)_r$ chosen also fixes the value of $(V_A)_f$, the volume of benzene sorbed by a volume V_f of filler at a pressure corresponding to the point $(\lambda_A)_r$. The corresponding value of V_A may now be found from eqs. (21) and (22) assuming either zero or immobile sorption by the filler. In this way, choosing several values of $(\lambda_A)_r$, the J_A versus λ_A curves for the various filled rubbers may be estimated and compared with the experimental curves.

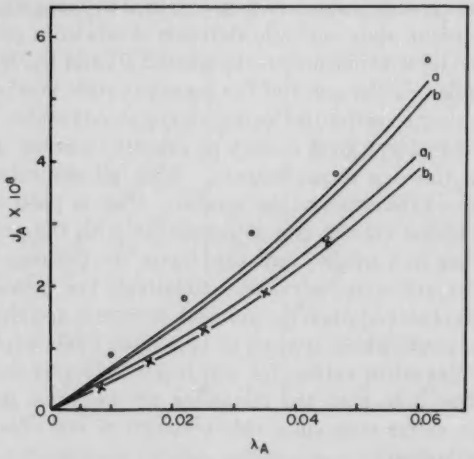

Fig. 10. J_A vs. λ_A for benzene at 40°C. (O) 10% ZnO. (×) 40% ZnO. Curve *a*, zero sorption by filler. Curve *b*, independent sorption by filler.

Some examples are given in Figure 10, but the analysis is not sufficiently accurate to distinguish between the two reference models.

Diffusion Coefficients

Steady state diffusion coefficients were calculated from eq. (17). Since the diffusion coefficient is concentration dependent the simple time-lag relationship of eq. (5) must be replaced by the general expression derived by Frisch.[12] However, the general expression for L may only be evaluated provided the form of the concentration dependence of the diffusion coefficient is known. It is assumed that the concentration dependence is the same for both transient and steady states of flow. The steady state diffusion coefficients were well represented not only by a polynomial but also by an equation proposed by Fujita and Kishimoto[13]:

$$D_{AB} = D_{\lambda_A=0}/(1 - b\lambda_A)^2 \tag{23}$$

This gives for the time lag,

$$L(\lambda_A) = \frac{l^2(1 - b\lambda_A)^2}{D_{\lambda_A=0}(b\lambda_A)^2}\left[\ln(1 - b\lambda_A) + \frac{1}{2(1 - b\lambda_A)} - \frac{1}{2}(1 - b\lambda_A)\right] \tag{24}$$

For all membranes the time lag was determined as a function of the concentration (λ_A) at the ingoing face of the membrane. Two values of $L(\lambda_A)$ were then chosen which with eq. (24) served to evaluate the parameters $D_{\lambda_A=0}$ and b. The values of these parameters for the different membranes are recorded in Table VII.

Substitution of these values in eq. (23) then gives D_{AB} for the transient state as a function of λ_A. From the coefficients D_{AB} the corresponding intrinsic diffusion coefficients were then obtained by using eq. (16). Steady state and transient state intrinsic diffusion coefficients are compared in Table VIII and for convenience are designated D_S and D_L, respectively.

For the unfilled rubber some of the transient state coefficients are even slightly larger than those for the corresponding steady state. However, the agreement is perhaps as good as may be expected bearing in mind the accuracy of the time-lag measurements. With all the other rubbers the transient state coefficients are the smaller. This is particularly true for the 40% ZnO-filled rubber and is consistent with the presence of dead volume resulting in a smaller structure factor for the transient state and hence a smaller diffusion coefficient. Relatively low transient state coefficients are also observed when the diffusion process is accompanied by slow relaxation processes, which appears to be a more likely explanation in the case of the sulfur-cured rubber for which the ZnO-filler content is small. However, if this is so then the relaxation process must in some way be specific to the sulfur cure since this behavior is not observed with the peroxide-cured rubber.

The effect of filler content on the diffusion coefficient is perhaps not so pronounced as expected, and in fact the steady state diffusion coefficients

TABLE VII
Parameters $D_{\lambda_A=0}$ and b of Equation (24)

T, °C.	b	$D_{\lambda_A=0}$ × 10^7, cm.^{2} sec.$^{-1}$
	Unfilled Rubber	
30	5.0	2.42
40	5.88	4.07
50	2.74	7.52
	Sulfur Cured	
30	3.2	1.98
40	2.2	3.10
50	3.7	5.00
	10% ZnO	
30	3.7	2.03
40	4.4	3.16
50	3.0	6.06
	40% ZnO	
40	2.05	2.35

for the 10% ZnO rubber are higher than for the unfilled rubber. This probably reflects some experimental error in those measurements although gas gaps in the filled rubber may also be partly responsible.

Concentration Dependence of Diffusion Coefficient in Filled Rubber

Figure 11*a* shows the steady state intrinsic diffusion coefficients as a function of benzene volume fraction in the various rubbers. It is of interest

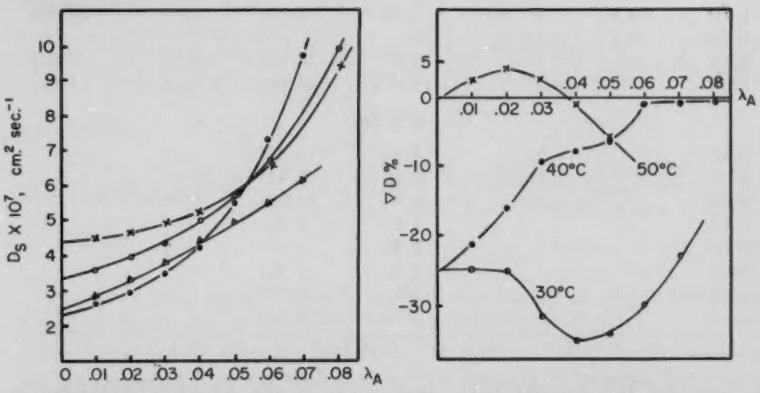

Fig. 11. (*a*) The steady state diffusion coefficient as a function of benzene volume fraction. (O) unfilled rubber, (●) sulfur cured, (×) 10% ZnO, and (△) 40% ZnO. (*b*) The divergence of $D_r(\lambda_A)$ and D_S plotted as a function of λ_A for the 10% ZnO-filled rubber.

TABLE VIII

Steady State and Transient State Intrinsic Diffusion Coefficients, D_S (D_L) $\times 10^7$ (cm.^{2} sec.$^{-1}$)

A	50°C.		40°C.		30°C.	
			Unfilled Rubber			
0.00	7.5	(7.5)	4.46	(4.07)	2.42	(2.42)
0.01	7.8	(8.03)	4.7	(4.64)	—	—
0.02	8.2	(8.6)	5.0	(5.33)	2.64	(3.05)
0.03	8.8	(9.3)	5.4	(6.18)	—	—
0.04	9.8	(9.9)	—	—	2.94	(3.94)
0.05	11.1	(10.6)	6.7	(8.60)	—	—
0.06	13.1	(11.5)	7.7	(10.30)	3.91	(5.24)
0.08	—	—	10.9	(15.8)	5.7	(7.31)
0.09	—	—	13.2	(19.4)	—	—
0.10	—	—	—	—	8.7	(10.8)
			Sulfur Cured			
0.00	5.6	(5.0)	3.4	(3.10)	2.3	(1.98)
0.01	6.0	(—)	4.6	(—)	2.33	(2.00)
0.02	6.5	(5.72)	3.9	(3.33)	—	—
0.03	7.5	(—)	4.4	(—)	2.49	(2.04)
0.04	9.2	(6.62)	5.2	(3.58)	2.67	(2.06)
0.05	11.7	(—)	6.5	(—)	2.97	(2.08)
0.06	—	(7.77)	8.3	(3.87)	3.40	(—)
			10% ZnO			
0.00	7.48	(6.06)	5.5	(3.16)	3.05	(2.03)
0.01	7.6	(6.38)	—	—	3.13	(—)
0.02	7.9	(6.7)	5.78	(3.72)	3.31	(2.32)
0.03	8.6	(7.1)	—	—	3.59	(—)
0.04	9.8	(7.5)	6.28	(4.47)	3.98	(2.69)
0.05	11.8	(7.97)	—	—	—	—
0.06	14.9	(8.48)	7.79	(5.49)	5.08	(3.15)
0.07	19.1	(9.0)	—	—	—	—
0.08	—	—	10.5	(6.93)	6.65	(3.77)
0.10	—	—	14.9	(9.07)	8.72	(4.61)
			40% ZnO			
0.00	—	—	3.38	(2.35)	—	—
0.01			3.82	(2.42)		
0.02			4.30	(2.50)		
0.03			4.81	(2.58)		
0.04			5.36	(2.67)		
0.05			5.93	(2.76)		
0.06			6.54	(2.88)		
0.07			7.19	(2.97)		

to consider the concentration dependence of the diffusion coefficient in such a complex system as filled rubber. To simplify what follows, it is again assumed that diffusion occurs only in the rubber phase, that sorption by the filler is zero, and that there are no gas gaps.

Consider a volume fraction of benzene λ_A referred to unit volume of swollen filled rubber and let $(\lambda_A)_r$ denote the volume fraction equivalent to λ_A but referred to unit volume of the swollen rubber phase. From eq. (19)

$$\frac{d(J_A)_r}{d(\lambda_A)_r} = \frac{1}{\kappa(1 - \lambda_f)} \cdot \frac{dJ_A}{d(\lambda_A)_r} \tag{25}$$

and so by eq. (16)

$$D_S = D_r(1 - \lambda_f)\kappa \cdot \frac{(1 - (\lambda_A)_r)}{(1 - \lambda_A)} \cdot \frac{d(\lambda_A)_r}{d\lambda_A} \tag{26}$$

If V_A denotes the volume of benzene in question then from eqs. (20) and (21) it follows that

$$\frac{d(\lambda_A)_r}{d\lambda_A} = \frac{V_r(V_r + V_f)}{(V_r + \lambda_A V_f)^2} \tag{27}$$

and so eq. (26) becomes

$$D_S = D_r \cdot \kappa \cdot \frac{(1 - \lambda_f)V_r(V_r + V_f)}{(V_r + \lambda_A V_f)^2} \cdot \frac{(1 - (\lambda_A)_r)}{(1 - \lambda_A)} \tag{28}$$

which for $\lambda_A = 0$ reduces to

$$D_S = \kappa \cdot D_r$$

Now, D_r refers to the diffusion coefficient in unfilled rubber at a volume fraction of benzene $(\lambda_A)_r$. In practice it is more convenient to effect a comparison at the same benzene volume fraction for both filled and unfilled rubber. Let $D_r(\lambda_A)$ be the diffusion coefficient for the unfilled rubber at a benzene volume fraction numerically equal to that for the filled rubber. Then from eq. (17) one has

$$\frac{D_r}{D_r(\lambda_A)} = \frac{(1 - \lambda_A)}{(1 - (\lambda_A)_r)} \cdot \frac{(A + 2B(\lambda_A)_r + 3C(\lambda_A)^2_r + \ldots)}{(A + 2B\lambda_A + 3C\lambda^2_A + \ldots)} \tag{29}$$

and finally,

$$D_S = \kappa \cdot D_r(\lambda_A) \cdot \frac{(1 - \lambda_f V_r)(V_r + V_f)}{(V_r + \lambda_A V_f)^2} \left[\frac{A + 2B(\lambda_A)_r + 3C(\lambda_A)^2_r + \ldots}{A + 2B\lambda_A + 3C\lambda^2_A + \ldots}\right] \tag{30}$$

It follows from eq. (27) that as λ_A increases the term within the square brackets decreases, as also does the term $[V_r(V_r + V_f)]/(V_r + \lambda_A V_f)^2$. The divergence between D_S and $D_r(\lambda_A)$ contained in the above two terms should therefore increase with the volume fraction of benzene for a given rubber. On the other hand, as λ_A increases the volume fraction of the continuous phase (rubber plus benzene) increases and therefore κ should increase towards unity [cf. eqs. (12) to (14)]. The term $(1 - \lambda_f)$ also in-

creases with λ_A. The possibility therefore arises of either maxima or minima in the divergence of D and $D_r(\lambda_A)$.

When the divergences expressed as $[D_r(\lambda_A) - D_S]/[D_r(\lambda_A)]$ were plotted as functions of λ_A curves showing minima were often obtained (Fig. 11*b*). However, although the foregoing treatment shows how maxima or minima could arise, such simplifying assumptions as the neglect of gas gaps make its application at best only qualitative. The treatment does, nevertheless, illustrate the complex concentration dependence of the observed diffusion coefficient in filled rubber systems.

Conclusion

The work described in this paper has demonstrated that the presence of filler particles can lead to considerable differences between diffusion coefficients evaluated by steady state and time-lag procedures, respectively. It has also shown that the variations of the diffusion coefficients with the volume fraction of penetrant is complex, and has given some guidance as to how these variations may be interpreted.

One of us (M. G. Rogers) wishes to acknowledge the award of a Gas Council Scholarship which enabled him to take part in this work.

List of Symbols

A, B, C, D	Constants in polynomial equation for the flux as a function of penetrant volume fraction λ_A.
$D_{\lambda_A=0}$	Diffusion coefficient at $\lambda_A = 0$.
D_{AB}, D_A	Interdiffusion and intrinsic diffusion coefficients, respectively, for the membrane (cm.^{2} sec.$^{-1}$).
D_S, D_L	Steady and transient state intrinsic diffusion coefficient, respectively, for the filled membrane (cm.^{2} sec.$^{-1}$).
D_r	Intrinsic diffusion coefficient for the unfilled rubber (cm.^{2} sec.$^{-1}$).
J	Permeation rate (cm.^{3} s.t.p./sec./cm.^{2}).
J_A	Permeation rate (cm.^{3} of liquid/sec./cm.^{2}).
L	Time lag, minutes.
l	Membrane thickness, mm.
$\overline{P}$	Permeability coefficient (cm.^{3} s.t.p./sec./cm.^{2}/cm./cm. Hg).
V	Volume, cm.^{3}
κ	Structure factors.
λ	Volume fraction.
ρ	Density, g./cm.^{3}
σ	Henry's law solubility coefficient (cm.^{3} s.t.p./cm.^{3} of membrane/cm. Hg).

Subscripts

A	With respect to penetrant (benzene).
f	With respect to filler.
g	With respect to gas gaps.
r	With respect to rubber.

References

1. Barrer, R. M., and R. R. Fergusson, *Trans. Faraday Soc.*, **54**, 989 (1958).
2. Barrer, R. M., J. A. Barrie, and M. G. Rogers, *Trans. Faraday Soc.*, **58**, 2473 (1962).
3. Barrer, R. M., J. A. Barrie, and N. K. Raman, *Polymer*, **3**, 605 (1962).
4. Smith, E. R., *J. Res. Natl. Bur. Std.*, **26**, 129 (1941).
5. Barrer, R. M., *Trans. Faraday Soc.*, **35**, 628 (1939).
6. Maxwell, J. C., *Electricity and Magnetism*, Vol. 1, Dover, New York, 1891.
7. Fricke, H., *Physics*, **1**, 106 (1931).
8. Rayleigh, Lord, *Phil. Mag.*, **34**, 481 (1892).
9. Meredith, R. E., and C. W. Tobias, *J. Appl. Phys.*, **31**, 1270 (1960).
10. Runge, I., *Z. tech. Physik.*, **6**, 61 (1925).
11. Hartley, G. S., and J. Crank, *Trans. Faraday Soc.*, **45**, 80 (1949).
12. Frisch, H. L., *J. Phys. Chem.*, **61**, 93 (1957).
13. Fujita, H., and A. Kishimoto, *J. Technol. Res., Eng. Dep. Kanto Gakuin Univ.*, **23**, 59 (1953).

Résumé

On a étudié la diffusion et la dissolution du propane et du benzène dans une série de membranes hétérogènes constituées de caoutchouc naturel et d'oxyde de zinc. Le volume de la charge en % variait de 0, 5, 10, 20, 30 et 40. Une interaction entre le caoutchouc et la charge a été mise en évidence de même que l'existence de trois phases dans certaines membranes: le polymère, la charge et les interstices libres entre les particules de la charge. Quoiqu'il n'existe aucune théorie rigoureuse de la diffusion dans les milieux rigides, on a cependant pu développer un modèle de deux phases interdispersées. Ce modèle a été discuté en relation avec les vitesses de perméation et les coefficients de diffusion. Les différences entre les coefficients de diffusion-temps et l'état stationnaire ont été attribuées à des facteurs de structure différents dans l'écoulement aux états stationnaire et transitoire. On a measuré la dépendance de l'interdiffusion et les coefficients de diffusion intrinsèque du benzène par rapport à la concentration. Les influences de la dépendance par rapport à la concentration, de la charge et du facteur de structure ont été combinées en une équation reliant le coefficient de diffusion intrinsèque dans le caoutchouc contenant une charge au coefficient pour la diffusion dans le caoutchouc exempt de charge et contenant la même fraction de volume de benzène. L'expression finale semble être apte à rendre compte de façon qualitative de certains comportements complexes observés dans l'étude de la diffusion.

Zusammenfassung

Die Diffusion und Lösung von Propan und Benzol in einer Reihe heterogener, Zinkoxyd-gefüllter Naturkautschukmembranen wurde in einem Temperaturbereich untersucht. Die Volum-% Füllstoff betrugen 0, 5, 10, 20, 30 und 40. Die Wechselwirkung zwischen Kautschuk und Füllstoff, sowie das Auftreten von drei Phasen in einigen Membranen, nämlich Polymeres, Füllstoff und offene Lücken zwischen Füllstoffteilchen, wurden nachgewiesen. Es gibt keine strenge Behandlung der Diffusion in heterogenem Medium; das Modell zweier ineinander verteilter Phasen wurde entwickelt und in bezug auf Permeationsgeschwindigkeit und Diffusionskoeffizienten diskutiert. Unterschiede zwischen den Diffusionskoeffizienten im stationären Zustand und den aus der Durchbruchszeit erhaltenen wurden auf verschiedene Struktureinflüsse beim stationären und nichtstationären Fließen zurückgeführt. Die Konzentrationsabhängigkeit der Interdiffusions- und spezifischen Diffusionskoeffizienten von Benzol wurde gemessen. Der Einfluss der Konzentrationsabhängigkeit, des Füllstoffs und des Strukturfaktors wurde in eine Beziehung zusammengefasst und damit eine Beziehung zwischen dem

spezifischen Diffusionskoeffizienten im gefüllten Kautschuk und dem Koeffizienten für die Diffusion in ungefülltem Kautschuk mit dem gleichen Volumbruch an Benzol hergestellt. Der resultierende Ausdruck bietet eine qualitative Erklärung für einen Teil des beobachteten, komplexen Diffusionsverhaltens.

Received May 11, 1962

JOURNAL OF POLYMER SCIENCE: PART A VOL. 1, PP. 2587–2600 (1963)

An Interpretation of Ethylene Polymerization with Alkyl-Promoted Transition-Metal Catalysts

WAYNE E. SMITH* and RALPH G. ZELMER, *Research Department, Amoco Chemicals Corporation, Whiting, Indiana*

Synopsis

A concept has been developed to explain the kinetic behavior of six transition-metal catalyst systems for ethylene polymerization: $CrO_3 \cdot SiO_2$ and $V_2O_5 \cdot SiO_2$ promoted by $(i\text{-}C_4H_{10})_3Al$; $VOCl_3$ promoted by $(C_2H_5)_2AlCl$; $TiCl_4$ promoted by $(C_2H_5)_3Al$ or $(i\text{-}C_4H_{10})_3Al$; and $(C_5H_5)_2TiCl_2$ promoted by $(CH_3)_2AlCl$. Despite obvious differences in the chemical nature of their active species and known behavioral differences, all of these systems show a second-order deactivation of active species with time. Production of polymer in batch polymerizations has been shown to obey an equation relating propagation and deactivation constants, monomer concentration, reaction time, and initial number of active sites. This equation has been extended to fit batch runs with continuous catalyst addition. One possible reaction mechanism has been proposed. Qualitative steps are: (*1*) complex formation between the transition-metal complex and alkyl, (*2*) alkylation of the complex, (*3*) polymerization by the alkylated species, and (*4*) second-order decay of active species.

The use of aluminum alkyls as promoters for the production of polyolefins has been generally studied. Several differing mechanisms for the polymerization have been proposed based on qualitative studies of specific catalyst systems. Kinetic data that would help in developing a mechanistic model for the polymerization are lacking. At present, there is no general agreement[1] as to whether the polymerization is ionic[2] or radical,[3] heterogeneous[4] or homogeneous,[5] or which transition metal is optimum.[6–8]

In hopes of unifying thinking in this field, a detailed kinetic study has been made of ethylene polymerization with alkyl-promoted chromia·silica, vanadia·silica, and titanium tetrachloride catalysts. Batch studies have been conducted at constant pressure with both slug addition and continuous addition of catalyst and alkyl. Fall off in reaction rate with time indicates that these catalysts follow the same kinetics in spite of obvious differences in the chemical nature of their catalytic species and their known behavioral differences. The alkyl and transition-metal compounds initially form a catalytically active species which deactivates with time. Deactivation of the active species is second order. The different catalyst systems exhibit differing deactivation rates at given reaction conditions, indicating significant differences in the chemical nature of their active

* Present address: Spencer Chemical Co., Merriam, Kansas.

catalytic species. The concept of second-order deactivation has not been heretofore proposed for alkyl-promoted heterogeneous catalysts. A similar kinetic behavior was noted for the homogeneous catalyst system bis-cyclopentadienyl titanium dichloride promoted with aluminum sesquihalide.[12]

Literature data for other heterogeneous catalyst systems, presented without kinetic interpretation, can be analyzed to fit a second-order deactivation. Performance of vanadium oxychloride promoted by aluminum sesquihalide,[9] titanium tetrachloride promoted by aluminum triethyl[7,10] all follow second-order kinetics for deactivition of active species.

Despite the chemical and behavioral differences of these catalyst systems, the similarity in their kinetic behavior suggests a unified concept for a mechanistic picture in which the rate determining step is a second-order decay of active catalyst species.

Experimental

Experimental vanadia-silica and chromia-silica catalysts were prepared in the laboratory by wet impregnation of the silica support with soluble salts. Most of the water was removed by evaporation at 95°C.; the rest just before use by calcination in air at 450°C. Catalysts varied from 3 to 8 wt.-% in content of transition-metal oxide.

Commercial grade titanium tetrachloride and aluminum triisobutyl were used without further purification. Because these catalysts are particularly sensitive to polar compounds, all runs were made with highly purified ethylene and hydrocarbon solvents. Neither solvent nor ethylene contained more than 20 ppm of water.

Polymerizations were conducted in batch runs in a one-gallon stirred autoclave. Runs were carried out at constant pressure to maintain constant monomer concentration in the reaction system. In most runs, hydrocarbon solvent was introduced into the reactor, catalyst and promoter were added by slug addition, and the reactor was pressured to operating level. Reaction rate was followed by monomer consumption at constant pressure and verified by isolating and weighing the final polymer. Monomer consumption and weighed product usually agreed within 5%. Repeatability in duplicate experiments was excellent.

Several batch runs were made under other conditions to obtain an independent verification of kinetics determined from slug addition runs. Some were made with continuous addition of catalyst and promoter. In others, catalyst and promoter were added to the reactor and preactivated for various times at reaction temperature before the reactor was pressured with ethylene.

All data presented are typical and were selected from studies of reaction temperature and pressure, catalyst concentration, and alkyl-to-catalyst ratio. All runs chosen for illustration were made at 160°C. and 750 psig. Because the catalysts used were experimental, the absolute activities could be affected by further refinements in preparation.

Results

Typical polymer yield curves for the three catalyst systems studied are given as a function of time after catalyst addition in Figure 1. In no case is polymer yield a linear function of reaction time.

Polymer production rates were determined from the slopes of curves in Figure 1. Rates are plotted as a function of time interval t in Figure 2. Base points for time intervals with $TiCl_4$, CrO_3, and V_2O_5, were 1, 7.5, and 4 min. after catalyst addition, respectively. For all three catalyst systems, polymer production rate decreases markedly with reaction time. At a given reaction temperature, rate fall off was most pronounced for the $TiCl_4$ system and least pronounced for the V_2O_5 system, indicating differences in the chemical nature of their active catalytic species.

Polymer production rate was directly proportional to catalyst concentration; thus, monomer diffusional limitations were absent.

To further substantiate the rapid deactivation of the catalyst and promoter with time, several runs were made in which catalyst and promoter were precontacted for various times before the introduction of ethylene.

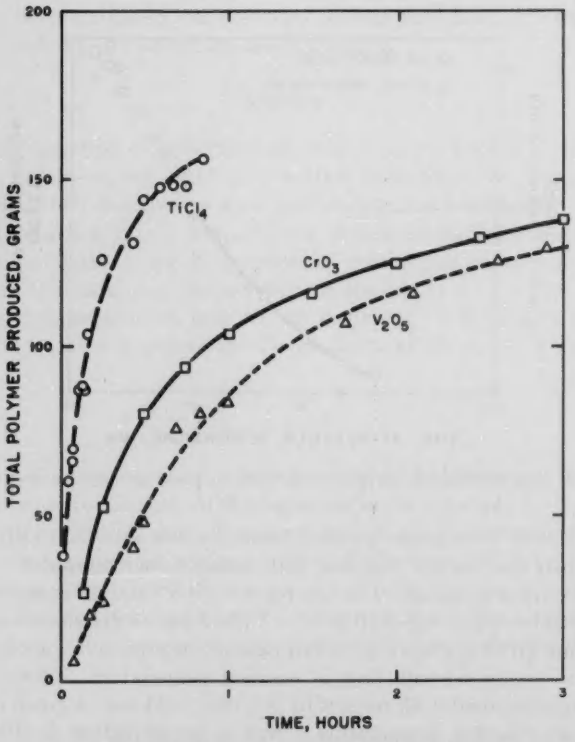

Fig. 1. Polymerization of ethylene with promoted catalysts.

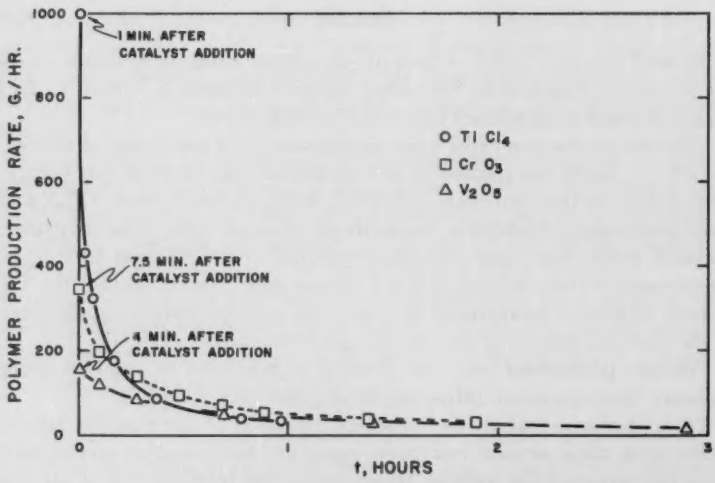

Fig. 2. Fall off in rate with reaction time.

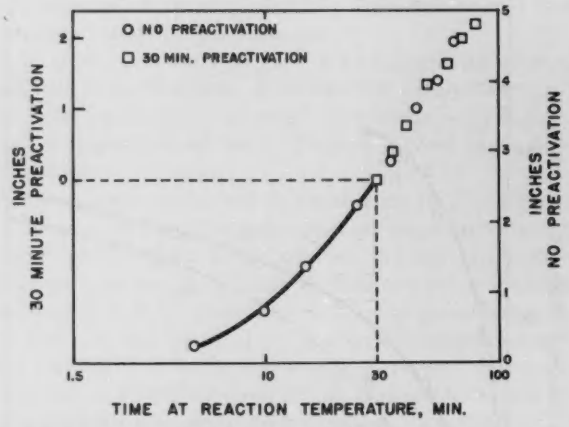

Fig. 3. Deactivation of catalysts with time. Uptake of ethylene over CrO_3.

Standard runs were made without preactivation in which ethylene was admitted to the reactor together with catalyst and promoter. In other runs, ethylene was admitted to the reactor after catalyst components had been precontacted for one-half hour. Yield data for runs made with CrO_3 catalyst are given in Figure 3. The origin of the preactivation run has been shifted to correspond with time at reaction temperature. The two curves can be superimposed with respect to polymer yield over a given increment of time at reaction temperature. But if preactivation is disregarded, runs without preactivation result in substantially more polymer per unit

time at reaction pressure (2.6 in. ethylene uptake over 30 min. vs. 2.2 in. ethylene uptake over 55 min.). The strong influence of preactivation on catalyst activity suggests an unstable alkyl-catalyst complex as the active species for polymerization.

Evidence for Complex Formation

The rapid fall off in production rate with reaction time might be due to decomposition of the alkyl promoter. Alkyls decompose at temperatures above 50 to 60°C.[11]

Data in Figure 2 indicate that the decrease in polymer production rate with time differs for the three catalyst systems studied, even though these runs were made at the same temperature with the same promoter. If thermal decomposition of the promoter were controlling, rate fall off should be independent of catalyst type.

Data reported[11] for thermal stability of $(i\text{-Bu})_3$ Al at 160°C. indicate the alkyl fraction remaining after 1 hr. would be 10^{-8}. Figure 2 shows that the polymer production rate after 1 hr. at a reaction temperature of 170°C. is still greater than 2% of the initial production rate. The alkyl must have been stabilized, undoubtedly through formation of a semistable complex involving the transition-metal catalyst.

Kinetics

In batch ethylene polymerizations with alkyl-promoted CrO_3, V_2O_5, and $TiCl_4$ catalysts, the alkyl and catalyst form an active complex, initially, which then deactivates with time at reaction conditions. Because polymer production rate is proportional to active-complex concentration, the fraction of active complex decomposed over a particular time interval is equal to the reduction in polymer production rate over the interval divided by the production rate at the beginning of the interval. Conversely, the fraction of active sites C_t remaining at the end of a time interval t is

$$C_t = P_t/P_0 \tag{1}$$

where P_t is the polymer production rate at the end of the time interval t, and P_0 is the production rate at the beginning of the interval.

Rate data in Figure 2 were substituted into eq. (1) to determine the fraction of active complex remaining at the end of a time interval t. Results of calculations are given in Figure 4.

The deactivation data in Figure 4 are best represented by a second-order rate equation. The integrated rate equation for a second-order deactivation reaction is

$$t = k_D \frac{(1 - C_t)}{C_t} \tag{2}$$

Figure 5 shows plots of $(1 - C_t)/C_t$ versus t, for data in Figure 4. The linearized plots verify the fall off in polymer production rate is in accord with second-order deactivation of active complex. Rate constants for deactivation k_D are equal to the slopes of the lines in Figure 5. The slopes or rate constants for deactivation differ widely for the three catalyst systems, even though the polymerizations were conducted under the same conditions (160°C. and 750 psig). Obviously, the chemical nature of

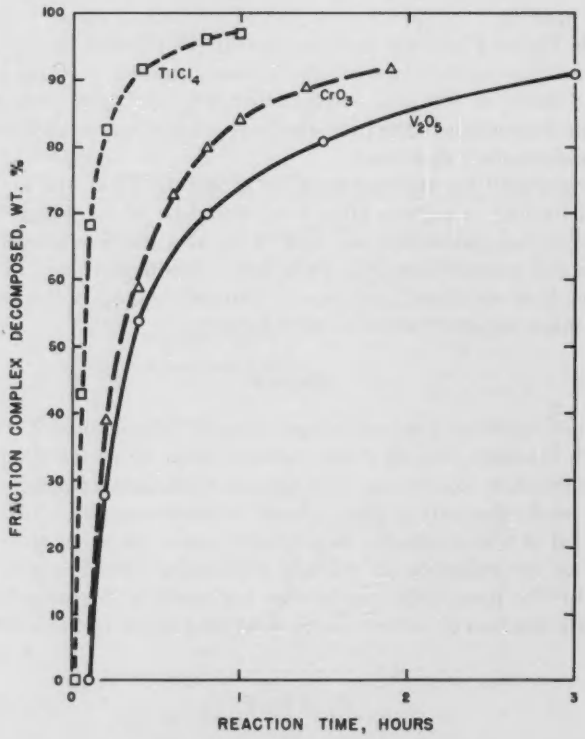

Fig. 4. Decomposition of complex.

their active complexes must differ, with the vanadia-alkyl complex being about ten times more stable than the $TiCl_4$-alkyl complex. Catalyst stability is an important factor in product yield, quality, and control.

Cumulative polymer production data from batch runs can be used directly to determine rate constants for deactivation of the alkyl-catalyst complex and for polymer formation. The rate equation for the propagation reaction in olefin polymerization is

$$dP/dt = k_P[M](C_t) \tag{3}$$

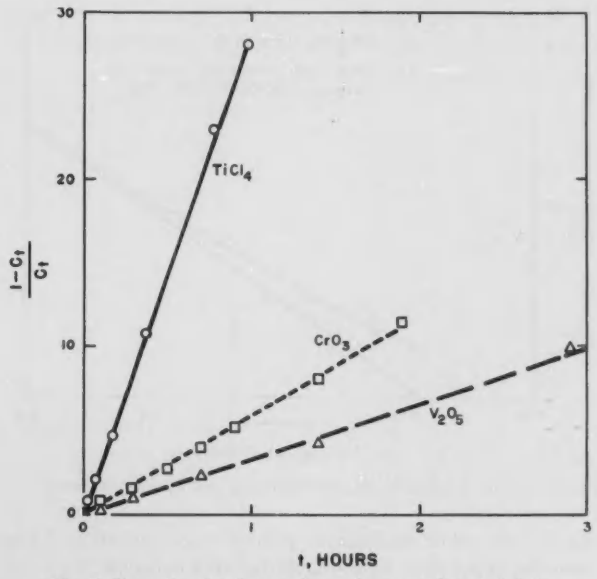

Fig. 5. Second-order decay of complex, experimental data.

where dP/dt is the rate of polymer formation, k_P is a rate constant for propagation, [M] is the monomer concentration, and C_t is molar concentration of active complex at time t. The differential rate equation for catalyst deactivation is

$$dC/dt = -k_D(C^2) \tag{4}$$

where C is the molar concentration of active sites. Integration of eq. (4) gives

$$C_t = \frac{1}{k_D t + \frac{1}{C_0}} \tag{5}$$

where C_0 is the concentration of active complex added to the reactor at the start of the batch polymerization. Substituting the value for C_t from eq. (5) into eq. (3) gives

$$\frac{dP}{dt} = k_P[\mathrm{M}] \frac{1}{k_D t + \frac{1}{C_0}} \tag{6}$$

Integration yields:

$$P = \frac{k_P}{k_D}[\mathrm{M}] \ln \left[\frac{t + \frac{1}{k_D C_0}}{\frac{1}{k_D C_0}} \right] \tag{7}$$

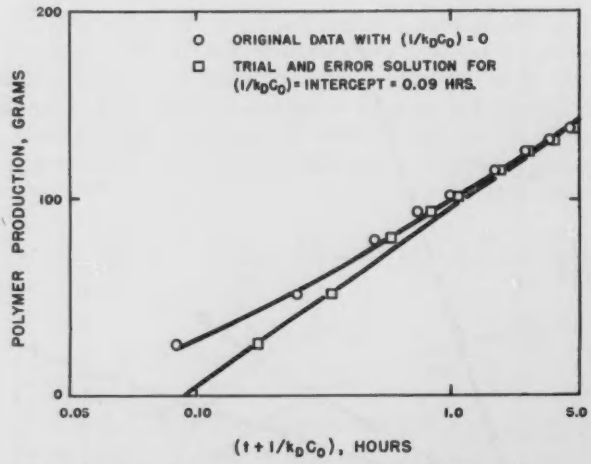

Fig. 6. Determination of rate constants k_D and k_P for CrO_3 catalyst.

Equation (7) describes cumulative polymer production as a function of reaction time for batch runs with slug addition of catalyst.

Determining rate constants k_P and k_D from cumulative production data involves a trial-and-error procedure. A semilogarithmic plot of cumulative polymer production versus $\ln (t + 1/k_DC_0)$ is a straight line with slope k_P/k_D and intercept $1/k_DC_0$. Construction of the plot involves a trial and error procedure to determine the value of $1/k_DC_0$ which, when added to t, results in a linearized plot with intercept $(1/k_DC_0)$. Figure 6 illustrates how cumulative polymer production data may be linearized by proper selection of $1/k_DC_0$.

Equation (7) can be extended to batch reactions with continuous addition of catalyst and promoter, where P_0 is polymer production at some time t_0, over which catalyst and promoter have been added to the batch reactor at constant addition rate W. For an incremental amount of catalyst Wdt added to the batch reactor at some time t, the incremental polymer production from this catalyst at some time t_0 is, from eq. (7),

$$dP_0 = Wdt \frac{k_P}{k_D} [\mathrm{M}] \ln \left[\frac{t_0 + \dfrac{1}{k_DC_0^*}}{\dfrac{1}{k_DC_0^*}} \right] \tag{8}$$

Integration for production from total catalyst added gives

$$P_0 = W \frac{k_P}{k_D} [\mathrm{M}] \left\{ \left[t_0 + \frac{1}{k_DC_0^*} \right] \ln \left[\frac{t_0 + \dfrac{1}{k_DC_0^*}}{\dfrac{1}{k_DC_0^*}} \right] - t_0 \right\} \tag{9}$$

Equation (9) can be used to predict polymer production as a function of catalyst addition for any time t_0 before catalyst addition is stopped.

Similarly, polymer production P_A, at any time t_A after catalyst addition is stopped, may be expressed as

$$P_A = \frac{Wk_P}{k_D}[\mathrm{M}]\left\{-\left[t_A - t_S + \frac{1}{k_DC_0^*}\right]\ln\left[\frac{t_A - t_S + \frac{1}{k_DC_0^*}}{\frac{1}{k_DC_0^*}}\right] + \left[t_A + \frac{1}{k_DC_0^*}\right]\ln\left[\frac{t_A + \frac{1}{k_DC_0^*}}{\frac{1}{k_DC_0^*}}\right] - t_S\right\} \quad (10)$$

where t_S the time catalyst addition was stopped.

Equations (9) and (10) can be used to find the value of reaction rate constants in batch runs with continuous addition of catalyst. A plot of P vs. $f(t)$, where

$$f(t) = \left\{\left[t_A + \frac{1}{k_DC_0^*}\right]\ln\left[\frac{t_A + \frac{1}{k_DC_0^*}}{\frac{1}{k_DC_0^*}}\right] - \left[t_A - t_S + \frac{1}{k_DC_0^*}\right]\ln\left[\frac{t_A - t_S + \frac{1}{k_DC_0^*}}{\frac{1}{k_DC_0^*}}\right] - t_S\right\}$$

for any time after catalyst addition was stopped, and

$$f(t) = \left\{\left[t_0 + \frac{1}{k_DC_0}\right]\ln\left[\frac{t_0 + \frac{1}{k_DC_0}}{\frac{1}{k_DC_0}}\right] - t_0\right\}$$

for any time before catalyst addition was stopped can be linearized by selecting the proper value of $1/k_DC_0$. The resultant slope is $Wk_P[\mathrm{M}]/k_D$. The following example illustrates the procedure.

Table I gives polymer production data for a batch polymerization with continuous addition of catalyst and promoter. These data can be used to develop the matrix also given in Table I, in which polymer production is related to $f(t)$ for various assumed values of $1/k_DC_0$. Figure 7 shows that a 0.25 value for $1/k_DC_0$ linearizes the data; the slope of the line is equal to $Wk_P[\mathrm{M}]/k_D$.

Other data, presented without previous kinetic interpretation, can be shown to fit the theory of second-order decay. Data from studies made on

TABLE I
Batch Polymerization with Continuous Catalyst Addition

		$f(t)$ for $(1/k_DC_0)$ =		
P, g.	t, hr.	0.05	0.25	0.60
8	0.20[a]	0.20	0.08	0.03
35	0.40[a]	0.59	0.26	0.11
64	0.60[a]	1.07	0.51	0.23
85	0.80[b]	1.39	0.73	0.36
103	1.00[b]	1.61	0.89	0.46
130	1.40[b]	1.85	1.11	0.61
155	1.80[b]	2.05	1.28	0.75

[a] Continuous catalyst addition.
[b] Catalyst addition stopped at 0.6 hr.

$VOCl_3 + (C_2H_5)AlCl$[9] and $TiCl_4 + (C_2H_5)_3Al$ at 40[7] and 80°C.[10] are plotted according to second-order kinetics in Figure 8. Even though these plots were interpolated from graphs in the literature, the degree of fit is good in each case. These data also show that reaction temperature, which

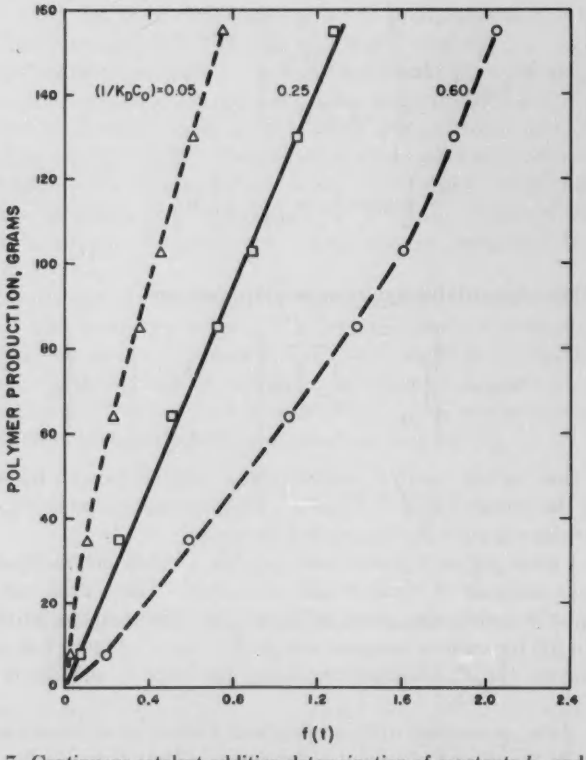

Fig. 7. Continuous catalyst addition determination of constants k_D and k_P.

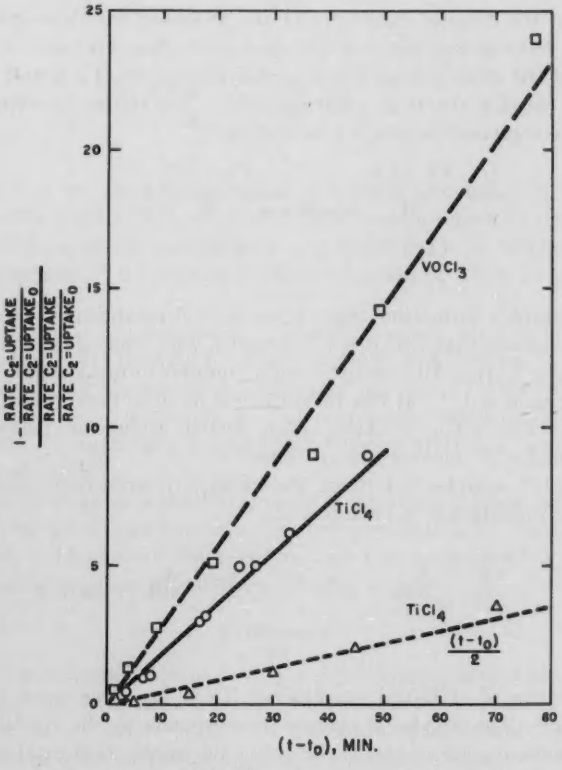

Fig. 8. Second-order decay of complex, literature data.

ranged from 40[7] to 160°C. (present work), only affects the relative rates and not the order of the kinetics, even though reaction conditions change from suspension to solution polymerization over this temperature range.

Mechanism

The preponderance of evidence for the second-order decay of active catalytic species leads the authors to propose a set of qualitative reactions that would account for such behavior. These reactions would be: (*1*) complex formation between the transition-metal compound and metal alkyl, (*2*) alkylation of the transition metal, (*3*) growth of polymer at the transition-metal-alkyl bond, and (*4*) disappearance of active sites by a second-order decay reaction.

Although steps (*1*) through (*3*) are well documented, step (*4*) is the key to the unifying theory. For homogeneous systems, only Chien[12] has reported second-order behavior; for heterogeneous systems, no kinetic data have heretofore been reported and interpreted as such in the literature.

Much of the detailed chemistry of the proposed reactions still remains obscure. Nonetheless, one can speculate as to what is actually happening. For one of the most-studied Ziegler-catalyst systems, $TiCl_4$ and AlR_3, the following possible reactions are suggested. The initial reaction between these two components is complex formation:

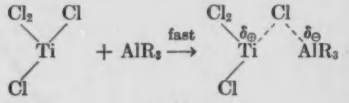

(I)

That complex formation takes place is well established.[12,13] Further, there is evidence that this is a 1:1 complex with some degree of stability. Data on the $(C_5H_5)_2$ AlCl system[12] show complex formation to be complete at a mole ratio of 1:1; at this ratio there is no detectable reduction of the titanium. The $TiCl_4$ + $Al(i\text{-}C_4H_{10})_3$ system shows no polymerization activity until a 1:1 mole ratio is reached.[14]

After a 1:1 complex is formed, the addition of more alkyl causes alkylation of the transition-metal compound.

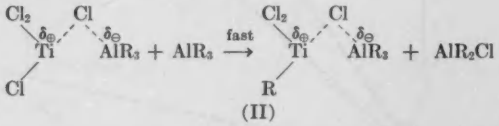

(II)

The ability of $(CH_3)_3Al$ to alkylate $TiCl_4$ has been used to prepare CH_3TiCl_3.[15] The alkylated complex corresponds to the symbol C given in the kinetic equations and is the active polymerization catalyst. There is some evidence to indicate that the Ti^{+4} is necessary for maximum activity.[6] Chain growth occurs at the transition-metal alkyl bond. Ample evidence for growth on the transition metal rather than the aluminum comes from studies of both homopolymerization[15–17] and copolymerization.[19]

For the second-order decay of active catalyst to be obeyed, two active sites must interact to form species of negligible activity. One possible scheme for this bimolecular reaction is

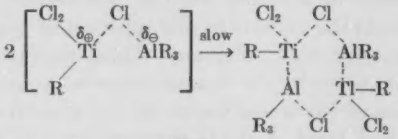

(III)

Recent evidence indicates the ability of titanium to form penta-coordinate compounds.[18] Complete justification of this "dimer" cannot be given; however, a six-membered ring compound seems possible as a nonstable intermediate state that disproportionates thusly:

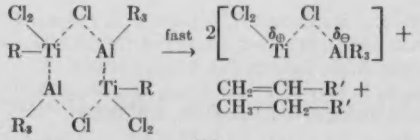

(IV)

Termination by disproportionation is favored because this system is similar to the $(C_5H_5)_2TiCl_2$ + (C_2H_5) AlCl system which forms polymer with 0.5 carbon-carbon double bond per molecule.[12] A reaction of this type was proposed[19] to account for the reduction of $TiCl_4$ by aluminum alkyls.

The Ti^{+3} complex in reaction (IV) is still an active catalyst for ethylene polymerization. Its activity for relatively short reaction times, however, is overshadowed by the extremely high activity of the Ti^{+4} species. Aging of transition-metal compounds in their maximum oxidation states with alkyl promoters is generally known to decrease catalytic activity for ethylene polymerization.

Whether the scission of the Ti-R bond during polymerization is homolytic or heterolytic is still not known. Because termination by combination is free radical, and homolytic reactions are known to obey second-order kinetics, such a mechanism must not be excluded.

Conclusion

A unifying concept has thus been developed from reaction kinetics that accounts for the behavior of several catalysts for low-pressure ethylene polymerization. Further work with transition-metal compounds having different types of substituents and other oxidation states would assist in the continuing effort to elucidate the mechanism of these reactions. Whether or not such data become available, a second-order decay of active catalytic species is well enough established that it must be included in any consideration of a mechanistic picture for the catalysts studied.

References

1. Carrick, W. E., et al., *J. Am. Chem. Soc.*, **82**, 3887 (1960).
2. Natta, G., *Chim. Ind. (Milan)*, **37**, 888 (1955).
3. Friedlander, H. N., and K. Oita, *Ind. Eng. Chem.*, **49**, 1885 (1957).
4. Nenitzescu, C. D., and A. H. Ciresicahuch, *Angew. Chem.*, **68**, 438 (1956).
5. Natta, G., et al., *J. Polymer Sci.*, **26**, 120 (1957).
6. Breslow, D. S., and N. R. Newburg, *J. Am. Chem. Soc.*, **81**, 81 (1959).
7. Lundlum, D. B., A. W. Anderson, and C. E. Ashby, *J. Am. Chem. Soc.*, **80**, 1380 (1958).
8. Carrick, W. L., *J. Am. Chem. Soc.*, **80**, 6455 (1958).
9. Bier, G., *Angew. Chem.*, **73**, 186 (1961).
10. Kodama, S., et al., *J. Appl. Polymer Sci.*, **3–4**, 20 (1960).
11. Knap, J. E., et al., *Ind. Eng. Chem.*, **49**, 874 (1957).
12. Chien, J. C. W., *J. Am. Chem. Soc.*, **81**, 86 (1959).
13. Natta, G., *J. Inorg. & Nuclear Chem.*, **8**, 589 (1958).
14. Jones, M. H., U. Martuis, and M. P. Thorne, *Can. J. Chem.*, **38**, 2303 (1960).

15. Karapinka, G. L., J. J. Smith, and W. L. Carrick, *J. Polymer Sci.*, **50**, 143 (1961).
16. Natta, G., P. Pino, and G. Mazzonti, *Chim. Ind.* (*Milan*), **39**, 1032 (1957).
17. Farbwerke Hoechst A. G., Belgian Pat. 553,477 (1957).
18. Karol, F. J., and W. L. Carrick, *J. Am. Chem. Soc.*, **83**, 2654 (1961).
19. Gilman, H., and G. Jones, *J. Org. Chem.*, **10**, 505 (1945).

Résumé

On a développé une théorie expliquant le comportement cinétique de six systèmes catalytiques de métaux de transition pour la polymérisation de l'éthylène: $CrO_3 \cdot SiO_2$ et $V_2O_5 \cdot SiO_2$ cocatalysé par $(i\text{-}C_4H_{10})_3Al$; $VOCl_3$ cocatalysé par $(C_2H_5)_2AlCl$; $TiCl_4$ cocatalysé par $(C_2H_5)_3Al$ ou $(i\text{-}C_4H_{10})_3Al$; et $(C_5H_5)_2\ TiCl_2$ cocatalysé par $(CH_3)_2AlCl$. En dépit de différences manifestes dans la nature chimique de leurs espèces actives et des différences de comportement connu, l'ensemble de ces systèmes montrent une désactivation du second ordre des espèces actives avec le temps. On montre que la production de polymère en masse obéit à une équation reliant les constantes de propagation et de désactivation, la concentration en monomère, le temps de réaction et le nombre initial de sites actifs. Cette équation a été établie pour adjuste les conditions de travail en masse avec addition continue en catalyseur. On a proposé un mécanisme de raction possible. Les étapes qualitatives sont: (*1*) formation d'un complexe entre le complexe "métal de transition et l'alcoyle," (*2*) alcoylation du complexe, (*3*) polymérisation par les espèces alcoyles, et (*4*) disparition de second ordre des espèces actives.

Zusammenfassung

Ein Konzept zur Erklärung des kinetischen Verhaltens von sechs Übergangsmetall-Katalysatorsystemen für die Äthylenpolymerisation-$CrO_3.SiO_2$ und $V_2O_5.SiO_2$ mit $(i\text{-}C_4H_{10})_3Al$; $VoCl_3$ mit $(C_2H_5)_2AlCl$; $TiCl_4$ mit $(C_2H_5)_3Al$ oder $(i\text{-}C_4H_{10})_3Al$ und $(C_5H_5)_2$-$TiCl_2$ mit $(CH_3)_2AlCl$-wurde entwickelt. Trotz der offenbaren Unterschiede in der chemischen Natur der aktiven Spezies und der bekannten Unterschiede im Verhalten zeigen alle diese Systeme eine Desaktivierung der aktiven Spezies mit der Versuchsdauer nach zweiter Ordnung. Für die Bildung des Polymeren bei diskontinuierlicher Polymerisation wurde das Bestahen einer Beziehung zwischen Wachstums- und Desaktivierungskonstanten, Monomerekonzentration, Reaktionsdauer und Anfangzahl der aktiven Stellen gezeigt. Diese Gleichung wurde ouf die Beschreibung von diskontinuierlechen Ansätzen mit kontinuierlichem Katalysatorzusatz ausgedehnt. Ein möglicher Reaktionsmechanismus wird vorgeschlagen. Folgende Schritte werden angenommen: (*1*) Komplexbildung zwischen dem Übergangsmetallkomplex und Alkyl, (*2*) Alkylierung des Komplexes, (*3*) Polymerisation durch die alkylierte Spezies und (*4*) Abklingen der aktiven Spezies nach zweiter Ordnung.

Received May 16, 1962

JOURNAL OF POLYMER SCIENCE: PART A VOL. 1, PP. 2601–2620 (1963)

The Chemical and Physicochemical Properties of Wheat Starch Mildly Oxidized with Alkaline Sodium Hypochlorite*

J. SCHMORAK and M. LEWIN, *Institute for Fibres and Forest Products Research, Ministry of Commerce and Industry, Jerusalem, Israel*

Synopsis

An attempt has been made to elucidate the nature of the reaction between alkaline hypochlorite and granular wheat starch. With this end in view various analytical determinations were carried out on starch samples oxidized under well-determined conditions. The reaction was found to be nonspecific, its main results being the formation of functional groups and the scission of glucosidic bounds. The functional groups formed were mainly carboxyls, some carbonyl formation taking place at lower pH values. The consumption of about 0.05 atom of oxygen/AGU resulted in an extensive degradation of both starch components. There are indications to the effect that degradation is random in type. On that assumption, 0.5 to 1 glucosidic bonds in 100 were scinded, each scission being accompanied by the formation of about two carboxyl groups and by an overall consumption of 4–5 oxygen atoms. The reaction apparently took place in the amorphous part of the granule. The amylose-amylopectin ratio, as well as the granule size remained unchanged. More than one-quarter of the total oxygen consumed reacted with the dissolved portion of the starch as the result of the oxidation.

Introduction

In a previous paper[1] the kinetic aspects of the mild oxidation of wheat starch by alkaline hypochlorite were reported. It was suggested that the reaction was of an apparent first order with respect to starch, and either of an apparent first order or fractional order with respect to hypochlorite. It appeared to follow the overall equation

$$\mathrm{NaOCl} + \mathrm{Starch} = \mathrm{Starch \cdot O} + \mathrm{NaCl}$$

It was thought likely that the undissociated hypochlorous acid rather than the hypochlorite ion was the active oxidizing species. The numerical values obtained for the activation energy of the reaction gave an additional indication of its essentially chemical mechanism. When the granular structure was destroyed and the starch went into solution, the rate of reaction was found to increase; this gave grounds for assuming that the

* This work forms part of the research being carried out at this Institute under Grant No. FG-Is-102-58, issued by the Agricultural Research Service, U. S. Department of Agriculture.

reaction might possibly take place only in the amorphous portion of the granule.

The kinetic approach, where conclusions were drawn from the variation of the rate of disappearance of the *oxidant*, is supplemented in the present paper by the description of the changes brought about in the *oxidized starch itself*. Experimentally, this amounts to a characterization of starches oxidized under known conditions and a search for a possible correlation between these characteristics and the conditions of oxidation.

Scant data are available in the literature on the properties of hypochlorite oxidized starches. They mostly concern starches oxidized under more drastic conditions than those described below. MacKillican and Purves[2] determined the carbonyl and carboxyl groups in thin boiling wheat starch oxidized in acid and neutral pH. Rassow and Lobenstein[3] determined the changes in the acidity, reducing power, and viscosity of potato starch oxidized with alkaline hypochlorite to the dextrin stage. Hullinger and Whistler[4] determined the carboxyl and carbonyl groups, uronic acids and changes in viscosity and retrogradation properties of wheat and potato amyloses oxidized at pH 7. Whistler et al.[5] identified low molecular degradation products of corn amylose and amylopectin fractions. Farley and Hixon[6] determined the hot viscosity, swelling, turbidity, gel strength, birefringence and action of beta-amylase on corn starch which had been strongly oxidized by the electrolytic method.

This paper deals with the changes in granule size, viscosity, x-ray pattern, molecular weights of amylose and amylopectin fractions, carbonyl and carboxyl group concentration, and amylose:amylopectin ratio, brought about by oxidizing wheat starch with alkaline hypochlorite under the experimental conditions described in the previous paper.[1] An attempt is also made to correlate the data obtained with the oxidation parameters and to establish a tentative oxygen balance.

Experimental conditions differ from those employed by the authors quoted above in that (*a*) the oxidation is conducted in alkaline rather than acid or neutral medium; (*b*) the extent of the oxidation is much smaller; and (*c*) the oxidation is conducted on granular starch, the granular structure being preserved throughout each experiment.

Materials and Methods

Starches

Starches were oxidized by the technique previously described[1]; the relevant oxidation parameters will be found in the tables. A "blank" sample means a starch sample prepared for comparison purposes under the same conditions of pH, temperature, consistency, and duration of treatment, but in the absence of hypochlorite.

Granule Size

Granule size was measured by counting 500–700 granules under the microscope and classifying them into 7 or 8 size groups. The arithmetical average and the 95% confidence limit of the standard error range were calculated in the usual way. This was necessary in view of the fact that the granule size varied between 4 and 27 μ in diameter.

Intrinsic Viscosities

Intrinsic viscosities were determined using a Fenske-Ostwald capillary viscometer. One-normal KOH was used as solvent (flow time in viscometer: 93 sec.) and no precaution was taken to exclude oxygen. This was in agreement with Lansky et al.[7] and has been confirmed by a separate experiment, when it was found that the viscosity of 1% solutions of starches in 1*N* KOH remained practically constant when exposed to the atmosphere for up to 48 hr. The expression $\ln \eta_{rel}/c$ was experimentally found to be constant within the concentration range 0.25 to 1.20% starch in all cases examined, and so was taken to be identical with the intrinsic viscosity.

Fractionations

Fractionations were carried out by thymol precipitation[8] followed by recrystallization of the crude amylose from butanol.

Amylose:Amylopectin Ratio

The amylose:amylopectin ratio was determined by potentiometric titration against iodine.[9]

Carboxyl Groups

Carboxyl groups were determined by the copper acetate method of Elizer.[10]

Carbonyl Groups

Carbonyl groups were determined by the method recently published.[11]

Periodate Oxidations

Periodate oxidations were made essentially by the method of Sloan et al.,[12] except that the nitrogen treatment was omitted. From the amount of formic acid evolved, the number-average molecular weights of amylose and amylopectin fractions were calculated from the formula:

$$\frac{3w}{F - \frac{1-w}{n} + 3\alpha w} \leqslant N_\alpha{}^A \leqslant \frac{2+w}{\mathrm{F} - \frac{1-w}{n_\alpha}} \leqslant N_\alpha{}^B \leqslant 1/\alpha$$

where $N_\alpha{}^A$ is the DP of the amylose fraction degraded to the extent α; $N_\alpha{}^B$ is the DP of amylopectin fraction degraded to the extent α; w is the

weight fraction of amylose in (whole) starch, F,F_α are moles of formic acid evolved by 162 g. of the original and the oxidized starch, respectively; n,n_α is the DP of the repeating chain length of the amylopectin fraction in the original and in the oxidized starch, respectively.

The justification of this procedure is given in separate papers.[13,14]

Sedimentation Velocities

The sedimentation velocities in ultracentrifugal field were determined in Spinco model E ultracentrifuge in the biophysical department of the Weizmann Institute of Science, Rehovoth, Israel. One-normal potassium hydroxide proved to be the best solvent in that it gave the most detailed Schlieren photographs; it had proved superior to water, and to acetone and butyl acetate solutions of starch acetates. The frequency distributions and sedimentation constants were calculated from Schlieren photographs by the method of Williams et al.[15] The extrapolation of the sedimentation constants to infinite dilution influenced their values only to a small extent and was dispensed with for comparative purposes; the concentration of 1% in starch was accordingly used throughout.

Starch Yield

Accurately weighed samples of starch were oxidized under the desired conditions. The suspension was then centrifuged, when a supernatant and a cake were obtained. The cake was washed with water until the washings were free of chlorides, then with methanol and ether, dried and weighed, quantitative conditions being observed throughout.

Dissolved Starch Recoverable as Glucose

The supernatant was then exactly neutralized with alkaline arsenite and an aliquot part acidified with sulfuric acid and hydrolyzed for 1 hr. under reflux. Glucose was then determined on the hydrolyzate after neutralization. The amount of glucose found multiplied by 0.93[16] then gave the amount of starch recoverable as glucose which had passed into solution.

Oxygen Taken up by the Dissolved Starch

An oxidation experiment was run under the desired conditions. Portions of the suspension were withdrawn with a pipette at specified time intervals, filtered, and the disappearance of the oxidant in the filtrate was followed as a function of time in the usual way.

Results

Granule Size

Starches oxidized with 1 mole of hypochlorite per 20 AGU's (anhydroglucose units) showed an approximate 16% increase in the diameter of

the granule, irrespective of the pH at which the oxidation had been conducted (Table I). The blank treatment may have possibly caused some slight diameter increase at higher pH values, which had remained, however, within the experimental error.

TABLE I

The Influence of Oxidation on Granule Size

(Oxidant absorbed: 1 mole per 20 AGU's; temp. of oxidation: 27°C.; starch consistency: 1:35; initial oxidant concentration: 15 mmoles/liter)

pH of oxidation	Granule diam., μ	
	Blank	Sample
Unoxidized	—	12 ± 0.42
7.5	11.5 ± 0.63	14.4 ± 0.54
8	10.4 ± 0.46	14.5 ± 0.50
9	12.5 ± 0.58	13.7 ± 1.54
10	13.4 ± 0.50	14.2 ± 0.58
11	12.4 ± 0.54	14.4 ± 0.50

Viscosities

The viscosities in 1*N* KOH of whole starches, amyloses, and amylopectins are seen to decrease as the amount of oxidant absorbed increases (Table II). At an oxidant consumption of about 1 mmole per 19 AGU's, the decrease in the intrinsic viscosity, as compared with the unoxidized material, was approximately as follows: whole starch, from 1.1 to 0.3, amyloses, from 0.60 to 0.25, and amylopectins, from 0.55 to 0.25.

The pH of the oxidation appears to be without influence on the intrinsic viscosities of the oxidized products.

X-Ray Examination

Both oxidized and unoxidized starches gave a perfectly unchanged *A* pattern throughout.[17]

Functional Groups

The functional group content of oxidized whole starches is given in Table III.

Carbonyl Groups

The amount of carbonyl groups formed in the pH range 9 through 11 was exceedingly small throughout (less than 1 group in 200 AGU's) and so could not be accurately determined. The carbonyl content at pH 7.5 and 8 was 1 carbonyl group in 110 and 170 AGU's, respectively.

Carboxyl Groups

More carboxyl groups were formed at higher than at lower pH values, but the carboxyl group formation only accounted for a part of the oxidant consumed (cf. Discussion).

TABLE II
Intrinsic Viscosities of Whole Starches and Starch Fractions
(Temperature: 27°C.; starch consistency during oxidation: 1:35; solvent: 1*N* KOH)

Description	pH of oxidation	Oxidant absorbed, AGU's/mole	$[\eta]$
Unoxidized, original starch	—	—	1.1
Amylose	—	—	0.60
Amylopectin	—	—	0.54
Whole starch, blank	8	—	1.1
Whole starch	8	100	0.80
Whole starch	8	67	0.56
Whole starch	8	40	0.51
Whole starch	8	31	0.40
Whole starch	8	26	0.45
Whole starch	8	19	0.40
Amylose	8	19	0.28
Amylopectin	8	100	0.65
Amylopectin	8	40	0.3
Amylopectin	8	26	0.39
Amylopectin	8	19	0.25
Whole starch, blank	9	—	1.3
Whole starch	9	20.6	0.3
Amylose	9	20.6	0.26
Amylopectin	9	20.6	0.25
Whole starch, blank	10	—	1.2
Whole starch	10	18.5	0.3
Amylose	10	18.5	0.21
Amylopectin	10	18.5	0.23

TABLE III
Functional Group Content of Oxidized Whole Starches[a]

pH of oxidation	Oxygen consumed, mmole/AGU	AGU's/ COOH group	AGU's/ CO group	Moles carboxyl/mole of oxygen consumed	Moles carbonyl/mole of oxygen consumed
7.5	0.069	97	110	0.148	0.132
8	0.053	80	170	0.236	0.111
9	0.048	67	>200	0.311	>0.100
10	0.054	54	>200	0.342	>0.100
11	0.060	36	>200	0.464	>0.100

[a] *Note:* Less than 1 carboxyl in 250 AGU's was found both in the original unoxidized starch and in blanks prepared at all pH values investigated.

Amylose:Amylopectin Ratio

This has remained unchanged throughout within the limits of the experimental error (Table IV).

TABLE IV
Amylose Content in Oxidized Starches[a]
(Oxygen absorbed: 1 mole/20 AGU's)

pH of oxidation	Amylose, %	
Unoxidized	20	± 1
7.5	22	± 1
8	21	± 1
9	21	± 1
10	20	± 1
11	18	± 1

[a] *Note:* The iodine binding power of pure amylose was taken as 20%.

TABLE V
Starch Dissolved on Oxidation
(Initial oxidant concentration: 30 mmoles of oxidant/liter; starch consistency: 54 g./liter)

pH	Moles of oxidant/AGU	Total starch dissolved, wt.-%	Reducing groups in dissolved material calcd. as glucose, %	Total starch recovered as glucose, %	Apparent DP of dissolved material
8	0.0526	5.45	1.55	5.06	3
9	0.0525	3.27	0.41	3	7
10	0.0534	1.74	0.15	2.60	17

TABLE VI
Ultracentrifugal Data
(All starches oxidized at pH = 8)

Description or product	AGU's per 1 mole of oxidant absorbed	s value of most frequent species $\times 10^{13}$	Highest value of s $\times 10^{13}$	Value of $g(s)$
Whole starch	100	4.4	41	12.7
Whole starch	65	2.3	19	20.1
Whole starch	38	2.9	14.1	20.4
Whole starch	25	2.6	14.8	22.3
Whole starch	19	2.2	14.8	18.2
Amylose	38	3	21.2	17.5
Amylose	25	2.2	7.2	28.8
Amylose	22.5	1.9	5.2	44.1
Amylopectin	100	6.6	57.6	4.7
Amylopectin	38	3.2	27.4	14.5
Amylopectin	25	2.7	15.4	16.5
Amylopectin	22.5	2.6	18	18.8

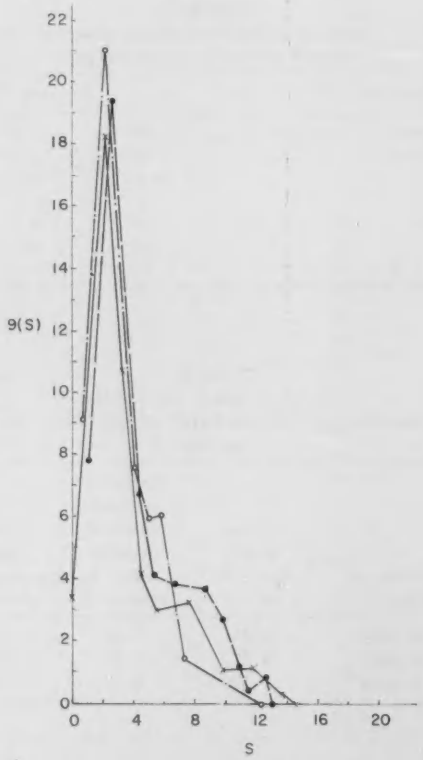

Fig. 1. Distribution of ultracentrifugal sedimentation constants of whole starches oxidized with 1 oxygen atom/19 AGU's, at different pH values: (×) pH = 8, (●) pH = 9, (○) pH = 10.

Yield of Oxidized Starch

As a result of the oxidation, a certain proportion of the starch passed into solution, practically all of which could be recovered as glucose (Table V).

Distribution of the Ultracentrifugal Sedimentation Constants

The following results were obtained (Table VI):

1. Whole starches oxidized with the same amount of oxidant at pH values of 8, 9, and 10, respectively, showed a very similar distribution (Fig. 1).

2. When whole starches were oxidized with increasing amounts of oxidant, other parameters remaining equal, it was observed that the *s* value of the most frequent species slowly decreased, and the highest

s values (over 15×10^{-13}) disappeared altogether. At the same time the $g(s)$ value of the peak increased, indicating homogenization (Fig. 2).

3. The amyloses, isolated from whole starches oxidized with increasing amounts of oxidant, showed a sharp homogenization accompanied by the disappearance of higher s values (Fig. 3).

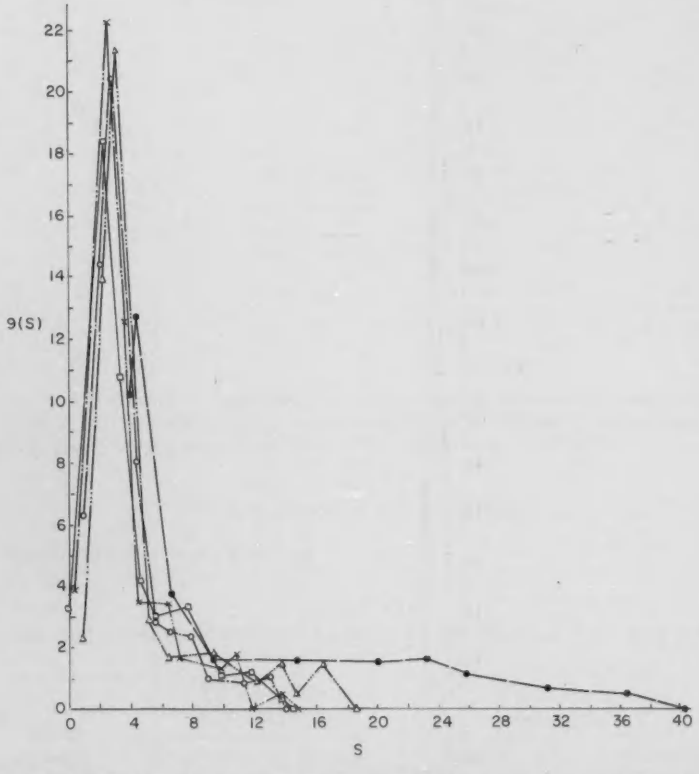

Fig. 2. Distribution of ultracentrifugal sedimentation constants of whole starches oxidized at pH = 8 with: (□) 1 oxygen atom/19 AGU's, (×) 1 oxygen atom/25 AGU'S, (○) 1 oxygen atom/38 AGU'S, (△) 1 oxygen atom/65 AGU's, (●) 1 oxygen atom/> 100 AGU's.

4. The amylopectins, isolated from whole starches oxidized with increasing amounts of hypochlorite, showed the following effects: (*a*) the s value of the most frequent species first dropped rapidly, but then decreased only very slowly; (*b*) there was a marked tendency to a homogenization of the material through the progressive disappearance of s values above 15×10^{-13}, accompanied by the increase in the $g(s)$ value of the most frequent species (Fig. 4).

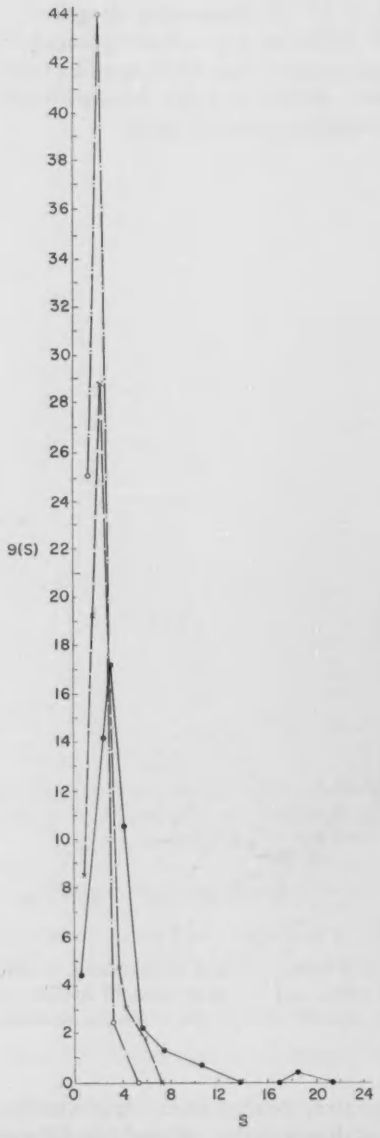

Fig. 3. Distribution of ultracentrifugal sedimentation constants of amyloses oxidized at pH = 8 with: (●) 1 oxygen atom/38 AGU'S, (×) 1 oxygen atom/25 AGU's, (○) oxygen atom/22.5 AGU's.

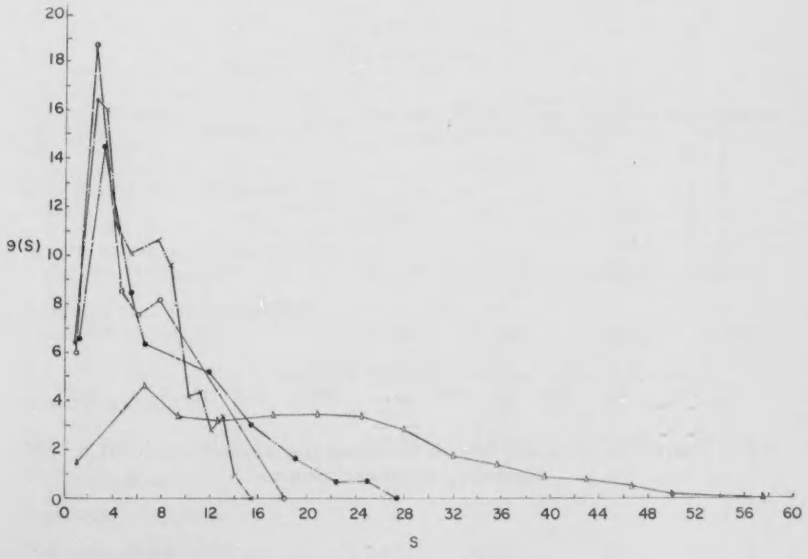

Fig. 4. Distribution of ultracentrifugal sedimentation constants of amylopectins oxidized at pH = 8 with: (△) 1 oxygen atom/>100 AGU'S, (●) 1 oxygen atom/38 AGU'S, (×) 1 oxygen atom/25 AGU'S, (○) 1 oxygen atom/22.5 AGU'S.

Number-Average Molecular Weights

Results are shown in Table VII.

TABLE VII
Formic Acid Evolved on Periodate Oxidation of Oxidized and Unoxidized Whole Starches

pH of oxidation	AGU's per mole of formic acid evolved		Calcd. approx. number-average DP	
	Blank	Sample	Amylose	Amylopectin
Unoxidized	26	—	—	—
7.5	26	18	153 ± 11	170 ± 6
8.0	26	17	131 ± 9	143 ± 4
9	25	17	131 ± 9	143 ± 4
10	25	15	99 ± 2	104 ± 3
11	23	16	114 ± 5	122 ± 3

Oxygen Consumed by the Dissolved Starch

Two experiments were carried out at pH = 8 and pH = 10 (Figs. 5 and 6; see also Table VIII). It will be seen on inspecting the diagrams that the oxidation of the dissolved starch is roughly an apparent zero-

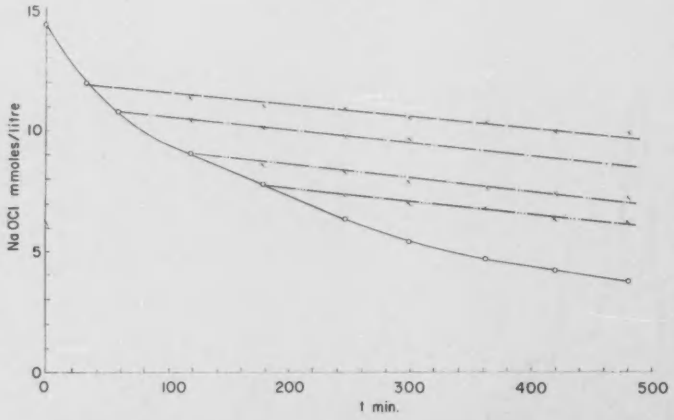

Fig. 5. Distribution of oxygen between suspended and dissolved starch pH 8. (O) Suspension, (×) filtered solutions.

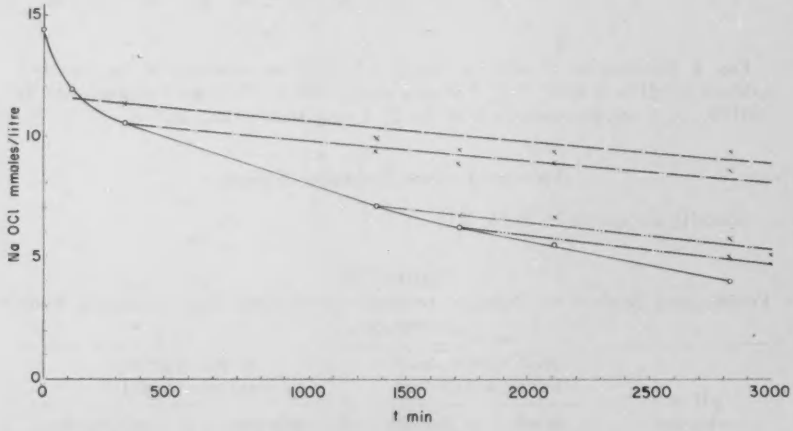

Fig. 6. Distribution of oxygen between suspended and dissolved starch at pH 10. (O) Suspension, (×) filtered solutions.

order reaction, and that the oxidant consumption in unit time remains approximately constant for a given pH.* By comparing the absolute amount of oxidant consumed by the suspension and the dissolved starch, respectively, in the course of the oxidation (the latter being allowed to proceed until 0.0525 atom of oxygen per AGU had been consumed in all) it could be calculated that about 26 and 28% of the total oxygen had been consumed by the dissolved starch at pH 8 and 10, respectively.

* This is irrespective of the time elapsed from the beginning of the oxidation of the suspension till the withdrawal and filtration of the sample.

TABLE VIII
Oxygen Balance

Molecular species	Amylose	Amylopectin	Amylose	Amylopectin
pH	8	8	10	10
Total oxygen consumed, atoms/AGU	0.0525	0.0525	0.0525	0.0525
Oxygen consumed by dissolved material, atoms/AGU	0.0137	0.0137	0.0150	0.0150
Oxygen consumed by undissolved material, atoms/AGU	0.0388	0.0388	0.0375	0.0375
	Undissolved Material Only			
Number-average DP	131	143	99	104
Carboxyls, groups/AGU	0.0125	0.0125	0.0185	0.0185
Carbonyls, groups/AGU	0.00588	0.00588	Nil	Nil
Carboxyls, groups/scission	1.64	1.79	1.83	1.93
Carbonyls, groups/scission	0.77	0.84	Nil	Nil
Oxygen consumed, groups/scission	5.09	5.55	3.72	3.90

Discussion

It is clear from the foregoing that the reaction between wheat starch and alkaline hypochlorite is not selective, and that at least two kinds of interaction may be distinguished: (*1*) formation of functional groups and (*2*) scission of glucosidic bonds (degradation).

There may also possibly be some oxidation beyond the glucose stage, as evidenced by the apparently excessive glucose recovery at pH 10 (cf. Table V).

Inspection of the results shows that the most conspicuous reaction occurring between alkaline hypochlorite and starch is the scission of glucosidic bonds, which may or may not have proceeded independently of the functional group formation. In what follows, the extent and the manner of that scission will be discussed.

The number-average molecular weights of both amyloses and amylopectins could be obtained from periodate measurements[13,14] within the error range indicated in Table VII. The weight-average molecular weights of each fraction could be calculated from the sedimentation velocity constant of the most frequent species, if Scheraga and Mandelkern's formula[18] is assumed to be valid. That formula is:

$$M = \left(\frac{\eta_0 N s_0}{\beta(1 - V\rho)}\right)^{3/2} [\eta^{1/2}]$$

where M is the molecular weight, s_0 is the sedimentation velocity constant extrapolated to zero concentration, ρ is the density of solvent, η_0 is the viscosity of solvent in poises, $[\eta]$ is the intrinsic viscosity of solute (cf. Table II), V is the partial specific volume of solute, N is Avogadro's number, and β is a hydrodynamic constant.

Since only an approximation was aimed at, the s value of the most frequent species at 1% concentration was equated to s_0 and η_0, V, ρ, and N were taken, respectively, as 1×10^{-2}, 0.6, 1 and 6×10^{23}, and β was taken as 2.6×10^6 and 2.13×10^6 for amylose and amylopectin, respectively.[18]

The viscosity-average DP of the amylose fraction was also calculated, using the modified form of the Staudinger equation developed by Husemann and co-workers[19] for 1% KOH solution as solvent:

$$[\eta] = 0.164 \times (\mathrm{DP})_{\mathrm{vis}}^{0.93}$$

Results are given in Table IX. It will be seen that for amylose, the viscosity-average DP is about twice the number-average DP, which would indicate random-type degradation; on this assumption, the ultracentrifugal sedimentation figures are low.

TABLE IX
Comparative DP Determinations
(pH = 8; oxygen absorbed: 0.0525 atom/AGU)

Molecular species	No.-av. DP (periodate)	$s \times 10^{13}$	Intrinsic viscosity	Wt.-av. DP[a]	Viscosity-av. DP[b]
Amylose	131 ± 9	2	0.28	128	250
Amylopectin	143 ± 4	2.5	0.25	229	—

[a] See ref. 18.
[b] See ref. 19.

It has been shown by Erlander and French[20] that in a sample of amylopectin having a random distribution of DP's, the weight-average:number-average DP ratio will depend on the structural model assumed for amylopectin, on the degree of branching, and on the molecular size itself. Formulas have been developed by these authors by means of which the number-average DP can be calculated if the weight-average DP is known and vice versa.

The repeating chain unit of the amylopectin sample was 21, and the number- and weight-average DP's were 115 and 229, respectively; when the calculations were carried out, it was found that neither the fully random statistical model nor the less random model V fitted the experimental results, though the latter model approached them much more closely than the former.

Expressions have been derived[21] for the distributions of molecular weights in a chain polymer degraded to the extent α; as α increases, the resulting chain mixture becomes at first less, then more homogeneous;

the peak of the most frequent species moves toward the ordinate axis first quite fast, then very slowly; there is a "tail" of high molecular weight material, which disappears at a later stage, but no corresponding tail of low molecular weight material. These considerations were shown to be essentially valid, irrespective of whether the original material was homogeneous or had an initially normal distribution.

An inspection of Figures 2, 3, and 4 will show that all these features are conspicuously present in whole starch, amylose, and amylopectin; this may be interpreted as indicative of a random type of degradation.

Additional insight into the nature of the reaction between wheat starch and hypochlorite may be gained on considering the oxygen balance.

Since, as has been seen, it is plausible to assume random degradation, it was thought interesting to attempt correlating the number of glucosidic bonds scinded on one hand, and the number of oxygen atoms adsorbed and of the functional groups formed per scission on the other. Such a correlation has actually been found for the oxidation of cotton in the 5–10 pH range.[22]

The calculations set out in Table VIII were carried out on *undissolved* starch only. It has been assumed that the weight percentage of the material passing into solution is the same for both amylose and amylopectin. Since the amount of oxygen consumed by the dissolved starch was known (cf. Results above), the amount of oxygen consumed by the undissolved material was taken to be the difference between that value and the total amount of oxygen consumed. Since, furthermore, the number-average DP was known (Table VII) as was the amount of carboxyl and carbonyl groups formed per AGU of the undissolved material (Table III), the following relationships could be applied:

Atoms of oxygen consumed per scission

$$= \text{atoms of oxygen consumed per AGU} \times \text{number-average DP}$$

Functional groups formed per scission

$$= \text{groups formed per AGU} \times \text{number average DP}$$

The results of the calculations set out in Table VIII indicate that the scission of one glucosidic bond is accompanied by the consumption of 4–5 atoms of oxygen and by the formation of nearly 2 carboxyl groups and up to one carbonyl group.

The number of oxygen atoms consumed per scission could be independently checked by making use of the solubility data in Table V and assuming the validity of certain molecular models. Kuhn[23] gives the following formulas for the weight fraction $F(n)$ and the number fraction $W(n)$ of fragments having a DP equal to n and formed from an originally infinite chain degraded to the extent α

$$W(n) = \alpha(1 - \alpha)^{n-1}$$
$$F(n) = n\alpha^2(1 - \alpha)^{n-1}$$

The number of oxygen atoms consumed per scission in amylose was calculated as follows: The proportion of the bonds scinded α was first calculated, using a formula developed elsewhere:[14]

$$\alpha = \frac{F_\alpha - F}{3}$$

where F and F_α are the number of moles of formic acid evolved per AGU-mole of the original and the oxidized starch, respectively (Table VII). The function $F(n)$ was then summated over $n = 1, 2, 3, \ldots k$ so as to make the value of $\sum_{n=1}^{k} F(n)$ numerically equal to the weight fraction of the starch dissolved, given in Table V.

The highest DP value of the amylose still in solution was then equal to k. The value of k thus obtained was then used to calculate $\sum_{n=1}^{k} W(n)$, the number fraction of the molecules dissolved. Since number-average DP is defined as the ratio of the total number of AGU's to the total number of molecules, the true number-average DP (i.e., that of the combined dissolved and undissolved material) could be obtained from the following relationship:

$$\text{Number-average DP of undissolved material} = \text{true number-average DP} \times \left[\frac{1 - \sum_{n=1}^{k} F(n)}{1 - \sum_{n=1}^{k} W(n)}\right]$$

and the number of oxygen atoms consumed per scission from the relationship:

$$\text{Oxygen atoms/scission} = \text{total oxygen atoms/AGU} \times \text{true number-average DP}$$

For amylopectin, the "less random model V" of Erlander and French[20] was assumed to be valid. The value of their statistical parameter β was calculated from the equation:

$$\text{Number-average DP of undissolved material} = Y/(1 - 2\beta) \text{ (from Table VII)}$$

where Y was the repeating chain length of the oxidized product.[14]

According to Erlander and French[20] the weight fraction $F(n)$ is then given by the expression:

$$F(n) = \left[\frac{(1 - 2\beta)(1 - \beta)}{\beta}\right] [(1 - \beta)\beta]^n \frac{(2n)!}{(n - 1)!\,(n + 1)!}$$

When the calculations were performed, it was found that monomeric fragments accounted by themselves alone for the entire material dissolved, i.e., $\sum_{n=1}^{k} F(n) = F(1)$ and $k = 1$. Since, for the value of β here employed, the

theoretical values of $F(n)$ diminish quite rapidly as n increases, the value of $W(1)$ could be easily obtained from the expression:

$$W(1) = \frac{F(1)}{\sum_{n=1}^{k} F(n)}$$

The calculations were then completed as for amylose and resulted in the approximate value of 4–5 atoms of oxygen consumed per scission (Table X), in fair agreement with the value in Table VIII.

It will be noted that the values of α and β have been calculated on the undissolved portion only, instead of on the total (dissolved and undissolved) starch. It may be shown[23] that the error thus introduced is negligible.

The resulting values of k appear to be too high for amylose and much too low for amylopectin, but are, surprisingly enough, in rough agreement with the experimental values for the apparent DP of the dissolved material as given in Table V. The *maximum* DP of the amylose dissolved at pH 8 is 60 according to Table X; taking 30 as the average value, the apparent DP of the dissolved starch will be $(0.2 \times 30 + 0.8 \times 1)$ or about 7, as compared with 3 given in Table V. A similar estimate for pH 10 gives the apparent DP as $(0.2 \times 17 + 0.8 \times 1)$, or about 4, as compared with 17 given in Table V; it is quite possible, however, that the latter value is too high,

TABLE X
Oxygen Consumed per Scission from Solubility Data

Molecular species	Amylose	Amylopectin	Amylose	Amylopectin
pH	8	8	10	10
Oxygen consumed, atoms/AGU	0.0525	0.0525	0.0525	0.0525
Wt.-% of starch dissolved, $= \sum_{n=1}^{k} F(n)$	6.4	6.4	3.8	3.8
No. % of molecules, dissolved, $= \sum_{n=1}^{k} W(n)$	34	41	29	26
Highest DP dissolved, $(=k)$	60	1	34	1
No.-av. DP of undissolved starch	131	143	99	104
Calcd. approx. No.-av. DP of total starch	90	90	80	80
Oxygen/scission, atoms	4.72	4.72	4.20	4.20

owing to a higher proportion of the reducing groups being oxidized to carboxyls at that pH value.

From the theoretical point of view the low value of k for amylopectins is a direct consequence of the molecular model adopted, whereas the rather high value of k for amyloses may perhaps be at least partly explained by assuming a solubilizing effect of the sodium carboxylates presumably formed on each amylose molecule.

It is noteworthy that in the case of the oxidation of cotton *ca.* 26 atoms of oxygen were found to be consumed per each scission,[22] as compared to 4–5 atoms found in the present work for wheat starch in similar experimental conditions. This seems to constitute a basic difference between the behavior of cotton and starch.

Summary and Conclusions

1. An attempt was made to elucidate the changes brought about in granular wheat starch, resulting from a mild oxidation by alkaline hypochlorite.

2. The reaction apparently takes place in the amorphous part of the granule, as no change in the x-ray pattern or its intensity was observed in oxidized starches.

3. The reactions found to take place were formation of functional groups and scission of glucosidic bonds.

4. The ultracentrifugal frequency distribution of molecular weights in oxidized samples appears to depend only on the amount of oxidant consumed and not on the pH of oxidation. The shape of the distribution curves of amylose and amylopectin components may indicate random-type degradation.

5. The consumption of about 0.0525 oxygen atoms/AGU was accompanied by extensive degradation of both starch components. The proportion of the glucosidic bonds thus broken was about 0.5 to 1%. The resulting DP's were 100–130 and 104–143 for amylose and amylopectin, respectively.

6. A study of the oxygen balance indicated that the scission of one glucosidic bond was accompanied by the consumption of 4–5 atoms of oxygen and by the formation of about two carboxyl groups. Carbonyl groups were formed in smaller amounts at pH values of 8 or lower.

The technical assistance of Miss J. Bel-Ayche and Miss E. Lipkin is gratefully acknowledged.

References

1. Schmorak, J., D. Mejzler, and M. Lewin, *J. Polymer Sci.*, **49**, 203 (1961).
2. MacKillican, M. E., and C. B. Purves, *Can. J. Chem.*, **32**, 312 (1954).
3. Rassow, B., and M. Lobenstein, *Kolloid Beih.*, **33**, 179 (1931).
4. Hullinger, C. H., and R. L. Whistler, *Cereal Chem.*, **28**, 153 (1951).
5. Whistler, R. L., E. G. Linke, and S. Kazeniac, *J. Am. Chem. Soc.*, **78**, 4704 (1956); R. L. Whistler and R. Schweiger, *ibid.*, **79**, 6460 (1957).

6. Farley, F. F., and R. M. Hixon, *Ind. Eng. Chem.*, **34**, 677 (1942).
7. Lansky, S., M. Kooi, and T. J. Schoch, *J. Am. Chem. Soc.*, **71**, 4066 (1949).
8. Haworth, W. N., S. Peat, and P. E. Sagrott, *Nature*, **157**, 19 (1946).
9. Wilson, E. J., Jr., T. J. Schoch, and C. S. Hudson, *J. Am. Chem. Soc.*, **65**, 1380 (1943).
10. Elizer, H., *Ind. Eng. Chem. Anal. Ed.*. **14**, 635 (1942).
11. Schmorak, J., and M. Lewin, *Anal. Chem.*, **33**, 1403 (1961).
12. Sloan, J. W., B. T. Hofreiter, R. L. Mellies, and I. A. Wolff, *Ind. Eng. Chem.*, **48**, 1165 (1956).
13. Schmorak, J., D. Mejzler, and M. Lewin, *J. Polymer Sci.*, **55**, 437 (1961).
14. Mejzler, D., J. Schmorak, and M. Lewin, *J. Appl. Polymer Sci.*, **7**, 1557 (1963).
15. Williams, J. W., R. L. Baldwin, W. M. Saunders, and P. G. Squire, *J. Am. Chem. Soc.*, **74**, 1542 (1952).
16. Noyes, W. A., G. Crawford, C. H. Jumper, E. L. Flory, and R. B. Arnold, *J. Am. Chem. Soc.*, **26**, 266 (1904).
17. Katz, J. R., and T. B. van Itallie, *Z. Physik. Chem. (Leipzig)*, **A150**, 90 (1930).
18. Scheraga, H. A., and L. Mandelkorn, *J. Am. Chem. Soc.*, **75**, 179 (1953).
19. Husemann, E., W. Burchard, B. Pfannemueller, and R. Werner, *Staerke*, **13**, 196 (1961).
20. Erlander, S., and D. French, *J. Polymer Sci.*, **20**, 7(1956).
21. Grassie, N., *The Chemistry of High Polymer Degradation Processes*, Butterworths, London, 1956, ch. 3.
22. Epstein, J. A., and M. Lewin, *Textil Rundschau* **16**, No. 9/10, (1961), p. 494.
23. Kuhn, W., *Ber.*, **63**, 1503 (1930).
24. Mejzler, D., unpublished results.

Résumé

On a essayé d'élucider la nature de la réaction entre les hypochlorites alcalins et l'amidon de blé. Dans ce but on a effectué différentes déterminations analytiques sur des échantillons d'amidon oxydé dans des conditions bien déterminées. On a trouvé que la réaction n'était pas spécifique et consistait principalement dans la formation de groupements fonctionnels et la scission des liaisons glucosidiques. Les groupements fonctionnels formés sont principalement des groupes carboxylés. Il se forme quelques groupes carbonyles à des valeurs de pH plus faibles. La consommation d'environ 0.05 atome d'oxygéne/AGU résulte d'une dégradation poussée des deux composants de l'amidon. Il y a des indications qui montrent que la dégradation est du type statistique. En supposant cela, sur 100 liaisons glucosidiques, il y en a 0.5 à 1 de scindée, chaque scission étant accompagnée de la formation d'environ deux groupes carboxyles et d'une consommation totale de 4–5 atoms d'oxygène. La réaction s'effectue apparemment dans la partie amorphe du grain. Le rapport amylose-amylopectine, ainsi que la dimension du grain restent inchangés. Plus d'un quart de l'oxygène total consommé réagit avec la partie de l'amidon dissoute, résultat de l'oxydation.

Zusammenfassung

Ein Versuch zur Aufklärung der Natur der Reaktion zwischen alkalischem Hypochlorit und gekörnter Weizenstärke wurde unternommen. Unter diesen Gesichtspunkten wurden verschiedene analytische Bestimmungen an unter gut definierten Bedingungen oxydierten Stärkeproben ausgeführt. Die Reaktion erwies sich als nicht spezifisch und führte in der Hauptsache zur Bildung funktioneller Gruppen und zur Spaltung glukosidischer Bindungen. Die gebildeten funktionellen Gruppen waren vornehmlich Karboxylgruppen, bei niedrigen pH-Werten trat auch aine gewisse Bildung von Karbonylgruppen auf. Der Verbrauch von etwa 0,05 Atomen Sauerstoff/AGU führte zu einem weitgehenden Abbau beider Stärkekomponenten. Es bestehen Hinweise auf eine statistische Natur

des Abbaus. Unter dieser Annahme wurden 0,5 bis 1 glukosidische Bindung gespalten wobei jede Spaltung von der Bildung von etwa zwei Karboxylgruppen und einem Bruttoverbrauch von 4–5 Sauerstoffatomen begleitet war. Die Reaktion fan doffenbar im amorphen Teil des Kornes statt. Das Amylose-Amylopektinverhaltnis und auch die Korngrösse blieben unverändert. Mehr als ein Viertel des verbrauchten Sauerstoffs reagiert mit dem als Folge der Oxydation in Lösung gegangenen Teil der Stärke.

Received May 18, 1962

JOURNAL OF POLYMER SCIENCE: PART A VOL. 1, PP. 2621–2650 (1963)

Infrared Spectra and Assignments for Polyvinyl Chloride and Deuterated Analogs

S. KRIMM, *Harrison M. Randall Laboratory of Physics, University of Michigan, Ann Arbor, Michigan*, and V. L. FOLT, J. J. SHIPMAN, and A. R. BERENS, *The B. F. Goodrich Company Research Center, Brecksville, Ohio*

Synopsis

Deuterated analogs of polyvinyl chloride (PVC) have been prepared and their infrared spectra analyzed as an aid to the more detailed assignment of bands in the spectrum of PVC. The following deuterated polymers were studied: PVC-αd_1, PVC-βd_1, PVC-$\alpha\beta d_2$, and PVC-d_3. These, as well as PVC, were polymerized in urea-complex, at −78°C., and at +50°C. in order to determine which bands are of crystalline origin and which of noncrystalline origin. Polarized spectra of oriented samples were obtained in each case to assist in the analysis. As a result of this study several of the previously uncertain assignments have been clarified. With the help of other studies on model chlorine-containing compounds it has been possible to identify the various conformations present in the polymer and to associate these with isotactic and syndiotactic pair configurations in the chain. A method is suggested for determining the proportion of each type of pair configuration in PVC.

INTRODUCTION

The infrared spectrum of polyvinyl chloride (PVC) has been the subject of several studies directed toward the detailed assignment of its spectral bands.[1–5] In part this was motivated by a desire to check the predictions of early x-ray work,[6] which had indicated that a major component of the structure is to be attributed to a syndiotactic chain configuration. Much evidence has accumulated, both x-ray[7] and infrared,[8–11] which supports the presence of a syndiotactic structure in PVC. A completely satisfactory analysis of the spectrum however, remains to be presented. A normal coordinate treatment has been given,[4] but in view of our presently limited knowledge of force fields in macromolecules it is necessary to verify such assignments experimentally. One way of doing this is by studying deuterated molecules, and in this paper we will discuss the assignments of bands in the PVC spectrum in terms of the analysis of the spectra of various deuterated PVC's. As will be seen, a fairly complete set of assignments of the bands above 500 cm.$^{-1}$ can be made.

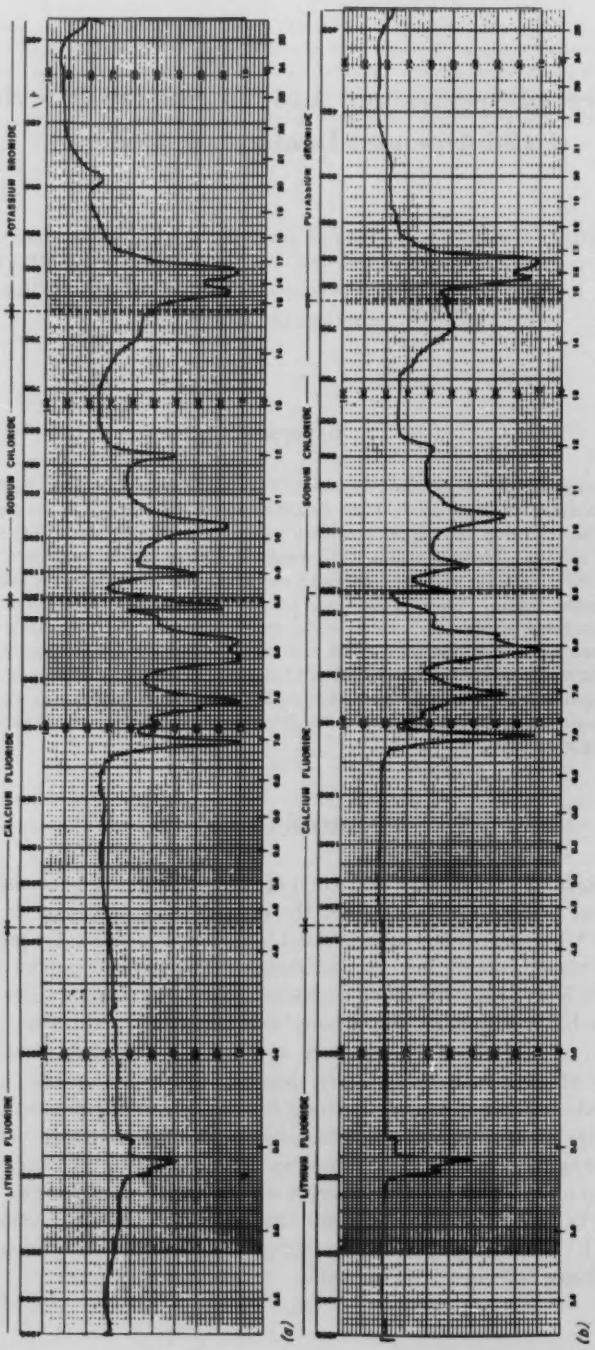
LITHIUM FLUORIDE
CALCIUM FLUORIDE
SODIUM CHLORIDE
POTASSIUM BROMIDE
(a)
(b)

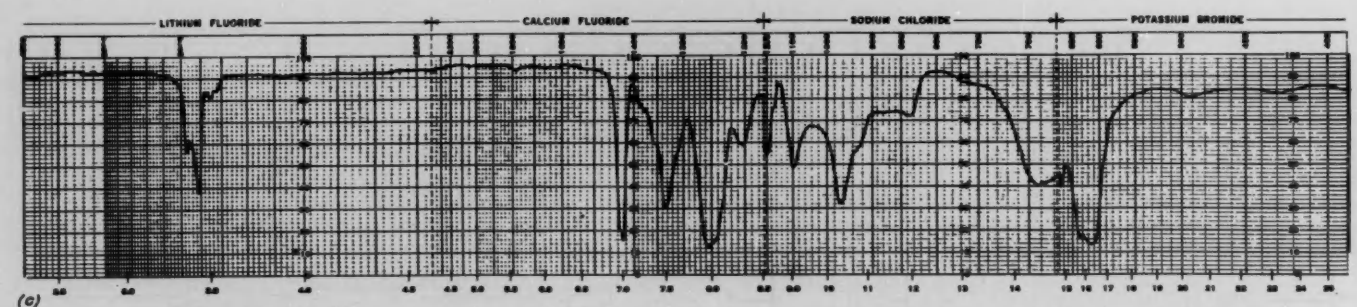

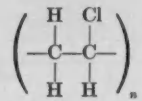

Fig. 1. Infrared spectra of polyvinyl chloride (from top to bottom): (*a*) polymerized in urea-complex; (*b*) polymerized at −78°C.; (*c*) polymerized at +50°C.; (*d*) polarized spectrum of oriented +50°C. polymer; (——) radiation with electric vector perpendicular to stretching direction, (- - - -) radiation with electric vector parallel to stretching direction.

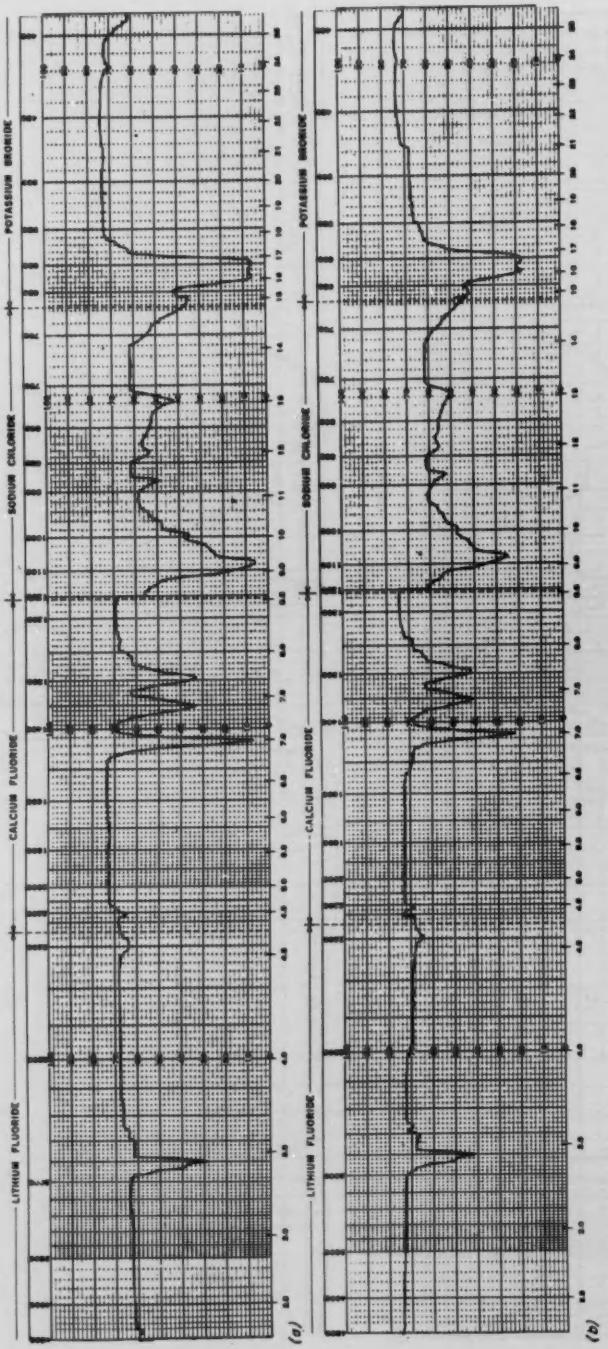
LITHIUM FLUORIDE
CALCIUM FLUORIDE
SODIUM CHLORIDE
POTASSIUM BROMIDE
(a)
(b)

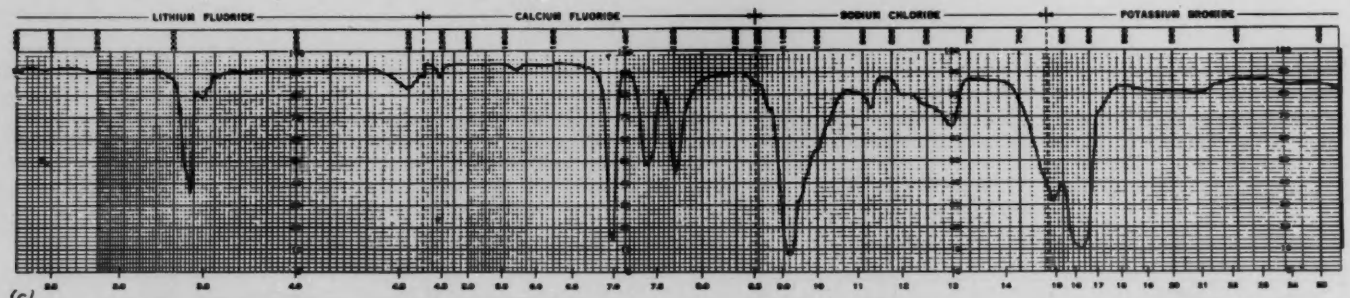

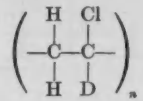

Fig. 2. Infrared spectra of polyvinyl chloride-ad_1 (from top to bottom): (*a*) polymerized in urea-complex; (*b*) polymerized at −78°C.; (*c*) polymerized at +50°C.; (*d*) polarized spectrum of oriented +50°C. polymer; (——) radiation with electric vector perpendicular to stretching direction; (- - - -) radiation with electric vector parallel to stretching direction.

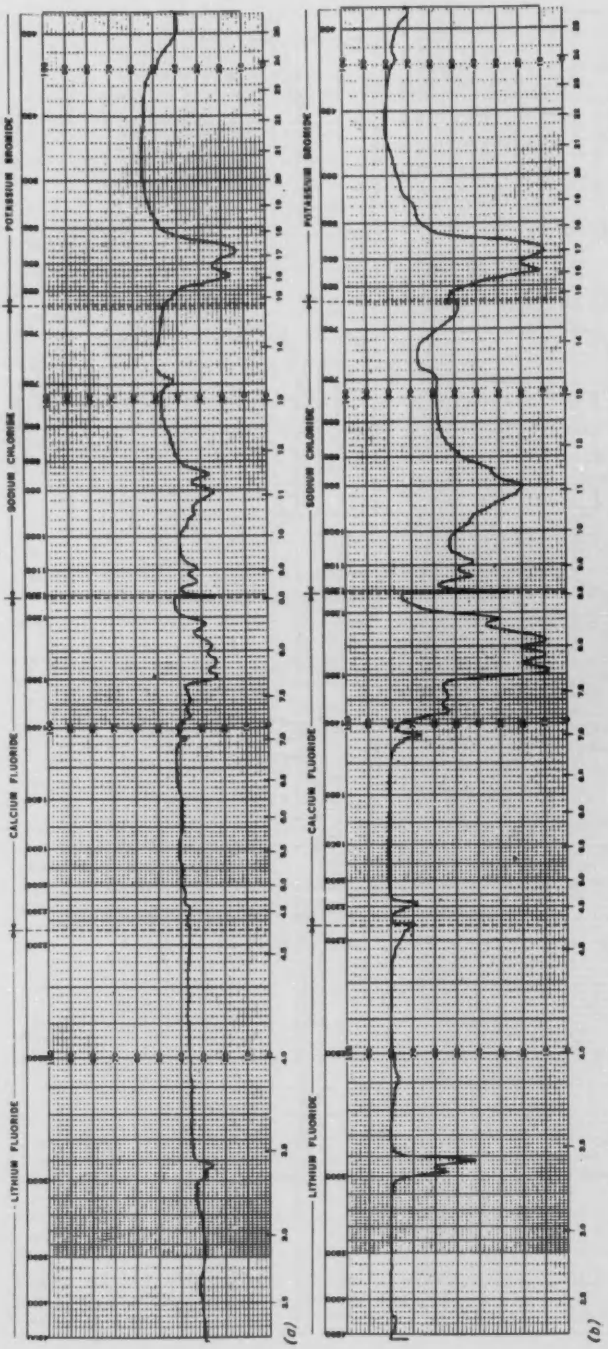
LITHIUM FLUORIDE
CALCIUM FLUORIDE
SODIUM CHLORIDE
POTASSIUM BROMIDE
(a)
(b)

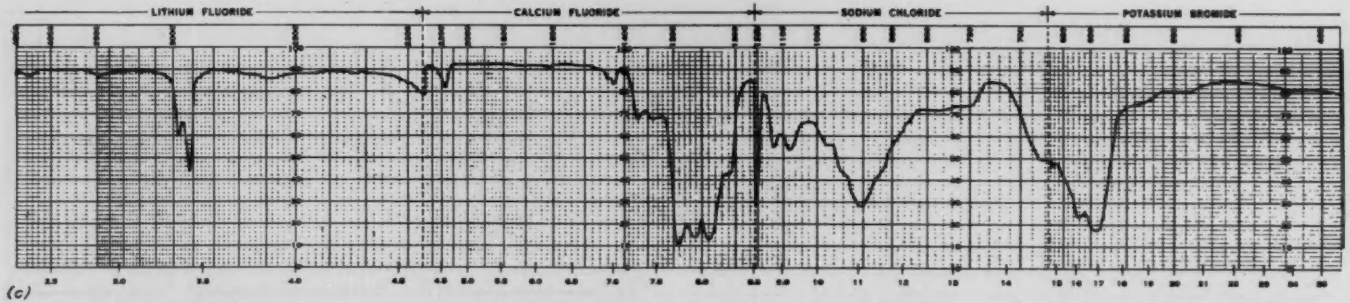

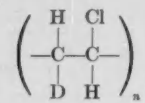

Fig. 3. Infrared spectra of polyvinyl chloride-βd_1 (from top to bottom): (*a*) polymerized in urea-complex; (*b*) polymerized at −78°C.; (*c*) polymerized at +50°C.; (*d*) polarized spectrum of oriented +50°C. polymer; (——) radiation with electric vector perpendicular to stretching direction, (- - - -) radiation with electric vector parallel to stretching direction.

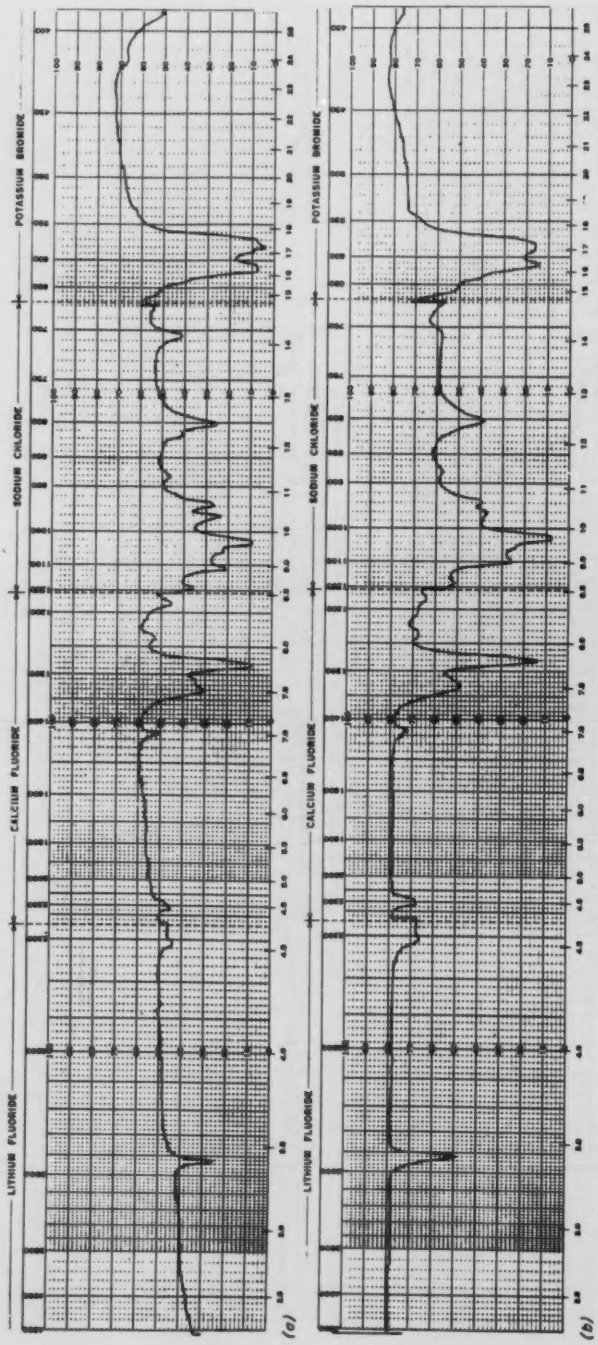
LITHIUM FLUORIDE
CALCIUM FLUORIDE
SODIUM CHLORIDE
POTASSIUM BROMIDE
(a)
(b)

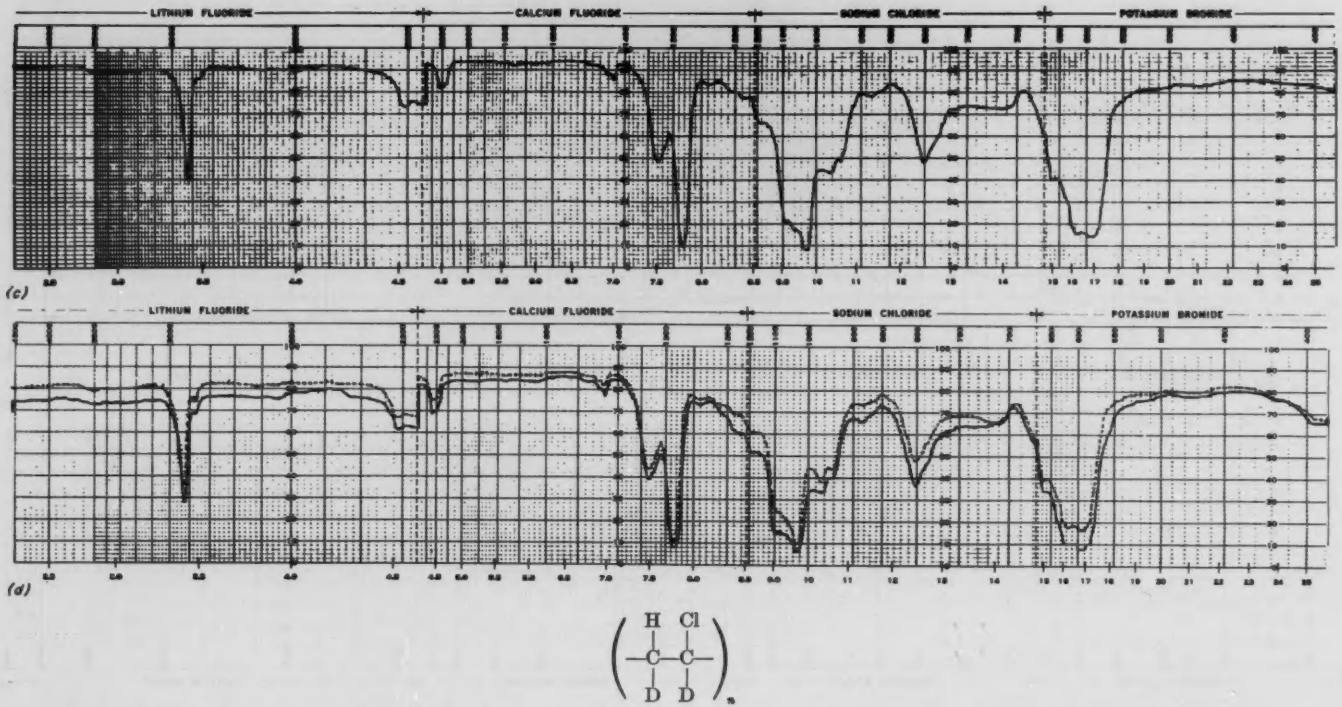

$$\left(\begin{array}{cc} H & Cl \\ | & | \\ -C- & -C- \\ | & | \\ D & D \end{array}\right)_n$$

Fig. 4. Infrared spectra of polyvinyl chloride-$\alpha\beta d_2$ (from top to bottom): (*a*) polymerized in urea-complex; (*b*) polymerized at −78°C.; (*c*) polymerized at +50°C.; (*d*) polarized spectrum of oriented +50°C. polymer; (——) radiation with electric vector perpendicular to stretching direction, (- - - -) radiation with electric vector parallel to stretching direction.

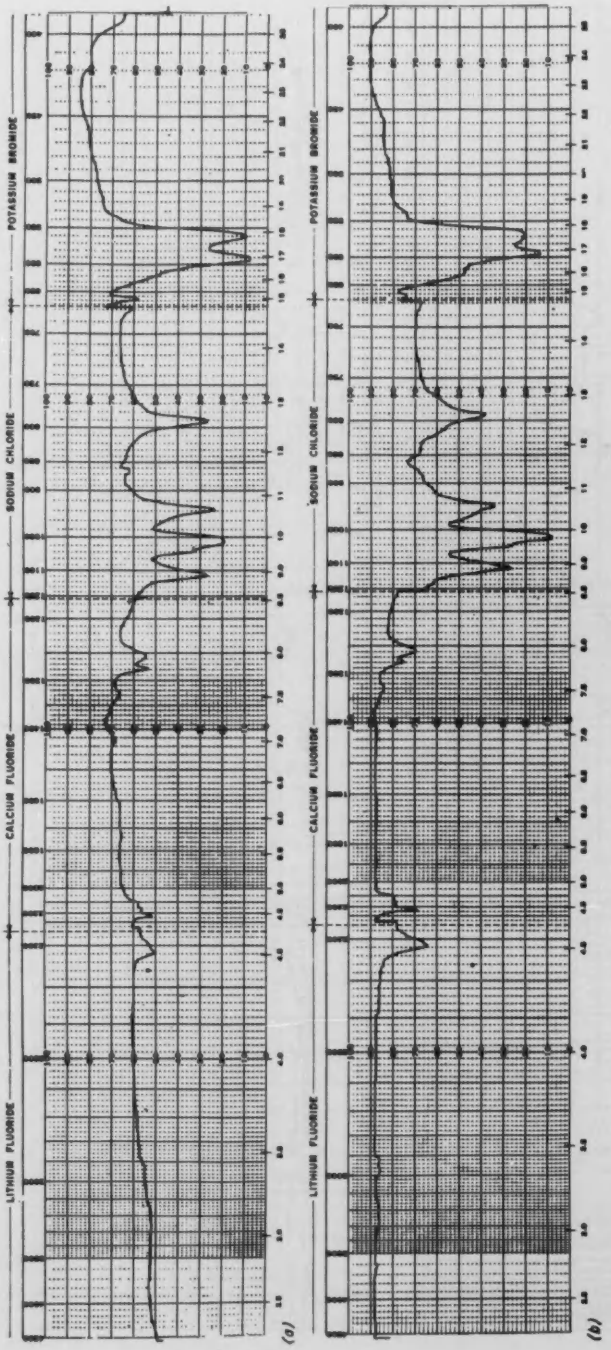
LITHIUM FLUORIDE
CALCIUM FLUORIDE
SODIUM CHLORIDE
POTASSIUM BROMIDE
(a)
(b)

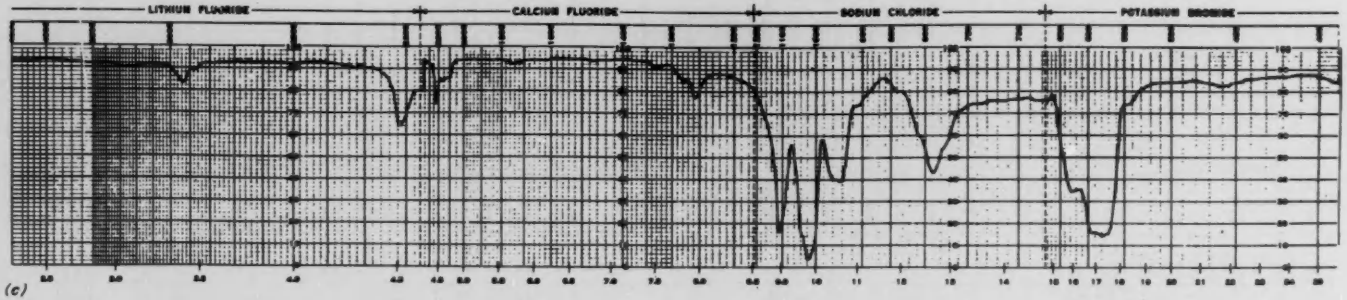

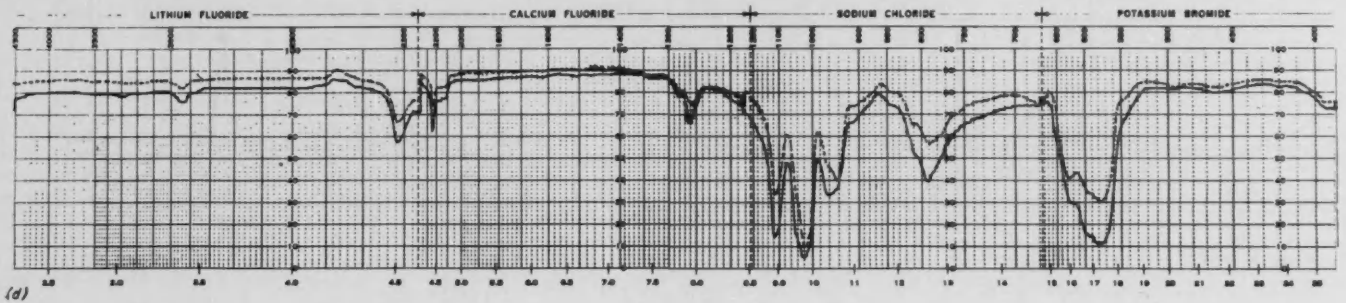

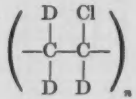

Fig. 5. Infrared spectra of polyvinyl chloride-d_3 (from top to bottom): (*a*) polymerized in urea-complex; (*b*) polymerized at −78°C.; (*c*) polymerized at +50°C.; (*d*) polarized spectrum of oriented +50°C. polymer; (——) radiation with electric vector perpendicular to stretching direction, (- - - -) radiation with electric vector parallel to stretching direction.

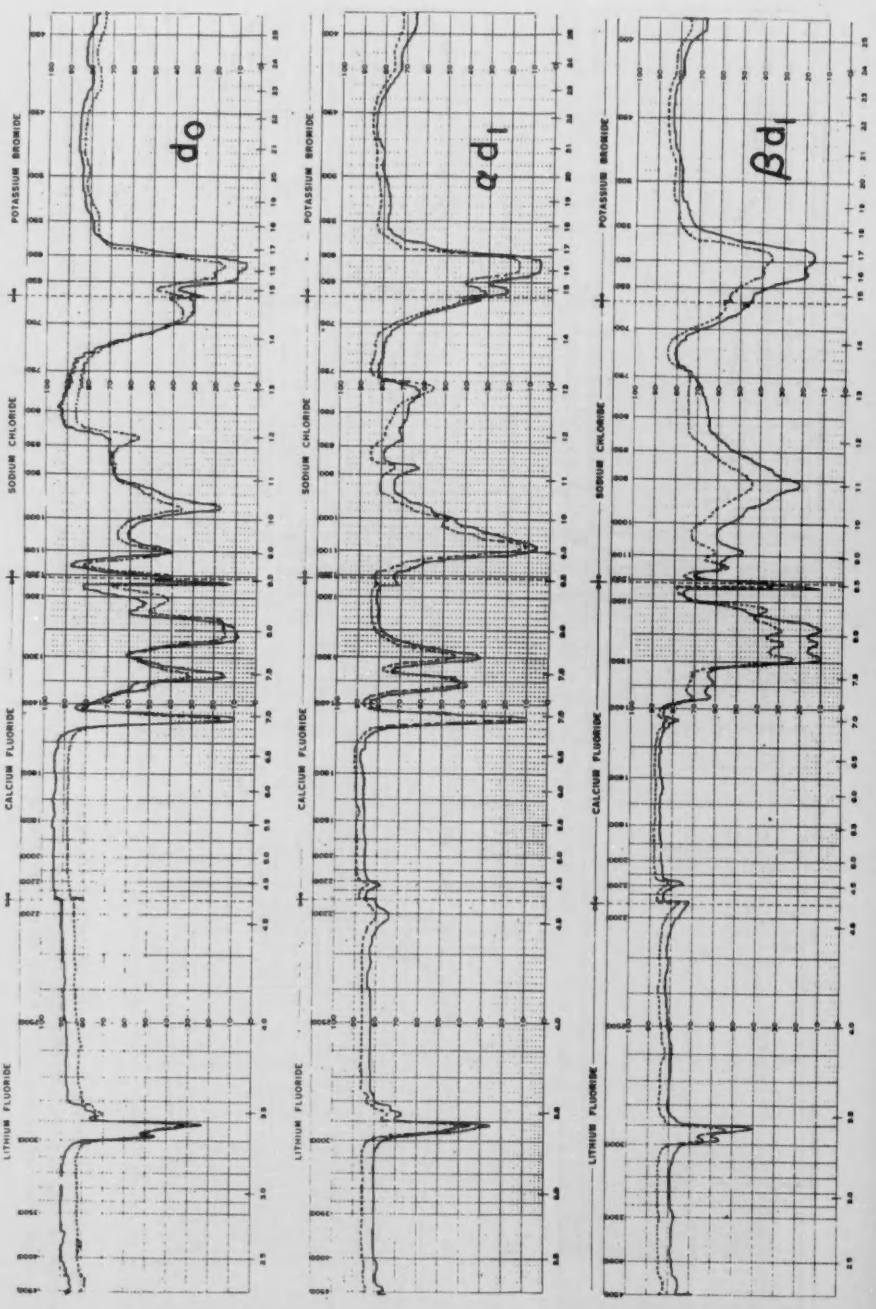
LITHIUM FLUORIDE
CALCIUM FLUORIDE
SODIUM CHLORIDE
POTASSIUM BROMIDE
d_0
αd_1
βd_1

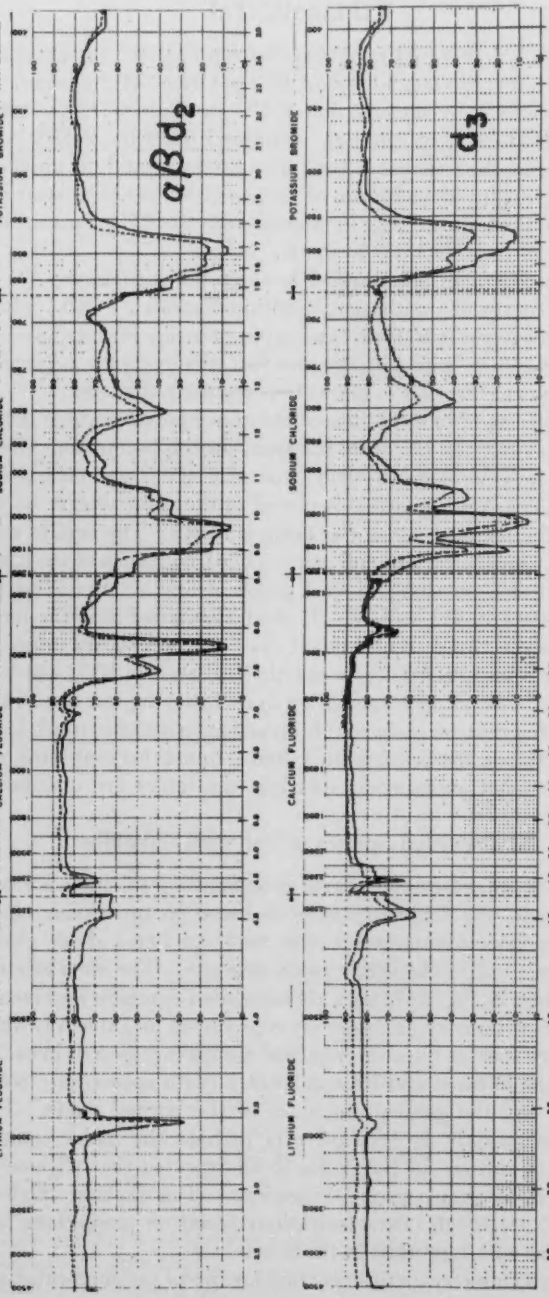

Fig. 6. Polarized infrared spectra of +50°C. polymers of polyvinyl chloride and deuterated analogs, (——) radiation with electric vector perpendicular to stretching direction, (- - - -) radiation with electric vector parallel to stretching direction.

EXPERIMENTAL

The following deuterated monomers were prepared: (*a*) vinyl chloride-βd_1, CHD=CHCl, by the addition of DCl to CH≡CH; (*b*) vinyl chloride-$\alpha\beta d_2$, CHD=CDCl, by the addition of HCl to CD≡CD; (*c*) vinyl chloride-αd_1, CH_2=CDCl, by the light catalyzed addition of DBr to CH_2 = CCl_2 followed by the removal of BrCl with Zn dust; and (*d*) vinyl chloride-d_3, CD_2 = CDCl, by the addition of DCl to CD≡CD. Nuclear magnetic resonance studies indicate that in monomer (*a*) the Cl is *trans* to the D and in monomer (*b*) the Cl is *trans* to the H.

The monomers were polymerized in three different ways: (*1*) in urea-complex, by means of γ-radiation;[12] (*2*) in ethanol at −78°C. with tri-isobutyl borane-oxygen initiation; and (*3*) in peroxide initiated aqueous suspension at +50°C. Low temperature and urea-complex polymerizations have been shown[8,9] to lead to more stereoregular polymers.

Infrared spectra of pressed films of the above polymers were obtained on the B. F. Goodrich double beam infrared spectrophotometer. Samples of the +50°C. polymer were stretched from 300–400% and polarized spectra obtained. (The AgCl polarizer is placed in the spectrometer between the source and the point at which the beam is split.) The results are shown in Figures 1–6 for the various polymers. The frequencies of the bands, their relative intensity, polarization, and phase of origin (crystalline or amorphous) are listed in Tables I–V. It should be noted that the term amorphous as used in the present context does not necessarily imply that the polymer component referred to is atactic.[13] Bands in PVC which show an inversion of dichroism with increasing draw ratio[5] are indicated in Table I. It is interesting that we observe this inversion to occur at much lower draw ratios, 10–20%, on the pressed films than is found[5] for cast films, viz., over 250%. The band assignments listed in the tables are discussed below.

Predicted Spectra of Polyvinyl Chlorides

Although in the crystalline form of syndiotactic PVC there are two chains in the unit cell,[7] the symmetry analysis based on two chains[3] does not at present seem more advantageous than that based on a single chain.[1] We will, therefore, utilize the single chain analysis. The structure of such a chain is shown in Figure 7, with its associated symmetry elements. The results of the symmetry analysis[1] are reproduced in Table VI, which gives the symmetry species, number of normal modes (n_i) present in each species, activity in the infrared and Raman spectra (with appropriate polarization properties), and the general character of the normal mode. The latter should be taken only as descriptive of perhaps the major component of the normal vibration, since it is not to be expected that all modes can be characterized as simple group vibrations. The skeletal modes, $\nu_+(0)$, $\nu(\pi/2)$, etc., are rough characterizations based on predictions for planar zig-zag chains with four units in the repeat.[14]

The above symmetry analysis is valid for two of the deuterated polymers,

TABLE I
Infrared Spectrum and Assignments for Polyvinyl Chloride

Frequency, cm.$^{-1}$	Polarization	Relative intensity	Phase[b]	Assignment[c]
418		vw	C	
~427	π?	vw	A	
492	π	vw	C	
540	π	vw	A	ν(CCl)T_{HHH}
570		vw(sh)	C	
588	σ	vw(sh)	A	ν(CCl) T_{HHC}
604	σ[a]	s	C	ν(CCl) B_1
615	σ	s	A	ν(CCl) S_{HH} (A)
~638	σ	ms	A	ν(CCl) S'_{HH} (A)
640	σ	ms	C	ν(CCl) A_1
685	σ	m	A	ν(CCl) S_{HC} (A)
693	π			
~710		vvw(sh)	A	ν(CCl) S'_{HC} (A)
768		vw	A	ν(CCl) S_{CC} (A)
835	π	mw	C	γ_r(CH$_2$) B_2
840	σ			
~880	π	vw	A	
~925	σ	w(sh)	A	
960	σ[a]	ms	C	γ_r(CH$_2$) B_1
970	σ	ms	A	γ_r(CH$_2$) (A)
~1030		vvw	C	
1090	σ[a]?	mw(sh)	C	$\nu_+(\pi/2)$ B_1
1105	σ	m	C,A	ν_+(O) A_1; ν_+(O) (A)
1122	π	w	A	$\nu_+(\pi)$ (A)
1170	σ	vw(sh)	A	
1195	π	w	C	$\nu_+(\pi)$ B_2
1203	π	w	A	γ_w(CH) (A)
1210	σ			
1230	π	mw	C	γ_w(CH) B_2
1245	σ	m(sh)	A	δ(CH) (A)
1258	σ[a]	s	C	δ(CH) B_1
1310	σ	vw(sh)	A	γ_t(CH$_2$) (A)
1338	σ	ms	C	δ(CH) A_1 (+ γ_t(CH$_2$) A_1?)
1355	σ[a]	w	C	γ_w(CH$_2$) B_1
1365	σ	w	A	γ_w(CH$_2$) (A)
1387	π	w	C	γ_w(CH$_2$) B_2
1428	σ	s	C	δ(CH$_2$) A_1
1438	σ	m	A	δ(CH$_2$) (A)
~1780		vvw		
2810	π?	vw	C	δ(CH$_2$)A$_1$ + γ_w(CH$_2$)B$_2$ = 2815 B_2
2820	σ?	vw	C	
2850	σ	vw	A	ν_s(CH$_2$) (A)?
2910	σ	s	C,A	ν_s(CH$_2$) A$_1$
2930	σ?	w	C,A	ν_a(CH$_2$) B$_1$
2970	σ	mw	C,A	ν(CH) A$_1$ and B$_1$

[a] Bands show π dichroism at low draw ratios.

[b] A: amorphous, C: crystalline.

[c] ν stretching, δ: bending, γ_w: wagging, γ_t: twisting, γ_r: rocking, s: strong, m: medium, w: weak, vw: very weak.

TABLE II
Infrared Spectrum and Assignments for Polyvinyl Chloride-αd_1

Frequency, cm.$^{-1}$	Polarization	Relative intensity	Phase	Assignment
418		vw		
480	σ	vw	A	
~567	σ	vvw		
~577	σ	vvw		
598	σ	s	C	ν(CCl) B_1
615	σ	s	A	ν(CCl) S_{HH}
625	σ	s	C,A	ν(CCl) A_1 and S'_{HH}
670	σ	m	A	ν(CCl) S_{HC}
676	π			
~700		vvw	C	
~730		vvw	A	
769	π	m	C	
775	σ			
805	σ	vw	A	
835	σ	w	C?	
883	π	mw	C,A	
888	σ			
970	σ	vvw		
1000	π	vw	C?	γ_w(CD)?
1020	σ	vw	C?	
~1080	σ	s		δ(CD) + ν_+(O)?
1110		vvw	C?	
1160		vvw		
~1240		vvw	C?	
1260		vvw	C	
1297	σ	ms		$\gamma_t(CH_2)$ A_1
1340	σ	w(sh)	A	
1353	π	ms		$\gamma_w(CH_2)$ B_2
1360	σ			$\gamma_w(CH_2)$ B_1
1430	σ	s	C	$\delta(CH_2)$ A_1
1440	σ	m	A	
~1510	σ	vw		
1750	π	vw		
2200	σ	w	C,A	ν(CD) A_1 and B_1
2780	π	vw		$\delta(CH_2)$ A_1 + $\gamma_w(CH_2)$ B_2 = 2783 B_2
~2815	σ	w		
2860	σ	w	A	$\nu(CH_2)(A)$
2910	σ	s	C,A	$\nu(CH_2)$ A_1
2935		mw(sh)	C,A	$\nu(CH_2)$ B_1

viz., PVC-αd_1 and PVC-d_2, since their symmetry in the planar zig-zag syndiotactic form is the same as that of PVC. The forms of the normal modes, however, may not be as simple as given in Table VI. It is likely that the CH modes of PVC can be replaced to first approximation by CD modes in PVC-αd_1. The situation probably is more complex in PVC-d_2, since normal vibration calculations[4] indicate a strong coupling between different modes. While the symmetry of a given vibration is unaltered, the mode

TABLE III
Infrared Spectrum and Assignments for Polyvinyl Chloride-βd_1

Frequency, cm.$^{-1}$	Polarization	Relative intensity	Phase	Assignment
418		vw		
488	σ	vw	A	
530	σ	vw	A	
560	σ	w(sh)	A	
580	σ	s	C	ν(CCl) B_1
592	σ	s	A	ν(CCl) S_{HH}
622	σ	s	C,A	ν(CCl) A_1 and S'_{HH}
~680	σ	m	A	ν(CCl) S_{HC}
747	π	mw	C	
872	σ?	m	C	
904	σ	ms	C,A	δ(CD) ?
950	σ?	w	C	
980	σ	w	A	
1070	σ?	vvw(sh)	C	
1090	σ	mw	C,A	
1140	π	mw	C,A	
1210	π	mw	C	γ_w(CH)
1240	σ	vs	C,A	$\delta(CH)_\beta$
1263	σ	ms	C,A	$\delta(CH)_\alpha$
1275		vw	C	
~1292	σ	vs	C,A	$\delta(CH)_\beta$
1340	σ	mw	C,A	$\delta(CH)_\alpha$
1372	σ	mw	C,A	
1428	σ	w	C	$\delta(CH_2)$ (impurity)
1440	σ	w	A	
~1640		vvw		
2170	σ	w	C,A	$\nu(CD)_\beta$
~2590	π?	vw	A?	
2920	σ	ms		$\nu(CH)_\beta$
2980	σ	m		$\nu(CH)_\alpha$

may no longer be as describable in terms of the vibrations of a restricted group of atoms as was the case for PVC. For PVC-βd_1 and PVC-$\alpha\beta d_2$ the symmetry of the planar zig-zag structure is lower than that of PVC. If the D atoms in PVC-βd_1 and the H atoms in PVC-$\alpha\beta d_2$ are in a syndiotactic arrangement along the chain as are the Cl atoms (i.e., there is no isomerization of the *trans* monomer in the polymerization process) then the structure will have a glide plane of symmetry and its symmetry group will be isomorphic with the point group C_s. If on the other hand the D and H atoms are randomly placed, even if the Cl atoms are in a syndiotactic arrangement, the structure will have no symmetry at all. We shall see later that the evidence favors the C_s structure for these polymers.

The discussion thus far has been concerned with the modes of an infinitely long planar zig-zag syndiotactic PVC chain. While such a chain exists (in an adequate approximation) in the crystalline regions of the polymer, it need not occut extensively in the amorphous regions. We must now evalu-

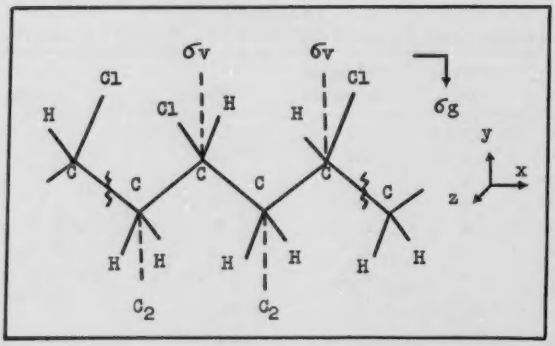

Fig. 7. Structure and symmetry elements of a syndiotactic planar zig-zag polyvinyl chloride chain, C_2 twofold axis, σ_v mirror plane, σ_g glide plane.

ate the effects on the spectrum of the presence of such noncrystalline components. These can be of several general types. First, the frequencies characteristic of a long planar zig-zag chain in the noncrystalline regions can be slightly different from those of a similar chain in the crystal. This is a consequence of the different potential field in which the molecule finds itself. Second, for short planar zig-zag chains (how short we do not know at present) we can expect a relaxation of the selection rules such that previously inactive modes, e.g. A_2 modes, could become spectrally active, probably with weak intensity. Third, an additional consequence of the shortening of the planar zig-zag syndiotactic sequence will be an activation of nonfactor group modes, i.e., modes in which (in distinction to the analysis represented in Table VI) motions in adjacent cells are no longer in phase with each other. In fact, the concept of a repeating unit along the chain loses its significance for such short chain segments, and we can expect new frequencies to appear which do not represent the few specific phase relationships to which the infinite chain is limited. Thus, for example, in the infinite PVC chain previously considered there are two ν(CCl) modes (A_1 and B_1 species), their frequencies being determined by interchain interactions between adjacent monomer units and by the relative phase of the vibrations in each unit (0 and π in this case). In a short chain segment the phases of such interactions would no longer be restricted as above, with the result that ν(CCl) vibrations in one monomer unit could in effect be independent of those in an adjacent unit. This would give rise to what might be termed an unperturbed ν(CCl) frequency, which could of course be different from the above two frequencies. Fourth, the presence of short planar zig-zag segments is a result of rotations about C—C bonds which produce a departure from an extended zig-zag conformation. Whether these bends in the chain are a result of chain entanglements or whether they arise from departures from stereoregularity, in either case they result in the presence of new rotationally isomeric structures. Since in general different rotational

TABLE IV
Infrared Spectrum and Assignments for Polyvinyl Chloride-$\alpha\beta d_2$

Frequency, cm.$^{-1}$	Polarization	Relative intensity	Phase	Assignment
418		vw	C	
475	σ	vw	A	
555	σ	w	A	
570	σ?	w?		
580	σ	s	C	ν(CCl) B_1
590	σ	ms	A	ν(CCl) S_{HH}
615	σ	s	C,A	ν(CCl) A_1 and S'_{HH}
638	σ	w		
667	σ	ms	A	
705	π	mw	C	ν(CCl) S_{HC}
710	σ			
783	σ	vw	A	
802	σ	m	C,A	
816		vw	C	
862	π?	vw	A	
880	σ	w	C,A	
918		vvw	C	
938	σ	mw	C	
962	σ	mw	C	
1025	σ	s	C,A	
1058	σ?	w		
~1100	σ	m	A	
~1115	π?	vw(sh)	C	
1185	σ	mw	C	
1208	σ	w	A	
1238	σ	w	C	
1275		vvw(sh)	C?	
1282	σ	s		δ(CH) B_1
1310		vw	C	
1330	σ	m		δ(CH) A_1
1428	σ	w		$\delta(CH_2)$ (impurity)
1445	σ	w	A	
2180	σ	w		$\nu(CD)_\beta$
2208	σ	w		$\nu(CD)_\alpha$
~2860	σ	vw	A	
2920	σ	ms	C,A	$\nu(CH)_\beta$

isomers associated with a given group have different frequencies, we may expect new spectral bands to appear which are derived from the bent regions of a polymer chain. As we shall see, the operation of the third and fourth factors can be detected fairly definitely in the spectrum of noncrystalline PVC. The effects of the first two factors are not as clearly observed.

The expected frequencies of the normal modes of planar zig-zag syndiotactic PVC have been given from normal vibration calculations.[4,5] While these are of help in assigning bands, and we shall make reference to them, they may contain ambiguities. These arise from the possible inapplicability of force constants transferred from smaller molecules, and are evidenced

TABLE V. Infrared Spectrum and Assignments for Polyvinyl Chloride-d_3

Frequency, cm.$^{-1}$	Polarization	Relative intensity	Phase	Assignment
418		vw	C	
460	σ	vw	A	
493	π	vw	A?	
540	π?	vw	A	
560	σ	s	C	ν(CCl) B_1
578	σ	s	A	ν(CCl) S_{HH}
595	σ	s	C,A	ν(CCl) A_1 and S'_{HH}
628	σ	m	A	ν(CCl) S_{HC}
~670		mw	C	
~680	π	mw	A?	
773	π?	vw	A	
792	σ	ms	C,A	
810	π?	vw	A	
840		vw	A	
865		vw	C	
910	σ?	w	A	
940	π?	m	C,A	
960	σ	m	A	
1010	σ	ms	C	
1020	σ	ms	A	
1040	σ	w	C,A	
~1100		vw	A	
1118	σ	ms	C	
1256	π	mw	C,A	
1279	σ	w	C	
1328		w		
1365		w	C	
2110	σ	mw		$\nu_s(CD_2)$ A_1
2160	σ	mw		$\nu_a(CD_2)$ B_1
2230	σ	m		ν(CD) A_1 and B_1
2870		w	A	
2940		w	A	
2975		w	C	ν(CH) (impurity)

TABLE VI
Symmetry Species, Number of Normal Modes, Selection Rules, and Mode Characteristics for Syndiotactic Polyvinyl Chloride

C_{2v}	E	C_2	σ_v	σ_g	n_i	IR	R	Mode Characterization[a]
A_1	1	1	1	1	10	σ	a	ν(CH), δ(CH), $\nu_s(CH_2)$, $\delta(CH_2)$, $\gamma_t(CH_2)$, ν(CCl), δ(CCl), ν_+(O), $\nu(\pi/2)$ T_y
A_2	1	1	−1	−1	7	f	a	γ_w(CH), $\nu_a(CH_2)$, $\delta(CH_2)$, $\gamma_t(CH_2)$, γ_w(CCl), $\nu_+(\pi/2)$, $\nu_-(\pi/2)$
B_1	1	−1	1	−1	11	σ	a	ν(CH), δ(CH), $\nu_a(CH_2)$, $\gamma_w(CH_2)$, $\gamma_r(CH_2)$, ν(CCl), δ(CCl), $\nu_+(\pi/2)$, $\nu_-(\pi/2)$, T_z, R_x
B_2	1	−1	−1	1	8	π	a	γ_w(CH), $\gamma_a(CH_2)$, $\gamma_w(CH_2)$, $\gamma_r(CH_2)$, γ_w(CCl), $\nu_+(\pi)$, $\nu(\pi/2)$, T_x

[a] σ: perpendicular, π: parallel, f: forbidden, a: active, ν: stretching, δ: bending, γ_w: wagging γ_t: twisting, γ_r: rocking, s: symmetric, a: antisymmetric.

by occasional lack of agreement between predicted and observed bands. In any event the caselculations require experimental verification. This is the main concern of the present paper.

Band Assignments

General Considerations. The first step in the assignment process is to correlate a given crystalline absorption band with a particular symmetry species. It is then necessary to determine the normal mode in this species which gives rise to the absorption band under consideration. Restricting our attention to the infrared-active species (no Raman data are available which would permit assignment of modes in the infrared-inactive A_2 species), we see from Table VI that the B_2 species modes are readily identified by their parallel (π) dichroism. A distinction between A_1 and B_1 modes would ordinarily not be possible, since they both exhibit perpendicular (σ) dichroism. However, a very fortunate circumstance in PVC permits their identification. It has been observed[5] that the σ bands fall into two groups (as a function of increasing draw ratio): bands in one group show initial σ dichroism which increases in magnitude at higher draw ratios; bands in the other group show initial π dichroism which changes to σ with increasing draw ratio. Without knowing the details of the orientation of PVC crystallites with increasing draw ratio which give rise to these effects, the above information suffices to identify the A_1 and B_1 species. Nor are the results of normal vibration calculations necessary at this point as claimed.[5] The identification proceeds as follows: The A_1 species contains a $\delta(CH_2)$ mode, the B_1 species does not. This mode is without question assignable to the band at 1428 cm.$^{-1}$ Since this band shows increasing σ dichroism with increasing draw ratio,[5] it follows that this characteristic is to be associated with the A_1 species modes. The bands which show inversion of dichroism with increasing draw ratio, therefore, belong to the B_1 species. Four such strong bands appear in the 550–1500 cm.$^{-1}$ region, as expected from the symmetry analysis. Having determined the symmetry species of the crystalline PVC bands, we can now turn to the assignment of individual modes.

CCl Stretching Modes. The assignment of the two ν(CCl) modes predicted for a planar zig-zag syndiotactic PVC chain (see Table VI) can be made without difficulty. The urea-complex PVC shows only two bands in the appropriate region,[9] at 604 cm.$^{-1}$ and at 640 cm.$^{-1}$. Progressive elongation studies[5] show that the former band undergoes an inversion of dichroism, thus indicating that it belongs to the B_1 species. The 640-cm.$^{-1}$ band exhibits the dichroic behavior expected of A_1 species modes. The general frequency region in which these bands are located accords with results obtained on model compounds,[11,15–17] and the relative frequencies of A_1 and B_1 species agrees with calculation[4] (although the values obtained, viz., 633 and 651 cm.$^{-1}$, are not in exact agreement with the observed bands). A comparable pair of bands is observed in all of the deuterated polymers, and can be assigned by analogy with the bands in PVC.

A glance at this region of the spectrum of a less crystalline polymer however, shows that the situation is much more complex than indicated above.

In particular, new bands make their appearance, the most prominent being at 615 cm.$^{-1}$ and at ca. 690 cm.$^{-1}$. On the basis of model compound studies,[15] it was soon recognized[8-11] that these bands could be associated with rotationally isomeric structures, the former corresponding to Cl *trans* to H and the latter to Cl *trans* to C. The underlying validity of this idea has been confirmed by recent studies[16] of 2,4-dichloropentane. The proposed assignment[5,16] of these bands to syndiotactic and isotactic components of the amorphous phase does not, however, completely clarify the origin of the bands in this region. Furthermore, we believe that there is evidence for the presence of another band, at ca. 638 cm.$^{-1}$, associated with the noncrystalline component. We arrive at this conclusion as follows. In the urea-complex PVC, the 604 cm.$^{-1}$ band is slightly more intense than the 640 cm.$^{-1}$ band. Yet in less crystalline PVC's there is still a band near 638 cm.$^{-1}$ even though there is no evidence of a comparably strong component at 604 cm.$^{-1}$. It cannot be argued that the latter band is overlapped by the 615 cm.$^{-1}$ amorphous band because in PVC-αd_1 and in PVC-d_3, where the separation of the comparable two bands is even greater, viz., 17 and 18 cm.$^{-1}$ respectively, an analogous effect is observed. Since we expect both the 604 and 640 cm.$^{-1}$ bands of PVC to diminish in intensity with a decrease in the relative proportion of planar zig-zag syndiotactic chains, we conclude that the ca. 638 cm.$^{-1}$ band is properly associated with the noncrystalline component.

A more detailed interpretation of the bands in the CCl stretching region of PVC can now be achieved on the basis of more complete studies on model compounds.[17] In the earlier studies of rotational isomerism in chlorine-containing molecules,[15] it was noted that the frequency of a ν(CCl) mode depended on whether a H atom or a C (or Cl) atom was *trans* to the Cl atom. Thus, secondary chloride frequencies were designated as S_H or S_X, and frequency ranges quoted for each. It is now observed[17] that the ν(CCl) frequency is determined by the nature of the substituents in the *trans* positions on *both* sides of the C—Cl bond. This requires that ν(CCl) modes now be characterized as S_{HH}, S_{HC}, or S_{CC}. There is also evidence[17] that the S_{HH} frequency depends on the conformation of the local carbon skeleton in the vicinity of the C—Cl bond. We designate by S_{HH} the frequency associated with the planar zig-zag form and by S'_{HH} the frequency associated with the bent skeletal form.[17] On the basis of the correlations of these rotationally isomeric forms with specific frequency regions,[17] we can assign the ca. 690 cm.$^{-1}$ band to an S_{HC} mode, the ca. 638 cm.$^{-1}$ band to an S'_{HH} mode, the 615 cm.$^{-1}$ band to an S_{HH} mode, and the 768 cm.$^{-1}$ band most probably to an S_{CC} mode. Weak bands at 540 and 588 cm.$^{-1}$ can be associated with tertiary Cl stretching modes.[17] The infrared spectra of some dichlorides[18] suggest that the weak band at ca. 710 cm.$^{-1}$ can also be an S_{HC} mode (we designate it S'_{HC}), perhaps due to structure II of Shimanouchi and Tasumi.[16] We see, therefore, that the CCl stretching region of the infrared spectrum gives evidence of the many local chain conformations that can exist in the vicinity of a C—Cl bond. It does this by distinguish-

ing between different rotationally isomeric forms (S_{HH}, S_{HC}, S_{CC}) and by demonstrating the presence of nonfactor-group modes (the 615-cm.$^{-1}$ band, associatee with the planar zig-zag chain conformation, probably corresponds to a ν(CCl) frequency unperturbed by interactions between adjacent C—Cl groups).

It is of interest to note that the ν(CCl) frequencies of syndiotactic PVC are lowered by deuteration of the molecule. The fact that there is a small lowering even for PVC-αd_1 indicates that the ν(CCl) mode cannot be taken to be a simple separable group frequency. This mode must involve motions of other atoms as well, a result which is also suggested by the large frequency difference (36 cm.$^{-1}$) between A_1 and B_1 species vibrations. This is consistent with the observed additional lowering in frequency upon increased deuterium substitution in the rest of the molecule. From the small shift in the B_1 and S_{HH} frequencies upon α deuteration (PVC to PVC-αd_1 and PVC-βd_1 to PVC-$\alpha\beta d_2$) we can say that these modes involve relatively little motion of the α hydrogen atom. On the other hand they do involve the motions of both β hydrogen atoms, since the frequency falls by about the same amount for each β hydrogen substitution (cf. PVC-βd_1 and PVC-d_3 with PVC). The A_1 mode involves both α and β hydrogen motions, as can be seen from the lowering in frequency upon either or both substitutions. The S_{HC} mode clearly is more complex in its dependence on mass increments. This band might be expected to reveal the location of the D atom relative to the Cl atom in PVC-βd_1, since of course no spectral differences as a function of D position can arise in the planar zig-zag syndiotactic structure. The observed results, however, do not permit a simple interpretation at the present time.

CH Stretching Modes. The assignment of the CH and CH_2 stretching modes can be done relatively unambiguously now with the help of the spectra of the deuterated PVC's. Thus, the disappearance of the 2970 cm.$^{-1}$ band upon deuteration shows that this band is to be assigned to ν(CH). Since no other bands in this region are affected by α deuteration, the 2970 cm.$^{-1}$ band probably represents overlapped A_1 and B_1 species modes. The shift of this frequency to 2200 cm.$^{-1}$ in PVC-αd_1, a shift ratio of 1.35, is in good agreement with the ratio of 1.34 which is expected on the basis of an isotopic frequency rule that is valid for separable group modes.[3,19] The appearance of a comparable band at 2217 cm.$^{-1}$ in PVC-d_3 is consistent with its assignment to the corresponding ν(CD) mode in this polymer. The two other bands in this region of the spectrum of PVC-d_3, viz., at 2110 and 2160 cm.$^{-1}$, must therefore be the CD_2 modes. If we consider the fact that the 2850 cm.$^{-1}$ band arises from the amorphous phase, that the ca. 2820 cm.$^{-1}$ band is probably at too low a frequency to be assigned to a $\nu_s(CH_2)$ mode, and that the predicted isotopic shift ratios are 1.38 for $\nu_s(CH_2)$ and 1.36 for $\nu_s(CH_2)$, then the assignments of the 2910 cm.$^{-1}$ band to $\nu_s(CH_2)$ and the 2930 cm.$^{-1}$ band to $\nu_s(CH_2)$ follow quite naturally. The observed frequency shift ratios are 1.38 and 1.35 respectively, in good agreement with prediction, and the 2930 cm.$^{-1}$ band seems to exhibit the dichroism inver-

sion required for its assignment to a B_1 mode. While the $\nu_s(CH_2)$ mode has a frequency much higher than that at ca. 2850 cm.$^{-1}$ found in many polymers, for example in polyethylene,[3] it agrees with the comparable frequency at 2910 cm.$^{-1}$ found in the spectrum of polyvinyl alcohol.[3] The reason for such large frequency shifts in the $\nu_s(CH_2)$ mode is not understood at present. It might be noted that the values calculated for these frequencies are:[4,5] $\nu(CH)$ — 2968, $\nu_s(CH_2)$ —2905, $\nu_t(CH_2)$ —2873. The spectra of PVC-βd_1 and PVC-$\alpha\beta d_2$ now permit an unambiguous identification of the $\nu(CH)_\alpha$ and $\nu(CH)_\beta$ frequencies and their deuterated counterparts, and these assignments are shown in Tables III and IV.

CH Deformation and Skeletal Modes. The $\delta(CH_2)$ A_1 mode can be assigned to the 1428 cm.$^{-1}$ band without any problem. The assignment of the 1438 cm.$^{-1}$ amorphous band will be considered later.

The assignment of the $\delta(CH)$ A_1 and B_1 modes has been the subject of some discussion. The correlation of these modes with bands at 1258 cm.$^{-1}$ and 1338 cm.$^{-1}$ respectively[1,3] has been questioned[4] on the basis that the normal vibration calculations predict only a very small splitting, viz., about 1 cm.$^{-1}$. It has been suggested[4,5] that the large separation between the above two bands is due primarily to a strong coupling between the $\delta(CH)$ and $\gamma_t(CH_2)$ modes. A study of the spectra of the deuterated PVC's shows that this may not be entirely true. The spectrum of PVC-$\alpha\beta d_2$ shows two crystalline σ bands at 1282 and 1330 cm.$^{-1}$. There is no obvious way in which these can be assigned to overtones or combinations, and their intensity also suggests that they are fundamentals. The only reasonable assignment of these bands, therefore, is to the two $\delta(CH)$ modes expected of the planar zig-zag C_s structure. Their 48 cm.$^{-1}$ separation indicates that a strong interaction can exist between syndiotactically placed β hydrogen bending modes which leads to a large splitting in the fundamental frequency. Splittings of this order are also observed in the spectrum of PVC-βd_1, although the detailed analysis of all of the components is not initially as straightforward. With a splitting of the order of 50 cm.$^{-1}$ observable for $\delta(CH)_\beta$ modes, it is possible that comparable or larger splittings can occur for the $\delta(CH)_\alpha$ modes.

That the situation in PVC may be more complex than this is indicated by an examination of the comparable region of the spectrum of PVC-αd_1, where three bands are found, at 1297 cm.$^{-1}$ (σ) and 1353 (π), 1360 (σ). These bands are most reasonably assigned to the $\gamma_t(CH_2)$ A_1 and $\gamma_w(CH_2)$ B_2 and B_1 modes respectively which are expected for the C_{2v} chain structure. Not only are other assignments difficult to support, but these modes are found in the spectra of other polymers at about the same frequencies.[3] It is, therefore, necessary to consider the possibility that in PVC these modes may interact with the $\delta(CH)$ modes. The observed inversion of dichroism[4] suggests that the 1355 cm.$^{-1}$ band should be assigned to $\gamma_u(CH_2)$ B_1. The only π band in this region is at 1387 cm.$^{-1}$, and this band is, therefore, most likely assigned to the $\gamma_w(CH_2)$ B_2 mode. The shift of these modes to higher frequencies in PVC as compared to PVC-αd_1 may

reflect the participation of the α hydrogen atom in the normal vibrations. The observed dichroism inversion for the 1258 cm.$^{-1}$ band indicates that it should be assigned to the δ(CH) B_1 mode. The 1338 cm.$^{-1}$ band is then reasonably assigned to the δ(CH) A_1 mode, possibly mixed with the $\gamma_t(CH_2)$ A_1 mode. This is permitted since both modes belong to the same symmetry species. If the intensity of $\gamma_t(CH_2)$ is as comparably low in PVC as compared to PVC-αd_1 as is the case for $\gamma_w(CH_2)$, this may account for only one of the two expected bands being observed. If this is the case, then the 1338 cm.$^{-1}$ band can be considered as essentially a δ(CH) mode. These considerations now permit some tentative assignments to be made of the δ(CH) modes of PVC-βd_1, and these are indicated in Table III.

Of the remaining deformation modes it is most likely that the γ_w(CH) B_2 mode is to be assigned to the crystalline band at 1230 cm.$^{-1}$ The only other unassigned CH_2 modes are the rocking vibrations. Band intensities and dichroism, as well as the results of normal vibration calculations,[4,5] indicate that the 835 cm.$^{-1}$ band should be assigned to $\gamma_r(CH_2)$ B_2 and the 960 cm.$^{-1}$ band should be assigned to $\gamma_r(CH_2)B_1$. It is interesting to note that these modes are much more poorly characterized as CH_2 vibrations then, say, were the $\nu(CH_2)$ modes. Thus, deuteration in the α position causes the 835 cm.$^{-1}$ band to shift to ca. 770 cm.$^{-1}$, a very large amount for substitution outside the CH_2 group. Furthermore, the frequency shift ratio (the band can be followed quite uniquely to ca. 675 cm.$^{-1}$ in PVC-d_3) is 1.24, which is quite significantly different from the ratio of 1.38 expected for a separable group frequency.[3] If the 960 cm.$^{-1}$ band moves in similar fashion to 792 cm.$^{-1}$ in PVC-d_3, as is indicated from the spectra, the shift ratio is 1.21. The comparable values of these ratios support the similar assignments of the 835 and 960 cm.$^{-1}$ bands. These considerations therefore indicate that the motions in the $\gamma_r(CH_2)$ modes are not restricted to the CH_2 group but probably involve appreciable movements of the α hydrogen atoms.

The remaining infrared active modes of the planar zig-zag syndiotactic structure in this region are the three skeletal modes, $\nu_+(0)$ A_1, $\nu_+(\pi)$ B_2, and $\nu_+(\pi/2)B_1$. For a polyethylene planar zig-zag chain the first two modes are found at 1061 and 1131 cm.$^{-1}$ respectively and the third[3] is calculated to occur at 983 cm.$^{-1}$. For PVC these three frequencies have been calculated[4] to be 1100, 1054, and 1071 cm.$^{-1}$ respectively. None of the above values correspond to bands in PVC, but they perhaps are indicative of the general region in which the skeletal modes are to be found. The observed bands seem in general to be at somewhat higher frequencies. The only crystalline π band in this region is the weak band at 1195 cm.$^{-1}$, and we believe that this is to be assigned to $\nu_+(\pi)$ B_2. Two other crystalline σ bands are found at 1105 cm.$^{-1}$ and 1090 cm.$^{-1}$, and it is possible that these are associated with the two other skeletal modes. No clear-cut differentiation is possible at present, but we prefer the assignment of the 1105 cm.$^{-1}$ band to the $\nu_+(O)$ A_1 mode and the 1090 cm.$^{-1}$ band to the $\nu_+(\pi/2)$ B_1 mode. This is based on the expectation that the $\nu_+(0)$ mode should be

associated with a stronger band than the $\nu_+(\pi/2)$ mode, and on the variation of dichroism with draw ratio,[5] which seems to indicate a possible inversion for the 1090 cm.$^{-1}$ band.

Some assignments of bands in the deuterated polymers are suggested in Tables II–V, but these must be considered as quite tentative, particularly in view of the extensive mixing of modes which is predicted by the normal vibration calculations.[4] This can also be seen from the departure of the isotopic shift ratios from predicted values. For example, if the crystalline σ band of PVC-d_3 at 1118 cm.$^{-1}$ is taken to be the $\delta(CD_2)$ mode then the frequency ratio is 1.28, significantly lower than the predicted ratio of 1.35.[3] If the 1279 cm.$^{-1}$ band is assigned to this mode,[4] then the ratio becomes 1.12. The departure from a simple group frequency is therefore very much larger than in the case of the $\nu(CH_2)$ modes.

Noncrystalline Bands. The discussion thus far has been concerned primarily with the assignment of modes of the planar zig-zag syndiotactic PVC chain. In the case of the $\nu(CCl)$ modes we saw that the noncrystalline bands could be assigned to rotationally isomeric forms of the chain. We wish now to consider the assignment of the other noncrystalline bands in the spectrum.

In most cases the specific origin of the noncrystalline bands is difficult to specify, although rotational isomerism seems the most likely cause. This appears to be indicated for example for the $\delta(CH_2)$ mode from the study of model compounds. Thus, it is found[16] that the $\delta(CH_2)$ mode of meso-2, 4-dichloropentane (corresponding to an isotactic placement of adjacent Cl atoms) is at a frequency ca. 13 cm.$^{-1}$ higher than that of dl-2,4-dichloropentane (corresponding to a syndiotactic placement of adjacent Cl atoms). This would suggest the assignment of the 1438 cm.$^{-1}$ band of PVC to the $\delta(CH_2)$ mode of such a conformation. In the case of all of the noncrystalline bands other than the $\nu(CCl)$ modes we have made no attempt to specify the exact origin of the mode other than to identify it nominally with the amorphous regions. Assignments are based tentatively on the general spectral region and the experience with assignments in other polymers. Thus: The 2850 cm.$^{-1}$ band could be a $\nu_s(CH_2)$ mode, although an overtone of the 1438 cm.$^{-1}$ band cannot be completely excluded. The weak 1365 cm.$^{-1}$ band could well be an unperturbed $\gamma_w(CH_2)$ mode; it is commonly found near this frequency.[3] Similarly, the 1310 cm.$^{-1}$ band would correspond to $\gamma_t(CH_2)$, as in polyethylene.[3] Because of its location and dichroism the 1245 cm.$^{-1}$ band would reasonably be assigned to the $\delta(CH)$ mode. A similar assignment of the 1203 cm.$^{-1}$ band to $\gamma_w(CH)$ is consistent with the absence of this band in PVC-αd_1. The assignments of the skeletal modes at 1122 and 1105 cm.$^{-1}$ and $\gamma_r(CH_2)$ at 970 cm.$^{-1}$ are perhaps less certain but not unreasonable. More definitive assignments in this region must await more detailed studies in the far infrared region of the spectrum.

Discussion

In the light of the above analysis it is of interest to consider what information the infrared spectrum can provide on certain aspects of the struc-

ture of PVC. The assignments of the crystalline bands are, as we have seen, completely consistent with a planar zig-zag syndiotactic structure for this component. The structure of the noncrystalline chain segments, however, is not as certain. Nevertheless, some relatively detailed information appears to be suggested by our assignments.

The premise upon which the following arguments are based is that the conformation of a chain is determined in first approximation by the relative configurations of nearest neighbor Cl atoms only. We can designate such adjacent Cl atoms as isotactic pairs (i) or syndiotactic pairs (s), depending on whether the two Cl atoms are on the same side or on opposite sides of the plane in which the carbon skeleton would assume a standard zig-zag form. From studies on 2,4-dichloropentane[16] it is known that one specific rotationally isomeric form of the molecule is preferred depending on whether the two Cl atoms are in an isotactic or a syndiotactic arrangement. Therefore, it may not be unreasonable to assume that the i or s character of a chain at a given point is the primary factor determining the conformation which the chain acquires at this location. If this is the case, then we can inquire into the structures which will result from i and s pairs. This can be done with the aid of space-filling molecular models and considerations concerning the relative energies of various PVC chain conformations.[20] The following results emerge. For the i pair the least stable structure is the planar zig-zag chain, since this places adjacent Cl atoms much too close to each other. By rotations about the CHCl—CH_2 or CH_2—CHCl bonds, the chain will assume a form in which one of the S_{HH} frequencies of the planar zig-zag i structure is replaced by an S'_{HH} or an S_{HC} frequency. The form giving rise to the S_{HC} frequency is the more stable,[16,20] but under the constraints imposed by chain entanglements, interchain interactions, etc., it is probable that some of the S'_{HH} structure will be present in the solid polymer at room temperature. Thus with each i pair a contribution to the S_{HC} or S'_{HH} band is introduced. For the s pair the planar zig-zag is the most stable structure.[16,20] Constraints may give rise to bends in the chain, but these will be limited to structures which introduce an S_{HC} frequency since the structure which gives an S'_{HH} frequency places adjacent Cl atoms in the same close contact as for the planar zig-zag isotactic structure, and is similarly very unlikely to be found. Each s pair, therefore, introduces a contribution to the S_{HH} or S_{HC} bands in the spectrum.

The above conclusions lead to the following interpretation of the origins of the noncrystalline bands in the spectrum of PVC. The 615 cm.$^{-1}$ band, assignable to an S_{HH} mode, must arise from the s pairs only in the chain. (These presumably are not part of long $ss\ldots$ sequences, so that the 604, 640 cm.$^{-1}$ interaction splitting does not occur.). The ca. 638 cm.$^{-1}$ band, assignable to an S'_{HH} mode, must be due to the i pairs only, originating from the less favorable rotationally isomeric structure. The ca. 690 cm.$^{-1}$ band contains contributions from both i and s pairs, comprising the most stable form of the former and the less stable form of the latter. It should be noted that although both i and s pairs can give S_{HC} frequencies, the adjacent structures need not be the same: for the i pair the C—Cl bond on

the trans carbon atom can be nearly coplanar with the first C—Cl bond and the intervening carbon skeleton, while for the *s* pair the two C—Cl bonds can be essentially perpendicular to each other. We may, therefore, expect that the S_{HC} frequency of an *i* pair could be slightly different from the S_{HC} frequency of an *s* pair.

The results of studies on heated PVC[11] seem to be consistent with the above ideas. When PVC is heated it is found that the ca. 638 cm.$^{-1}$ band weakens markedly and the maximum of the ca. 690 cm.$^{-1}$ band shifts from 693 cm.$^{-1}$ to 685 cm.$^{-1}$ We would expect that heating would release some of the constraints on the polymer chains, thus making it possible for the more favorable conformations to be assumed. This would account for the weakening of the ca. 638 cm.$^{-1}$ band, which arises from the less favorable isomeric structure of the *i* pairs. Presumably a similar situation occurs with respect to the *s* pairs, and is reflected in the frequency shift of the maximum of the ca. 690 cm.$^{-1}$ band. On the basis of these considerations we would associate the 685 cm.$^{-1}$ component with the S_{HC} frequency of the *i* pairs and the 693 cm.$^{-1}$ component with the S_{HC} frequency of the *s* pairs. This would be consistent with the observed dichroism for these components: 685 σ and 693 π. Such successions of *i* pairs as existed would be expected to form short helical segments which upon orientation would give rise to a strong σ ν(CCl) mode, while the bends at the *s* pairs, which result in the associated S_{HC} frequency, can become oriented in such a way as to give rise to a predominantly π ν(CCl) mode. It should be noted that this provides a reasonable alternative explanation for the frequency difference between π and σ components of the ca. 690 cm.$^{-1}$ band. Previous suggestions[5,16] associated these two components with A and E species modes respectively of an isotactic helix, and resulted in the conclusion that the noncrystalline chain segments were stereoblock in character. However, since the 615 cm.$^{-1}$ band suggests the presence of relatively short *ss*. . . sequences, it does not seem likely that significantly longer *ii* . . . sequences would occur. We believe it more probable that the noncrystalline PVC chains are more satisfactorily described as atactic than as stereoblock copolymers of syndiotactic and isotactic sequences of appreciable length.

If the above interpretations are correct, they suggest a method for determining the relative number of *i* and *s* pairs without regard to their distribution in the chain. In a heated specimen the proportion of less favored conformations decreases, if not actually to zero then seemingly so for practical purposes. Thus the integrated area associated with the 615 cm.$^{-1}$ band should be proportional to the number of *s* pairs while the integrated area associated with the ca. 690 cm.$^{-1}$ band would be proportional to the number of *i* pairs. While exact data are not available on polymers, spectra of model compounds[16] indicate these two bands to have essentially equal extinction coefficients. A calculation based on this assumption would probably not be seriously in error.

We are indebted to Dr. R. J. Fawcett for the preparation of vinyl chloride-αd_1 and to Dr. F. A. Regenass for the preparation of the other deuterated monomers. We wish to thank Dr. J. H. Goldstein for providing the NMR data on some of the monomers. One of us (S. K.) wishes to acknowledge support in part from the National Science Foundation, grant G17469.

References

1. Krimm, S., and C. Y. Liang, *J. Polymer Sci.*, **22**, 95 (1956).
2. Narita, S., S. Ichinohe, and S. Enomoto, *J. Polymer Sci.*, **37**, 273, 281 (1959).
3. Krimm, S., *Fortschr. Hochpolym.-Forsch.*, **2**, 51 (1960).
4. Shimanouchi, T., and M. Tasumi, *Bull. Chem. Soc. Japan*, **34**, 359 (1961).
5. Tasumi, M., and T. Shimanouchi, *Spectrochim. Acta*, **17**, 731 (1961).
6. Fuller, C. S., *Chem. Rev.*, **26**, 143 (1940).
7. Natta, G., and P. Corradini, *J. Polymer Sci.*, **20**, 251 (1956).
8. Grisenthwaite, R. J., and R. F. Hunter, *Chem. Ind. (London)*, **1958**, *Ibid.*, **1959**, 433.
9. Krimm, S., A. R. Berens, V. L. Folt, and J. J. Shipman, *Chem. Ind. (London)*, **1958**, 1512; *Ibid.*, **1959**, 433.
10. Shimanouchi, T., S. Tsuchiya, and S. Mizushima, *J. Chem. Phys.*, **30**, 1365 (1959).
11. Shimanouchi, T., S. Tsuchiya, and S. Mizushima, *Kobunshi*, **8**, 202 (1959).
12. White, D. M., *J. Am. Chem. Soc.*, **82**, 5678 (1960).
13. Folt, V. L., J. J. Shipman, and S. Krimm, *J. Polymer Sci.*, **61**, 517 (1962).
14. Liang, C. Y., G. B. B. M. Sutherland, and S. Krimm, *J. Chem. Phys.*, **22**, 1468 (1954).
15. Mizushima, S., T. Shimanouchi, K. Nakamura, M. Hayashi, and S. Tsuchiya, *J. Chem. Phys.*, **26**, 970 (1957).
16. Shimanouchi, T., and M. Tasumi, *Spectrochim. Acta*, **17**, 755 (1961).
17. Shipman, J. J., V. L. Folt, and S. Krimm, *Spectrochim. Acta*, **48**, 1603 (1962).
18. Lím, D., and M. Kolínský, *J. Polymer Sci.*, **53**, 173 (1961).
19. Krimm, S., *J. Chem. Phys.*, **32**, 1780 (1960).
20. Fordham, J. W. L., *J. Polymer Sci.*, **39**, 321 (1959).

Résumé

On a préparé des analogues deutérés du chlorure de polyvinyle (PVC) et les spectres infrarouges ont été analysés dans le but de caractériser d'une façon plus détaillée les bandes obtenues dans le spectre du PVC. Comme polymères deutérés on a étudié: PVC-αd_1, PVC-βd_1, PVC-$\alpha\beta d_2$ et PVC-d_3. Ces polymères ainsi que le PVC ont été obtenus dans un complexe d'urée, à -78°C et à $+50$°C dans le but de déterminer quelles bandes sont d'origine cristalline et lesquelles sont d'origine non-cristalline. Des spectres polarisés des échantillons orientés ont été obtenus dans chaque cas de manière à faciliter l'analyse. Plusieurs conclusions incertaines obtenues antérieurement ont été élucidées grâce à cette étude. A l'aide d'autres études sur des composés chlorés, il a été possible d'identifier les différentes conformations présentes dans le polymère et de relier celles-ci avec les configuration isotactiques et syndiotactiques de la chaîne. On présente une méthode pour déterminer la proportion de chaque type de configuration dans le PVC.

Zusammenfassung

Deuterierte Analoga von Polyvinylchlorid (PVC) wurden dargestellt und ihre Infrarotspektren zur Ermöglichung einer detailierteren Zuordnung der Banden im PVC-Spektrum untersucht. Die Untersuchung erstreckte sich auf folgende deuterierte Polymere: PVC-αd_1, PVC-βd_1, PVC-$\alpha\beta d_2$ und PVC-d_3. Diese und ebenso PVC wurden im Harnstoffkomplex, bei -78°C und bei $+50$°C, polymerisiert, um festzustellen welche Banden den kristallinen und welche den nichtkristallinen Bereichen zugehören. In

jedem Falle wurden zur Erleichterung der Analyse Polarisationsspektren orientierter Proben aufgenommen. Als Ergebnis dieser Untersuchung konnten einige der früher ungewissen Zuordnungen geklärt werden. Mit Hilfe von Untersuchungen an chlorhältigen Modellverbindungen war es möglich die verscheidenen, im Polymeren vorhandenen Konformationen zu identifizieren und mit isotaktischen und syndiotaktischen Paarkonfigurationen in der Kete in Verbindung zu bringen. Eine Methode zur Bestimmung des Anteils jedes Typs von Paarkonfiguration in PVC wird angegeben.

Received April 30, 1962

JOURNAL OF POLYMER SCIENCE: PART A VOL. 1, PP. 2651–2666 (1963)

Study of Entanglement of Polymers in Solution by Viscosity Measurements. II. Polymethyl Methacrylate in Various Solvents

SAMUEL H. MARON and THOMAS T. CHIU, *Department of Chemistry, Case Institute of Technology, Cleveland, Ohio*

Synopsis

A study has been made of the flow behavior at 30°C. of solutions of three samples of polymethyl methacrylate in three solvents in both the Newtonian and non-Newtonian regions. The concentration range covered was approximately 0–16% by weight. By application of the Ree-Eyring theory it was found possible to represent the observed data in terms of two flow units, and to obtain from the parameters of the theory the effective hydrodynamic volume occupied by the polymer in solution, ϵv_2. Here v_2 is the volume fraction of the polymer and ϵ an effective volume factor. The volume factor, ϵ, was found to be dependent on both solvent and molecular weight only up to ca. $v_2 = 0.04$. Beyond $v_2 = 0.04$, ϵ is independent of solvent and is a function of molecular weight only. These observations indicate that chain entanglement in solution is not probable. Rather, the polymer chain curls on itself, and compacts to a small mass when the effective concentration $\epsilon v_2 = 1$ and the viscosity becomes infinite. The concentration at which this occurs, v_∞, is given by $v_\infty = 1/\epsilon_\infty$. The quantity ϵ_∞ has been found to be a linear function of molecular weight, M. Further, the value of ϵ at $v_2 = 0$, ϵ_0, has been found to be an exponential function of M, and to yield expressions relating intrinsic viscosity to molecular weight in good accord with published results.

INTRODUCTION

The first paper of this series[1] described a study of the flow behavior of solutions of a single sample of polystyrene in five solvents in both the Newtonian and non-Newtonian flow regions at temperatures between 20° and 50°C. The concentration range covered was approximately 0–20% by weight. By application of the Ree-Eyring theory,[2] it was found possible to represent the observed data in terms of two flow units, and to obtain from the parameters of the Ree-Eyring equation the effective hydrodynamic volume occupied by the polymer in solution, ϵv_2. Here v_2 was the volume fraction of polymer in solution and ϵ was an effective volume factor.

For any given solvent, ϵ was found to vary from $[\eta]_{v_2}/2$ at $v_2 = 0$, (where $[\eta]_{v_2}$ is the intrinsic viscosity expressed in volume fractions as the concentration unit) to ϵ = ca. 4 at v_∞, the volume fraction at which $\epsilon v_2 = 1$ and the viscosity becomes infinite. Again, for all concentrations except the very dilute ones, ϵ proved to be essentially independent of temperature.

Finally, for any given value of v_2, ϵ was a function of the nature of the solvent only between $v_2 = 0$ and $v_2 = 0.04$. Above the latter concentration, ϵ was completely independent of the solvent in which the polystyrene was dissolved, and became merely a function of the solution concentration.

These results were interpreted to indicate that at concentrations below ca. $v_2 = 0.25$ no entanglement of polymer chains took place in solution, and that the configuration of polymer chains, as reflected in the effective volume they occupied, was governed only by the nonspecific factor of the space available for occupancy by each molecule. As this space decreased with an increase in concentration, the polymer molecule was forced to reduce its effective volume by coiling into a tighter mass. This process continued until $\epsilon v_2 = 1$, at which point the state of tightest coiling was reached without a change in the nature of the flow.

This paper presents the results obtained in the rheologic study of polymethacrylate solutions ranging in concentrations up to 16% of polymer by volume with various molecular weight polymers and solvents. Attempts were made to measure the flow of solutions at concentrations higher than 16% by means of the Ferranti-Shirley cone-and-plate viscometer, but it was found that degradation and evaporation made the results obtained meaningless. The objectives of the study were (*1*) to check the above observations and conclusions on a system involving a polymer of a different type, such as a polyester, and (*2*) to ascertain the effect of molecular weight on the flow parameters and the effective volume factors.

EXPERIMENTAL

The polymers studied in this investigation consisted of three fractionated samples of polymethyl methacrylate whose molecular weights were determined by intrinsic viscosity[3,4] to be 75,000, 361,000, and 617,000, respectively. The solvents used (redistilled toluene, monochlorobenzene, and chloroform) were chosen to give a good spread of solvent effect action. Solutions of these polymers in the different solvents were prepared by completely dissolving weighed samples of polymethyl methacrylate in a definite volume of solution with the aid of a wrist-action shaker.

Viscosity measurements on the most dilute samples were made in spiral-shaped modified Ostwald pipettes and also ordinary Ostwald viscometers. At concentrations where non-Newtonian behavior was not very pronounced, the low shear capillary viscometer of Maron and Belner[5] was employed. In the range of concentrations where non-Newtonian behavior was more pronounced, the capillary viscometer of Maron, Krieger, and Sisko[6] was used. With combinations of different-sized capillary units, this viscometer furnished shear stresses ranging from 0–1800 dynes/cm.^{2}.

The non-Newtonian data were reduced to shear stress and rate of shear by methods appropriate to each viscometer.[5,6] As a check, a Burroughs 220 electronic digital computer was employed to recalculate the data, and the results of the two methods were found to agree very satisfactorily.

All viscosity measurements were made at 30°C. To convert weight to volume concentrations, the bulk density of polymethyl methacrylate, 1.16 g./cc. was used.

Dependence of Viscosity on Rate of Shear

The generalized theory of flow presented by Ree and Eyring[2] considers a system to be composed of a number of flow units, each characterized by its mean relaxation time, β_n, by x_n, the fractional area of the shear surface which the flow unit occupies, and by α_n, a characteristic shear volume divided by kT. The resulting equation gives for the viscosity η (defined as F/G, where F is the shear stress and G the rate of shear) the expression

$$\eta = \sum_{n=1}^{n} \frac{x_n \beta_n}{\alpha_n} \frac{\sinh^{-1} \beta_n G}{\beta_n G} \tag{1}$$

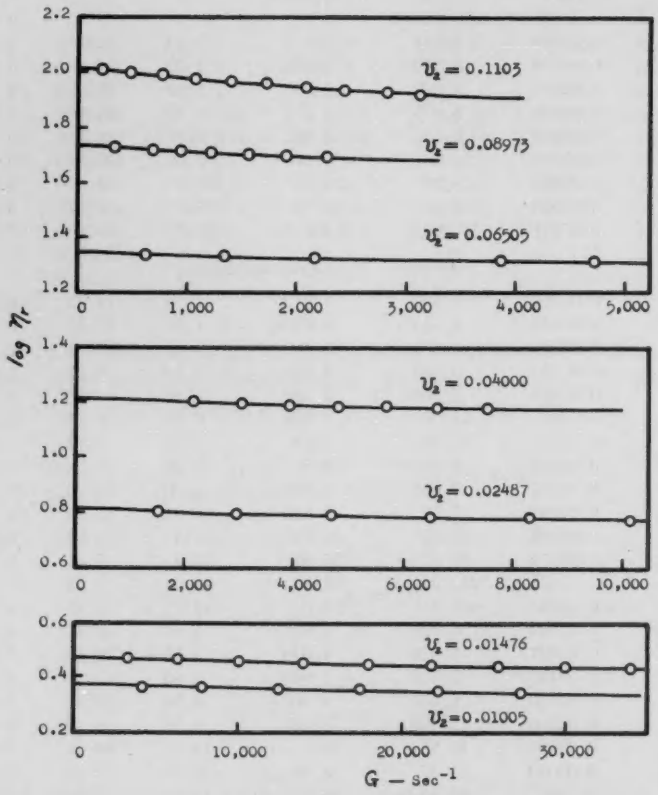

Fig. 1. Plots of log η_r vs. G for polymethyl methacrylate in toluene at 30°C. (Sample II: $M = 3.61 \times 10^6$) (——) calculated; (O) observed.

TABLE I
Flow Parameters for PMMA Solutions in Non-Newtonian Region at 30°C.

Sample	v_2	$a \times 10^2$	$b \times 10^2$	$\beta \times 10^4$	ϵ	ϵv_2
			Solvent: Toluene			
I	0.01775	0.8964	0.0050	1.00	12.65	0.2246
	0.02580	1.125	0.0064	1.20	11.93	0.3078
	0.04322	1.787	0.0146	1.70	10.43	0.4508
	0.06446	2.646	0.102	2.40	8.51	0.5487
	0.09514	6.373	0.284	3.60	7.45	0.7092
	0.1130	10.13	0.670	4.30	6.81	0.7694
	0.1610	29.56	4.60	7.00	5.37	0.8650
II	0.01005	1.139	0.116	1.00	31.04	0.3120
	0.01476	1.405	0.183	1.50	25.79	0.3807
	0.02487	2.893	0.523	2.30	22.85	0.5683
	0.04000	7.593	1.070	4.80	18.34	0.7335
	0.06505	9.955	1.713	7.50	11.80	0.7674
	0.08973	23.70	4.964	13.5	9.46	0.8492
	0.1103	38.76	15.88	18.5	8.00	0.8821
III	0.01010	1.381	0.444	1.50	37.16	0.3753
	0.10753	2.500	1.080	2.20	30.56	0.5357
	0.02092	3.080	2.000	3.00	27.80	0.5816
	0.02900	5.925	3.675	5.50	24.08	0.6984
	0.03029	6.531	3.862	5.90	23.53	0.7127
	0.03796	11.00	8.170	9.30	20.51	0.7786
	0.04868	18.20	25.05	15.2	17.01	0.8279
	0.05950	33.30	56.45	25.0	14.67	0.8728
	0.07971	72.00	282.1	67.0	11.46	0.9135
			Solvent: Monochlorobenzene			
I	0.02251	1.566	0.0126	1.30	14.42	0.3246
	0.03636	2.423	0.0274	1.70	12.57	0.4571
	0.05058	3.339	0.0623	2.20	10.63	0.5375
	0.07155	5.453	0.230	3.10	8.92	0.6380
	0.09895	9.796	0.400	4.30	7.38	0.7300
	0.1306	18.36	0.960	6.10	6.15	0.8028
	0.1671	34.00	5.20	8.70	5.12	0.8551
II	0.01012	1.838	0.398	2.10	37.22	0.3767
	0.02997	7.030	1.775	5.30	22.73	0.6813
	0.04987	17.10	6.840	10.3	15.95	0.7956
	0.06996	34.05	21.30	18.5	12.22	0.8552
	0.09471	88.00	55.00	39.0	9.61	0.9099
	0.1247	233.2	186.8	95.0	7.58	0.9447
	0.1609	469.0	916.0	210.0	5.97	0.9610
III	0.01009	2.545	0.825	4.80	46.61	0.4703
	0.02097	5.620	4.040	5.50	30.69	0.6435
	0.02440	6.360	5.960	5.80	27.25	0.6649
	0.02926	9.680	8.400	8.50	24.89	0.7284
	0.02986	9.460	9.120	8.30	24.29	0.7253
	0.03983	15.85	20.05	12.5	19.78	0.7877
	0.05080	29.52	38.08	21.1	16.62	0.8444
	0.06011	43.35	66.20	30.0	14.50	0.8717
	0.06247	48.10	81.60	33.8	14.06	0.8782
	0.08129	120.8	221.2	85.0	11.36	0.9231
	0.1034	240.0	626.4	142.0	9.14	0.9454

(continued)

TABLE I (*continued*)

Sample	v_2	$a \times 10^2$	$b \times 10^2$	$\beta \times 10^4$	ϵ	ϵv_2
			Solvent: Chloroform			
I	0.00861	0.7848	0.0275	1.00	22.15	0.1907
	0.01724	1.105	0.0356	1.30	18.45	0.3180
	0.04300	2.554	0.165	2.10	12.82	0.5513
	0.06006	3.835	0.270	2.90	10.54	0.6330
	0.08000	6.011	0.432	3.80	8.85	0.7076
	0.1292	15.80	1.78	6.10	6.34	0.8196
	0.1600	23.65	3.65	9.00	5.33	0.8526
II	0.00766	1.363	0.279	2.30	50.38	0.3859
	0.01114	1.976	0.652	2.90	43.99	0.4900
	0.03027	7.200	3.190	6.50	24.21	0.7328
	0.05000	19.50	9.400	11.8	16.75	0.8376
	0.06511	34.74	20.26	18.0	13.49	0.8784
	0.08100	56.70	41.80	28.0	11.17	0.9048
	0.1008	130.6	70.90	58.0	9.30	0.9373
	0.1296	295.5	156.0	115	7.39	0.9583
	0.1639	747.4	422.0	242	5.94	0.9738
III	0.01008	2.360	1.280	4.20	52.91	0.5333
	0.02019	6.250	4.820	9.50	35.32	0.7132
	0.03376	14.94	14.80	16.0	24.13	0.8145
	0.03651	17.95	20.80	19.0	22.76	0.8309
	0.05546	49.10	72.60	42.5	16.19	0.8977
	0.07764	121.0	201.5	80.0	12.04	0.9348
	0.08001	144.5	245.3	103	11.75	0.9404
	0.1091	475.0	777.0	250	8.86	0.9671

The summation indicated has to be carried over the number of flow units required to represent the η versus G data. For two flow units, a Newtonian solvent and a non-Newtonian polymer unit, eq. (1) takes the form

$$\eta = \frac{x_1\beta_1}{\alpha_1} + \frac{x_2\beta_2}{\alpha_2}\left(\frac{\sinh^{-1}\beta_2 G}{\beta_2 G}\right) = a + b\theta \tag{2}$$

where

$$a = \frac{x_1\beta_1}{\alpha_1} \tag{3}$$

$$b = \frac{x_2\beta_2}{\alpha_2} \tag{4}$$

and

$$\theta = \frac{\sinh^{-1}\beta_2 G}{\beta_2 G} = \frac{\sinh^{-1}\beta G}{\beta G} \tag{5}$$

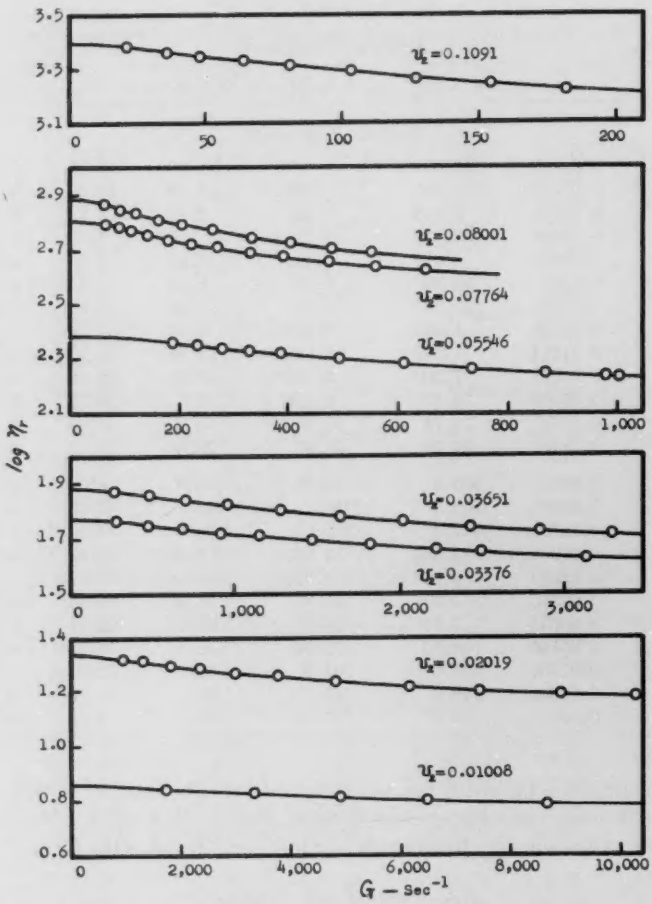

Fig. 2. Plots of log η_r vs. G for polymethyl methacrylate in chloroform at 30°C. (Sample III: $M = 6.17 \times 10^5$) (——) calculated; (O) observed.

In these equations a gives the contribution made by the solvent to the viscosity, and $b\theta$ gives the contribution of the polymer unit. Since the latter may be non-Newtonian, its viscosity contribution may depend on G as contained in the expression for θ.

To fit the non-Newtonian viscosity data obtained at various concentrations to eq. (2), a trial-and-error procedure was employed. At each concentration 3 or 4 values of β were selected, and these were used to calculate the θ's at the experimental shear rates. The parameters a, b, and $(a + b)$ were evaluated next from the viscosities and corresponding θ's, and plots of β versus $(a + b)$, β versus a, and β versus b were prepared. Meanwhile,

samples of various concentrations were measured in Maron and Belner's low shear capillary viscometer[5] at a shear stress range of 0.06–20 dynes/cm.[2] These measurements gave viscosities which were equal to $(a + b)$, since at such low shear the solutions behave Newtonian. From the value of $(a + b)$ obtained from these independent measurements, the plot of β versus $(a + b)$ yielded β, and the β versus, a, and β versus b plots allowed the estimation of a and b. The values of a and b thus obtained should give the best straight line when viscosities are plotted against the θ's corresponding to the experimental shear rates.

Typical examples of the fitting thus obtained are shown in Figures 1 and 2. In these figures the points are experimental, while the solid lines were calculated from the evaluated parameters. The agreement between the two has been found to be similarly satisfactory in all the systems investigated.

Table I gives a summary of the flow parameters thus obtained in the non-Newtonian region for the samples studied in the various solvents. Samples I, II, and III correspond, respectively, to polymethyl methacrylate of 0.75×10^5, 3.61×10^5, and 6.17×10^5 molecular weight.

Dependence of Parameters on Concentration

The variation of the parameter a with volume fraction v_2 is taken to be[1]

$$a = \frac{\eta_0}{(1 - \epsilon v_2)^2} \tag{6}$$

where η_0 is the viscosity of the pure solvent. This equation allows the evaluation of ϵ from the observed values of a. The values of ϵ and ϵv_2 thus obtained are shown in the last two columns of Table I. It can be seen that in every solvent ϵ decreases with increasing v_2, while the product ϵv_2 increases.

TABLE II
Constants for Eqs. (7) and (8)

Solvent	Sample	$\eta_0 \times 10^3$ poises	$K_b \times 10^3$ poises	m	$K_\beta \times 10^5$ sec.	p
Toluene	I	5.390	0.503	2.0	7.6	1.22
	II	5.390	2.70	1.9	6.0	1.62
	III	5.390	12.6	2.4	4.5	2.00
Monochloro-benzene	I	7.141	0.393	1.4	7.8	1.28
	II	7.141	5.67	1.7	8.2	1.65
	III	7.141	13.8	2.0	7.7	1.87
Chloroform	I	5.140	0.694	1.2	7.9	1.26
	II	5.140	3.31	1.2	10.0	1.48
	III	5.140	8.32	1.6	12.0	1.57

Using these values of ϵ, it was found possible to represent b and β as functions of ϵv_2 by the relations

$$b = \frac{K_b(\epsilon v_2)^m}{(1 - \epsilon v_2)^2} \tag{7}$$

$$\beta = \frac{K_\beta}{(1 - \epsilon v_2)^p} \tag{8}$$

The costants K_b, K_β, m, and p thus obtained are summarized in Table II.

TABLE III
Flow Data for PMMA Solutions in Newtonian Region at 30°C.

Sample	v_2	η_r	ϵ	ϵv_2
		Solvent: Toluene		
I	0.005553	1.1717	13.67	0.07591
	0.007579	1.2377	13.29	0.1007
	0.008809	1.2793	13.09	0.1153
II	0.003457	1.3707	40.71	0.1407
	0.004940	1.5506	38.16	0.1885
	0.006112	1.6962	36.21	0.2213
III	0.001529	1.2290	61.67	0.09429
	0.001900	1.2889	59.81	0.1136
	0.002736	1.4328	56.22	0.1538
	0.003302	1.5300	53.56	0.1769
		Solvent: Monochlorobenzene		
I	0.001203	1.0505	20.10	0.02418
	0.002400	1.1024	19.67	0.04721
	0.003760	1.1617	19.04	0.07159
	0.005124	1.2228	18.50	0.09479
II	0.002760	1.4531	56.70	0.1565
	0.003926	1.6725	52.51	0.2062
	0.004821	1.8516	49.75	0.2398
III	0.001141	1.2646	88.67	0.1012
	0.001602	1.3825	83.40	0.1336
	0.002405	1.6026	75.96	0.1827
		Solvent: Chloroform		
I	0.002133	1.1325	27.30	0.05823
	0.003467	1.2208	26.39	0.09149
	0.004332	1.2782	25.68	0.1113
	0.005464	1.3564	24.91	0.1361
	0.006448	1.4265	24.29	0.1566
II	0.001896	1.4283	73.06	0.1385
	0.002931	1.7027	67.86	0.1989
	0.003430	1.8262	64.70	0.2219
	0.004812	2.2438	59.46	0.2861
III	0.001017	1.3529	121.2	0.1233
	0.001912	1.7044	103.9	0.1987
	0.002531	1.9757	95.65	0.2421

Flow in Newtonian Region

At the low concentrations where the solutions exhibit Newtonian behavior, it is no longer possible to evaluate the separate contributions of polymer and solvent by the method described above. In this region viscosity is independent of rate of shear, $\theta = 1$, and eq. (2) reduces to

$$\eta = a + b \tag{9}$$

Substituting for a and b the expressions in eq. (7) and (8), eq. (9) becomes

$$\eta = \frac{\eta_0}{(1 - \epsilon v_2)^2} + \frac{K_b(\epsilon v_2)^m}{(1 - \epsilon v_2)^2} \tag{10}$$

or

$$\eta_r = \frac{1}{(1 - \epsilon v_2)^2} + \frac{K_b}{\eta_0} \frac{(\epsilon v_2)^m}{(1 - \epsilon v_2)^2} \tag{11}$$

Therefore, by knowing η_r at various low concentrations in the Newtonian region, ϵ can be found from eq. (11). Data for flow of the polymethyl methacrylate solutions in the Newtonian region, along with the values of ϵ and ϵv_2 obtained in this manner, are given in Table III.

Dependence of ϵ on Concentration

The variation of ϵ with concentration is typified by the ϵ versus v_2 plot shown in Figure 3, where the results obtained from measurements in both the Newtonian and non-Newtonian regions are combined. Similar plots were obtained in all the solvents with polymers of various molecular weights. It will be noticed that ϵ starts with a high value at $v_2 = 0$, and decreases rapidly with an increase in v_2 down to a limiting value. In turn, plots of $1/\epsilon$ versus v_2 were found to be linear, Figure 4, and hence the variation of ϵ with v_2 can be represented by the relation

$$1/\epsilon = A + Sv_2 \tag{12}$$

The significance of A and S is obtained by substituting two boundary conditions into eq. (12), namely, that when $v_2 = 0$, $\epsilon = \epsilon_0$, and when $v_2 = v_\infty$, $\epsilon_\infty v_\infty = 1$. With these substitutions we obtain

$$A = 1/\epsilon_0 \tag{13}$$

and

$$S = (\epsilon_0 - \epsilon_\infty)/\epsilon_0 \tag{14}$$

On insertion of eq. (13) and (14) into eq. (12) we get

$$\frac{1}{\epsilon} = \frac{1}{\epsilon_0} + \left(\frac{\epsilon_0 - \epsilon_\infty}{\epsilon_0}\right) v_2 \tag{15}$$

and consequently both ϵ_0 and ϵ_∞ can be found from plots such as those in Figure 4.

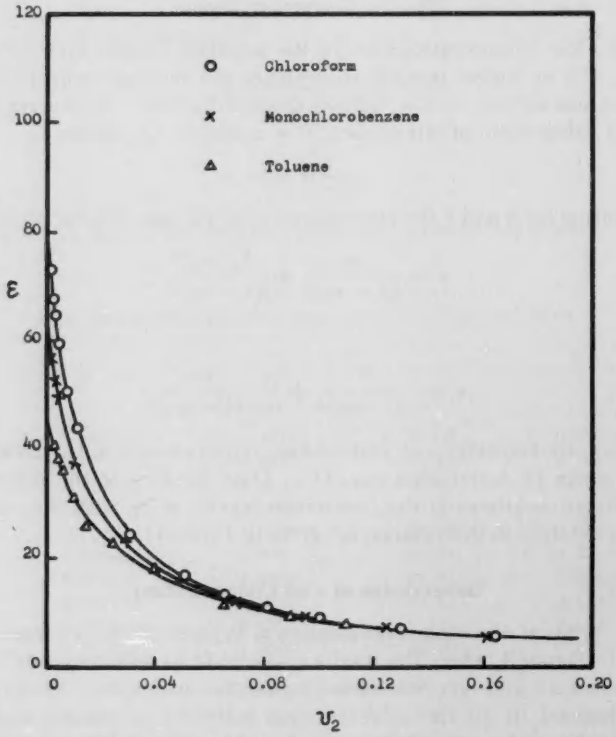

Fig. 3. Plot of ϵ vs. v_2 for polymethyl methacrylate in several solvents at 30°C. (Sample II: M = 3.61×10^6).

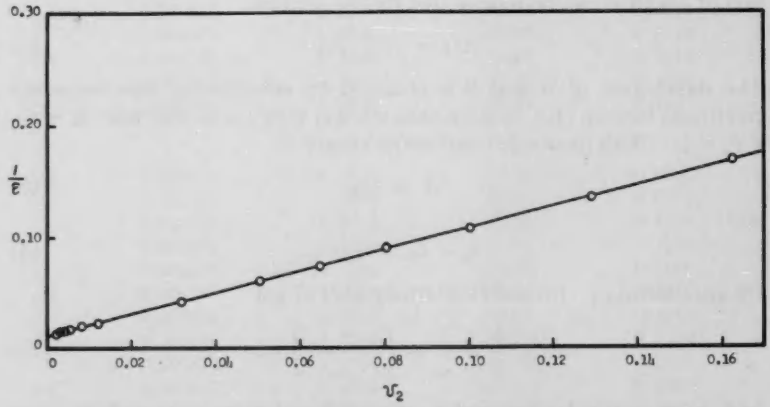

Fig. 4. Plot of $1/\epsilon$ vs. v_2 for polymethyl methacrylate in chloroform at 30°C. (Sample II: M = 3.61×10^6).

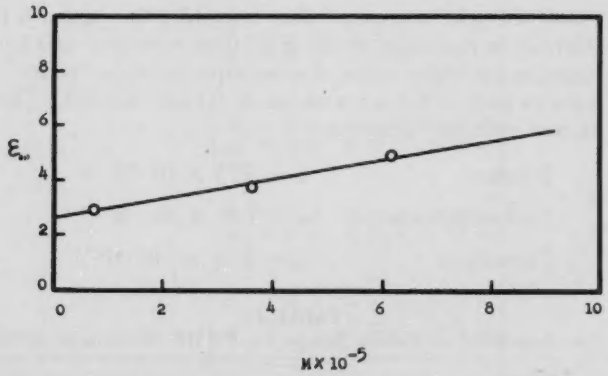

Fig. 5. Plot of ϵ_∞ vs. M for polymethyl methacrylate at 30°C.

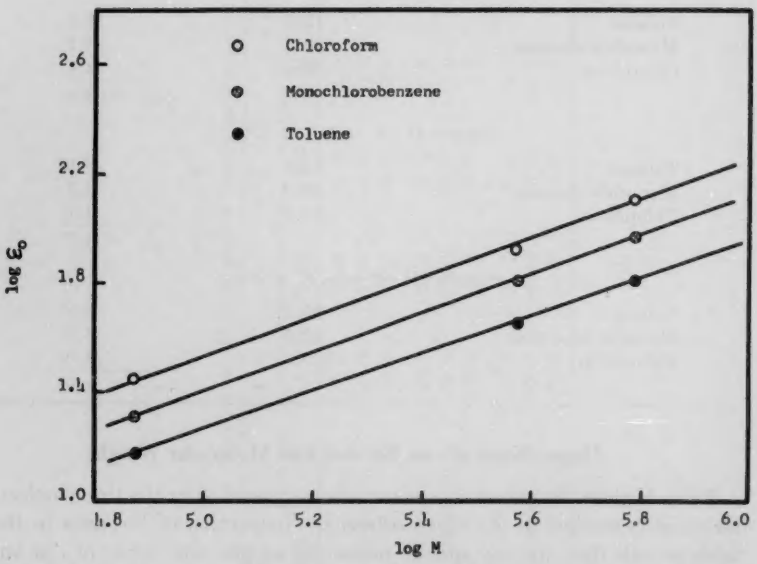

Fig. 6. Plot of log ϵ_0 vs. log M for polymethyl methacrylate in several solvents at 30°C.

The values of ϵ_0 and ϵ_∞ obtained in this manner are given in Table IV. The values of ϵ_∞ are small and range only from 2.0–5.9 for the various solvents and molecular weights. It will be observed that the value of $\epsilon_{\infty av.}$, averaged over all three solvents for a given sample, increases with an increase in molecular weight. Figure 5 shows the plot of $\epsilon_{\infty av.}$ against molecular weight, M. The equation for this straight line is

$$\epsilon_{\infty av.} = 2.60 + 0.34 \times 10^{-5} M \tag{16}$$

The ϵ_0 values are quite large, and range from 15–130. Again, ϵ_0 increases with an increase in molecular weight in all three solvents; and for a given polymer sample, the higher value of ϵ_0 corresponds to the "better" solvent. Figure 6 shows plots of log ϵ_0 versus log M for each solvent. These plots are linear, and yield the equations

$$\text{Toluene:} \quad \epsilon_0 = 5.75 \times 10^{-3} M^{0.70} \tag{17}$$

$$\text{Monochlorobenzene:} \quad \epsilon_0 = 7.09 \times 10^{-3} M^{0.71} \tag{18}$$

$$\text{Chloroform:} \quad \epsilon_0 = 8.54 \times 10^{-3} M^{0.72} \tag{19}$$

TABLE IV
Limiting Effective Volume Factors for PMMA Solutions at 30°C.

Solvent	ϵ_0	ϵ_∞
Sample I ($M = 0.75 \times 10^5$)		
Toluene	15.0	3.7
Monochlorobenzene	20.4	3.1
Chloroform	28.0	2.0
		$\epsilon_{\infty av.} = 2.9$
Sample II ($M = 3.61 \times 10^5$)		
Toluene	45.6	3.6
Monochlorobenzene	65.8	3.7
Chloroform	84.2	3.7
		$\epsilon_{\infty av.} = 3.7$
Sample III ($M = 6.17 \times 10^5$)		
Toluene	65.0	5.9
Monochlorobenzene	92.3	4.2
Chloroform	129.2	4.5
		$\epsilon_{\infty av.} = 4.9$

Dependence of ϵ on Solvent and Molecular Weight

Table V gives the values of ϵ at rounded values of v_2 for the three molecular weights studied in the three solvents. Inspection of the data in this table reveals that, for any specific molecular weight, the values of ϵ at any given v_2 vary significantly with solvent only when $v_2 = 0$, $v_2 = 0.01$, and $v_2 = 0.02$. At higher concentrations ϵ is essentially independent of solvent, and varies only with v_2 and with molecular weight. In other words, at and above $v_2 = 0.04$, the values of ϵ are independent of the nature of the solvent, whether the solvent is "good" or relatively "poor." This behavior is in complete accord with the results Maron, Nakajima, and Krieger[1] found for polystyrene. At and above $v_2 = 0.04$ the values of ϵ at any given v_2 are dependent only on the molecular weight, and this dependency can be found by inserting into eq. (15) eq. (16) for ϵ_∞, and any one of the eqs. (17–19) for ϵ_0.

TABLE V
Dependence of ϵ on Molecular Weight and Solvent at 30°C.

M	Solvent	ϵ at v_2 = 0	0.01	0.02	0.04	0.06	0.08	0.10	0.12	0.16
0.75×10^5	Toluene	15.0	13.2	12.0	10.3	8.9	8.0	7.1	6.4	5.4
	Monochlorobenzene	20.4	17.5	15.3	12.0	9.9	8.5	7.3	6.5	5.4
	Chloroform	28.0	22.4	18.3	13.2	10.7	9.0	7.6	6.7	5.4
3.61×10^5	Toluene	45.6	31.5	24.3	17.0	13.0	10.5	8.8	7.5	6.0
	Monochlorobenzene	65.8	40.8	29.0	18.9	14.0	11.1	9.1	7.8	6.0
	Chloroform	84.2	46.5	31.7	19.7	14.5	11.3	9.2	7.8	6.0
6.17×10^5	Toluene	65.0	41.2	29.6	19.2	14.3	11.3	9.5	8.1	—
	Monochlorobenzene	92.3	49.5	33.2	20.0	14.7	11.6	9.6	8.1	—
	Chloroform	129.2	59.0	38.0	21.3	15.1	11.7	9.6	8.1	—

DISCUSSION AND CONCLUSIONS

Except for the effect of temperature, which was not investigated here, the results of this paper confirm in every respect the findings and conclusions of Maron, Nakajima, and Krieger[1]. In addition, the present work shows that ϵ_∞ is a function of molecular weight but not essentially of solvent, and ϵ_0 is a function of both molecular weight and solvent. Since ϵ is related to both of these quantities, eq. (15), the resultant effect on ϵ is that ϵ is dependent on both solvent and molecular weight only up to ca. $v_2 = 0.04$. Beyond $v_2 = 0.04$, ϵ becomes independent of solvent, and is only a function of molecular weight.

The values of ϵ_∞ given in Table IV for the polymethyl methacrylate samples of three different molecular weights in various solvents vary from 2.0–3.7 for sample I of lowest molecular weight, stay constant at 3.7 for sample II, and vary from 4.2–5.9 for sample III of highest molecular weight. It is believed that the variation for each sample is due to extrapolation uncertainties. However, the averaged ϵ_∞ of each sample in the three solvents increases smoothly and linearly with an increase in the molecular weight. The relation between $\epsilon_{\infty av.}$ and M, as shown in Figure 5, seems to suggest that, although at $\epsilon v_2 = 1$ the polymer molecule "balls up" to a fairly tightly wound coil, the molecules of higher molecular weight cannot wind themselves as tightly as those with lower molecular weight. This effect may be due to steric hindrances in rotation of molecular segments about their bonds in the higher molecular weight molecules, an effect which is less significant in the shorter chains.

The straight lines found for the plots of log ϵ_0 versus log M in all three solvents are practically parallel, the slopes being 0.70, 0.71, and 0.72 for toluene, monochlorobenzene, and chloroform respectively. However, the intercepts increase in magnitude for the solvents in the order listed, as may be seen from eq. (17–19). This latter fact reveals that in a "good" solvent, where the interaction between polymer and solvent is pronounced, ϵ_0 of a given polymer molecule is larger than in a "poorer" solvent, where the environment is less favorable to molecular relaxation.

Maron, Nakajima, and Krieger[1] have shown that $[\eta]_{v_2} = 2\epsilon_0$, where $[\eta]_{v_2} = \left[\frac{\eta_{sp}}{v_2}\right]_{v_2 \to 0}$ is the intrinsic viscosity with the concentration expressed in volume fractions. Therefore, in terms of $[\eta]_{v_2}$ eqs. (17–19) become

$$\text{Toluene:} \qquad [\eta]_{v_2} = 11.50 \times 10^{-3} M^{0.70} \tag{20}$$

$$\text{Monochlorobenzene:} \qquad [\eta]_{v_2} = 14.18 \times 10^{-3} M^{0.71} \tag{21}$$

$$\text{Chloroform:} \qquad [\eta]_{v_2} = 17.08 \times 10^{-3} M^{0.72} \tag{22}$$

Generally intrinsic viscosities are calculated for concentration in g./100 cc. of solution, C. C is related to v_2 by the relation

$$v_2 = C/100\rho_2 \tag{23}$$

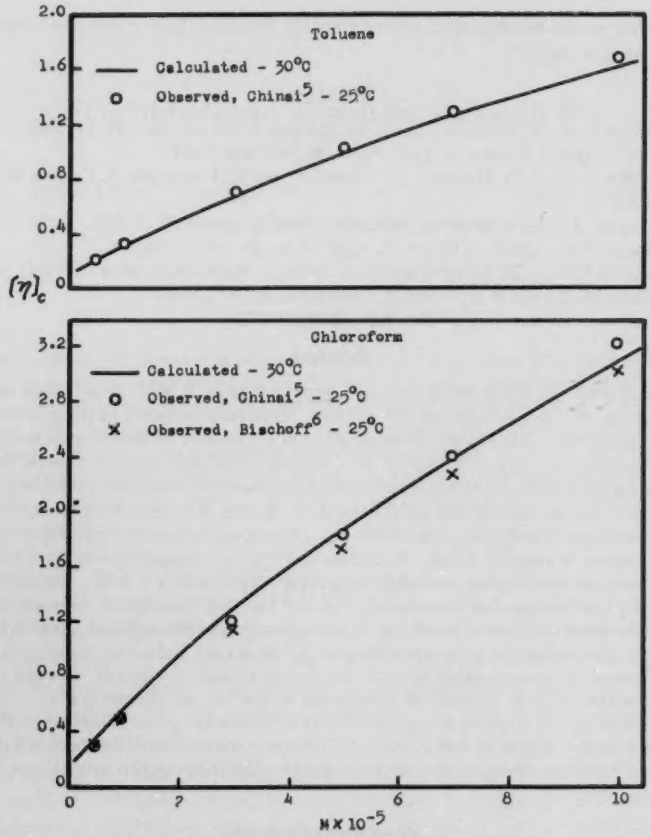

Fig. 7. Comparison of intrinsic viscosity—molecular weight relations for polymethyl methacrylate in toluene and chloroform.

where ρ_2 is the density of polymer. Hence in terms of $[\eta]_C$ eqs. (20–22) are:

$$\text{Toluene:} \qquad [\eta]_C = \left[\frac{\eta_{sp}}{C}\right]_{C\to 0} = 9.91 \times 10^{-5} M^{0.70} \tag{24}$$

$$\text{Monochlorobenzene:} \qquad [\eta]_C = 12.22 \times 10^{-5} M^{0.71} \tag{25}$$

$$\text{Chloroform:} \qquad [\eta]_C = 14.72 \times 10^{-5} M^{0.72} \tag{26}$$

The comparisons of eq. (24) with Chinai's[3] equation and of eq. (26) with the equations of Chinai[3] and Bischoff[5] obtained for these systems are shown in Figure 7 by plotting $[\eta]_C$ against rounded values of M covering the molecular weight range studied in this paper. The agreement between the $[\eta]_C$ values obtained from all these equations is satisfactory. This result confirms the findings of Maron and coworkers[1,7,8] for synthetic rubber latex and polystyrene solutions, namely, that

$$[\eta]_{\epsilon_2} = 2\epsilon_0$$

and hence ϵ_0 can be obtained independently from intrinsic viscosity measurements as $\epsilon_0 = [\eta]_{v_2}/2$.

References

1. Maron, S. H., N. Nakajima, and I. M. Krieger, *J. Polymer Sci.*, **37**, 1 (1959).
2. Ree, T., and H. Eyring, *J. Appl. Phys.*, **26**, 793, 800 (1955).
3. Chinai, S. N., J. D. Matlack, A. L. Resnick, and R. J. Samuels, *J. Polymer Sci.*, **17**, 391 (1955).
4. Bischoff, J., and V. Desreux, *Bull. Soc. Chim. Belges*, **61**, 10 (1952).
5. Maron, S. H., and R. J. Belner, *J. Appl. Phys.*, **26**, 1457 (1955).
6. Maron, S. H., I. M. Krieger, and A. W. Sisko, *J. Appl. Phys.*, **27**, 971 (1954).
7. Maron, S. H., and P. E. Pierce, *J. Colloid Sci.*, **11**, 80 (1956).
8. Maron, S. H., and A. W. Sisko, *ibid.*, **12**, 99 (1957).

Résumé

On a effectué une étude sur le comportment rhéologique à 30°C de solutions de trois échantillons de polyméthacrylate de méthyle, dans trois solvants et dans les régions d'écoulement Newtonien et non-Newtonien. On a parcouru un domaine de concentration allant approximativement de O à 16% en poids. En appliquant la théorie de Ree-Eyring, il a été possible de repreésenter les résultats observés dans les deux unités d'écoulement et d'obtenir, à partir des paramètres de la théorie, le volume hydrodynamique effectif occupé par le polymère en solution, ϵv_2. Ici v_2 est la fraction de volume du polymére et ϵ un facteur de volume effectif. Le facteur de volume, ϵ, dépend du solvant et du poids moléculaire, seulement pour une valeur de v_2 situé au dessus de $v_2 = 0.04$. En dessous de $v_2 = 0.04$, ϵ est indépendant du solvant et est une fonction uniquement du poids moléculaire. Ces observations indiquent que l'enchevêtement des chaînes n'est pas probable en solution. La chaîne de polymère s'enroule plutôt sur elle-même, et forme une petite masse lorsque la concentration effective $\epsilon v_2 = 1$ et lorsque la viscosité edevient infinie. La concentration pour laquelle ce phénomène a lieu, v_∞ est donnée par $v_\infty = 1/\epsilon_\infty$. On a trouvé que la quantité ϵ_∞ est une fonction linéaire du poids moélculaire, M. De plus, la valeur de ϵ pour $v_2 = 0$, ϵ_0, est une fonction exponentielle de M et fournit des expressions reliant la viscosité intrinsèque au poids moléculaire en bon accord avec les résultats publiés.

Zusammenfassung

Eine Untersuchung des Fliessverhaltens der Lösungen von drei Polymethylmethacrylatproben in drei Lösungsmitteln bei 30°C im Newtonschen und nicht-Newtonschen Bereich wurde durchgeführt. Der Konzentrations-bereich unfasste etwa 0–16 Gew.%. Durch Anwendung der Ree-Eyring Theorie war es möglich die Versuchsdaten durch zwei Fliesseinheiten darzustellen und aus den theoretischen Parametern das vom Polymeren in der Lösung eingenommene, effektive hydrodynamische Volumen, ϵv_2, zu erhalten. Hier bedeutet v_2 den Volumbruch des Polymeren und ϵ einen Faktor für das effektive Volumen. Der Volumsfaktor, ϵ, zeigte nur bis hinauf zu ca $v_2 = 0{,}04$ eine Abhängigkeit vom Lösungsmittel und Molekulargewicth. Oberhalb $v_2 = 0{,}04$ ist ϵ vom Lösungsmittel unabhängig und nur eine Funktion des Molekulargewichts. Diese Beobachtungen zeigen, dass eine Kettenverschligung in Lösung nicht wahrscheinlich ist. Die Polymerkette verknäuelt sich vielmehr in sich selbst und wird bei der effektiven Konzentration $\epsilon v_2 = 1$ und bei Unendlichwerden der Viskosität eine kompakte, kleine Masse. Die Konzentration, bei welcher dieses Verhalten eintritt, v_∞, ist gegeben durch $v_\infty = 1/\epsilon_\infty$. Die Grösse ϵ_∞ erwies sich als lineare Funktion des Molekulrgewichts, M. Weiters wurde gefunden, dass der Wert von ϵ bei $v_2 = 0$, ϵ_0, eine Exponentialfunktion von M ist und Beziehungen zwischen Viskositätszahl und Molekulargewicht in guter Übereinstimmung mit Literaturangaben liefert.

Received May 21, 1962

JOURNAL OF POLYMER SCIENCE: PART A VOL. 1, PP. 2667–2678 (1963)

Turbidimetric Titration of Nylon 66

G. J. HOWARD,* *Research Department, British Nylon Spinners Ltd., Pontypool, Monmouthshire, England*

Synopsis

The turbidimetric titration of nylon 66 is reported. It is shown that the precipitation of any species is independent of polymer species differing in molecular weight and that the precipitability is a function of both polymer concentration and degree of polymerization. The construction of molecular weight distributions from turbidity results is described. The distribution obtained for a reference polymer is sharper than that from a careful fractional precipitation but is superior to a simple single-stage preparative fractionation. Distribution curves are given for other nylon 66 polymers, including photodegraded yarns.

INTRODUCTION

Since its introduction by Morey and Tamblyn,[1] turbidimetric titration has been employed to estimate the distribution of molecular weights in a number of polymers. The present paper describes the application of the method to nylon 66. In general, turbidimetric titration gives only the overall shape of the molecular weight distribution;[2] however, the technique is less laborious than the more accurate methods of polymer fractionation. The lack of precision arises, in part because a single-stage cumulative precipitation method is employed which, in many cases, involves non-equilibrium precipitation conditions. The high dilutions employed should tend however, to improve the efficiency of fractionation.

EXPERIMENTAL

The turbidimeter is a double-beam instrument which was designed for continuous titration work. White light is used; preliminary trials, by continuous turbidimetric titration, showed that essentially identical curves were traced with white, yellow, and blue-green incident light. The square cross-sectioned test cell is of optical quality glass and is of about 40 ml capacity. This cell and a similar comparison cell, which contains water, are positioned in a small water bath at 25 ± 0.05°C. supplied from an external thermostat.

The mode of action of the instrument may be seen from the block diagram (Fig. 1): the extent to which the optical wedge is rotated by the

* Present address Department of Textile Chemistry, College of Science and Technology, Manchester, England.

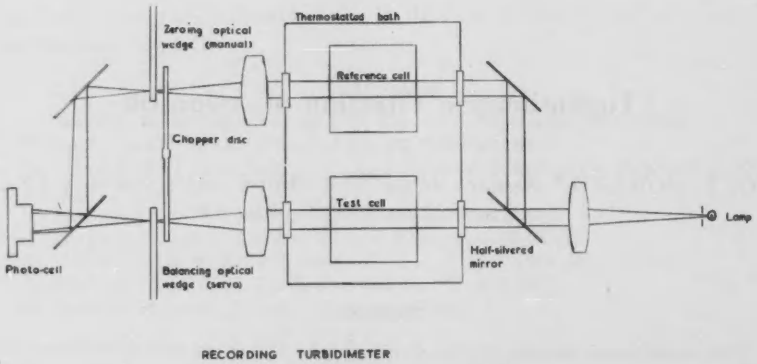

Fig. 1. Recording turbidimeter.

servo mechanism to maintain the equivalence of the light intensities in each beam is recorded by the pen of a chart recorder. The scale of this recorder is linear in optical density and all turbidities are given in the arbitrary units of the chart paper. A neutral density filter (Ilford) of rated optical density 0.49 is used as a day-to-day standard and gives a recording of 4.975 ± 0.005 units.

Titration Procedure

The procedure described below is noncontinuous in the sense that the system is brought to a predetermined solvent/nonsolvent content and the turbidity produced by the stable emulsion of precipitated polymer species allowed to reach a steady value. The turbidimetric titration curve is obtained from a series of such experiments, covering a suitable range of solvent/nonsolvent compositions; the total polymer concentration is kept constant throughout the titration. The experimentally obtained turbidimetric titration curve relates τ, the turbidity of the precipitate, to γ, the volume fraction of nonsolvent. By suitable calibration, the titration curve is converted to an integral distribution curve.

The solvent and nonsolvent chosen for this work are *m*-cresol and cyclohexane respectively; these are satisfactory in fractional precipitation,[3] in that a liquid precipitated phase is formed. *m*-Cresol/cyclohexane mixtures are prepared to give a series covering the required range of compositions; the liquids are freshly distilled and well-dried. A known volume (usually 1 ml.) of a dilute polymer solution in *m*-cresol is placed in the optical cell from a calibrated pipette and a volume (usually 35 ml.) of one of the diluent solutions added from a calibrated burette. The contents are stirred at a slow and constant speed for 40 sec., the cell closed by a well-fitting lid and placed in the cell compartment of the turbidimeter. This standard procedure is used throughout. For titration work, the polymer concentration was kept within the range 1.00–2.70 mg./100 ml. To obtain

the relation between turbidity and concentration of precipitated polymer, the concentration range was extended to lower values (*ca.* 0.10 mg./100 ml.).

The deflection of the recorder pen was noted when the turbidity reached a constant value. The time taken for the turbidity of the system to attain the equilibrium value depended upon the concentration of precipitated polymer and varied from about 10 min. at the lowest concentrations (*ca.* 0.1 mg./100 ml.) to about 80 min. at concentrations of 2.0 mg./100 ml. and above. Once equilibrium was reached, the turbidity remained constant for several hours before slowly decreasing. The cell must be closed with a well-fitting lid in order to prevent the evaporation of cyclohexane, as loss

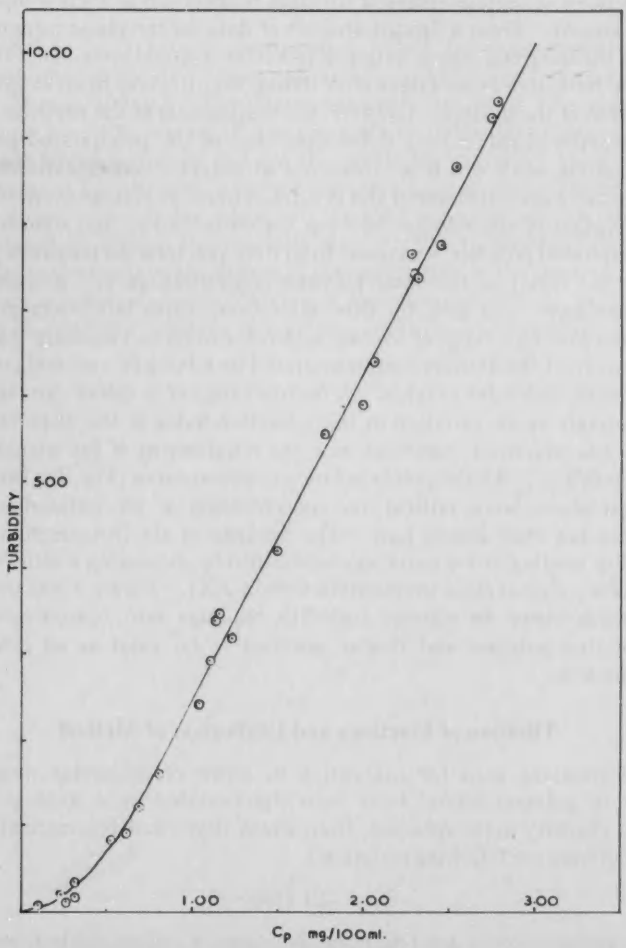

Fig. 2. Relation between turbidity and concentration of precipitated polymer.

of nonsolvent in this manner causes a drop in turbidity. Equilibrium turbidity values are usually reproducible to 0.10 units or better.

Concentration Dependence of Turbidity

The turbidity developed will be a function of the concentration of precipitated polymer, the size of the emulsion particles, and the refractive indices of both the particles and the liquid medium. The extreme compositions of the solvent/nonsolvent mixtures used correspond to a range of 1.450–1.434 for the refractive index of the medium: the variation in any one turbidimetric titration will not be so wide. The refractive index of the particles at various stages of titration is uncertain as their composition is not known. From a limited amount of data on the phase compositions during the fractional precipitation of nylon 66, it would seem likely that the particle refractive index might alter during the titration to an extent similar to that of the medium: however, the composition of the particles during turbidimetric titration may differ from that of the precipitated phase in fractionation work which is carried out at polymer concentrations higher by a factor of several hundred and in a different range of nonsolvent content.

Derivation of the relation between turbidity and c_p, the concentration of precipitated polymer, was made from fully precipitated polymers so that c_p was set equal to the total polymer concentration, c_t. A number of polymers have been used for this calibration: three laboratory-prepared samples covering a range of average molecular weights, two sharp fractions, and one broad distribution sample produced by mixing two normal polymers of different molecular weights. A narrow range of γ values (giving a correspondingly small variation in the refractive index of the dispersion medium) was employed consistent with the requirement of full precipitation of the polymer. All the points fall on a common curve (Fig. 2); this curve is linear above some critical low concentration of precipitated polymer but does not obey Beer's Law. The linearity of the instrument up to a turbidity reading of 1.4 units was established by measuring a series of dilutions of a colloidal silica preparation (Syton 2 X). Figure 2 was used as a calibration curve to convert turbidity readings into concentrations of precipitated polymer and it was assumed to be valid at all extents of precipitation.

Titration of Fractions and Calibration of Method

The fractions used for calibration in terms of molecular weight (or degree of polymerization) have been characterized by a single-point intrinsic viscosity approximation, from which degrees of polymerization are deduced from the following equation.[3]

$$\bar{x}_v = 421\ ([\eta])^{1.34} \tag{1}$$

The fractions cover a ten-fold range in degree of polymerization and have been subjected to two or three fractional precipitation stages; they are

TABLE I
Fractions Used for Calibration

Fraction	Degree of polymerization
F/3	45
E/3	111
A/5/b	131
C/3	202
A/1/c	276
B/2/a	343
A/2/a	434
A/1/b	487

considered to be of narrow distributions. Each fraction was titrated at three concentrations: the concentration range covered was limited to about 1.00–2.70 mg./100 ml. The lower concentration limit was chosen to permit an accurate tracing of the complete turbidimetric titration curve while the upper limit was set by the maximum turbidity value on the instrument. The titration curves of one sample are shown as Figure 3.

The nonsolvent content, when half the total polymer concentration was precipitated, is termed the precipitability $\bar{\gamma}$; this parameter depends on both the concentration and degree of polymerization of the fraction. Over the range studied, the precipitability is linearly related to c_s, the concentration of polymer remaining in solution. Within experimental error, the

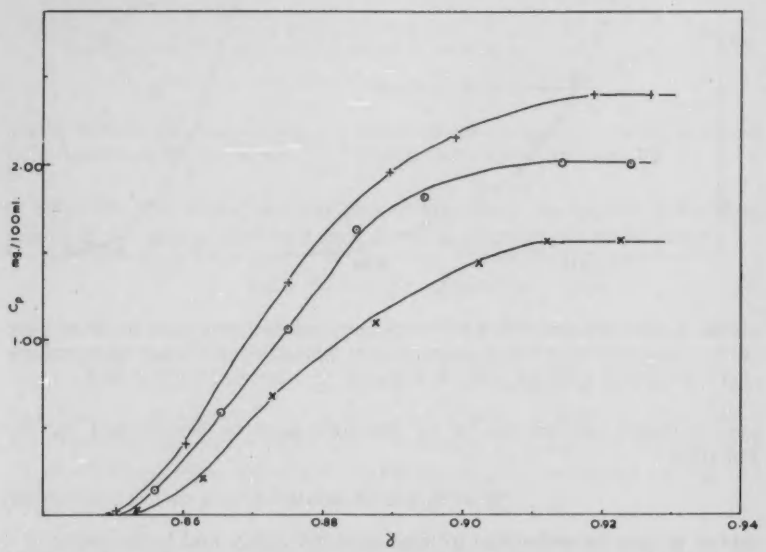

Fig. 3. Turbidimetric titration curves of fraction C/3. Polymer concn. (+) 2.40 mg./100 ml.; (O) 2.02 mg./100 ml.; (×) 1.56 mg./100 ml.

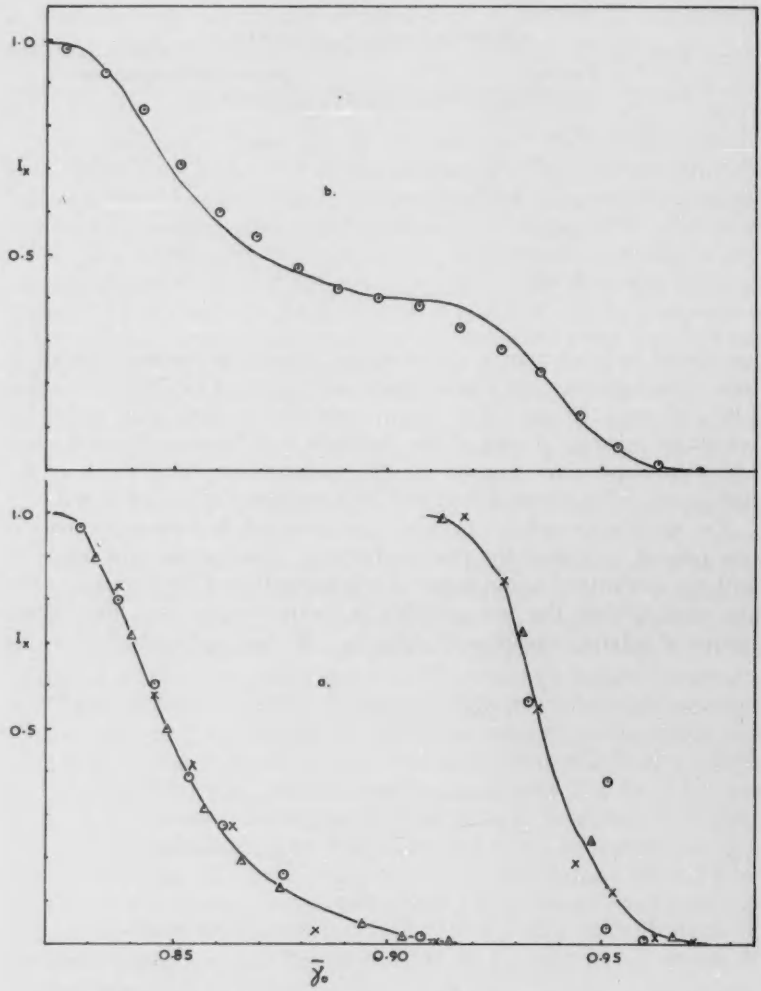

Fig. 4. Turbidimetric titration curves corrected for concentration dependence. (*a*) separate titrations of two polymers, each at three differing polymer concentrations: (*b*) (⊙) titration of a mixture of the two polymers; (—) calculated curve from (*a*).

concentration dependence of all fractions may be represented by the equation

$$\bar{\gamma}_0 = \bar{\gamma} + 2.50 \times 10^{-3} c_s \qquad (2)$$

where $\bar{\gamma}_0$ may be called the intrinsic precipitability and is the value of $\bar{\gamma}$ at infinite dilution. In eq. (2) the concentration of polymer in solution c_s is in mg./100 ml.

To extend the calibration procedure based on fractions to whole polymers requires that the precipitation of any species is not affected by the presence of lower molecular weight species remaining in solution. The titration of a mixture of two polymer samples with nonoverlapping distributions is found to be very little different to the curve calculated from the titration of the separate polymers (Fig. 4). The derivations are within the repeatability of the titration procedure (cf. Fig. 5) and the independent titration of species of differing molecular weight may, therefore, be assumed.

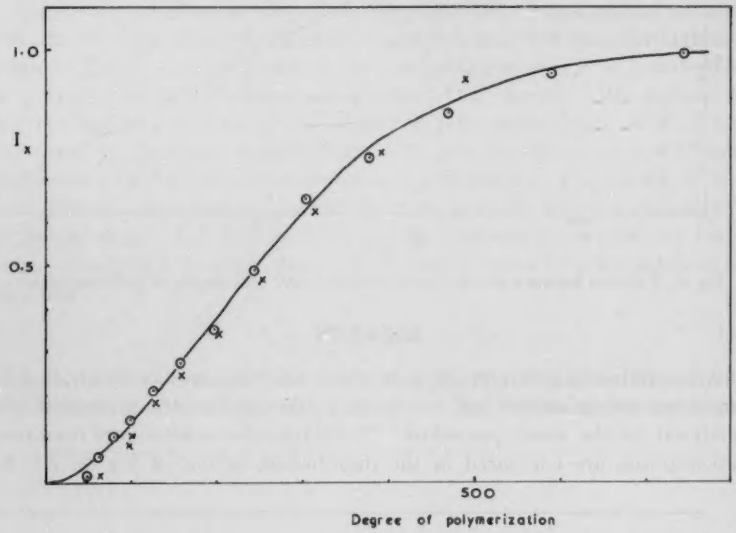

Fig. 5. Integral distribution curve of a vacuum-finished polymer: (⊙) polymer concentration 2.74 mg./100 ml.; (×) polymer concentration 1.89 mg./100 ml.

From the determined intrinsic precipitabilities of the series of calibrating fractions, the dependence on degree of polymerization was found to be

$$\log x = 11.725 - 10.750\ \bar{\gamma}_0 \tag{3}$$

and the data were graphed in Figure 6. The procedure for estimating the distribution curve of a whole polymer was based on Figure 2 and eq. (2–3). The equilibrium turbidity was measured at various γ values; c_p was calculated from Figure 2 and hence c_s was found. From the latter value the correction to each γ value was determined from eq. (2); the values of $\bar{\gamma}_0$ so obtained were converted to degrees of polymerization by eq. (3). As the cumulative weight fraction I_x was given by

$$I_x = c_s/c_t \tag{4}$$

the integral distribution curve may be plotted.

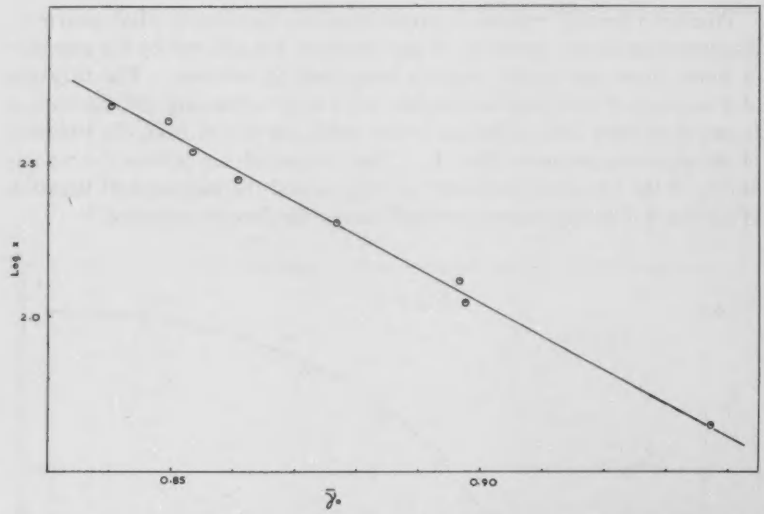

Fig. 6. Relation between the intrinsic precipitability and degree of polymerization.

RESULTS

An equilibrium nylon 66 polymer which has been previously studied by fractional precipitation[3] and by thermal diffusion[4] has been titrated and analyzed by the above procedure. Turbidimetric titration and fractional precipitation are compared in the distribution curves of Figure 7. Al-

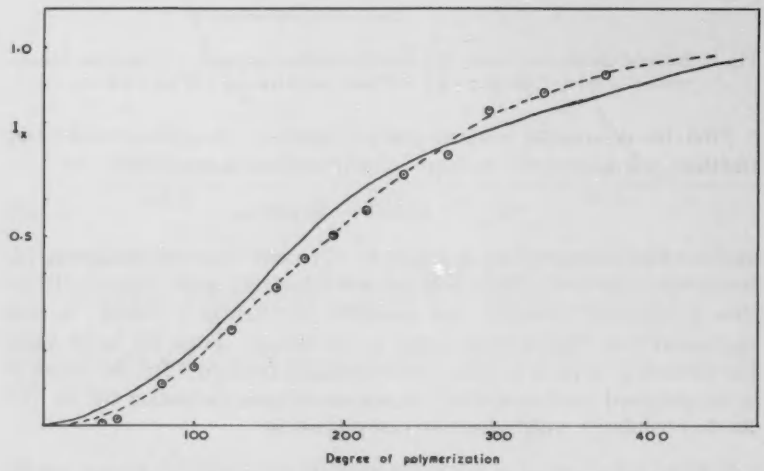

Fig. 7. Integral distribution curve of reference polymer: (—) fractional precipitation (ref. 3); (⊙) turbidimetric titration; (– –) Tung function fitted to titration data.

though the two distribution curves are not dissimilar, the turbidimetric method was less satisfactory in that a sharper distribution was indicated. Thus, turbidimetric titration gives $\bar{x}_w/\bar{x}_n$ as 1.64, whereas fractional precipitation gives a value of 1.87. It should be appreciated that the fractional precipitation involved three fractionation stages and, as a consequence, was a lengthy experiment. The apparent distribution given by the turbidimetric titration method described here is similar to that from a fractional precipitation involving two fractionation stages[3] but is much superior to a single-stage process.

Unlike the distribution curve from the preparative fractionation method, the one derived from turbidimetric titration does not pass through the origin. This is a consequence of the breakdown of eq. (3) at low degrees of polymerization. Equation (3) predicts that species with degrees of polymerization less than 10 are soluble in pure nonsolvent. This is not the case: all polymers examined are fully precipitated at $\gamma = 0.97$ and oligomers of nylon 66 are insoluble in cyclohexane. The failure of the turbidimetric titration analysis to describe properly the low end of the molecular weight distribution curve may be overcome in an arbitrary fashion by fitting the results to the empirical distribution function introduced by Tung[6]

$$I_x = 1 - \exp.\ (-ax^b) \tag{5}$$

The parameters of this equation are obtained by a suitable graphical plot of the experimental results; this plot is such that the low molecular weight

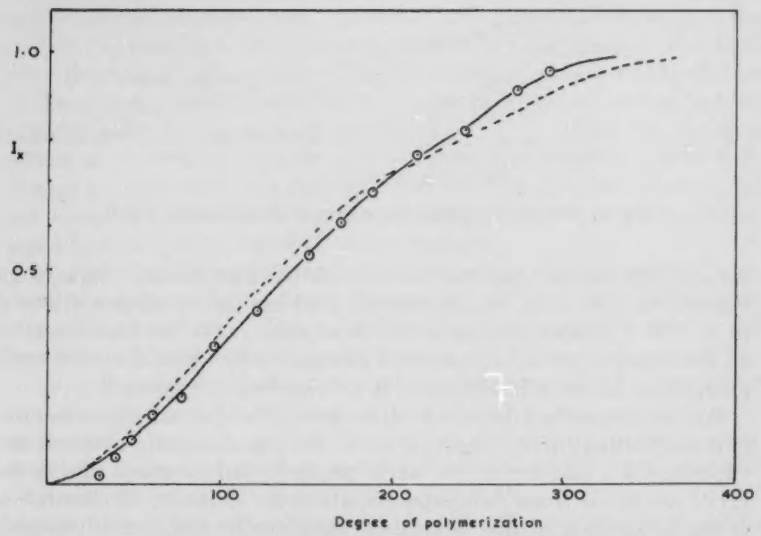

Fig. 8. Integral distribution curve of mixture of two polymers. (⊙) turbidimetric titration; (—) two-part Tung function; (– –) calculated curve for mixture.

region of the distribution is accorded little weight. Curve fitting to the Tung distribution equation is illustrated by the full-line curve of Figure 5, from which the nature of the correction imposed may be assessed.

A number of other equilibrium nylon 66 polymers have been examined by the technique of turbidimetric titration. For example, a higher molecular weight nylon 66 prepared by conducting the final stages of the polycondensation under vacuum is shown as Figure 5. Here, the results of two titrations, at total polymer concentrations of 2.74 and 1.89 mg./100 ml. are given; again, the smooth curve drawn through the points is the appropriate Tung distribution function. Despite the arbitrary correction involved in employing the Tung function to represent the distribution, the

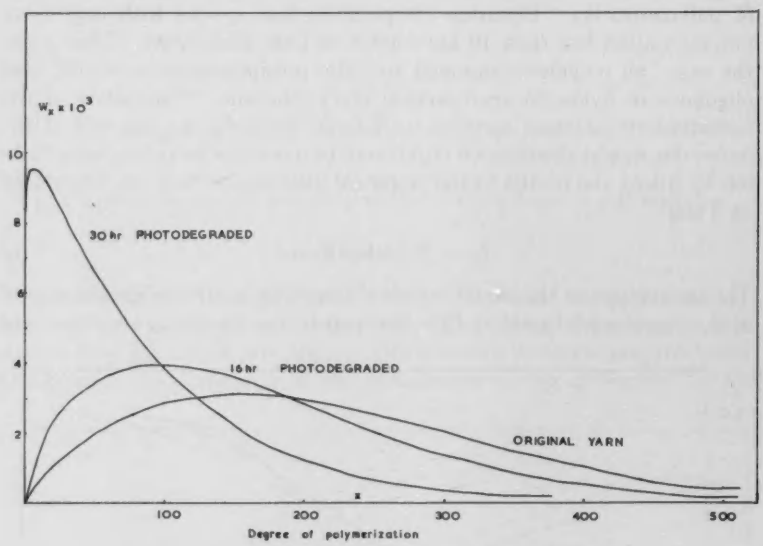

Fig. 9. Differential distribution curves of photodegraded yarns.

curve is still sharper than the "most probable" distribution. Thus, from Figure 5 the ratio $\bar{x}_z/\bar{x}_w = 1.35$, whereas the Flory theory requires this ratio to be 1.50. This sharpening of the distribution curve has been found in all examinations of well-equilibrated polymers which should obey Flory's distribution and must be attributed to deficiencies in the method.

Further, the method described will not readily detect small discontinuities in a distribution curve. Figure 8 shows the experimentally obtained distribution for a mixture of two whole polymers and compares this to the curve calculated from their separate titrations. Finally, an illustration of the application of this method of turbidimetric titration to research problems is provided by the examination of undelustred nylon 66 multifilament yarns after periods of photo-oxidation (mercury arc). The

changes in the distribution are best visualized by plotting the differential distribution curves from

$$W_x = abx^{b-1} \exp. (-ax^b) \quad (6)$$

The changes in the distribution function (Fig. 9) are such that the photodegradation of these samples is not a process of uniform random scission.

DISCUSSION

Two comments must be made on the calibration method. First, the selection of the point of half precipitation as the precipitability which is related to the viscosity-average degree of polymerization is an arbitrary procedure, although one adopted by some previous workers in this field.[9,10] However, the alternative approach taken by other investigators, namely, to define a precipitability in terms of the point of initial precipitation, must be regarded as much less satisfactory in that a disproportionate influence is exerted by the highest molecular weight species in the sample. Secondly, a linear dependence of the precipitability on polymer concentration is found to fit the experimental results within the range for which turbidimetric titration is possible: it is not suggested that eq. (2) may be extrapolated to less dilute systems. Although a relation of this form was apparently observed in a study of cellulose acetate,[7] other authors find that the precipitability (however defined) is linearly related to the logarithm of the polymer concentration. The present results can in fact be fitted to such a logarithmic dependence, with slopes varying with the degree of polymerization of the fraction. However, this variation of the slope of the plot of $\bar{\gamma}$ against log c_s is in the sense opposite to that expected; that is to say, the efficiency of separation of adjacent species decreases with dilution of the system. A calibration procedure has been devised on the basis of $\bar{\gamma}/\log c_s$ plots having slopes proportional to log x. When the titration results of the well-characterized reference polymer described above were treated by this calibration procedure the resulting distribution curve did not agree with that from fractional precipitation but was much sharper and displaced to lower degrees of polymerization.

In conclusion, the turbidimetric titration method described in this paper must be considered to yield only the approximate form of the distribution of a nylon 66 polymer. This is, perhaps, to be anticipated in view of the assumptions introduced by (*a*) application of the relation between τ and c_p to all stages of precipitation, (*b*) extrapolation of eq. (2) to low polymer concentrations and, (*c*) the breakdown of eq. (3) at low degrees of polymerization. The only previously reported turbidimetric titration study of a polyamide, by Griehl[8] on nylon 6, found, as in this work, that the derived distribution curves were rather sharper than the "most probable" distribution. Thus with polyamides, as with other systems,[2] it is fair to conclude that turbidimetric titration is not capable of accurately deducing the absolute molecular weight distribution, but that the rapidity of the

method makes it suitable for less demanding work such as comparative studies of distributional changes.

The author is indebted to members of the Experimental Engineering Group of this company for the design and construction of the turbidimeter and to Mr. A. G. Edwards for experimental assistance. This paper is published by permission of British Nylon Spinners Ltd.

References

1. Morey, D. R., and J. W. Tamblyn, *J. Appl. Phys.*, **16**, 419 (1945).
2. Hall, R. W., in *Techniques of Polymer Characterisation*, P. W. Allen, ed., Butterworths, London, 1959.
3. Howard, G. J., *J. Polymer Sci.*, **37**, 310 (1959).
4. Krejsa, J., unpublished results quoted in ref. (5).
5. Howard, G. J., *Progress in High Polymers*, Vol. I, J. Robb and F. W. Peaker, eds., Heywood, London, 1961.
6. Tung, L. H., *J. Polymer Sci.*, **20**, 495, (1956).
7. Bischoff, J., and V. Desreux, *Bull. Soc. Chim. Belges*, **60**, 137 (1951).
8. Griehl, W., *Faserforsch. Textiltech.*, **6**, 260 (1955).
9. Oth, A., *Bull. Soc. Chim. Belges*, **58**, 285 (1949).
10. Krasovec, F., N. Vene, and A. Peterlin, *Rept. J. Stefan Inst.*, **4**, 165 (1957).

Résumé

On décrit la titration turbidimétrique du nylon 66. On montre que la précipitation d'une fraction est indépendante de la présence d'autres fractions polymériques de poids moléculaire différent. La possibilité de précipitation dépend de la concentration en polymère et de son degré de polymérisation. On décrit la méthode pour construire la distribution des poids moléculaires à partir des résultats turbidimétriques. La distribution qu'on obtient pour un polymère de référence est un peu plus étroite que celle qui résulte d'un fractionnement préparatif en une étape. On donne des courbes de distribution pour d'autres polymères de nylon 66 y compris des fils dégradés par l'action de la lumière.

Zusammenfassung

Es wird über Trübungstitrationen an Nylon 66 berichtet. Die Fällung einer Molekülart ist unabhängig von Polymermolekülen mit anderem Molekulargewicht und die Fällbarkeit ist eine Funktion der Polymerkonzentration und des Polymerisationsgrades. Die Gewinnung von Molekulargewichtsverteilungen aus Trübungsergebnissen wird beschrieben. Die für ein Standardpolymeres erhaltene Verteilung ist um einiges schärfer als die aus einer sorgfältigen, fraktionierten Fällung gewonnene, ist aber einer einfachen präparativen Einstufenfraktionierung überlegen. Verteilungskurven für andere Nylon-66-polymere, einschliesslich eines photochemisch abgebauten Garnes, werden angegeben.

Received May 22, 1962

JOURNAL OF POLYMER SCIENCE: PART A VOL. 1, PP. 2679–2695 (1963)

The Emulsion Polymerization of 2,3-Dimethylbutadiene-1,3*

MAURICE MORTON and WILLIAM E. GIBBS,† *Institute of Rubber Research, University of Akron, Akron, Ohio*

Synopsis

A study has been carried out on the kinetics of the emulsion polymerization of 2,3-dimethylbutadiene-1,3. The kinetic treatment of Smith and Ewart was applied for the direct determination of the absolute propagation rate constant k_p. The following expression was obtained: $k_p = 8.9 \times 10^7 \exp\{-9000/RT\}$ liter/mole/sec. A previously developed treatment was applied to the determination of the relative and absolute crosslinking rates of 2,3-dimethylbutadiene-1,3. The results led to the following expression for the absolute crosslinking rate constant k_x: $k_x = 3.0 \times 10^6 \exp\{-14400/RT\}$ liter/mole/sec. A comparison of these rate constants was made for the three dienes, viz., butadiene, isoprene, and dimethylbutadiene. The propagation rate constants were found to vary only by a factor of 2–3. However, the crosslinking rates were found to decrease considerably in going from butadiene to isoprene to dimethylbutadiene. This was attributed, mainly, to the decreased side-vinyl content of the latter two monomers, compared to butadiene, as well as to the steric hindrance imposed by the presence of the methyl group.

Introduction

2,3-Dimethylbutadiene-1,3 (DMBD) is best known as the basis of "methyl rubber" produced in Germany during World War I. An account of this thermal polymerization has been given by Gottlob[1] and also summarized by Whitby and Katz.[2] Other studies of the bulk polymerization of this monomer, thermal and catalyzed, were carried out by Whitby and Crozier,[3] Conant and Tanberg,[4] and Starkweather et al.[5] A more recent study of the bulk polymerization of DMBD is reported by Konigsberger and Salomon,[6] who measured the rates of both the catalyzed and uncatalyzed processes. In addition to these studies, there can be found a fairly substantial number of references in the patent literature to methods of polymerizing this monomer.

The emulsion polymerization of DMBD has been mentioned in the

* Presented in part at the 126th meeting of the American Chemical Society, Division of Polymer Chemistry at New York, September 1954.

† Taken in part from the dissertation submitted by William E. Gibbs in partial fulfillment of the requirements for the degree of Doctor of Philosophy, University of Akron, June, 1959. Present address: Polymer Branch, Non-Metallic Materials Laboratory, Aeronautical Systems Division, Wright-Patterson AFB, Ohio.

patent literature as early as 1929.[7,8] A study of the emulsion copolymerization of this monomer with butadiene and acrylonitrile is described by Konigsberger and Salomon[9] in a more recent publication, while Marvel and Williams[10] carried out a more detailed study of the emulsion copolymerization of DMBD with butadiene at 50°C. Recently, Gilbert and Williams[11] determined the reactivity ratios of this monomer in copolymerizations with butadiene and isoprene at 5°C.

The above studies contain little or no kinetic data on the behavior of DMBD in emulsion polymerization. Hence it was thought desirable to study the polymerization of this monomer by the same approach previously applied to butadiene[12,13] and isoprene.[14,15] In this way it was hoped to determine values for the absolute propagation and crosslinking reaction rate constants.

Experimental

Materials

Acetone (Eimer and Amend reagent grade)—dried over calcium chloride 24 to 48 hr. and used immediately.

Benzene (Baker's reagent grade, thiophene free)—when used in monomer synthesis—dried 24 to 48 hr. over calcium chloride and used immediately, otherwise used as received.

Calcium chloride (Eimer and Amend reagent grade)—used as received.

Diisopropylbenzene monohydroperoxide(DIBHP)—used as received from the Hercules Powder Co. Stated to contain about 60% active hydroperoxide.

2,3-Dimethylbutadiene-1,3—obtained in part from the Borden Co. It was fractionated, and the portion boiling between 68.5 and 69.0°C. at 760 mm. Hg was retained for use. Most of this monomer, however, was prepared in this laboratory by the procedure discussed later.

Hydrobromic acid—kindly provided by the Goodyear Tire and Rubber Co. Research Laboratory as a 48% aqueous solution. Used as received.

Isopropanol (Commercial Solvents Co., technical grade)—used as received.

Magnesium metal (Baker's analytical reagent grade turnings)—used immediately after opening.

Mercaptan (Sulfole B-8 mercaptan, Phillips Petroleum Co.), stated to be a mixture of isomeric tertiary dodecyl mercaptans. However, its molecular weight (cryoscopic, in benzene) of 193 g./mole indicates an average of an undecyl mercaptan. It was chosen because its chain transfer activity with other monomers has been extensively studied. It was distilled at reduced pressure and the central fraction retained for use.

Mercuric chloride (Baker's analytical reagent)—used as received.

Potassium chloride (Baker's analytical reagent grade)—used to reduce latex viscosity at high conversions.

Potassium persulfate (Baker's analytical reagent grade)—used as received.

Soap—Office of Synthetic Rubber potassium fatty acid soap flakes (KOSR). This is a mixture of mainly potassium stearate, palmitate and oleate. Used as received.

Tetraethylene pentamine (TEP) (Carbide and Carbon Chemical Co., technical grade)—distilled at reduced pressure and the central fraction, boiling between 170 and 180°C., retained for use.

Tripotassium phosphate (Eimer and Amend C.P. grade)—used as received to buffer the system when "peroxamine" initiation was employed.

Procedures

Monomer Synthesis

Two sources of monomer were used. Initially the DMBD was obtained via the synthesis from acetone. Later, a small quantity was obtained from a commercial source.

The synthesis method used in our laboratory followed the procedures of Adams and Adams[16] and Allen and Bell.[17] This involves, essentially, the condensation of two moles of acetone in the presence of magnesium amalgam to form pinacol, isolated as the hydrate, followed by the dehydration of the hydrate by azeotropic distillation with benzene and reaction of the anhydrous pinacol with hydrobromic acid to yield the diene. Variations in the prescribed procedures were made in minor instances. Overall yields were in the proximity of 25% based on the molar quantity of magnesium used initially. The monomer was inhibited with *tert*-butyl catechol and stored in a Dry Ice chest. It was fractionated through a a packed column immediately before use. The infrared spectrum of the monomer supplied by the Borden Co. was identical to that published by the American Petroleum Institute[18] for this monomer prepared from acetone. The physical constants given in Table I were found for the monomer synthesized in this laboratory.

TABLE I
Physical Constants of DMBD

	Refractive index, n_D^{20}	Boiling point, 760 mm.
Observed	1.4379	68.5–69.°C.
Literature[a]	1.4377	68.8–68.9°C.

[a] See ref. 19.

Polymerization

The bottles used were either four or eight ounce round-form type, fitted with a metal screw cap lined with extracted butyl rubber and nitrile rubber gaskets. The caps were perforated to enable sampling by the hypodermic

syringe technique. The recipes used for the propagation and crosslinking rate studies are given in Table II. The charging and sampling techniques are adequately discussed elsewhere.[14]

TABLE II
2,3-Dimethylbutadiene-1,3 Emulsion Recipes

Component	Parts by weight	
	Propagation studies	Crosslinking studies
Distilled water	180	180
Monomer	100	100
KOSR soap	5	5
Potassium chloride	1.0	0.7
Tripotassium phosphate	0.4	—
Tetraethylene pentamine	0.4	—
Diisopropylbenzene monohydroperoxide	0.2	—
Potassium persulfate	—	Variable
Sulfole mercaptan	—	Variable

Particle Size and Number Determination

Measurements of the latex particle size and, hence, the number of latex particles were carried out using the soap titration method of Maron et al.[20-22] The determinations were made at 50°C. using KOSR soap and a duNouy tensiometer. The complete technique used has been described elsewhere.[13]

Intrinsic Viscosity Measurements

The viscosity measurements were made with a modified dilution-type Ubbelohde viscometer, having a bulb capacity of 250 ml. The outflow time for benzene was in excess of 100 sec. and no kinetic energy correction was necessary. Viscosity measurements using benzene as the solvent were carried out in the usual manner. However, nearly all the viscosity measurements reported here used the Vistex viscosity method of Henderson and Legge.[23] The Vistex solvent (80 volumes benzene and 20 volumes of isopropanol) was employed whereby a sample of latex could be dispersed directly without having to isolate the polymer. Dilution of this solution was made with pure benzene, however, so that the intrinsic viscosity obtained was the same as if pure benzene had been used as the original solvent. All measurements were made at 30°C.

Mercaptan Analysis

The residual mercaptan in the polymerized latex was determined by Kolthoff and Harris' method[24] of amperometric titration as modified by Morton and Salatiello.[12]

Osmotic Pressure

Osmotic pressure measurements were made using a modified "thistle-tube" osmometer of the Sands and Johnson type. Sylvania No. 300 regenerated cellulose was used as the membrane material. The membranes were conditioned by the usual procedures. The measurements were performed at 30 ± 0.002°C., using benzene as the solvent.

Monomer-Polymer Ratio

The equilibrium concentration of DMBD in the polymer latex particles was determined by a procedure similar to that described by Morton et al.[14] for isoprene.

Results and Discussion

Propagation Rate Studies

Determinations of the rate per particle in DMBD polymerization was carried out at temperatures of 5 and 15°C. Figure 1 illustrates the rate curves obtained. As in the cases of butadiene[12] and isoprene,[14] it was found necessary to use booster charges of initiator to prevent a dying out of the polymerization rate due to initiator consumption, particularly at the higher temperature. These booster charges were always added at conversions of 30% or greater, where it would be expected that all the soap micelles had disappeared, hence no new particles should be formed. It was always found that the initiator added served only to maintain the same rate already observed in the polymerization, and under no conditions was

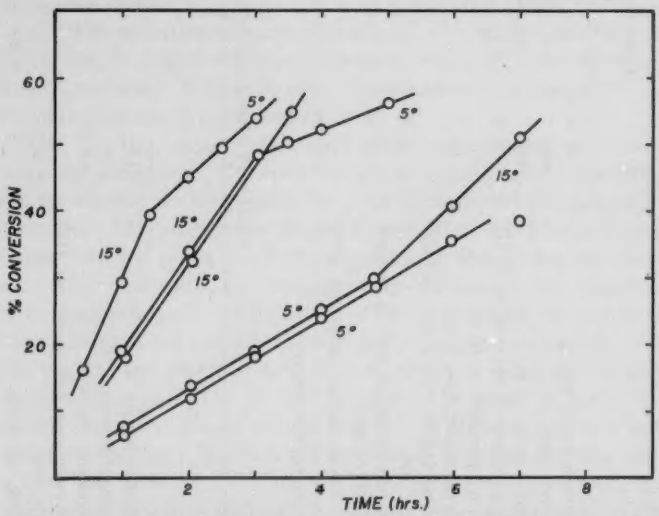

Fig. 1. Rate curves for dimethylbutadiene polymerization with peroxamine initiation.

TABLE III. Polymerization Rates and Particle Numbers in PolyDMBD Latex
(Initial catalyst charge: 0.2 DIBHP + 0.4 TEP; booster charge at 30% conversion: same)

	Polymerization temp., 15°C.			Polymerization temp., 5°C.		
Conversion of latex, %	69.3	61.9	61.5	61.3	77.8	65.5[a]
Particle diam. A, D_s	630	570	740	720	870	780
Particle diam. A, D_n	465	420	540	530	640	570
No. particles/ml. H_2O ($\times 10^{-15}$)	5.2	5.6	4.1	3.7	3.3	2.9
Av. no. particles ($\times 10^{-15}$)		4.9			3.3	
Polymerization rate, %/hr.	15	15.3	15	5.9	5.7	—
Polymerization rate, g./sec./ml. H_2O ($\times 10^{8}$)	2.32	2.36	2.32	0.91	0.88	—
Av. polymerization rate, g./sec./ml. H_2O ($\times 10^{8}$)		2.33			0.90	
Av. rate per particle, g./sec. ($\times 10^{21}$)		4.75			2.72	

[a] No booster charge.

TABLE IV. Rates and Activation Energies for the DMBD Propagation Reaction

	Bottle series					
	No. 1		No. 2		No. 3	
Initiation temp., °C.	15	15	15	15	5	5
Propagation temp., °C.	15	5	15	5	5	15
Polymerization rate, %/hr.	15.0	8.4	15.3	8.8	5.7	10.1
Polymerization rate, g./sec./ml. H_2O ($\times 10^{8}$)	2.32	1.30	2.36	1.36	0.88	1.56
E_p, kg. cal./mole	9.3		8.6		9.1	
Av. no. particles/ml. H_2O ($\times 10^{-15}$)	4.9		4.9		3.3	
Rate per particle, g./sec. ($\times 10^{21}$)	4.7	2.6	4.8	2.8	2.7	4.7

an increase in rate over this ever found. Using this technique, it was possible to extend the expected zero-order rate to conversions of 50 to 60%, at which point monomer depletion causes a decrease in rate.

Table III gives the rates of reaction and numbers of particles obtained in these polymerizations. Booster charges of initiators were used in all except one case. The values of the surface-to-volume average particle diameters were determined by soap titration. The member-average diameters were obtained by use of the factor 0.735, found by Maron et al.[20] from a study of the distributions of particle sizes in similar latex systems. The per cent conversion values of the latices are included to illustrate that the particle distributions involved here should be comparable to one another.

Table IV gives a summary of the data from which it is possible to calculate values of E_p, the activation energy for the propagation reaction. Two methods were used for the determination of this parameter. The first involved calculation of E_p from the ratio of rates per particle obtained in two polymerizations carried out at different temperatures. The second method involved using the ratio of overall polymerization rates at two temperatures for a single reaction. In the latter case a reaction was started at one temperature and the rate measured. After all the particles had been formed and the rate was firmly established at this temperature, the bottle was withdrawn and placed in another bath maintained at a different temperature. After allowing time to establish thermal equilibrium, rate measurements were continued. Since the same number of particles were involved in both cases, E_p could be determined directly from the overall polymerization rates. Values of E_p calculated using the latter method do not include, therefore, any errors that might have arisen due to error in the determination of particle numbers. A comparison of E_p values derived by the two methods shows the same order of variation obtained within each method. Hence, it would appear that errors in particle number determination are not too serious here.

In Table IV, the terms "initiation" and "propagation" temperatures have a specific meaning. The initiation phase is that period, up to 30–40% conversion, wherein the latex particles are all formed and increase to a constant number. The propagation period is, then, the period from about 30% conversion until the point at which the free monomer phase had been expended. After this point, the monomer concentration is not constant and the theory does not apply. The values of the polymerization rate, listed in Tabel IV, pertain to the overall rate during the propagation period.

Table V gives the rate per particle data obtained using the persulfate-mercaptan system at 60°C. As may be noted, the particle number in this case is about the same as was obtained at 5°C. with peroxamine initiation, mentioned previously. The overall rate here, however, is only slightly higher than the value at 5°C. Hence, then persulfate-mercaptan system must show considerably less than the optimum rate per particle This has previously been found with both isoprene and butadiene. In the case of

DMBD the observed value at 60°C. is low by a factor of about 10 when compared with the calculated rate at 60°C. for the peroxamine system. In the case of butadiene[12] and isoprene [14] these differences involved factors of about 20 and 10, respectively.

TABLE V
Polymerization Rate and Particle Number in PolyDMBD Latex
(Persulfate initiation)

Polymerization temp., °C.	60
Conversion of latex, %	62.3
Particle diam. A, D_s	775
Particle diam. A, D_n	570
No. of particles/ml. H_2O ($\times 10^{-15}$)	3.20
Polymerization rate, %/hr.	8.9
Polymerization rate, g./sec./ml. H_2O ($\times 10^{5}$)	1.36
Av. rate per particle, g./sec. ($\times 10^{21}$)	4.2
Calcd. rate per particle at 60°C. with the peroxamine system, g./sec. ($\times 10^{21}$)	39.3

If it may be assumed that the case II treatment of Smith and Ewart[25] is applicable here, calculations of the absolute propagation rate constant should follow directly from the following expression:

$$k_p = 2(-d[\mathrm{M}]/dt)/[\mathrm{M}]N$$

where k_p is the absolute propagation rate constant (liter/mole/sec.), [M] is the monomer concentration in the latex particles (moles/liter), N is the number of latex particles per millititer of aqueous phase, and $d[\mathrm{M}]/dt$ is the rate of polymerization expressed as molecules reacted/milliter of aqueous phase/second.

The results of these calculations may be expressed, together with the values calculated for the activation energy and frequency factor, in an Arrhenius-type expression:

$$k_p = 8.9 \times 10^7 \exp\{-9000/RT\}$$

A discussion of the significance of the results will appear later combined with a discussion of the results from the crosslinking reaction studies.

Crosslinking Rate Studies

In order to apply the theoretical considerations of Flory,[26] Bardwell and Winkler,[27] and Morton et al.[13] to the determination of the crosslinking rate of DMBD, it is first necessary to elucidate the processes which determine the molecular weight of the polymer formed in DMBD polymerization. For butadiene[13] and isoprene[15] polymerizations, carried out using the persulfate-mercaptan initiator system, the exclusive reaction controlling molecular weight was found to be chain transfer with mercaptan. However, this is not known to be necessarily true for DMBD and must be proved.

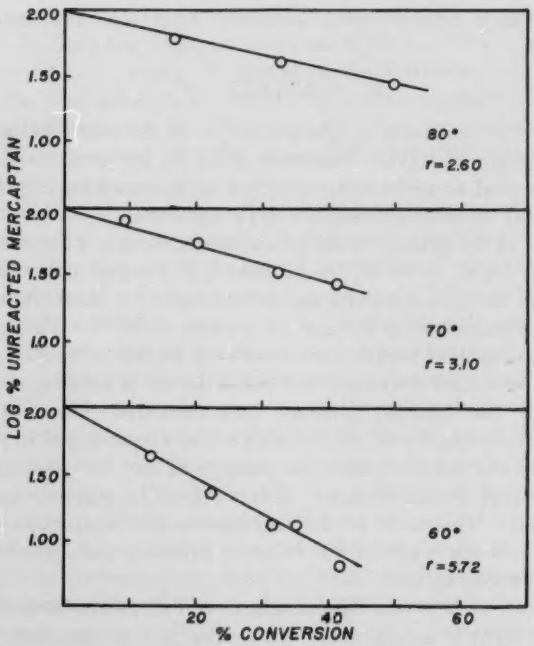

Fig. 2. Mercaptan disappearance curves for dimethylbutadiene polymerization.

Figure 2 shows the mercaptan disappearance curves for the DMBD system initiated with persulfate, at 60, 70, and 80°. These plots indicate a first-order disappearance rate for mercaptan up to 50–60% conversion. From the slope of the linear portions of these curves, the value of the regulating index r at each temperature may be determined.[12] As with butadiene and isoprene, the values of r decrease with increasing temperature. This is attributed to the smaller activation energy associated with the process as against the propagation reaction. The value of r at 60°C. appears to be somewhat higher than would be expected from the values at 70 and 80°C. From values of r at these higher temperatures, an activation energy difference ($E_p - E_{tr}$) of 4.5 kg. cal./mole can be estimated. Using this value, it is possible to calculate an r value of 3.75 at 60°C. The reason for the higher observed value of r at 60°C. is not apparent.

To determine whether chain transfer with mercaptan is the main process controlling the molecular weight of the polymer, a polyDMBD was prepared at 70°C. to 37.3% conversion. Initial concentrations of mercaptan and persulfate were 0.20 and 0.30 PHM (parts per hundred monomer), respectively. From the rate of mercaptan disappearance at this temperature, it is possible to calculate, according to Bardwell and Winkler,[27] the primary number-average polymer molecular weight from the following relation, as-

suming that chain transfer with mercaptan is the sole process determining chain length:

$$\bar{M}_r = M_0\alpha/R_0(1 - e^{-r\alpha})$$

where $\bar{M}_r$ is the molecular weight predicted on the above basis, M_0 is the molecular weight of DMBD monomer, R_0 is the initial mercaptan concentration expressed as moles mercaptan per mole monomer, r is the regulating index, and α is the fractional extent of conversion.

The value of the primary number-average molecular weight of the poly-DMBD was found to be 52,200 g./mole. The actual polymer was then isolated from the system and its molecular weight was determined by osmotic pressure measurements in benzene solution at 30°C. The actual number-average molecular weight was found to be 68,500 ± 3,000 g./mole. It should be mentioned that care was taken to use a solution of the whole polymer for the osmotic pressure measurements. The polymer was obtained from a coagulation of the latex in pure isopropanol to remove the soap. Care was taken to note the passage of any low molecular weight material through the membrane. About 1% of the polymer was found to have diffused. The value of the polymer-solvent interaction parameter, estimated from the slope of the osmotic pressure plot, was 0.41. This value appears reasonable.

The agreement between the calculated and measured osmotic pressure molecular weight is satisfactory. It would be expected that the actual number-average value would be somewhat higher than the primary value, since the latter does not take into account the crosslinking reaction. Actually, a crosslinking rate of the order found for the 1,3-dienes is far from suf-

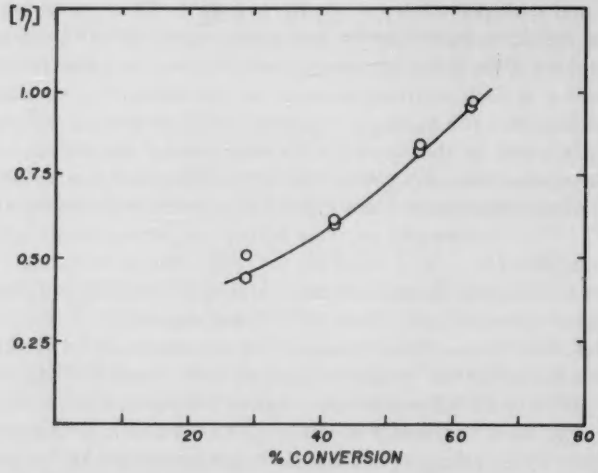

Fig. 3. Intrinsic viscosity—conversion data for dimethylbutadiene—polymerization (60°C., 0.20% mercaptan): (O) dry polymer in benzene; (⟨◯⟩) latex in Vistex.

ficient to account for the above disparity in molecular weights, which is more likely due to osmotic membrane permeability. However, from these values of molecular weight it appears certain that transfer with mercaptan is the dominant process controlling molecular weight in the above DMBD polymerization. If this were not true the measured polymer molecular weight should actually be lower than that calculated from mercaptan disappearance.

The method chosen in this work for the determination of the gel-point conversion was the Vistex viscosity technique.[23] The Vistex method has considerable advantage over the use of conventional viscosity procedures (which usually involve the isolation of the polymer, followed by drying and solution in a pure solvent), since it obviates possible extraneous crosslinking which may take place during the isolation and drying operations. With the Vistex procedure, however, it is necessary to ascertain that the viscosity data give the same intrinsic viscosities as the conventional viscosity procedures. To test this, a polymerization was carried out at 60°C. wherein samples for both viscosity procedures were removed at the same time. For the Vistex method, a 1- m. sample of latex was dispersed directly in 100 m. of Vistex solvent. A 5-ml. sample of latex was coagulated in rapidly stirred isopropanol, and the coagulum removed and dried overnight *in vacuo* 40°C. An appropriate quantity of the dried polymer was then dissolved in 100 ml. of pure benzene. The results of the viscosity measurements from these two methods are shown in Figure 3. In both cases the dilutions were made with pure benzene. It may be seen from Figure 3 that the intrinsic viscosities by the two methods agree very well. In most cases the results are almost identical. It may be assumed, therefore, that the Vistex viscosity technique gives as accurate a representation of the molecular weight of the polymer as the conventional viscosity methods.

Intrinsic viscosity versus per cent conversion measurements were carried out with the DMBD system at three temperatures, 60, 70, and 80°C. in an attempt to determine the gel-point conversions for various initial mercaptan concentrations. From the results at 60°C., it was immediately obvious that considerably lower quantities of transfer agent were required with DMBD than with either butadiene or isoprene, in comparable systems. Whereas with isoprene, which has a considerably lower crosslinking rate than butadiene, gel points at 60°C. had been found with as high as 0.05 PHM of mercaptan, it was not possible to produce insoluble polymer with DMBD at 60°C. at conversions below 60% even with as little as 0.01 PHM of mercaptan.

Since the 60°C. polymerizations of DMBD at the lowest practical mercaptan levels had failed to produce insoluble polymer, succeeding reactions were carried out at higher temperatures. A series of polymerizations was carried out at 80°C., wherein the initial mercaptan concentrations were in the range of 0.010 to 0.013 PHM. In view of these low quantities of transfer agent used, other means of transfer or termination, not usually considered significant, such as initiator, may become important. One means of

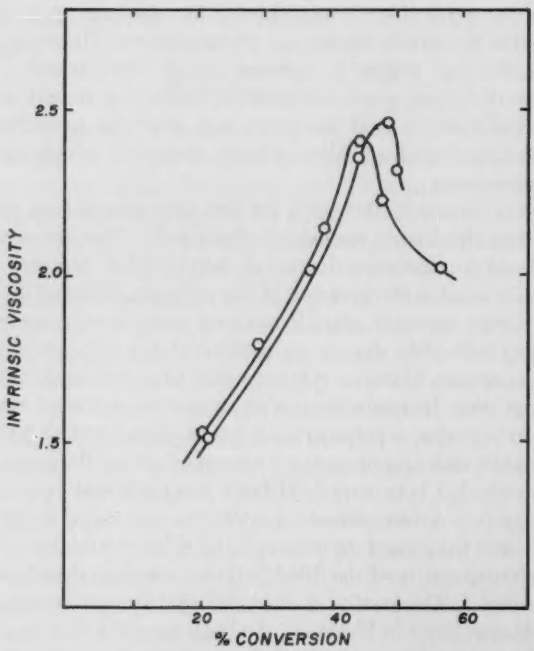

Fig. 4. Gel-point curves for dimethylbutadiene polymerization at 70°C.: (O) 0.010% RSH, 0.10% $D_2S_2O_8$; (⬭) −0.010% RSH, 0.08% $K_2S_2O_8$.

avoiding such termination processes could be to reduce the quantity of initiator used. From that point on all polymerizations were carried out at initial persulfate concentrations not exceeding 0.10 PHM.

The gel-point curves at 70°C. are given in Figure 4. It may be noted that, at 70°C., the difference in gel-point conversions was due to a 20% reduction in the concentration of persulfate (0.10–0.08%) rather than a change in mercaptan concentration. This pair of reactions was carried out to test if the persulfate was contributing significantly to the polymer chain termination at these low mercaptan levels. One would expect that, if persulfate were contributing to the termination reaction, a reduction in persulfate would lead to a lower gel-point conversion, due to the greater primary chain length thus obtained. In isoprene polymerization[15] with initial mercaptan levels of the order of 0.05 PHM, persulfate was found to contribute to the polymer chain termination only at initial persulfate concentrations higher than 0.03 PHM. Below this concentration, variation in persulfate level was not found to affect the gel-point conversion. However, at higher concentrations an increase in persulfate shifted the gel-point conversions to higher values. As may be noted from Figure 5, a decrease in persulfate concentration, from 0.10 to 0.08 PHM, here brought about a slight increase (45–49%) in the gel-point conversion. In addition a slightly higher value

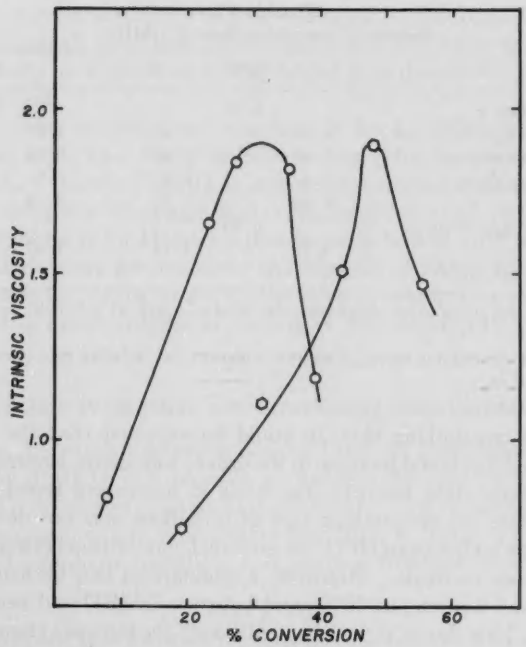

Fig. 5. Gel-point curves for dimethylbutadiene polymerization at 80°C.: (O) 0.010% RSH, 0.10% $K_2S_2O_8$; (◯) −0.013% RSH, 0.10% $K_2S_2O_8$.

for the intrinsic viscosity at the gel-point was observed at the lower persulfate level. It appears, therefore, that at the level of 0.10 PHM, persulfate is contributing to some chain termination but not to a significant degree. The slightly higher values of conversion and intrinsic viscosity at the gel-point are probably within the limits of experimental accuracy at these low mercaptan levels.

The gel-point curves for the 80°C. polymerizations are shown in Figure 5. As may be seen from these curves, fairly sharp gel-point were obtained. Both maxima in the curves at 80°C. occurred at the same intrinsic viscosity. This is in accord with the theoretical prediction that the value of the chain length at the gel point is constant at a particular temperature. Both the low amounts of mercaptan used to produce gel, and the significant change in gel. point conversion caused by changing the mercaptan charge from 0.010 to 0.013 PHM, are indicative of a very low crosslinking rate for DMBD. The results obtained at both temperatures are given in Table VI.

A comparison of the intrinsic viscosities at the gel point for the various diene monomer systems discloses an interesting situation. The values for butadiene, isoprene, and DMBD are shown in Table VII. Since the value of the critical molecular weight for gelation should be an inverse function of

TABLE VI
Relative Crosslinking Rate of DMBD

	70°C.		80°C.	
Regulating index, r	3.10		2.70	
Mercaptan charge, R_0 ($\times 10^5$)	4.28	4.28	4.28	5.55
Gel-point conversion, α	0.45	0.49	0.32	0.47
$[\eta]$ at gel-point, dl./g.	2.4	2.5	1.9	1.9
$\bar{y}_{wg}$ ($\times 10^{-4}$)[a]	3.28	3.52	2.72	2.70
Monomer/polymer ratio, m	0.80		0.80	
K ($\times 10^5$)[b]	1.22	1.14	1.47	1.48
$E_x - E_p$, kg. cal./mole	5.4			

[a] Here, $\bar{y}_{wg}$ the cumulative weight-average chain length at gel point $= 2(e^{r\alpha} - 1)/r^2\alpha R_0$.

[b] Here, K is the relative crosslinking rate constant, i.e., relative rate of crosslinking to propagation (k_x/k_p).

the relative crosslinking rate, it would be expected that the critical intrinsic viscosities should increase in the order: butadiene, isoprene, DMBD, since the above data indicate this trend in decreasing crosslinking rate. Unfortunately, the crosslinking rate of butadiene was not determined at temperatures higher than 60°C., so no direct comparison between the three monomers can be made. However, a comparison can be made between butadiene and isoprene at 60°C. and between DMBD and isoprene at 70 and 80°C. This shows at once that, although the intrinsic viscosities of the polybutadiene and polyisoprene have the expected relation, this is not the case for the polyDMBD, which has consistently lower intrinsic viscosities at the gel point than polyisoprene.

TABLE VII
$[\eta]$ at Gel Point for Butadiene, Isoprene, and DMBD

Polymerization temp., °C.	Intrinsic viscosity (C_6H_6) at gel point, (dl. g.$^{-1}$)				
	Butadiene		Isoprene	DMBD	
60	2.6	2.6	4	—	—
70	—		3.7	2.4	2.4
80	—		3	1.9	1.9

Fortunately, it can be shown qualitatively that the above anomaly is due to the markedly different viscosity-molecular weight relationship for polyDMBD as compared to the other two polymers. Although this relationship has not actually been determined, it is possible to compare the isoprene and DMBD systems on the basis of data obtained in this paper and previous work. Thus, it had been found previously[14] that polyisoprene having an osmotic molecular weight of 79,000 gave an intrinsic viscosity of 1.3 dl. g.$^{-1}$, in benzene at 30°C. On the other hand, the polyDMBD previously described, which had an osmotic molecular weight of 68,5000, showed an intrinsic viscosity of only 0.66 dl. g.$^{-1}$. This indicates

the markedly lower intrinsic viscosity exhibited by the DMBD polymers. Orr and Williams[28] have also found that polyDMBD shows a lower intrinsic viscosity for a given molecular weight than does either polyisoprene or polybutadiene.

The relative crosslinking rate constant K for DMBD is shown for 70 and 80°C. in Table VI. Using the value obtained for the activation energy difference ($E_x - E_p$) for DMBD, it is possible to calculate the value of K at 60°C., for purposes of comparison with butadiene and isoprene. The calculated value of K for DMBD is thus found to be 9×10^{-6}, as compared with the values found for butadiene and isoprene of 200×10^{-6} and 34×10^{-6}, respectively. Thus, at 60°C., the relative crosslinking rate constant for DMBD is one-twentieth of butadiene and one-fourth that of isoprene.

Absolute Propagation and Crosslinking Rate Constants

Using the Arrhenius expression obtained for the propagation rate constant (k_p) for DMBD, it is possible to calculate the absolute value of the crosslinking rate constant (k_x) for this monomer. The Arrhenius constants for both propagation and crosslinking are listed in Table VIII, together with those constants for butadiene and isoprene, from previous work.

TABLE VIII
Absolute Rate Constants for Butadiene, Isoprene and DMBD

Monomer	Reaction	A	E	k_{60}
Butadiene	Propagation	1.2×10^8	9.3	100
Isoprene	Propagation	1.2×10^8	9.8	50
DMBD	Propagation	8.9×10^7	9	120
Butadiene	Crosslinking	1.9×10^9	16.8	0.020
Isoprene	Crosslinking	8.5×10^8	14.8	0.0017
DMBD	Crosslinking	3.0×10^8	14.4	0.0011

In the case of the propagation reaction, both the A and E values are quite similar for the three monomers. This is not surprising, particularly for the activation energy values, since these all involve similar bond structures, viz., the 1,3-dienes. As for the A values, the presence of the methyl substituents on the 2 or 3 positions would not be expected to interfere seriously with radical attack on the terminal carbon atoms, which is known to occur during the propagation step.

On the other hand, since the crosslinking reaction involves the attack of a growing radical on a polymer double bond, and the subsequent growth of this new radical, a variation in the nature of the substituents on the doubly bonded carbons would be expected to affect the crosslinking rate. It has previously been shown[14] that the frequency factor A_x decreases markedly in going from butadiene to isoprene. This marked decrease was attributed both to the added shielding of the polymer double bonds by the methyl

substituent and to the reduced quantity of pendant unsaturated groups in polyisoprene. Thus, in emulsion polyisoprene, there are about 6% each of the 1,2-and 3,4-side-chain structures, as compared to about 20% of 1,2-structure in polybutadiene.[29] Since the side-chain unsaturation is generally much more reactive than the internal double bonds, it may be considered as the controlling factor in crosslinking. Furthermore, in the case of the polyisoprene, the effect of the reduced amount of side-chain unsaturation is further exaggerated by the fact that about half of these double bonds, in addition to *all* of the internal double bonds, are shielded by the methyl substituent.

Polydimethylbutadiene has been found[30] to contain about the same total amount of pendant unsaturation as isoprene (about 13%). Since DMBD is a symmetrical monomer, this pendant unsaturation is all of the same type, corresponding closely to the 3,4-addition product in polyisoprene. Hence DMBD should have an A_x value still lower than that of isoprene, since all the pendant unsaturation in polyDMBD is shielded, to some extent, by the methyl groups. From the results listed in Table VIII it may be seen that these predictions prove to be true. The values of the absolute crosslinking rate constant at 60°C. effectively illustrate the difference. Thus, DMBD shows a rate constant one-twentieth and two-thirds the rate constants of butadiene and isoprene, respectively. The difference in rate constants between isoprene and DMBD resides mainly in the lower A_x value of DMBD, as might be expected.

The activation energies for the crosslinking reaction for these three monomers are in the region of 14.4 to 16.8 kg. cal./mole, with the highest being that for butadiene and the lowest that found for DMBD. However, this small decrease in activation energy with increased methyl substitution is not sufficient to overcome the very marked decrease in A_x values.

This investigation was carried out under the sponsorship of the Office of Synthetic Rubber, Reconstruction Finance Corp. in connection with the Government Synthetic Rubber Program.

References

1. Gottlob, K., *Gummi-Ztg.*, **33**, 508, 534, 551, 576, 599 (1919).
2. Whitby, G. S., and M. Katz, *Ind. Eng. Chem.*, **25**, 1204, 1338 (1933).
3. Whitby, G. S., and R. N. Crozier, *Can. J. Res.*, **6**, 203 (1932).
4. Conant, J. B., and C. O. Tanberg, *J. Am. Chem. Soc.*, **52**, 1659 (1930).
5. Starkweather, H. W., et al., *Ind. Eng. Chem.*, **39**, 210 (1946).
6. Konigsberger, C., and G. Salomon. *J. Polymer Sci.*, **1**, 200 (1946).
7. Dinsmore, R. P., U. S. Pat. 1,732,795 (1929).
8. Goodyear Tire and Rubber Co., Brit. Pat. 297,050 (1929).
9. Konigsberger, C., and G. Salomon, *J. Polymer Sci.*, **1**, 353 (1946).
10. Marvel, C. S., and J. R. Williams, *J. Polymer Sci.*, **4**, 264 (1949).
11. Gilbert, R. D., and H. L. Williams, *J. Am. Chem. Soc.*, **74**, 4114 (1952).
12. Morton, M., and P. P. Salatiello, *J. Polymer Sci.*, **6**, 225 (1951).
13. Morton, M., P. P. Salatiello, and H. Landfield, *J. Polymer Sci.*, **8**, 215 (1952).
14. Morton, J. A. Cala, and I. Piirma, *J. Polymer Sci.*, **15**, 167 (1955).
15. Morton, M., P. P. Salatiello, and H. Landfield, *J. Polymer Sci.*, **8**, 279 (1952).

16. Adams, R., and E. W. Adams, in *Organic Syntheses, Collected Vol. I*, 2nd Ed., H. Gilman and A. H. Blatt, eds., Wiley, New York, 1955, p. 459.
17. Allen, C. F. H., and A. Bell, in *Organic Syntheses, Collected Vol. III*, 2nd Ed., E. C. Horning, ed., New York, 1955, p. 312.
18. American Petroleum Institute, *Spectrograph*, No. 451.
19. *Beilstein's Handbuch der organischen Chemie*, Band I, Springer, Berlin, 1923, p. 256.
20. Maron, S. H., M. E. Elder, and I. N. Ulevitch, *J. Colloid Sci.*, **9**, 89 (1954).
21. Maron, S. H., M. E. Elder, and C. Moore, *J. Colloid Sci.*, **9**, 104 (1954).
22. Maron, S. H., and M. E. Elder, *J. Colloid Sci.*, **9**, 263, 347, 353 (1954).
23. Henderson, D. A., and N. R. Legge, *Can. J. Res.*, **B27**, 666 (1949).
24. Kolthoff, I. M., and W. E. Harris. *J. Polymer Sci.*, **2**, 49 (1947).
25. Smith, W. V., and R. H. Ewart, *J. Chem. Phys.*, **16**, 592 (1948).
26. Flory, P. J., *J. Am. Chem. Soc.*, **69**, 2893 (1947).
27. Bardwell, J., and C. A. Winkler, *Can. J. Res.*, **27B**, 116, 128, 139, (1949).
28. Orr, R. J., and H. L. Williams, *Can. J. Chem.*, **30**, 108 (1952).
29. Foster, F. C., and J. L. Binder, *Advan. Chem. Ser.*, **19**, 27 (1957).
30. Saffer, A., and B. L. Johnson, *Ind. Eng. Chem.*, **40**, 538 (1948).

Résumé

On a étudié la cinétique de la polymérisation en émulsion du 2,3-diméthylbutadiène-1,3. Le traitement cinétique de Smith et Ewart a été appliqué pour la détermination directe de la constante de vitesse de propagation absolue, k_p. On a trouvé la relation suivante: $k_p = 8.9 \times 10^7 \exp\{-9000/RT\}$ liter/mole/sec. Un traitement développé antérieurement a été appliqué pour la détermination des vitesses de réticulation absolue et relative du 2,3-diméthylbutadiène-1,3. Les résultats pour la constante de vitesse de réticulation absolue, k_x nous donnent l'expression suivante: $k_x = 3.0 \times 10^6 \exp\{-14400/RT\}$ liter/mole/sec. On a comparé les constantes de vitesse de trois dienes suivants: butadiène, isoprène et diméthylbutadiène. On a trouvé que les constantes de vitesse de propagation ne varient que par un facteur de 2,3-. Toutefois on a trouvé que les vitesses de réticulation diminuent considérablement si l'on passe du butadiène à l'isoprene et a diméthylbutadiène. Ceci est attribué principalement à une diminution du pourcentage de groupements vinyliques latéraux pour les deux derniers monomères, comparé au butadiène, aussi bien que l'empêchement stérique dû à la présence de groupements méthyliques.

Zusammenfassung

Eine Untersuchung der Kinetik der Emulsionspolymerisation von 2,3-Dimethylbutadien-1,3 wurde ausgeführt. Die kinetische Behandlung von Smith und Ewart wurde zur direkten Bestimmung der absoluten Wachstumsgeschwindigkeitskonstanten k_p angewendet. Folgender Ausdruck wurde erhalten: $k_p = 8{,}9 \times 10^7 \exp(-9000/RT)$ 1/Mol/sek. Die Bestimmung der relativen und absoluten Vernetzungsgeschwindigkeit von 2,3-Dimethylbutadien-1,3 wurde nach einem früher entwickelten Verfahren vorgenommen. Die Ergebnisse führten zu folgendem Ausdruck für die absolute Vernetzungsgeschwindigkeitskonstante, k_x: $k_x = 3{,}0 \times 10^6 \exp(-14400/RT)$ 1/Mol/sek. Ein Vergleich dieser Geschwindigkeitskonstanten wurde für die drei Diene, Butadien, Isopren und Dimethylbutadien, durchgeführt. Die Wachstumsgeschwindigkeitskonstante variierte nur um einen Faktor 2–3. Die Vernetzungsgeschwindigkeit nahm jedoch beim Übergang von Butadien zu Isopren zu Dimethylbutadien beträchtlich ab. Das wurde hauptsächlich auf den herabgesetzten Gehalt an Vinylseitengruppen der letzteren beiden Monomeren im Vergleich zu Butadien zurückgeführt, sowie auf die sterische Hinderung durch die Anwesenheit der Methylgruppen.

Received May 24, 1962

JOURNAL OF POLYMER SCIENCE: PART A VOL. 1, PP. 2697–2709 (1963)

Studies on Crystallization of High Polymers by Differential Thermal Analysis

MASAKAZU INOUE, *Plastics Laboratory, Toyo Rayon Company, Ltd., Tokodori, Showaku, Nagoya, Japan*

Synopsis

Differential thermal analysis was applied for the investigation of melting and crystallization behavior of high polymers. The heats of fusion of crystalline regions were obtained as follows: 45.6 cal./g. for nylon 6, 46.8 cal./g. for nylon 66, 47.9 cal./g. for nylon 610, 54.1 cal./g. for nylon 11, 58.7 cal./g. for polyoxymethylene, 64.8 cal./g. for high density polyethylene, 15.9 cal./g. for polypropylene, and 35.4 cal./g. for poly-(3,3-bischloromethyl oxacyclobutane). In the course of crystallization, the exothermic peak appears in the temperature range of 20 to 100°C. below the melting point. The effect of melting temperature and molecular weight on the thermograms of crystallization of nylon 6 and polyoxymethylene was discussed and compared with the results obtained by dilatometry. For polymers such as nylon 6 with higher molecular weight and polyoxymethylene, two exothermic peaks of crystallization were observed, and it was found that the peak shape depends on the molecular weight. Nylon 6 containing nucleating agent shows only one exothermic peak independent on the molecular weight. It is presumed that the discontinuity of the growth rate of crystals is responsible for the thermograms having two peaks.

Introduction

Most of the studies on crystallization of high polymers have been restricted so far to the growth of spherulites, the morphology of spherulites, single crystals, and the isothermal crystallization kinetics by the use of dilatometry.

Recently, differential thermal analysis has become one of the useful techniques for the investigation of transition behavior of high polymers. However, this is used mainly for the study of thermal behavior such as melting temperature and heat of fusion. The glass transition of high crystalline polymers could hardly be detected by differential thermal analysis, since the endothermic mass in this transition is much smaller than that of melting transition.

As to the thermal properties of polymers, the melting behaviors of polyamide,[1] single crystals of polyethylene,[2] polyethylene,[3] and polyolefin have been reported.[4]

In this paper, the melting and crystallization phenomena are treated as a reversible transition; the crystallization behaviors are studied mainly by differential thermal analysis. The overall rate of crystallization is

proportional to the rate of nucleation and to that of growth. Both rates have maximum values below the melting point. The temperature range in which the rate of crystallization occurs at an appreciable rate is not very wide. If the melt of polymer specimen is cooled continuously and slowly, the thermograms obtained would have exothermic peak due to the heat of crystallization. The present paper deals with the thermograms of melting and crystallization in some crystalline polymers. Moreover, the thermograms of nylon 6 of various molecular weight are obtained at various crystallization conditions such as melting temperature and nucleating effect and are discussed in detail.

Experimental

Description of Specimens

The crystalline polymers used for the experiments are listed in Table I. Nylon 6 specimens of various molecular weights were prepared in our laboratory. Lead phosphate was used as a nucleating agent for nylon 6.[5]

TABLE I
Materials Used for the Experiments

Polymer	Manufacturer	Tradename	Viscosity
Nylon 6	Toyo Rayon	CM 1001	η_r[a] = 2.35
	Toyo Rayon	Special	2.67
	Toyo Rayon	Special	3.00
	Toyo Rayon	Special	3.23
	Toyo Rayon	CM 1011	3.40
	Toyo Rayon	CM 1021	4.51
	Toyo Rayon	Special	4.80
Nylon 66	Toyo Rayon	CM 3001	2.30
Nylon 610	Toyo Rayon	CM 2001	2.45
Nylon 11	Organico	Rilsan BMn	2.35
Polyoxymethylene	Du Pont	Delrin 500	η_{inh}[b] = 1.45
	Du Pont	Delrin 150	1.75
Polyethylene	Mitsui Petrochem.	Hizex 1000	η_{inh}[c] = 1.177
Polypropylene	Avisun	Avisun 1014	η_r[d] = 1.320
Poly-(3,3-bischloromethyloxacyclobutane)	Hercules	Penton	η_r[e] = 1.52

[a] 1 g./100 cc. in 98% H_2SO_4 at 25°C.
[b] 0.5 g./100 cc. in *p*-chlorophenol at 60°C.
[c] 0.1 g./100 cc. in tetralin at 100°C.
[d] 0.2 g./100 cc. in tetralin at 135°C.
[e] 1 g./100 cc. in cyclohexane at 50°C.

Apparatus and Measurements

Conventional apparatus of differential thermal analysis, DT-10 type, manufactured by Shimazu Seisakusho Ltd., was used. It consists of a

heating block, a sample chamber, and a recorder. The inner diameter of the heating block is 35 mm. and the length is 100 mm. The sample chamber is made of nickel block which has two holes: one is for sample cell and the other is for reference sample cell. The temperature of the sample chamber and the difference between the temperatures of the sample and the reference sample were determined by thermocouples connected with the potentiometer. The cells for the sample and the reference sample are made of platinum having a diameter of 6 mm. They are inserted into the holes of the sample chamber. Alpha-alumina powder was used for the reference sample. The sample measured was in the form of polymer chip; the diameter is about 1 mm. and the length is about 1.5 mm. In each measurement, 50 mg. of sample was taken.

The heats of fusion and crystallization were quantitatively evaluated by determining the endothermic and exothermic peak areas, which were compared with the melting peak area of benzoic acid. The heat of fusion of benzoic acid is 33.9 cal./g.[6].

Results and Discussions

Melting Transition of Some Crystalline Polymers

The thermograms of melting of each crystalline polymer yields an endothermic peak corresponding to fusion of the crystalline region of the polymer. Figure 1 shows the thermograms of melting of crystalline polymers. All of the crystalline region is lost at the peak. At the temperature slightly below the melting point, most of crystallinity begins to decrease by increasing temperature.

The densities of samples were measured at 25°C. by the use of a density gradient tube, and the degree of crystallinity was calculated using the well-known values of the crystalline and amorphous densities. The heats of fusion of sample and crystalline region were estimated from the peak areas. The heat of fusion of a crystalline polymer is the amount of heat required to melt the crystalline region. The heat of fusion of crystalline region, ΔH_c is obtained by (1):

$$\Delta H_c = \Delta H_{ac}/X \tag{1}$$

where ΔH_{ac} is the difference of the enthalpies of the amorphous and crystalline regions and is the observed heat of fusion, and X is the degree of crystallinity. The results obtained are given in Table II. The melting points and the heats of fusion agree well with the values cited in the literatures.

The heats of fusion of crystalline regions of nylon 11 and poly-(3,3-bischloromethyl oxacyclobutane), which have never been reported, are found to be 54.1 cal./g. (9900 cal./mole) and 35.4 cal./g. (5487 cal./mole), respectively. Accordingly, the entropies of fusion are 23.6 cal./deg./mole (1.8 cal./deg./bond) and 10.2 cal./deg./mole (1.5 cal./deg./bond) re-

TABLE II
Heat of Fusion and Crystallinity

Polymer	Density at 25°C., g./cc.	Crystallinity from density, %	Starting of melting, °C.	Melt peak temp., °C.	Heat of fusion of specimen $(\Delta H_{ac})_{obs.}$, cal./g.	Heat of fusion of crystalline region (ΔH_c), cal./g.	
						$(\Delta H_c)_{obs.}$	Other authors
Nylon 6	1.134	30.5	210	228	13.9	45.6	45[a]
Nylon 66	1.140	37.2	245	268	17.4	46.8	45[b]
Nylon 610	1.075	29.3	205	225	14	47.9	46.2[c]
Nylon 11	1.028	19.4	185	198	10.5	54.1	—
Polyoxymethylene	1.421	70.7	160	180	41.5	58.7	53.3[d]
Polyethylene	0.988	93	103	134	60.2	64.8	67,[e] 66.5[f]
Polypropylene	0.921	83.9	146	170	13.3	15.9	15.4[g]
Poly-(3,3-bischloro-methyloxacyclobutane)	1.396	29.2[h]	157	171	8.6	35.4	—

[a] Dole, M., and B. Wunderlich, *J. Polymer Sci.*, **24**, 139 (1957).
[b] Dole, M., and B. Wunderlich, *Macromol. Chem.*, **34**, 29 (1959).
[c] Kee, B., and A. W. Sisko, *J. Polymer Sci.*, **50**, 87 (1961).
[d] Inoue, M., *J. Polymer Sci.*, **51**, S18 (1961).
[e] Quinn, F. A., and L. Manderkern, *J. Am. Chem. Soc.*, **80**, 3178 (1958).
[f] Wunderlich, B., and M. Dole, *J. Polymer Sci.*, **34**, 201 (1957).
[g] Kee, B., *J. Polymer Sci.*, **42**, 15 (1960).
[h] The values of densities, 1.47 g./cc. (crystalline) and 1.386 g./cc. (amorphous), were used for the calculation.

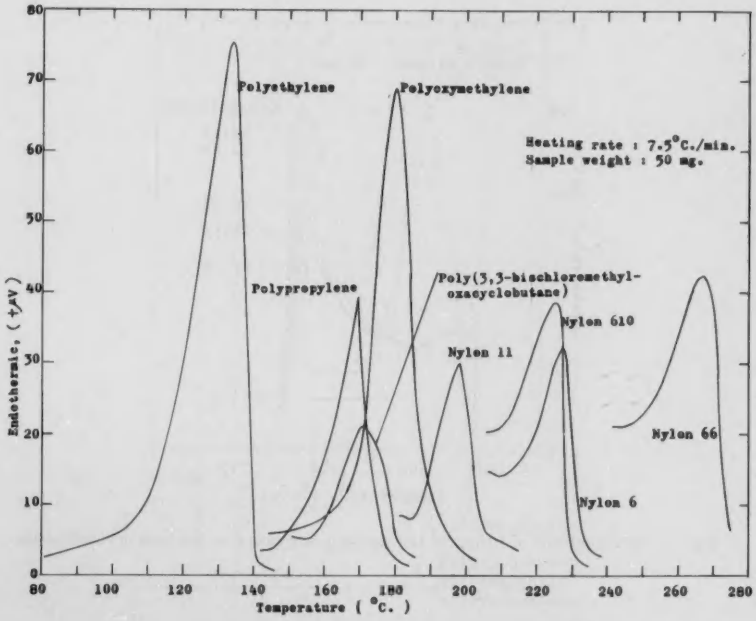

Fig. 1. Thermograms of fusion of some crystalline polymers.

spectively. They agree well with the values for other crystalline polymers reported by Flory.[7]

Figure 2 illustrates thermograms of the melting of nylon 6. The peak area depends on the degree of crystallinity. Figure 3 shows the plot of heat of fusion obtained by the peak area against the crystallinity obtained by the density. The linear relation is obtained and the heat of fusion of the crystalline region is found to be 45.6 cal./g. (5153 cal./mole) by extrapolating to 100% crystallinity. The value agrees well with the value reported by Dole and Wunderlich.[8]

Crystallization of Some High Polymers

Figures 4 and 5 illustrate the thermograms of crystallization. Each polymer gives the exothermic peak due to crystallization, corresponding to the endothermic peak due to fusion. Characteristic supercooling is observed for the polymers studied in the present investigation. Remarkable exothermic crystallization occurs in the range of 30 to 50°C. in all polymers. As shown in Figure 4, the degree of supercooling in polyethylene is much smaller than that in polypropylene. Polyoxymethylene gives two exothermic peaks of crystallization. This will be discussed later. The heat of crystallization was estimated from the peak areas and the degree of crystallization was calculated by comparing the heat of crys-

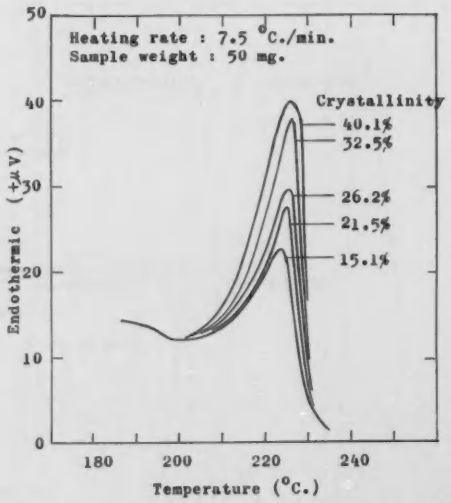

Fig. 2. Thermograms of fusion of the melting of nylon 6 at various crystallinities.

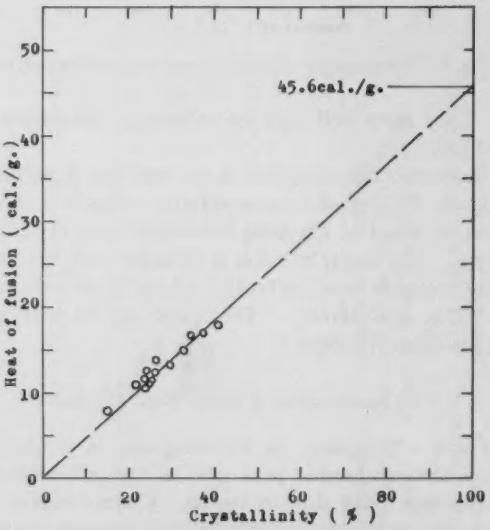

Fig. 3. Heat of fusion and crystallinity of nylon 6.

tallization with the heat of fusion in the crystalline region. The results are summarized in Table III. It is well known that the degree of crystallinity of most high polymers exists in a range independent of the condition of crystallization, which is inherent to a specific polymer; for ex-

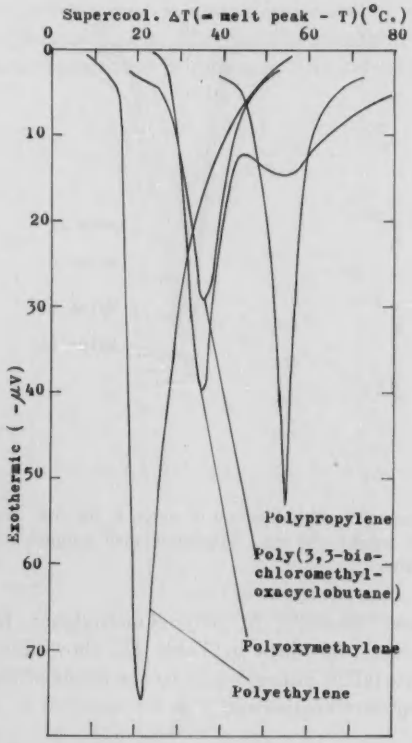

Fig. 4. Thermograms of crystallization of some crystalline polymers. Cooling rate: 6°C./min. Sample weight: 50 mg. Maximum melt temperature: 15°C. above the melt peak temperature.

TABLE III
Crystallization of Some Crystalline High Polymers

Polymer	Starting of crystn., °C.	Peak temp., °C.	Heat of crystn., cal./g.	Degree of crystn., %
Nylon 6	195	186	11.1	24.4
Nylon 66	238	229	12.8	27.4
Nylon 610	191	183	10.1	21.2
Nylon 11	168	160	9.6	17.7
Polyoxymethylene	153	145	50.5	86
Polyethylene	119	112	50.1	77.3
Polypropylene	127	115	14	88.2
Poly-(3,3-bischloromethyl-oxacyclobutane)	145	135	10.4	29.4

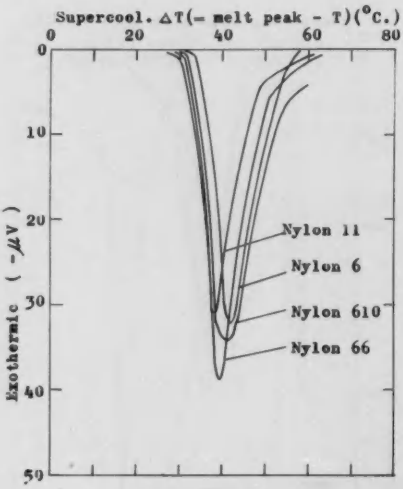

Fig. 5. Thermograms of crystallization of nylon 6, 66, 610, and 11. Cooling rate: 6°C./min. Sample weight: 50 mg. Maximum melt temperature: 15°C. above the melt peak temperature.

ample, in nylons: 10–40%, in polyoxymethylene: 60–80%, in polyethylene: 80–95%. The data in Table III show that the supercooled polymer melts crystallize almost equal to the levels of their inherent crystallinity in the region of exothermic peak.

Crystallization of Nylon 6 and Polyoxymethylene

In a previous paper,[9] it was reported that the rate of crystallization of nylon 6 at a given temperature decreases with the increase of melting temperature. Figure 6 shows the effect of maximum melt temperature on the thermograms of crystallization of nylon 6. The temperature of crystallization, the peak temperature, and the peak area decrease with the increase of melt temperature. The experimental data are illustrated in Figure 7. It was reported in the previous paper that the rate of crystallization at 190°C. is affected by the melt temperature until about 300°C.[9] This fact agrees well with the thermograms shown in Figure 7.

The rate of crystallization decreases with the increase of molecular weight. Figure 8 shows the thermograms of crystallization of nylon 6 of various molecular weights. The exothermic peak areas decrease with the increase of molecular weight. The crystallization temperature is almost invariable, and two exothermic peaks are observed. In low molecular weight, however, only one peak appears. The heights of both upper and lower peaks decrease with the increase of molecular weight. The temperature of upper peak increases and the height decreases with the increase of molecular weight, whereas the temperature of lower peak de-

creases and the height increases reciprocally compared with the height of the upper peak of polymers of the same molecular weight.

These results were summarized in Figure 9. As indicated in Figure 10,

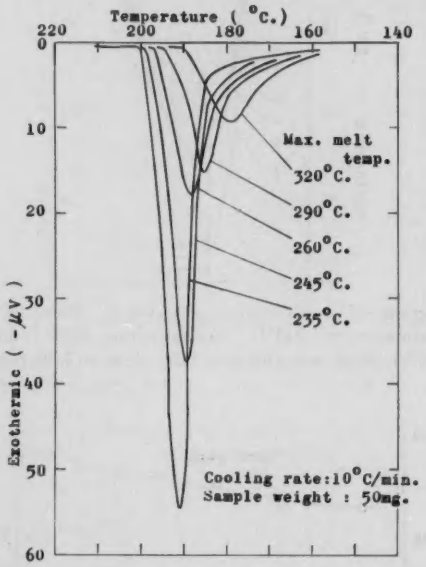

Fig. 6. Thermograms of crystallization of nylon 6. Effect of maximum melt temperature.

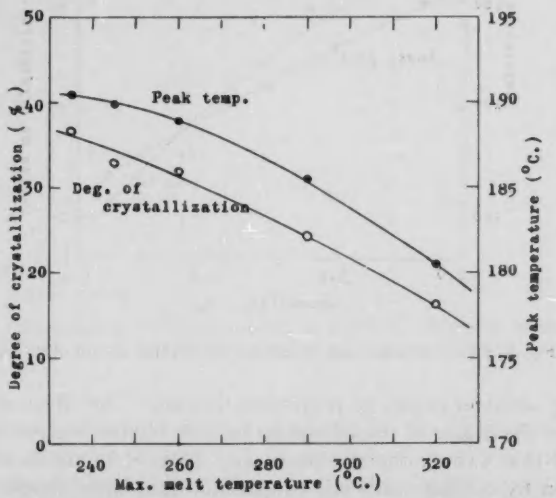

Fig. 7 Effect of maximum melt temperature on the crystallization of nylon 6.

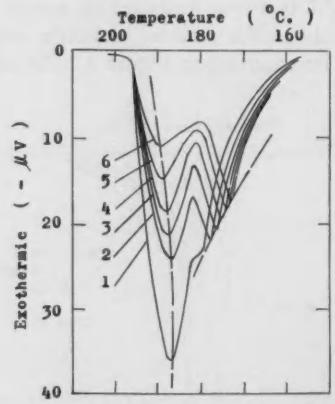

Fig. 8. Thermograms of crystallization of nylon 6. Effect of molecular weight. Maximum melt temperature: 240°C. Cooling rate: 10°C./min. Sample weight: 50 mg. (*1*) $\eta_5 = 2.35$, (*2*) $\eta_5 = 3$, (*3*) $\eta_5 = 3.23$, (*4*) $\eta_5 = 3.40$, (*5*) $\eta_5 = 4.51$, and (*6*) $\eta_5 = 4.80$.

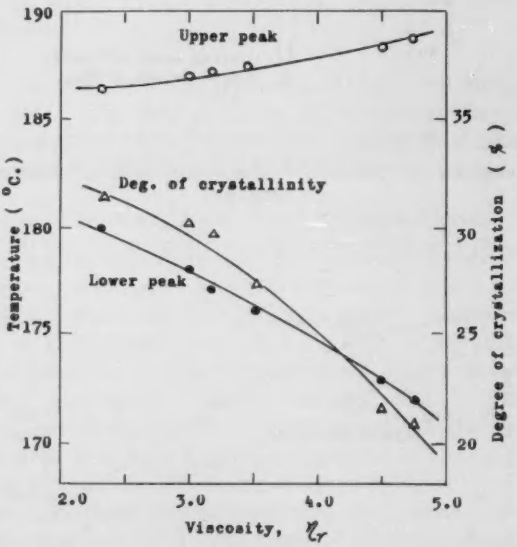

Fig. 9. Effect of molecular weight on the crystallization of nylon 6.

the same behavior occurs in polyoxymethylene. The effect of molecular weight on the degree of crystallization in this polymer is given in Table IV. The fact that two exothermic peaks are observed in the course of crystallization by cooling, leads one to conclude that there should be discontinuity of dependence of crystallization rate on temperatures. The peaks

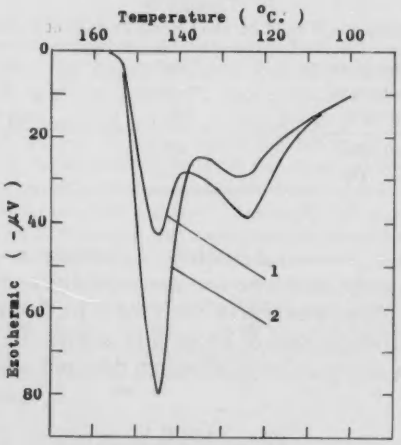

Fig. 10. Thermograms of crystallization of polyoxymethylene. Cooling rate: 8.5°C./min. Sample weight: 50 mg. (*1*) η_{inh} = 1.75 and (*2*) η_{inh} = 1.45.

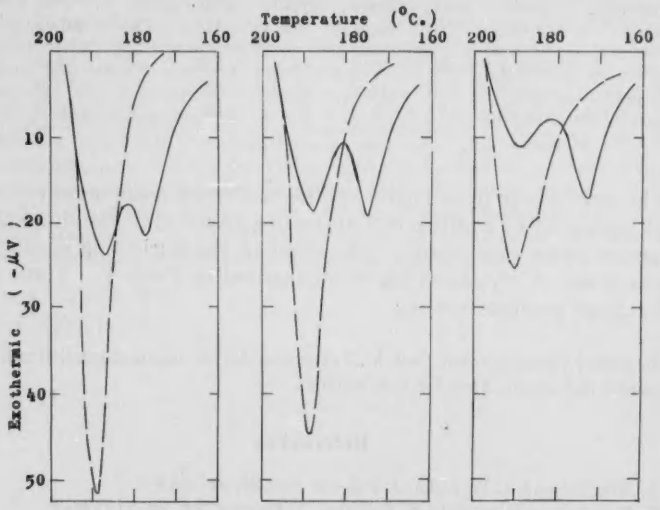

Fig. 11. Thermograms of crystallization of nylon 6. Effect of nucleating agent. (——) Base polymer, (—) nucleating agent, 0.1%. (*a*) η_r = 3, (*b*) η_r = 3.40, and (*c*) η_r = 4.80.

at lower temperatures of nylon 6 disappear by the addition of nucleating agents as shown in Figure 11. In poly(ethylene adipate) reported by Takayanagi and Yamashita,[10] the dependence of the growth rate of spherulites on temperature is divided into three parts, and each gives different

TABLE IV
Effect of Molecular Weight on the Crystallization of Polyoxymethylene

Number-average molecular weight	Heat of crystn., cal./g.	Degree of crystn., %
40,000	50.5	86
75,000	44.5	75

morphological structure of spherulites. According to the author's observation, it presumably relates to the discontinuity of the rate of crystallization. These phenomena will be discussed in forthcoming reports.

The rate of crystallization of nylon 6 is accelerated by the nucleating agent, while the degree of crystallization does not always increase.[5] As

TABLE V
Effect of Nucleating Agent on the Crystallization of Nylon 6

Base polymer viscosity, η_r	No nucleating agent				Nucleating agent, 0.1%			
	Upper peak, °C.	Lower peak, °C.	Heat of crystn., cal./g.	Deg. of crystn., %	Upper peak, °C.	Lower peak, °C.	Heat of crystn., cal./g.	Deg. of crystn., °C.
3	187.1	178	13.7	30.3	188	—	14.2	31.1
3.40	188	176	12.6	27.5	188.5	—	12.9	28.3
4.80	188.8	172	9.2	21	190	—	10.3	22.6

can be seen clearly from Figure 11, the exothermic peak areas are not always influenced by addition of a nucleating agent, while the shape of thermograms varies remarkably. The effect of the nucleating agent on the thermograms of crystallization is summarized in Table V. These results also support previous results.[5]

The author wishes to thank Prof. M. Takayanagi for his helpful discussion and Dr. M. Watanabe and Dr. N. Yoda for their advice.

References

1. Kee, B., and A. W. Sisko, *J. Polymer Sci.*, **50**, 87 (1961).
2. Wunderlich, B., and W. H. Kashdan, *J. Polymer Sci.*, **50**, 71 (1961).
3. Kee, B., *J. Polymer Sci.*, **50**, 79 (1961).
4. Kee, B., *J. Polymer Sci.*, **42**, 15 (1960).
5. Inoue, M., *J. Polymer Sci.*, **A1**, 2013 (1963).
6. Andrews, D. H., G. Lynn, and J. Johnstone, *J. Am. Chem. Soc.*, **48**, 1274 (1926).
7. Flory, P. J., *Principles of Polymer Chemistry*, Cornell Univ. Press, Ithaca, N. Y., 1953.
8. Dole, M., and B. Wunderlich, *J. Polymer Sci.*, **24**, 139 (1957).
9. Inoue, M., *J. Polymer Sci.*, **55**, 753 (1961).
10. Takayanagi, M., and T. Yamashita, *J. Polymer Sci.*, **22**, 552 (1956).

Résumé

On applique l'analyse thermique différentielle à l'étude de la fusion et de la cristallisation des hauts polymères. Les chaleurs de fusion des régions cristallines sont obtenues; elles s'élevent à: 45,6 cal/gr pour le nylon 6, 46,8 cal/gr pour le nylon 66, 47,9 cal/gr pour le nylon 610, 54,1 cal/gr pour le nylon 11, 58,7 cal/gr pour le polyoxyméthylène, 64,8 cal/gr pour le polyéthylène de haute densité, 15,9 cal/gr pour le polypropylène et 35,4 cal/gr pour le poly-(3,3-bischlorométhyloxacyclobutane). Dans la cristallisation à partir de la fusion, les pics exothermiques se présentent dans un domaine de température de 20 á 100°C. en dessous du point de fusion. On étudie l'effet de la température de fusion et du poids moléculaire sur les thermogrammes de cristallisation du nylon 6 et du polyoxyméthylène et l'on compare aux résultats obtenus par dilatométrie. Dans certains polymères tels que le nylon 6 avec des poids moléculaires plus élevés et le polyoxyméthylène, il se présente des pics de cristallisation en plus; les dimensions de ceux-ci dépendent du poids moléculaire. Le nylon 6 contenant des additifs en tant qu'agent nucléant ne montre qu'un seul pic exothermique indépendant du poids moléculaire. Ces thermogrammes à deux pics pourraient correspondre à la discontinuité de la vitesse de croissance des cristaux.

Zusammenfassung

Die Untersuchung des Schmelz- und Kristallisationsverhaltens von Hochpolymeren wurde mittels Differentialthermoanalyse durchgeführt. Folgende Schmelzwärmen für kristalline Bereiche wurden erhalten: 45,6 cal/g für Nylon 6, 46,8 cal/g für Nylon 66, 47,9 cal/g für Nylon 610, 54,1 cal/g für Nylon 11, 58,7 cal/g für Polyoxymethylen, 64,8 cal/g für Polyäthylen hoher Dichte, 15,9 cal/g für Polypropylen und 35,4 cal/g für Poly-(3,3)-bischlormethyloxacyclobutan. Bei Kristallisation aus der Schmelze tritt das exotherme Maximum in einem Temperaturbereich 20–100°C unterhalb des Schmelzpunktes auf. Der Einfluss von Schmelztemperatur und Molekulargewicht auf die Kristallisationsthermogramme von Nylon 6 und Polyoxymethylen wurde aufgeklärt und mit den dilatometrischen Ergebnissen verglichen. Vei manchen Polymeren, wie höhermolekularem Nylon 6 und Polyoxymethylen, tritt un ein exothermes Kristallisationsmaximum mehr auf, dessen Gestalt vom Molekulargewicht abhängt. Nylon 6, das keimbildende Zusätze enthält, zeigt unabhängig vom Molekulargewicht nur ein exothermes Maximum. Die Thermogramme mit zwei Maxima sollten zur Diskontinuität der Wachstumsgeschwindigkeit der Kristalle in Beziehung gebracht werden.

Received April 24, 1962
Revised May 27, 1962

JOURNAL OF POLYMER SCIENCE: PART A VOL. 1, PP. 2711–2730 (1963)

Photochlorination of Poly(methyl Methacrylate) in Aqueous Suspension*

F. H. OWENS and F. E. ZIMMERMAN, *Research Laboratories, Rohm & Haas Company, Bristol, Pennsylvania*

Synopsis

The aqueous suspension chlorination of poly(methyl methacrylate) using incandescent light produces polymer having up to one chlorine atom per monomer unit. The mechanism of aqueous suspension chlorination is the same as that for solution chlorination, i.e., free radical substitution; the rate of chlorination at constant chlorine flow rate depends on the time, the concentration of the polymer, and the size or porosity of the polymer particles. The structures of suspension and solution chlorinated poly(methyl methacrylate) were established by comparison of their NMR spectra with those of poly(methyl methacrylate), poly(chloromethyl methacrylate), and a copolymer of methyl α-chloromethylacrylate with methyl methacrylate. In chlorinated poly(methyl methacrylate) having 0.5 chlorine atoms per monomer unit, half of the chlorine is on the ester methyl group and half is on the β-carbon atom. In the suspension chlorinated sample containing one chlorine per monomer unit, 20% of the chlorine is present as $OCHCl_2$ groups, 40% as OCH_2Cl groups, 30% as —CHCl— groups, and 10% as C—CH_2Cl groups. In a solution chlorinated sample containing two chlorine atoms per monomer unit, the chlorine is distributed: 40% as OCH_2Cl, 40% as —CHCl— and/or C—CH_2Cl, and 20% as $OCHCl_2$.

INTRODUCTION

The primary objective of the investigation described here was to study the factors affecting the photochlorination of poly(methyl methacrylate) (PMMA) in aqueous suspension and to determine the structure of the chlorinated polymer, i.e., the position of substitution of the chlorine.

Photochlorination of PMMA in solution has been described by several workers.[1–4] Hahn and Grafmüller[2] showed that photochlorination of PMMA in carbon tetrachloride resulted in a decrease in the degree of polymerization (DP) from 1119 for unchlorinated material to 209 for chlorinated polymer containing approximately two chlorine atoms per monomer unit. They attributed this decrease in DP to the reaction as shown on the following page:[2]

* Presented before the Division of Polymer Chemistry at the 141st Meeting of the American Chemical Society, Washington, D.C., March 1962.

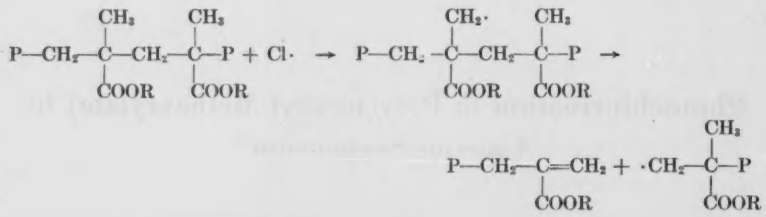

where P denotes the polymer chain and R is CH_3.

Smets and Fournaux[3] investigated the photochlorination of poly(methyl acrylate) (PMA), poly(ethyl acrylate)(PEA), and PMMA in solution. They found that these polymers were photochlorinated at a constant rate up to a degree of substitution (DS) of two. [Chlorinated PMMA has the compositions $(C_5H_7ClO_2)_n$, $(C_5H_{6.5}Cl_{1.5}O_2)_n$, and $(C_5H_6Cl_2O_2)_n$ for degrees of substitution of 1, 1.5, and 2, respectively.] They interpreted this constancy of rate as indicating that up to a DS of two, the ester alkyl group was not chlorinated. The chlorinated polymers were treated with aniline—a reagent which they felt would replace only chlorine attached to the β-methylene group in the case of PMA and PEA and would replace only chlorine attached to the α-methyl group in the case of PMMA. They found that in the case of PMA and PEA at DS $\leqq$ 1, 66% of the chlorine was replaceable by aniline, and they interpreted these data as indicating that the chlorine was distributed statistically according to the number of hydrogens on the carbon atom, i.e., 66% on the β-carbon atom and 33% on the α-carbon atom. With PMA and PEA at DS = 2, 50% of the

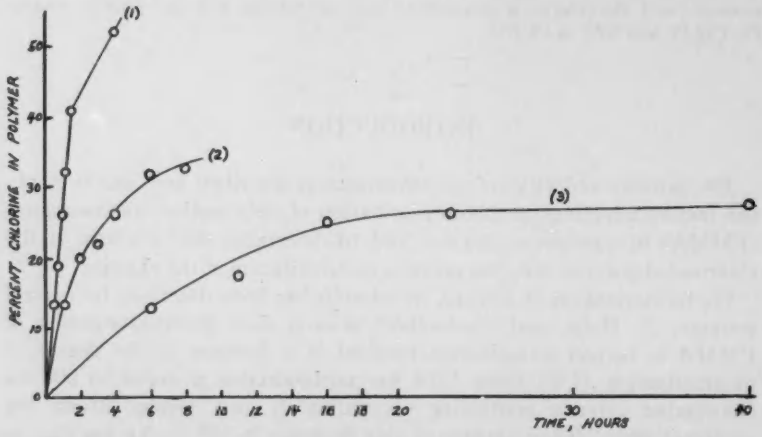

Fig. 1. Chlorine in the polymer as a function of the time of chlorination: (*1*) ultraviolet-catalyzed solution chlorination, data of Smets and Fournaux;[3] (*2*) suspension chlorination, 20 g. of polymer in 600 ml. of water; (*3*) suspension chlorination, 100 g. of polymer in 1 l. of water.

TABLE I
Aqueous Suspension Chlorination of Poly(methyl Methacrylate) with Incandescent Light

Run no.	Weight of polymer, g.	Volume of water, ml.	Time, hr.	Chlorine, %	DS	RSV, dl./g.[a]	$\bar{M}_n$	$\overline{DP}_n$
Starting material						0.59	41,700	416.5
4701	20.0	600	1	13.54	0.44	0.36	36,600	317.4
4702	20.0	600	2	20.13	0.71	0.27	31,700	254.7
4703	20.0	600	3	22.15	0.80	0.21	20,000	156.7
4704	20.0	600	4	26.12	0.99	0.15		
480	20.0	600	6	32.10	1.32	0.15		
483	20.0	600	8	32.65	1.35	0.14		
Starting material						0.65		
533	700	7000	6	13.13	0.43	0.33		
534	600	6000	11	15.00	0.50	0.32		
536	600	6000	16	25.10	0.94	0.12		
537	600	6000	23	26.10	0.99	0.15		
538	600	6000	40	27.60	1.06	0.12		

[a] Reduced specific viscosity in ethylene dichloride

chlorine was replaced by aniline; to these materials they assigned a structure having one chlorine on each of the backbone carbon atoms.

In chlorinated PMMA at DS $\leqq$ 1, 60% of the chlorine was replaced by aniline, and at DS = 2, 50% of the chlorine was replaced. Chlorinated PMMA was assigned a structure having 60% of the chlorine on the α-methyl group for DS = 1 and a structure having one chlorine each on the α-methyl and β-methylene groups for DS = 2. Their conclusion, based on the constant rate of chlorination and the reaction of the chlorinated polymers with aniline, was that photochlorination in solution up to DS = 2 directs the chlorine statistically without substitution on the ester alkyl group and without disubstitution on any one carbon atom.

In the work presented here we studied the photochlorination of PMMA in aqueous suspension with special regard to the structure of the resulting polymer. Since the structure of the polymer obtained from photochlorination in aqueous suspension was not the same as the structure assigned to solution chlorinated polymer, we reinvestigated the structure of the polymer obtained by solution chlorination and found that the structure previously assigned to this polymer by Smets and Fournaux[3] is incorrect.

DISCUSSION

Reaction Conditions

The polymer samples were suspended in water, and chlorine gas was bubbled into the suspension for a specified period of time with no attempt at metering the flow. The rate of flow of chlorine was kept approximately constant from experiment to experiment by visual observation of a bubbler. The chlorinated polymer was isolated by filtration, washed with water, and dried. That the reaction was light-catalyzed was demonstrated by conducting a chlorination in the absence of light; after 4 hr. the polymer contained no chlorine. Although ultraviolet photochlorination introduces slightly more chlorine per unit time, incandescent light was used for convenience.

In Table I are shown the results of a series of chlorinations of finely divided PMMA. As can be seen, the rate of chlorine uptake is proportional to the time and to the concentration of the polymer. These data are presented graphically in Figure 1. It is also noteworthy that the rate of chlorination decreases rapidly at DS = 1.

For comparison purposes, the data of Smets and Fournaux[3] on the ultraviolet-catalyzed solution chlorination of PMMA are included in Figure 1. Here the rate increases constantly until DS = 2 is reached. A series of samples was chlorinated in chloroform solution under both ultraviolet and incandescent light. These data are shown in Table II. The solution chlorinations proceed much faster to a DS $\sim$ 2, in agreement with the data of Smets and Fournaux. Indeed, it was necessary to reduce drastically the amount of chlorine passed into the solution in order to obtain a polymer with DS $<$ 1.

TABLE II
Chlorination of Poly(methyl Methacrylate) in Chloroform Solution[a]

Run no.	Catalysis	Time, hr.	Chlorine, %	DS	$[\eta]$, dl./g.[b]
7471A	Incandescent light	1	37.91	1.70	0.106
7472A	" "	2	38.72	1.75	0.105
7473A	" "	3	42.08	2.01	0.065
7474A	" "	4	42.91	2.08	0.074
749	Ultraviolet light	1	37.30	1.65	0.147
7661[c]	" "	0.5	14.17	0.46	0.57
7662[c]	" "	1	21.37	0.76	0.51

[a] All runs were made with 20 g. of Y-100 ($[\eta]$ = 0.59 dl./g.) in 500 ml. of chloroform.
[b] All intrinsic viscosities run in ethylene dichloride.
[c] Chlorine passed into the solution at a very slow rate.

A study was made of the effect of the particle size on the rate of chlorination. For this purpose, samples of PMMA of various particle sizes and two samples of highly crosslinked PMMA macroreticular beads[5] were chlorinated in aqueous suspension. The results, shown in Table III, indicate that for linear PMMA the particle size has a pronounced effect on the rate of chlorination, there being essentially no chlorination of the large-particled Y-100. In the case of the macroreticular resins,[5] not the particle size but the porosity is the controlling factor, as might be expected, since the rate of chlorination depends on the surface area exposed to chlorine.

Hahn and Grafmüller showed that photochlorination of PMMA in carbon tetrachloride resulted in a decrease in DP.[2] From the data in Table I, it can be seen that aqueous suspension chlorination of PMMA causes a decrease in DP from 416.5 for unchlorinated material to 156.7 for chlorinated polymer, DS = 0.80.

All of the above data indicate that aqueous suspension chlorination proceeds by the same mechanism as solution chlorination, i.e., free radical substitution, and that the rate of chlorination depends on the accessibility of the molecule to the chlorine, with the highest rate for solution chlorination and the lowest rate for large particle, low porosity material.

The Structure of Chlorinated Poly(methyl Methacrylate)

A comparison of the infrared spectra of PMMA and chlorinated PMMA reveals that on chlorination, two new maxima at 720 and 1340 cm.$^{-1}$ appear, the maximum at 990 cm.$^{-1}$ increases in intensity and is displaced to slightly higher frequency, and the ester carbonyl maximum at 1730 cm.$^{-1}$ for PMMA is considerably broader in chlorinated PMMA. The spectra of polymers containing equivalent amounts of chlorine were identical whether the polymer was chlorinated in solution or aqueous suspension. The new band at 720 cm.$^{-1}$ can be attributed to the C—Cl stretching mode. It was at first thought that the new maximum at 1340 cm.$^{-1}$ might be due to substitution on the α-methyl group; however, a deter-

TABLE III
Effect of Particle Size and Porosity on Aqueous Suspension Chlorination of Poly(methyl Methacrylate) with Incandescent Light

Run no.	Sample no.	Polymer	Particle size	Weight of polymer, g.	Volume of water, ml.	Time, hr.	Chlorine, %	DS
496	Y-100	Poly(methyl-	45–500μ, bulk 75–200μ	10	200	4	1.63	
7471B	7470	methacrylate)	5–1000μ, bulk 30–300μ	20	1000	1	11.77	0.37
7472B	7470		5–1000μ, bulk 30–300μ	20	1000	2	10.33	0.32
7473B	7470		5–1000μ, bulk 30–300μ	20	1000	3	18.93	0.65
7474B	7470		5–1000μ, bulk 30–300μ	20	1000	4	20.33	0.72
487	16027		1.5–16μ, bulk 3–10μ	140	2000	5	18.94	0.66
532	1323		2–20μ, bulk 8–10μ	500	7000	6	22.85	0.83
639	4419B[a]	Macroreticular	100–525μ, bulk 250–450μ	54	3000	4	8.83	
640	4419E[b]	resin	1–2 mm.	53	3000	4	16.43	

[a] Highly crosslinked PMMA, porosity 0.231 ml./ml.
[b] Highly crosslinked PMMA, porosity 0.635 ml./ml.

mination of the ratio of absorbances of the maxima at 1340 cm.$^{-1}$ and at 1392 cm.$^{-1}$ reveals that this ratio is directly related to the total per cent chlorine. Therefore, the maximum at 1340 cm.$^{-1}$ must be an overtone of a fundamental C-Cl vibration, probably below 650 cm.$^{-1}$.

The broadening of the C—O—C ester band at 1100 cm.$^{-1}$ and of the ester carbonyl band at 1730 cm.$^{-1}$ are hardly explicable on the basis of substitution only on the α-methyl group and the β-methylene group as suggested by Smets and Fournaux.[3] In order to establish the structure of these chlorinated materials, an attempt was made to prepare homopolymers and copolymers with methyl methacrylate of methyl α-chloromethylacrylate (Ib), methyl β-chloromethacrylate (IIb), and chloromethyl methacrylate (III):

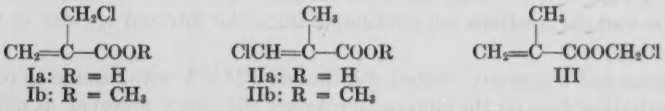

The acid Ia was prepared by the method of Ferris and Marks, pyrolysis of chloroacetone cyanohydrin acetate followed by hydrolysis of the α-chloromethylacrylonitrile.[6] Esterification with methanol containing anhydrous hydrogen chloride gave the ester Ib. Homopolymerization of methyl α-chloromethylacrylate in benzene yielded only 8% of a polymer of very low molecular weight. Copolymerization of equal weights of Ib and methyl methacrylate in benzene solution gave a 60% yield of copolymer containing 35.4% methyl α-chloromethylacrylate and having a reduced specific viscosity in ethylene dichloride of 0.07 dl./g. The infrared spectrum of this copolymer showed carbonyl maxima at 1730 and 1740 cm.$^{-1}$ and a shoulder on the maximum at 750 cm.$^{-1}$ but no maximum at 1340 cm.$^{-1}$. The ester carbonyl maximum at 1740 cm.$^{-1}$ is attributed to the dipolar interaction of the halogen with the carbonyl group across space and is normal for this type of interaction.

Methyl β-chloromethacrylate (IIb) was obtained by esterification of the acid IIa, prepared by dehydrochlorination of sodium α,β-dichloroisobutyrate with sodium hydroxide.[7] This monomer did not homopolymerize and copolymerized only very poorly with methyl methacrylate, so that no definitive spectral data could be obtained. However, a chlorine on the β-carbon atom would be expected to have little, if any, effect on the position of the ester carbonyl maximum.

Chloromethyl methacrylate (III) was prepared by the reaction of methacrylyl chloride containing a small amount of anhydrous zinc chloride with paraformaldehyde.[8] Chloromethyl methacrylate homopolymerizes well in benzene solution to give a polymer having a reduced specific viscosity in ethylene dichloride of 0.23 dl./g. Copolymerization of an equimolar mixture of III and methyl methacrylate in benzene gave a polymer having a reduced specific viscosity in ethylene dichloride of 0.38 dl./g. and containing 55.6 mole-% chloromethyl methacrylate. The ester carbonyl

maximum of poly(chloromethyl methacrylate) occurs at 1760 cm.$^{-1}$, and in the copolymer of chloromethyl methacrylate and methyl methacrylate, in addition to the normal maximum for PMMA at 1730 cm.$^{-1}$, there is a maximum at 1760 cm.$^{-1}$ attributable to the chloromethyl methacrylate portion of the copolymer. The additional maxima noted in the spectra of chlorinated PMMA are also present in the homopolymer and copolymer of III; however, the ratios of the absorbances at 1340 and 1392 cm.$^{-1}$ do not lie on the curve of absorbance versus per cent chlorine found for chlorinated PMMA. The reason for this discrepancy is not known.

Because of the nature of the ester carbonyl maxima and the ester C—O—C bands in chlorinated PMMA, it is evident that in chlorinated PMMA a substantial part of the substitution of the chlorine is on the methyl ester group. However, no quantitative data on the amount of substitution at the various positions are obtainable from the infrared spectra of these materials.

Smets and Fournaux treated chlorinated PMMA with aniline to obtain quantitative data on the amount of primary chlorine;[3] however, as pointed

TABLE IV
Determination of Primary Chlorine in Chlorine-Containing Acrylic Polymers

Polymer no.	Chlorine in polymer, %	DS	Chlorine replaced by NaI, %	Chlorine replaced by $C_6H_5NH_2$, %	Nitrogen in polymer, %	
					Found	Theor.[a]
Homopolymers and Copolymers						
1509[b]	26.24	1.0	101.5	88.4	8.10	6.69
908[b]	26.30	1.0	100.0			
756[c]	15.92	0.53	100.1	99.2	3.34	3.98
8732[d]	11.2	0.35	20.2			
Solution-Chlorinated Poly(methyl Methacrylate)						
7471A	37.91	1.70	44.3	78.7	4.89	7.98
7472A	38.72	1.75	44.5	79.6	5.98	8.16
7473A	42.08	2.01	40.8	80.5	4.86	8.68
7474A	42.91	2.08	37.4	80.9	5.71	8.82
749	37.30	1.65	43.2	79.5	4.58	7.95
7661	14.17	0.46	54.6	57.0	2.17	2.83
7662	21.37	0.76	40.5	59.5	3.15	4.18
Suspension-Chlorinated Poly(methyl Methacrylate)						
7471B	11.77	0.37	52.4	64.2	1.43	2.66
7472B	10.33	0.32	53.4	57.7	2.35	2.15
7473B	18.93	0.65	49.3	67.7	1.67	4.20
7474B	20.33	0.72	49.2	77.0	2.01	4.95
533	13.13	0.43	50.0			
537	26.10	0.99	48.0			

[a] Theoretical per cent nitrogen calculated on the basis of a direct nucleophilic displacement of chlorine by aniline.

[b] Poly(chloromethyl methacrylate).

[c] Copolymer of chloromethyl methacrylate and methyl methacrylate.

[d] Copolymer of methyl α-chloromethylacrylate and methyl methacrylate.

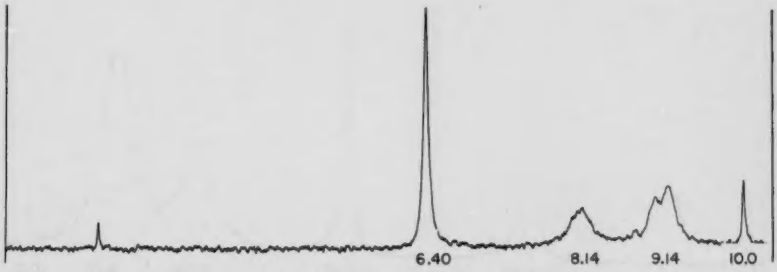

Fig. 2. NMR spectrum of poly(methyl methacrylate).

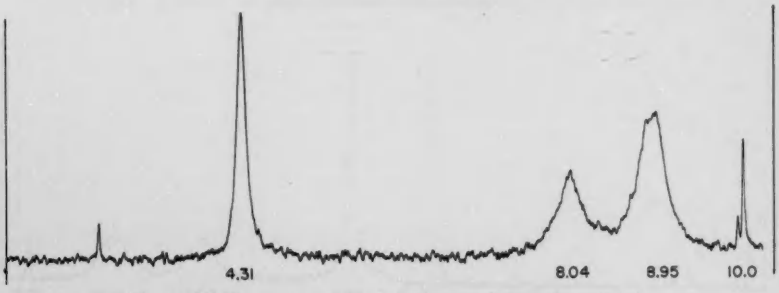

Fig. 3. NMR spectrum of poly(chloromethyl methacrylate).

out above, they assumed no substitution on the methyl ester group below DS = 2, and they assumed that the reaction of aniline with the chlorinated polymer would only be one of nucleophilic displacement of primary chlorine by aniline. It was felt that a better measure of the primary halogen might be obtained by treatment of the chlorinated polymer with sodium iodide in acetone followed by a determination of the acetone-insoluble sodium chloride. In Table IV are shown the data obtained on treatment of various chlorine-containing acrylic polymers with aniline and with sodium iodide in acetone. From these data it can be seen that there is no agreement between the two methods, and there is little agreement with the data of Smets and Fournaux. Furthermore, in all the cases except poly(chloromethyl methacrylate) the per cent nitrogen found falls below that calculated for a simple nucleophilic displacement of chlorine by aniline, indicating that the reaction with aniline is more complex. The data on the replacement of sodium iodide show that the method is valid for chlorine attached to the methyl ester group, but that only 20% of the chlorine attached to the α-methyl group is replaced. The reason for this discrepancy is not immediately obvious but is probably connected with the steric hinderance about the α-methyl group. The sodium iodide data show that there is primary chlorine present, but little indication is given as to the position of that primary chlorine, since it is not known what would be the result from a copolymer of chloromethyl methacrylate and methyl

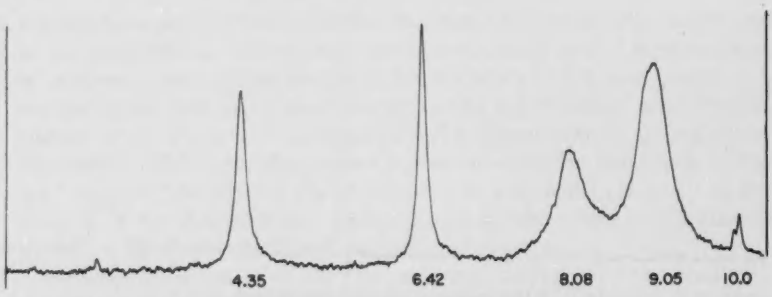

Fig. 4. NMR spectrum of a copolymer containing 44% methyl methacrylate and 56% chloromethyl methacrylate.

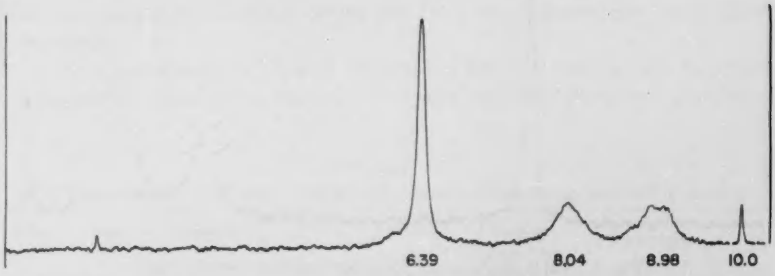

Fig. 5. NMR spectrum of a copolymer containing 65% methyl methacrylate and 35% methyl α-chloromethylacrylate.

α-chloromethylacrylate and since disubstitution on any one carbon atom would be unaffected by sodium iodide in acetone.

In Figures 2 to 7 are shown the nuclear magnetic resonance spectra of four polymers of known structure and two chlorinated PMMA polymers. In the spectrum of PMMA, Bovey and Tiers have attributed the peak at 6.40τ to the methyl ester group, the peak at 8.14τ to the β-methylene group, and the triad at 8.78, 8.98, and 9.14τ to the α-methyl group.[9] The areas of these peaks, in Figure 2, are in the ratio 3.04:1.78:3.18. The peaks in the spectrum of poly(chloromethyl methacrylate) are assigned as follows: 4.31τ (area ratio 2.03), chloromethyl ester group; 8.04τ (area ratio 1.69), β-methylene group; 8.95τ (area ratio 3.03), α-methyl group. In the case of the copolymer containing ca. 60% chloromethyl methacrylate, there are peaks at 4.35τ (OCH_2Cl, area ratio 1.20), 6.42τ (OCH_3, area ratio 1.21), 8.08τ (—CH_2 group, area ratio 1.97), and 9.05τ (—CH_3, area ratio 3.05). In the spectrum of the copolymer of methyl α-chloromethylacrylate (35%) and methyl methacrylate (65%), there are peaks at 6.39τ (area ratio 3.91), 8.04τ (area ratio 1.88), and a triad at 8.78, 8.98, and 9.14τ (area ratio 1.88). In this spectrum the peak attributable to the protons on the C—CH_2Cl group must lie under the OCH_3 peak at 6.39τ. The chemical shift of these protons from ca. 9.0 to 6.4τ is reasonable in view of the shift

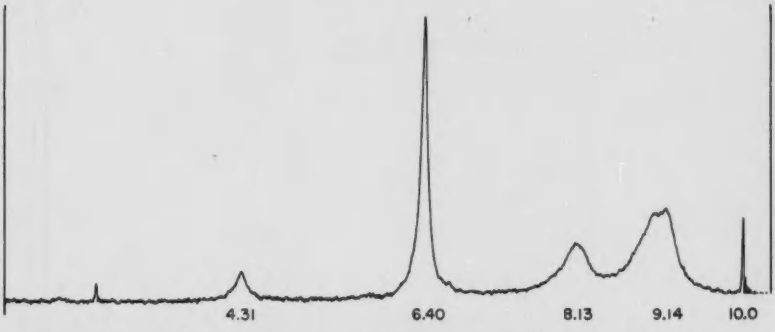

Fig. 6. NMR spectrum of suspension chlorinated poly(methyl methacrylate), DS = 0.43.

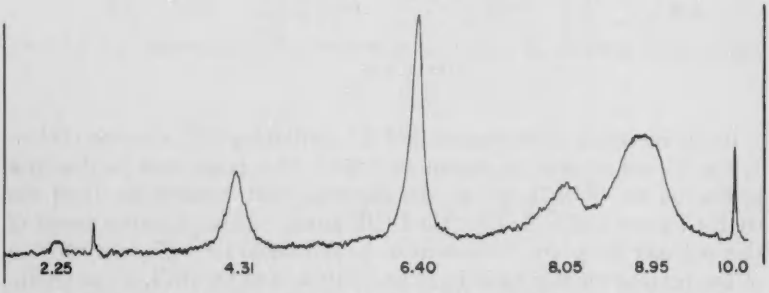

Fig. 7. NMR spectrum of suspension chlorinated poly(methyl methacrylate), DS = 0.99.

of the protons on the OCH_2Cl peak from 6.4 to 4.35τ for chloromethyl methacrylate. The area ratios are also in reasonable agreement with this formulation, the expected ratios being 3.7:2.0:1.95 for the peaks at 6.39, 8.04, and the triad centered at 8.98τ, respectively.

If in considering the spectrum of chlorinated PMMA containing 13% chlorine (DS = 0.4, Fig. 6) a segment of 10 units is taken, there are 76 hydrogen atoms and 4 chlorine atoms to be accounted for. The number of protons accounted for by each peak, on this basis, are: OCH_2Cl, 44; β-methylene, 16; α-methyl, 30; the peak at 6.40τ then accounts for 26 protons. Since there are thus 10 α-methyl groups, 8 β-methylene groups, and 2 chloromethyl ester groups, there must be 8 OCH_3 groups and 2 —CHCl— groups; therefore, the peak attributable to the —CHCl— proton must lie under the OCH_3 proton peak at 6.40τ. It will be noted that this peak is asymmetric, the asymmetry being due to the presence of two peaks. This shift from 8.12 to ca. 6.40τ is also reasonable. Thus, 50% of the chlorine is on the methyl ester group and 50% is on the β-carbon atom. This result is in good agreement with the results of the sodium iodide reaction (Table IV, No. 533).

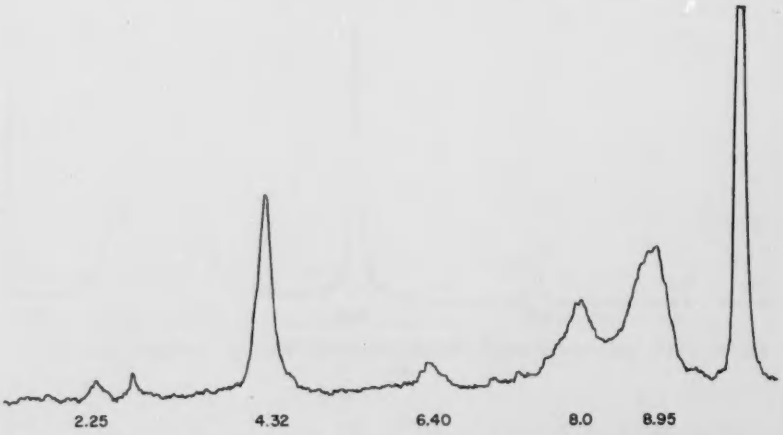

Fig. 8. NMR spectrum of suspension chlorinated poly(chloromethyl methacrylate), DS = 1.36.

In the spectrum of chlorinated PMMA containing 26% chlorine (DS = 1, Fig. 7), a new peak is present at 2.25τ. This peak must be due to a proton on an $OCHCl_2$ group, the chemical shift being 2.05τ from the OCH_2Cl group and 4.11τ from the OCH_3 group. In a ten-unit segment of this polymer there are 70 protons to be accounted for. The distribution of the protons on this basis is: 1 as $OCHCl_2$, 8 as OCH_2Cl, 15 as OCH_3, 3 as —CHCl—, 2 as C—CH_2Cl, and 7 as C—CH_3; therefore, the chlorine is distributed 10% on the α-methyl group, 30% on the β-methylene group, and 60% on the ester methyl group, 40% as monosubstitution, and 20% as disubstitution. These data are in agreement with the sodium iodide titration data, since the 40% of the chlorine which is on the methyl ester group (monosubstitution) and the 10% which is on the α-methyl group should be replaceable by iodide ion, the actual amount of chlorine replaced by sodium iodide being 48% (Table IV, No. 537). Since there is little substitution on the α-methyl group, probably because of steric hinderance, it is not too surprising that almost all of this chlorine is replaced, whereas in the copolymer of methyl α-chloromethylacrylate and methyl methacrylate only 20% of the chlorine is replaced.

Confirmation of the assignment of the $OCHCl_2$ band at 2.25τ and the —CHCl— band at ca. 6.4τ is obtained from the NMR spectrum of poly(chloromethyl methacrylate) which was chlorinated in aqueous suspension (Fig. 8). In this spectrum there are bands at 2.25τ (area ratio 0.2), 4.32τ (area ratio 1.65), 6.40τ (area ratio 0.2), 8.0τ (area ratio 1.5), and 8.95τ (area ratio 3.0). Thus, on the basis of the decrease in area ratios of the peaks at 4.3τ and 8.0τ and the appearance of the two bands at 2.25τ and 6.4τ, these latter bands must be assigned to the groups $OCHCl_2$ and —CHCl—, respectively.

TABLE V
NMR Analyses of Chlorinated Polymers

Sample	DS	Chlorine substituted, %				Chlorine replaceable by KI, %
		OCH_2Cl	—CHCl—	C—CH_2Cl	$OCHCl_2$	
Poly(chloromethyl methacrylate)	1.0	100				100
Copolymer of MMA and chloromethyl methacrylate	0.53	100				100
Copolymer of MMA and methyl α-chloromethylacrylate	0.35			100		20
Suspension-chlorinated PMMA	0.5	50	50			50
Suspension-chlorinated PMMA	0.6	50	50			47
Suspension-chlorinated PMMA	0.8	50	38	12		68
Suspension-chlorinated PMMA	1.0	40	30	10	20	48
Solution-chlorinated PMMA	0.5	60	40			55
Solution-chlorinated PMMA	0.8	38	62			41
Suspension-chlorinated poly(chloromethyl methacrylate)	1.4	57	14		29[a]	73

[a] This value represents only 15% chlorine introduced during the chlorination since the other half was originally present on this carbon atom.

It is interesting to note that the initial substitution patterns for PMMA and poly(chloromethyl methacrylate) are the same—half of the attack is on the ester alkyl group and half on the β-methylene group.

Table V is a recapitulation of the data on the position of substitution of chlorine as determined by NMR spectral analysis for a number of chlorinated polymers. From these data it can be seen that there is a slight difference between the substitution pattern for PMMA chlorinated in solution and in aqueous suspension, but the differences at DS<1 are so slight as to be negligible.

Fig. 9. NMR spectrum of solution chlorinated poly(methyl methacrylate), DS = 2.02.

Figure 9 shows the NMR spectrum of a sample of solution chlorinated PMMA, DS = 2. It can be seen that the peaks assigned to the ester methyl and β-methylene groups are no longer readily separable; thus, it is not possible to obtain quantitative data on the amount of chlorine substituted as —CHCl— or C—CH_2Cl. Consequently, in samples with DS>1, it is necessary to lump these two values together. In Table VI are shown the data obtained on the position of substitution of samples of solution-chlorinated PMMA at DS>1.

TABLE VI
NMR Analyses of Solution-Chlorinated PMMA

	Chlorine substituted, %			
DS	OCH_2Cl	—CHCl— and C—CH_2Cl	$OCHCl_2$	Chlorine replaceable by KI, %
1.6	50	47	3	43
1.7	41	47	12	41
2.0	40	40	20	41

From the data in Tables V and VI it can be seen that at equivalent DS, there is less disubstitution on the ester methyl group when the polymer is chlorinated in solution. It is interesting to note that above DS = 0.8, disubstitution on the ester alkyl group isp referred to substitution on the α-methyl group and that the substitution both in suspension and in solution chlorination is *not* statistical as suggested previously.[3] There is no obvious explanation for these observations.

EXPERIMENTAL

Materials

Y-100 is a commercial poly(methyl methacrylate) made by the Rohm & Haas Co. The finely divided samples were prepared by dissolving Y-100 in acetone and precipitating it into a large volume of water in a Waring Blendor. The chlorine was obtained from the Matheson Co. and was used as received. Methacrylyl chloride was obtained from the J. T. Baker Chemical Co. and was used as received. Sodium α,β-dichloroisobutyrate is a Rohm & Haas Co. product (Mendok) and was untreated. The paraformaldehyde (Fisher Scientific Co., U.S.P.) and the sodium iodide (J. T. Baker Chemical Co., crystal) were used as received. The 0.1*N* silver nitrate and 0.1*N* ammonium thiocyanate solutions were obtained from the Hartman Leddon Co. All solvents were reagent grade.

Viscosity Measurements

Intrinsic viscosities were determined in chloroform or ethylene dichloride solution at 25 ± 0.01°C. Reduced specific viscosities were determined in chloroform or ethylene dichloride solution at 25 ± 0.01°C. at a concentration of 2 g./l. The reduced specific viscosity is defined as RSV = η_{sp}/C.

Osmotic Measurements

Osmotic pressure measurements were made in benzene at 30 ± 0.005°C. using a modified Schulz-Wagner osmometer equipped with the "allerfeinst" grade of Ultrafein filter (Membranfilter Gesellschaft, Göttingen, Germany) described by Vaughan.[10]

Spectroscopic Analyses

The infrared spectra were obtained on a Perkin-Elmer model 21 double-beam recording spectrometer equipped with rock salt optics. The samples were cast as thin films from benzene solution onto silver chloride plates and were heated at 60°C. *in vacuo* overnight. The NMR spectra were obtained by Varian Associates on an A-60 spectrometer or in these laboratories on an HR-60 spectrometer. The samples were determined in deuterochloroform solution, and the areas of the various peaks were determined with a planimeter.

Chlorinations

The general procedures for the chlorinations in suspension and in chloroform solution are illustrated by the specific directions for the 4-hr. chlorinations of PMMA.

Aqueous Suspension Chlorination of PMMA (4701)

Water and polymer were placed in a reaction vessel equipped with a mechanical stirrer, water-cooled reflux condenser, thermometer, and an inlet

tube for chlorine gas which extended below the surface of the water. The exit from the condenser was connected to a trap containing aqueous base. The flask was illuminated with a 200-w. incandescent bulb placed adjacent to the side of the flask. With stirring, chlorine gas was passed through a water bubbler into the flask for 4 hr. No attempt was made to measure the amount or rate of chlorine, but the rate was kept approximately constant from run to run by visual observation of the bubbler. The polymer was filtered, washed three times with a large volume of water in a Waring Blendor, and dried *in vacuo* at 60°C. for 48 hr. In chlorinations requiring more than 8 hr., the sample was chlorinated for 8 hr. and was allowed to stand overnight. The procedure was repeated until the required time had elapsed. The polymers were isolated, washed, and dried as above. The data are shown in Tables I and III.

Chloroform Solution Chlorination of PMMA (7474A)

The polymer and chloroform were placed in a reaction vessel equipped as above. The flask was illuminated with a 200-w. incandescent bulb or a Sylvania 15-w. Blacklite placed adjacent to the side of the flask. The mixture was stirred until the polymer dissolved. With continued stirring, chlorine gas was passed through a chloroform bubbler into the solution for 4 hr. Nitrogen gas was then bubbled through the solution for 1 hr. to remove the excess chlorine gas. The polymer was precipitated into 10 volumes of vigorously stirred methanol, was washed three times with water in a Waring Blendor, and was dried *in vacuo* at 60°C. for 48 hr. In experiments 7661 and 7662, it was necessary to reduce the chlorine flow rate to avoid overchlorination.

Methyl α-Chloromethylacrylate (Ib)

A solution of 30 g. of α-chloromethylacrylic acid (Ia), prepared by the method of Ferris and Marks,[6] in 200 ml. of methanol was added with stirring to 200 ml. of methanol saturated with dry hydrogen chloride gas. The solution was allowed to stand overnight and was then poured into 1 l. of water containing ice. The ester was extracted with three 500-ml. portions of ether. The ethereal solution was washed with two 250-ml. portions of a 5% aqueous solution of sodium carbonate and two 250-ml. portions of water and was dried with anhydrous magnesium sulfate. The ether was removed *in vacuo*, and the residue was distilled. There was obtained 11.3 g. of methyl α-chloromethylacrylate, b.p. 57–58°C./13 mm.

ANAL. Calcd. for $C_5H_7ClO_2$: C, 44.63%; H, 5.24%; Cl, 26.35%. Found: C, 44.71%; H, 5.21%; Cl, 26.05%.

Homopolymerization of Methyl α-Chloromethylacrylate (8731)

A mixture of 0.057 g. of azobisisobutyronitrile, 5 g. of methyl α-chloromethylacrylate, and 25 ml. of benzene in an ampule was degassed on a high vacuum line by alternate freezing and thawing three times. The ampule

was sealed under vacuum and was heated at 60°C. for three days. The ampule was opened, and the polymer was precipitated by pouring the benzene solution into 10 volumes of a vigorously agitated mixture of 10 parts of water and 90 parts of methanol. There was obtained 0.4 g. (8%) of low molecular weight polymer.

ANAL. Calcd. for $(C_5H_7ClO_2)_n$: Cl, 26.35%. Found: Cl, 25.15%.

Copolymerization of Methyl α-Chloromethylacrylate with Methyl Methacrylate (8732)

A mixture of 0.057 g. of azobisisobutyronitrile, 2.5 g. of methyl α-chloromethylacrylate, 2.5 g. of methyl methacrylate, and 25 ml. of benzene in an ampule was degassed on a high vacuum line by alternate freezing and thawing three times. The ampule was sealed under vacuum and was heated at 60°C. for three days. The ampule was opened, and the polymer was precipitated by pouring the benzene solution into 10 volumes of a vigorously stirred mixture of 10 parts of water and 90 parts of methanol. There was obtained 3.0 g. (60%) of copolymer having a reduced specific viscosity in ethylene dichloride of 0.07 dl./g. and containing 11.19% chlorine. This value corresponds to 35.4% of methyl α-chloromethylacrylate in the copolymer.

Methyl β-Chloromethacrylate (IIb)

To 1074 g. (6 moles) of sodium α,β-dichloroisobutyrate in 1200 ml. of water was added 250 g. (6.25 moles) of sodium hydroxide in 250 ml. of water. The solution was warmed on a steam bath for 30 min. and was then cooled to room temperature. Concentrated hydrochloric acid (550 ml.) was added while the temperature was maintained below 25°C. The precipitate was extracted with hot benzene, and the benzene solution was filtered to remove the salt and was dried with anhydrous magnesium sulfate. Methanol (500 ml.) and 50 ml. of concentrated sulfuric acid were added. The mixture was heated at reflux for 60 hr., whereupon it was cooled to room temperature. The benzene and methanol were removed *in vacuo* without heating. The residue was taken up in 1 l. of ether, were washed with 500 ml. of water, three 500-ml. portions of a 10% aqueous solution of sodium carbonate, and 500 ml. of water, and was dried. The ether was removed *in vacuo*, and the residue was distilled. After a forerun (b.p. 53–57°C./25 mm., 3.4 g.) there was obtained 215.5 g. (27% based on Mendok) of methyl β-chloromethacrylate, b.p. 59°C./28 mm., n_D^{25} 1.4543 (lit.[7] b.p. 41–50°C./10 mm., n_D^{25} 1.4536).

ANAL. Calcd. for $C_5H_7ClO_2$: C, 44.63%; H, 5.24%; Cl, 26.35%. Found: C, 44.66%; H, 5.36%; Cl, 26.69%.

Attempted Homopolymerization of Methyl β-Chloromethacrylate

A mixture of 34 g. of methyl β-chloromethacrylate, 170 ml. of benzene, and 0.23 g. of azobisisobutyronitrile was deaerated by bubbling nitrogen

through the solution for 1 hr. and was heated at reflux with stirring overnight. The mixture was cooled to room temperature and was poured into 10 volumes of vigorously stirred methanol containing 10% by volume of water. No solid polymer was obtained.

Attempted Copolymerization of Methyl β-Chloromethacrylate with Methyl Methacrylate

A mixture of 17 g. (0.125 mole) of methyl β-chloromethacrylate, 12.5 g. (0.125 mole) of methyl methacrylate, 170 ml. of benzene, and 0.23 g. of azobisisobutyronitrile was deaerated by bubbling nitrogen through the solution for 1 hr. and was heated at reflux with stirring overnight. The mixture was cooled to room temperature and was poured into a vigorously stirred mixture of 90 parts of methanol and 10 parts of water. There was obtained 3.8 g. of polymer containing 0.56% chlorine.

Chloromethyl Methacrylate (III)

In a 1-l., three necked flask equipped with a mechanical stirrer, a water-cooled reflux condenser, and a thermometer were placed 246 g. (2.35 moles) of methacrylyl chloride and 5 g. of anhydrous zinc chloride. The mixture was stirred, and 74 g. (2.46 moles) of paraformaldehyde was added in portions over 1 hr. while maintaining the temperature at 25–35°C. The mixture was then stirred for 1.5 hr., whereupon the condenser was replaced with a 6-in. Vigreaux volumn connected to a distilling head with vacuum take-off. The receiver was cooled in a mixure of Dry Ice–acetone, and the reaction mixture was flash-distilled at a pressure of ca. 5 mm. Redistillation gave 110 g. (35% yield based on methacrylyl chloride) of chloromethyl methacrylate boiling at 45–46°C. at 15 mm. (lit.:[8] b.p. 63–65°C./62 mm.). The lachrymatory, colorless liquid was pure by gas chromatography.

Homopolymerization of Chloromethyl Methacrylate

A mixture of 25 g. of chloromethyl methacrylate, 225 ml. of benzene, and 0.086 g. of azobisisobutyronitrile was deaerated with nitrogen gas for 1.5 hr. and was then heated at 70°C. for 5 hr. The solution was cooled to room temperature and was poured into 10 volumes of vigorously agitated methanol. The polymer was dried *in vacuo* at room temperature for 5 days. There was obtained 10.8 g. (44.5%) of polymer having a reduced specific viscosity in chloroform of 0.23 dl./g.

ANAL. Calcd. for $(C_5H_7ClO_2)_n$: C, 44.63%; H, 5.25%; Cl, 26.35%. Found: C, 44.58%; H, 5.45%; Cl, 26.35%.

Copolymerization of Chloromethyl Methacrylate with Methyl Methacrylate

A mixture of 17 g. (0.125 mole) of chloromethyl methacrylate, 12.5 g. (0.125 mole) of methyl methacrylate, 225 ml. of benzene, and 0.082 g. of azobisisobutyronitrile was deaerated with nitrogen gas for 1.5 hr. and was

heated at 70°C. for 5 hr. The solution was cooled to room temperature and was poured into 10 volumes of vigorously stirred methanol. The polymer was dried *in vacuo* without heat for 5 days. There was obtained 10.4 g. of copolymer having a reduced specific viscosity in chloroform of 0.38 dl./g.

ANAL. Calcd. for $(C_5H_{7.44}Cl_{0.56}O_2)_n$: C, 50.29%; H, 6.28%; Cl 16.62%. Found: C, 50.29%; H, 6.08%; Cl, 16.58%.

Determination of Primary Chlorine in Chlorinated Acrylic Polymers by Reaction with Sodium Iodide in Acetone

In a 125-ml. Erlenmeyer flask equipped with a condenser connected to a drying tube containing Drierite were placed an accurately weighed sample (ca. 0.5 g.) of chlorine-containing material, 5 g. of sodium iodide, and 50 ml. of acetone. The mixture was heated at reflux for 72 hr., whereupon it was cooled to room temperature. The precipitated sodium chloride was removed by filtration through paper, was washed with 15 ml. of acetone, was dissolved in 25 ml. of water, and was titrated with silver nitrate by the Volhard method. Blank determinations using unchlorinated poly(methyl methacrylate) were made, and the value form the blank determination was subtracted from the values obtained on the chlorine-containing polymer.

Determination of the Amount of Chloride Ion Liberated by Reaction with Aniline

An accurately weighed sample (ca. 0.2 g.) of the polymer was placed in an ampule. Aniline (4 ml.) was added, and the mixture in the ampule was frozen in a mixture of Dry Ice–acetone. A moderate vacuum (ca. 2 mm.) was drawn on the ampule, and it was sealed. The sealed ampule was placed in an oven maintained at 100°C. for 17 hr. The ampule was cooled to room temperature and was opened. The polymer was precipitated in a solution of 5 ml. of concentrated nitric acid in 45 ml. of water and was filtered and washed with additional nitric acid solution. The combined nitric acid solution was titrated with silver nitrate solution by the Volhard method. The polymer was washed with water and was dried *in vacuo* at 60°C. overnight. Blank determinations were run on unchlorinated poly(methyl methacrylate), and the amount of silver nitrate consumed was subtracted from the value for the chlorinated polymer. The polymer from the blank determinations contained no nitrogen.

The authors wish to express their appreciation to Messrs. Fettes, Fellmann, and Dunkelberger for preparing some of the samples used in this work, to Dr. B. Storey for the macroreticular resins, to Dr. K. McCallum and Mr. F. Jackson for obtaining some of the NMR spectra, to Mr. Findlay for the viscosity determinations, to Mrs. E. Cohn-Ginsberg for the osmotic measurements, and to Mr. C. Nash for the microanalyses.

References

1. Bauer, W., U. S. Pat. 2,021,763 (1935).
2. Hahn, W., and F. Grafmüller, *Makromol. Chem.*, **21**, 121 (1956).
3. Smets, G., and J. Fournaux, *Makromol. Chem.*, **23**, 133 (1957).
4. Ridbo Laboratories, Brit. Pat. 657,811 (1951).
5. Kunin, R., E. Meitzner, and N. Bortnick, *J. Am. Chem. Soc.*, **84**, 305 (1962).
6. Ferris, A. F., and I. G. Marks, *J. Org. Chem.*, **19**, 1971 (1954).
7. Hurd, C. D., and C. H. Rector, Jr., *J. Org. Chem.*, **10**, 441 (1945).
8. Yakubovich, A. Y., V. V. Razumovskiĭ, Z. N. Vostrukhina, and S. M. Rozenshtein, *Zhur. Obsch. Khim.*, **28**, 1930 (1958).
9. Bovey, F. A., and G. V. D. Tiers, *J. Polymer Sci.*, **44**, 173 (1960).
10. Vaughan, M. F., *J. Polymer Sci.*, **33**, 417 (1958).

Résumé

La chloration d'une suspension aqueuse de polyméthacrylate de méthyle, initiée par une lampe incandescente, produit un polymère possédant un seul atome de chlore par unité monomérique. Le mécanisme de la chloration d'une suspension aqueuse est le même que celui de la chloration d'une solution par substitution radicalaire. La vitesse de chloration, à vitesse constante de barbottage du chlore, dépend à la fois du temps, de la concentration en polymère, et de la dimension ou de la porosité des particules de polymère. Les structures du polyméthacrylate de méthyle chloré par suspension ou en solution ont été établies en comparant leur spectre MNR avec ceux du polyméthacrylate de méthyle, du polychlorométhacrylate de méthyle et d'un copolymère d'α-chlorométhacrylate de méthyle avec le méthacrylate de méthyle. En chlorant le polyméthacrylate de méthyle ayant 0.5 atome de chlore par unité monomérique, une moitié du chlore est sur le groupe méthyle de l'ester et l'autre sur l'atome de carbone en position β. Dans l'échantillon, chloré en suspension, contenant un chlore par unité monomérique, 20% du chlore est présent sous forme de groupements —$OCHCl_2$, 40% comme —OCH_2Cl, 30% sous forme de —CHCl— et 10% sous forme de C—CH_2Cl. Dans l'échantillon, chloré en solution, contenant 2 atomes de chlore par unité monomérique, le chlore est distribué de la facon suivante: 40% de OCH_2Cl, 40% de —CHCl— et/ou et C—CH_2Cl et 20% de $OCHCl_2$.

Zusammenfassung

Die Chlorierung von Polymethylmethacrylat in wässriger Suspension unter Bestrahlung mit weissem Licht liefert ein Polymeres mit bis zu einem Chloratom pro Monomereinheit. Der Mechanismus der Chlorierung in wässriger Suspension ist der gleiche wie bei der Chlorierung in Lösung, nämlich eine radikalische Substitution; die Chlorierungsgeschwindigkeit bei konstanter Chlor-Strömungsgeschwindigkeit hängt von der Dauer, der Polymerkonzentration und der Grösse oder Porosität der Polymerteilchen ab. Die Struktur der in Suspension und Lösung chlorierten Polymethylmethacrylate wurde durch Vergleich ihrer NMR-Spektren mit denjenigen von Polymethylmethacrylat, Polychlormethylmethacrylat und einem Copolymeren von Methyl-α-chlormethylacrylat mit Methylmethacrylat festgelegt. In chloriertem Polymethylmethacrylat mit 0,5 Chloratomen pro Monomereinheit befindet sich die Hälfte des Chlors an der Estermethylgruppe und die andere Hälfte am β-Kohlenstoffatom. In der suspensionschlorierten Probe mit einem Chlor pro Monomereinheit sind 20% des Chlors als $OCHCl_2$-Gruppen, 40% als OCH_2Cl-Gruppen, 30% als —CHCl-Gruppen und 10% als C—CH_2Cl-Gruppen vorhanden. In einer lösungs-chlorierten Probe mit zwei Chloratomen pro Monomereinheit ist das Chlor folgendermassen verteilt: 40% als OCH_2Cl, 40% als —CHCl- und C—CH_2Cl und 20% als $OCHCl_2$.

Received May 31, 1962

JOURNAL OF POLYMER SCIENCE: PART A VOL. 1, PP. 2731–2739 (1963)

Further NMR Studies of Polydimethylsiloxanes: Effects of Radiation-Induced Crosslinking

C. M. HUGGINS, L. E. ST. PIERRE, and A. M. BUECHE, *General Electric Research Laboratory, Schenectady, New York*

Synopsis

Previous nuclear magnetic resonance measurements on a polymethylsiloxane gum (MW = 75,000) had been interpreted to indicate the presence of considerable segmental motion in both the amorphous and crystalline components at temperatures above the glass temperature. Further investigation again showed the NMR line to be completely narrowed just above the glass point indicating such motions must extend into the crystalline component. This work was extended by the measurement of NMR absorption line widths for temperatures of 80–300°K. on samples of the same gum subjected to gradually-increased crosslinking by electron doses of 3–600 $\times$ 10^6 rep. Here, no change in the NMR properties of low temperature, rigid states were observed, but the room temperature line width progressively increased from 0.019 gauss to over 0.100 gauss peak-to-peak due to the increase in bulk viscosity of the liquid. The "first-order" activation energy associated with the temperature-dependent line narrowing decreased from 10 to 2 kcal./mole. The NMR data indicate that the primary effects of radiation-induced crosslinking are to reduce the chain rotational energy by the creation of defects and to increase the short-range viscosity by the lowering of translational freedom.

Introduction

The contributions of nuclear magnetic resonance (NMR) studies to the understanding of molecular motion in polymers are firmly established.[1–3] Polydimethylsiloxanes have been the polymers of choice in a number of such investigations. The authors have recently reported[4] the results of a detailed NMR study on a high molecular weight (MW = 75,000) polydimethylsiloxane gum. The findings were in agreement with previously reported work where narrow line widths, indicative of gross translational motion, persisted to surprisingly low temperatures.[5–7] In addition, the data indicated that considerable translational motion persisted in the crystalline phase of these polymers down to temperatures approaching the glass temperature for the amorphous polymer.

The relationship between the physical properties of a polymer specimen and the degree of crosslinking present has been the subject of much work. In the polydimethylsiloxanes the effect of crosslinking on ultimate elongation[8] have been studied in this laboratory. The gross changes related to degree of crosslinking are readily apparent, but its effect on the amount and ease of segmental motion within the polymer has not been established.

This paper describes a study of the changes in proton magnetic resonance spectra as the degree of radiation-induced crosslinking in a polydimethylsiloxane was increased.

Experimental

The NMR equipment, techniques, and materials used were as previously described.[4] The spectrometer was a Varian Associates V-4300B dual-purpose operating at 40 megacycles and 9400 gauss. The polydimethylsiloxane sample had a viscosity of $\eta = 2.95 \times 10^4$ cpoises at 25°C. and a weight-average molecular weight of 7.5×10^4. Prior to irradiation, the liquid sample was degassed by evacuating to 10^{-4} mm. at 100°C. for 24 hr. The samples were then irradiated under nitrogen atmosphere with the 800-k.v.p. General Electric resonant transformer[11] to doses of 3, 6, 25, 60, and 600 Mrep.

The number of crosslinks present in the various samples irradiated up to doses of 60 Mrep has been shown to be 2.5 crosslinks per 100 e.v.,[10] the G value for crosslinking being independent of dose to that point. (A conversion factor of 5.8×10^{19} e.v./g./rep was used in calculating the G value.) At a dose of 600 Mrep this value probably can no longer be applied. The sample irradiated to 600 Mrep can be assumed to be a very highly crosslinked material which has undergone a large amount of dealkylation.

Results and Discussion

Before pursuing the study of the effect of crosslinking on the NMR spectra, it was necessary to reinvestigate the NMR properties of the unirradiated siloxane. In the previous work,[4] the polydimethylsiloxane gum ($\eta = 2.95 \times 10^4$ cpoises) was reported to exhibit an NMR line width of 4.9 gauss (peak-to-peak) at 80°K., which narrowed smoothly and completely to less than 0.019 gauss peak-to-peak at about 140–180°K. Considerable discussion was expended on the apparent absence of a residual wide line in the range 200–240°K., where x-ray studies had shown the sample to be at least 50% crystalline. Conflicting evidence on the NMR properties of polydimethylsiloxanes has come from the work of Powles,[3] who reports both a narrow and a wide line for a polydimethylsiloxane grease at temperatures from the second-order transition at 180°K. up to the melting point, ca. 230°K. The wide line was assigned to a crystalline fraction of 90% by analogy to polyethylene and similar polymers. By comparison, our previous work[4] shows the data for the lighter oil, where the total line narrows abruptly to about 0.019 gauss peak-to-peak at about −100°C. It is in this range of −110 to −40°C. that we expected and searched for a crystalline wide line of 50% relative area. Figure 1 shows a selected series of our spectra run under a large range of instrumental variables designed to optimize the detection of any hidden wide line.

The spectra shown in Figure 1 were recorded by a conventional, phase-sensitive detector using sinusoidal field modulation at 40 cycles/sec. Full details of this detection scheme are covered in most texts on magnetic

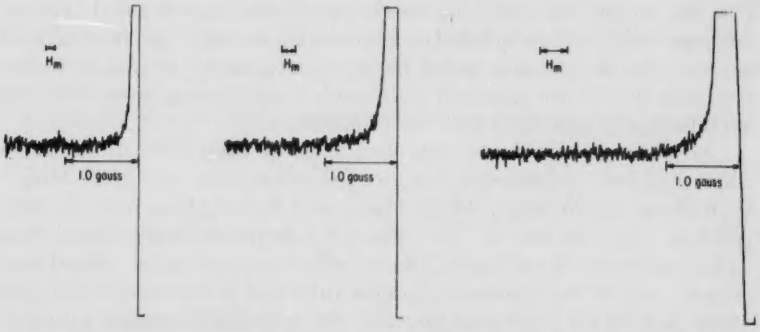

Fig. 1. Observed NMR absorption bands for unirradiated polydimethyl-siloxane ($\eta = 2.95 \times 10^4$ cpoises) at 223°K. Gain and modulation field increased to optimize response to any wide line present.

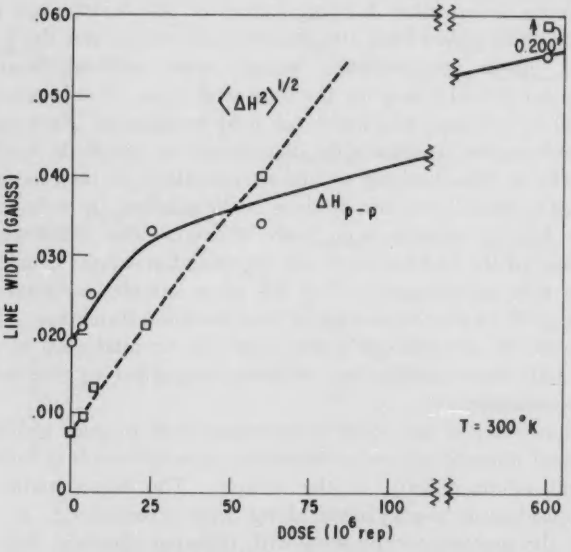

Fig. 2. NMR line widths of irradiated siloxane gum at 300°K.

resonance. Of concern here is the fact that the resulting spectrum closely resembles the derivative of the absorption line. This derivative presentation does tend to increase the relative amplitude of a narrow line if the field-modulation amplitude is small compared to the line width. The maximum sensitivity to a wide line is achieved when the field-modulation amplitude is comparable to the width of the line to be observed. However, once the field-modulation amplitude exceeds the true line width, the observed line width is essentially equal to the modulation amplitude itself.

For this reason, the optimum resolution of two superimposed lines of different widths will be achieved by a modulation amplitude intermediate between the narrow and broad lines. Consequently, it was necessary to obtain the silicone spectrum for a series of modulating fields to ensure not missing any significant wide-line components.

Line-width measurements were then made on samples of this siloxane which had been subjected to electron radiation doses of Ia, (3 Mrep); Ib, 6 Mrep; Ic, 25 Mrep; Id, 60 Mrep; and If, 600 Mrep, over the temperature range 80–300°K. The measured derivative peak-to-peak line widths are recorded on Figure 2, along with the data for the unirradiated sample. All of the irradiated samples exhibited a low-temperature line width (ΔH) of 4.8 gauss peak-to-peak; the unirradiated sample measured 4.9 gauss. This difference is considered to be within the probable experimental error. Upon warming, each underwent a relatively well-defined transition to a narrow line characteristic of the amount of radiation the sample had received.

The room temperature limiting values of line widths are plotted in Figure 2, which shows both the peak-to-peak values and the root second moments. Both measurements include some residual magnetic field inhomogeneity broadening for the narrower lines. It was not considered profitable to attempt to correct for field broadening, since calibrations with water varied considerably, depending on magnetic cycling. The magnitudes of these limiting widths are considered to be a measure of the hindrance to gross interchain motions in the polymer, intrachain rotational motions having already been fully excited. The exact temperature dependence of the line width for the unirradiated sample is masked somewhat by field inhomogeneity, but the other samples are seen to exhibit only negligible further narrowing beyond the main transition. This would be expected if the residual width were due to hindrance of interchain motion and these motions were severely restrained by the radiation-induced crosslinking.

The divergence of the room temperature peak-to-peak widths and the root second moment curves is considered to be the result of increasing the structural inhomogeneity in the sample. The larger radiation doses effect considerable dealkylation along with crosslinking, so that now some of the protons occupy sites with differing chemical and structural environments. The composite absorption curve is, then, a superposition of the resonances of each of the individual environments. It can be easily shown that such a composite absorption band yields peak-to-peak line widths weighted very heavily by the narrower components; the root second moment, on the other hand, closely approximates an arithmetic mean of the various components.

The line widths and second moments, $<\Delta H^2> = 7.0 \pm 0.2$ gauss^2 at -180°C. are observed to be independent of dose. The apparent constancy of the second moment with radiation dose and, consequently, crosslinking is evidence that the structure of the low temperature rigid form of the

polymer is not seriously perturbed by crosslinkkng, that is, the "crystal" or glass structure is not significantly changed by crosslinking up to a ratio of about one crosslink for every five monomer units. This is a natural

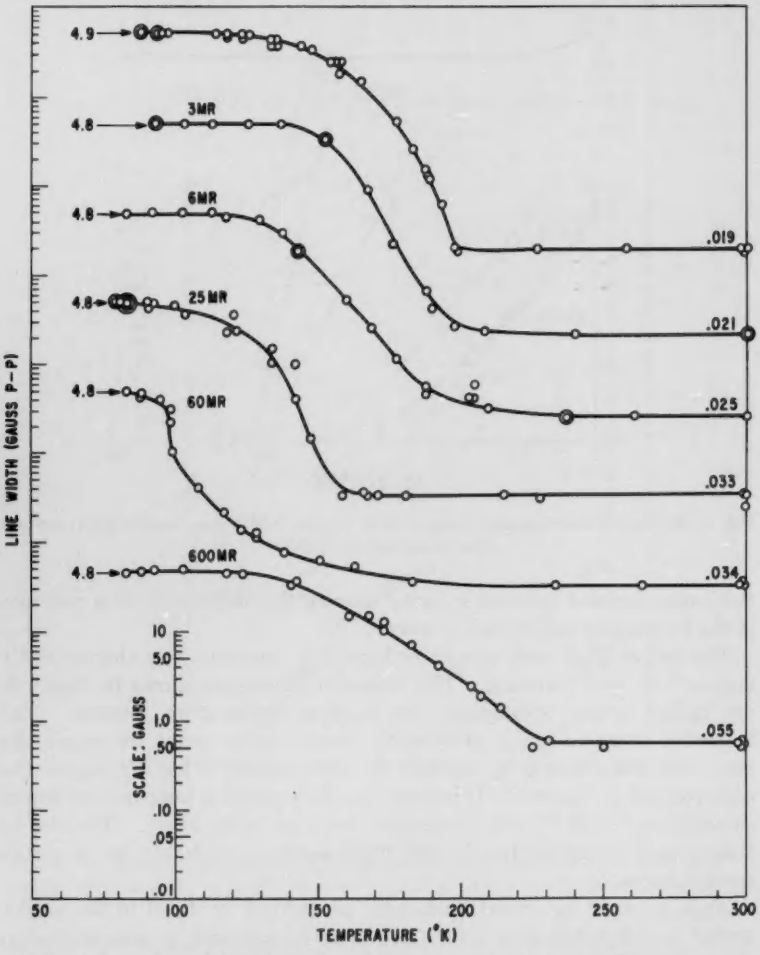

Fig. 3. Temperature dependences of NMR line widths of irradiated siloxane gum. A sliding vertical scale is used; the low and high temperature limits are given for each curve.

consequence of the short-order nature of the NMR perturbations and is similar to the findings of Slichter and Mandell[12] for irradiated polyethylene. Similarly, Mandelkern, Roberts, Halpin, and Price[13] report no change in the x-ray crystal spacings for polyethylene irradiated up to 50 Mrep,

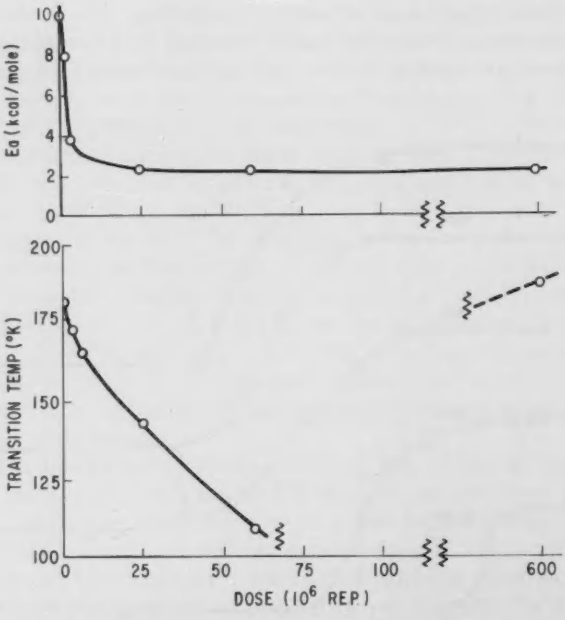

Fig. 4. Activation energies and temperatures of the NMR line narrowing transition for irradiated siloxanes.

but rather a small increase in x-ray line width attributable to a decrease in the average crystallite size or order.

The line width of each sample underwent a transition to a characteristic narrow line upon warming. The transition ranges, as shown in Figure 3, are rather diffuse, extending over a wide temperature interval. The transition temperature is arbitrarily defined as the point for which the line width has changed by one-half the total change in log ΔH to give the data plotted in Figure 4. It is seen that the transition temperature lowers smoothly to -160°C. for irradiation doses up to 60 Mrep. The rise in transition temperature for the 600 Mrep sample is probably due to structural changes.

Application of the usual, first-order procedures, outlined in the earlier work,[4] to the NMR data results in the activation energy plots shown on Figure 5. The data are reasonably fitted by a family of straight lines; the corresponding activation energies are also shown on Figure 4. There appears to be a rather smooth change in activation energy with increasing radiation dose and crosslinking. This decrease is a quantitative statement of the qualitative observation that the transition becomes more diffuse with increasing crosslinking.

Two features of the above data are both consistent with the narrowing mechanism proposed earlier:[4] the decreasing activation energy and the

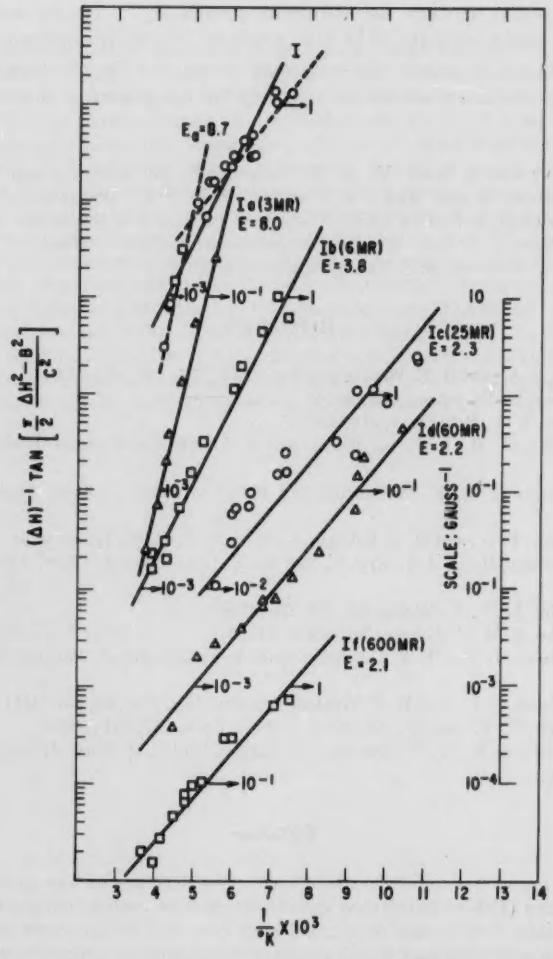

Fig. 5. Temperature dependences of NMR correlation times for irradiated siloxanes. A sliding vertical scale is used; relative vertical positions are indicated on each line.

increasing room temperature line width. It is suggested that in the uncrosslinked material, a high degree of cooperativeness is necessary to effect the rotational transition; hence, the large activation energy. As the number of crosslinks (defects) is increased, the resulting loss in long-range order lowers the degree of cooperativeness necessary for rotational freedom—hence, a general decrease in activation energy. However, in the high temperature limit, it is not expected that such small amounts of crosslinking would influence short-range rotational motion. The observed increase in line width must then be due to the hindrance

to translational motion as discussed previously.[4] In summary then, the NMR data indicate that the primary effects of radiation-induced crosslinking are to reduce the rotational energy by the creation of defects and to increase the short-range viscosity by the lowering of translational freedom.

The authors wish to thank Mr. D. R. Carpenter for performing a large part of the NMR measurements and Miss Ann Warner for help in the associated computations. They are also indebted to Dr. A. C. Martellock for supplying the sample and to Drs. A. A. Miller and E. J. Lawton for performing the irradiations. The many discussions with Drs. F. P. Price and B. H. Zimm are appreciated.

References

1. Sauer, J. A., and A. E. Woodward, *Rev. Mod. Phys.*, **32**, 88 (1960).
2. Slichter, W. P., *Advan. Polymer Sci.*, **1**, 35 (1958).
3. Powles, J. G., *Polymer*, **1**, 219 (1960).
4. Huggins, C. M., L. E. St. Pierre, and A. M. Bueche, *J. Phys. Chem.*, **64**, 1304, (1960).
5. Honnold, V. R., F. McCaffrey, and B. A. Mrowca, *J. Appl. Phys.*, **25**, 1219 (1954).
6. Rochow, E. G., and H. G. LeClair, *J. Inorg. Nucl. Chem.*, **1**, 92 (1955).
7. Kusomoto, H., I. J. Lawrence, and H. S. Gutowsky, *J. Chem. Phys.*, **32**, 724 (1960).
8. Bueche, A. M., *J. Polymer Sci.*, **19**, 275 (1956).
9. Bueche, A. M., *J. Polymer Sci.*, **15**, 97 (1955).
10. St. Pierre, L. E., H. A. Dewhurst, and A. M. Bueche, *J. Polymer Sci.*, **36**, 105 (1959).
11. Charleton, E. E., and W. F. Westendorp, *Gen. Elec. Rev.*, **44**, 652 (9411).
12. Slichter, W. P., and E. R. Mandell, *J. Phys. Chem.*, **62**, 334 (1958).
13. Mandelkern, L., D. E. Roberts, J. C. Halpin, and F. P. Price, *J. Am. Chem. Soc.*, **82**, 46 (1960).

Résumé

Des mesures antérieures de résonance magnétique nucléaire sur une gamme de polyméthylsiloxane (PM = 75.000) avaient été interprêtées comme indiquant l'existence de considérables mouvements de segment aussi bien dans le composant amorphe que dans le composant cristallin à des températures supérieures à la température de vitrification. Des recherches ultérieures ont montré que la ligne NMR était complètement amincie au-dessus du point de vitrification indiquant donc que de tels déplacements doivent s'étendre au composant cristallin. Ce travail a été complèté par des mesures de largeurs des lignes d'absorption NMR à des températures de 80 à 300°K sur des échantillons de la même gomme dont le taux de pontage est augmenté progressivement sous l'effet des doses d'électrons de 3–600 $\times$ 10^6 rep. Il n'y a aucun changement dans les propriétés NMR aux basses températures; des états rigides ont été observés mais la largeur de la ligne à température de chambre augmente progressivement de 0.019 gauss jusqu'à plus de 0.100 gauss à cause de l'augmentation de la viscosité du liquide. L'énergie d'activation de "premier ordre" décroît de 10 à 2 kcal/mole associée au retrécissement de la ligne dépendant de la température. Les données NMR indiquent que les effets primaires du pontage induit par irradiation consistent à réduire l'énergie rotationnelle de la chaîne par la création de défauts, et d'augmenter la viscosité à courte distance en diminuant la liberté de translation.

Zusammenfassung

Frühere kernmagnetische Resonanzmessungen an einem Polymethylsiloxangummi (MW = 75000) wurden als Anzeichen für eine starke Segmentbewegung sowohl im amorphen als auch im kristallinen Anteil bei Temperaturen oberhalb der Glastemperatur gedeutet. Weitere Untersuchungen zeigten wieder, dass die NMR-Linie unmittelbar über dem Glaspunkt vollständig verengt wird, was beweist, dass sich solche Bewegungen in den kristallinen Anteil hinein erstrecken müssen. Die Untersuchung wurde auf die Messung der NMR-Absorptionslinienbreite bei Temperaturen von 80–300°K an Proben des gleichen Gummis bei schrittweise erhöhter Vernetzung durch Elektronendosen von 3–6000 $\times$ 10^6 rep ausgedehnt. Hier wurde keine Anderung der NMR-Eigenschaften der starren Tieftemperatursysteme beobachtet, die Linienbreite bei Raumtemperatur nahm hingegen wegen des Anstiegs der Viskosität der Flüssigkeit stetig von 0,019 Gauss auf über 0,100 Gauss p–p zu. Die Aktivierungsenergie "erster Ordnung" für die temperaturabhängige Linienverengung nahm von 10 auf 2 kcal/Mol ab. Die NMR-Daten zeigen, dass die Primäreffekte der strahlungs-induzierten Vernetzung in einer Herabsetzung der Kettenrotationsenergie durch Defektbildung und in einer Erhöhung der Viskosität in kleinen Bereichen durch Erniedrigung der Translationsmöglichkeit besteht.

Received September 12, 1962

to translational motion as discussed previously.[4] In summary then, the NMR data indicate that the primary effects of radiation-induced crosslinking are to reduce the rotational energy by the creation of defects and to increase the short-range viscosity by the lowering of translational freedom.

The authors wish to thank Mr. D. R. Carpenter for performing a large part of the NMR measurements and Miss Ann Warner for help in the associated computations. They are also indebted to Dr. A. C. Martellock for supplying the sample and to Drs. A. A. Miller and E. J. Lawton for performing the irradiations. The many discussions with Drs. F. P. Price and B. H. Zimm are appreciated.

References

1. Sauer, J. A., and A. E. Woodward, *Rev. Mod. Phys.*, **32**, 88 (1960).
2. Slichter, W. P., *Advan. Polymer Sci.*, **1**, 35 (1958).
3. Powles, J. G., *Polymer*, **1**, 219 (1960).
4. Huggins, C. M., L. E. St. Pierre, and A. M. Bueche, *J. Phys. Chem.*, **64**, 1304, (1960).
5. Honnold, V. R., F. McCaffrey, and B. A. Mrowca, *J. Appl. Phys.*, **25**, 1219 (1954).
6. Rochow, E. G., and H. G. LeClair, *J. Inorg. Nucl. Chem.*, **1**, 92 (1955).
7. Kusomoto, H., I. J. Lawrence, and H. S. Gutowsky, *J. Chem. Phys.*, **32**, 724 (1960).
8. Bueche, A. M., *J. Polymer Sci.*, **19**, 275 (1956).
9. Bueche, A. M., *J. Polymer Sci.*, **15**, 97 (1955).
10. St. Pierre, L. E., H. A. Dewhurst, and A. M. Bueche, *J. Polymer Sci.*, **36**, 105 (1959).
11. Charleton, E. E., and W. F. Westendorp, *Gen. Elec. Rev.*, **44**, 652 (9411).
12. Slichter, W. P., and E. R. Mandell, *J. Phys. Chem.*, **62**, 334 (1958).
13. Mandelkern, L., D. E. Roberts, J. C. Halpin, and F. P. Price, *J. Am. Chem. Soc.*, **82**, 46 (1960).

Résumé

Des mesures antérieures de résonance magnétique nucléaire sur une gamme de polyméthylsiloxane (PM = 75.000) avaient été interprêtées comme indiquant l'existence de considérables mouvements de segment aussi bien dans le composant amorphe que dans le composant cristallin à des températures supérieures à la température de vitrification. Des recherches ultérieures ont montré que la ligne NMR était complètement amincie au-dessus du point de vitrification indiquant donc que de tels déplacements doivent s'étendre au composant cristallin. Ce travail a été complèté par des mesures de largeurs des lignes d'absorption NMR à des températures de 80 à 300°K sur des échantillons de la même gomme dont le taux de pontage est augmenté progressivement sous l'effet des doses d'électrons de 3–600 $\times$ 10^6 rep. Il n'y a aucun changement dans les propriétés NMR aux basses températures; des états rigides ont été observés mais la largeur de la ligne à température de chambre augmente progressivement de 0.019 gauss jusqu'à plus de 0.100 gauss à cause de l'augmentation de la viscosité du liquide. L'énergie d'activation de "premier ordre" décroît de 10 à 2 kcal/mole associée au retrécissement de la ligne dépendant de la température. Les données NMR indiquent que les effets primaires du pontage induit par irradiation consistent à réduire l'énergie rotationnelle de la chaîne par la création de défauts, et d'augmenter la viscosité à courte distance en diminuant la liberté de translation.

Zusammenfassung

Frühere kernmagnetische Resonanzmessungen an einem Polymethylsiloxangummi (MW = 75000) wurden als Anzeichen für eine starke Segmentbewegung sowohl im amorphen als auch im kristallinen Anteil bei Temperaturen oberhalb der Glastemperatur gedeutet. Weitere Untersuchungen zeigten wieder, dass die NMR-Linie unmittelbar über dem Glaspunkt vollständig verengt wird, was beweist, dass sich solche Bewegungen in den kristallinen Anteil hinein erstrecken müssen. Die Untersuchung wurde auf die Messung der NMR-Absorptionslinienbreite bei Temperaturen von 80–300°K an Proben des gleichen Gummis bei schrittweise erhöhter Vernetzung durch Elektronendosen von 3–6000 $\times$ 10^6 rep ausgedehnt. Hier wurde keine Änderung der NMR-Eigenschaften der starren Tieftemperatursysteme beobachtet, die Linienbreite bei Raumtemperatur nahm hingegen wegen des Anstiegs der Viskosität der Flüssigkeit stetig von 0,019 Gauss auf über 0,100 Gauss p–p zu. Die Aktivierungsenergie "erster Ordnung" für die temperaturabhängige Linienverengung nahm von 10 auf 2 kcal/Mol ab. Die NMR-Daten zeigen, dass die Primäreffekte der strahlungs-induzierten Vernetzung in einer Herabsetzung der Kettenrotationsenergie durch Defektbildung und in einer Erhöhung der Viskosität in kleinen Bereichen durch Erniedrigung der Translationsmöglichkeit besteht.

Received September 12, 1962

JOURNAL OF POLYMER SCIENCE: PART A VOL. I, PP. 2741–2752 (1963)

Ultraviolet Irradiation of Plastics. IV. Further Studies of Environmental Effects on Films and Fibers*

C. V. STEPHENSON† AND W. S. WILCOX,‡ *Southern Research Institute, Birmingham, Alabama*

Synopsis

Polyethylene, nylon, Mylar, Teflon, and Dacron all deteriorated more rapidly during ultraviolet irradiation when irradiated in oxygen than when irradiated in nitrogen. Deterioration during vacuum irradiation is less rapid than it is during oxygen or nitrogen irradiations for all of these polymers except Teflon, in which case it is more rapid. Environmental effects were not evident during the irradiation of HT-1. A scission-to-crosslinking ratio of 0.93 has been determined for ultraviolet-irradiated polyethylene.

INTRODUCTION

The results of studies of the deteriorating effect of ultraviolet light on polyethylene, nylon, Mylar, Acrilan, and Teflon irradiated *in vacuo* and in nitrogen have been presented in three previous articles.[1–3] It was shown in those articles that films of polyethylene, nylon, and Mylar and fibers of Acrilan deteriorate more rapidly when irradiated in nitrogen than when irradiated *in vacuo*. This conclusion was based on a more rapid deterioration of tensile properties and on a higher scission-to-crosslinking ratio during nitrogen irradiation. Teflon film, however, was found to deteriorate more rapidly when irradiated *in vacuo* than when irradiated in nitrogen. The rates of deterioration of all five polymers were found to vary directly with the energy of the ultraviolet photon, and evidence was found that the principal mechanism of the deterioration of at least three of these polymers was the photolytic scission (direct or indirect) of the carbon–carbon single bond.

Additional work on the photolytic degradation of polymeric materials has extended the previous studies to include a determination of the effects of an oxygen atmosphere and various conditions of vacuum on the rates of deterioration of the materials previously studied. A comparison has also been made of deterioration rates in films and fibers of the same material.

* This work was supported by the Directorate of Materials and Processes, Aeronautical Systems Division, Wright-Patterson Air Force Base, Ohio, under Contract AF 33(616)-7701.

† Present address: Vanderbilt University, Nashville, Tennessee.

‡ Present address: Birmingham-Southern College, Birmingham, Alabama.

The effect of ultraviolet light on an experimental fiber, HT-1, has also been determined. These results as well as the results of some other studies which were made to clarify unexplained observations reported in the previous articles will be presented in this paper.

EXPERIMENTAL APPARATUS AND PROCEDURES

Most of the experimental procedures and techniques have already been described[1-3] and need not be repeated in detail here. As before, irradiation units have used either G30T8 germicidal lamps or the high intensity A-H6 lamps. The G30T8 lamp is a low pressure mercury arc that emits more than 90% of its radiant intensity at 253.7 mμ. It has been used as a monochromatic source. The A-H6 is a high pressure mercury arc that emits a broad continuum that extends below 220 mμ. Bands of ultraviolet have been selected from this continuum by using either interference filters or a grating monochromator.

One significant change in experimental conditions has been to extend the vacuum range during irradiation down to about 10^{-6} mm. This vacuum has been achieved with a Varian Vac Ion pump.

During the tensile testing of the fibers it became obvious that the fibers were not uniform in size. The denier of the fibers was determined by weighing a few hundred to a few thousand meters of fiber length. However, it was found that there was considerable variation of the denier along the length of one fiber and from one fiber to the next. Consequently, control samples were taken from the same fiber from which samples were taken for irradiation and immediately adjacent to the samples taken for irradiation. The tensile properties of the irradiated samples were then determined as a fraction of the physical properties of the controls. The numerical values of the tensile properties given in this report are the product of this fractional factor and the value of the tensile properties found by taking the average of a large number of unirradiated samples.

RESULTS

Polyethylene

Tensile Properties. Polyethylene film has been irradiated in vacua of 5×10^{-2} and 1×10^{-6} mm. and in oxygen. The rate of degradation during both conditions of vacuum was essentially the same as was reported previously[1] at 5×10^{-3} mm. However, polyethylene film irradiated in oxygen deteriorates much more rapidly. For comparison, the variations of the tensile strength and ultimate elongation of polyethylene film irradiated in oxygen, in nitrogen, and in a vacuum of 5×10^{-3} mm. are given in Figure 1.

Polyethylene in the form of 169 den. fibers has also been irradiated in nitrogen with bands of ultraviolet light centered at 369 mμ and 244 mμ. It is difficult to directly compare the changes in tensile properties of films

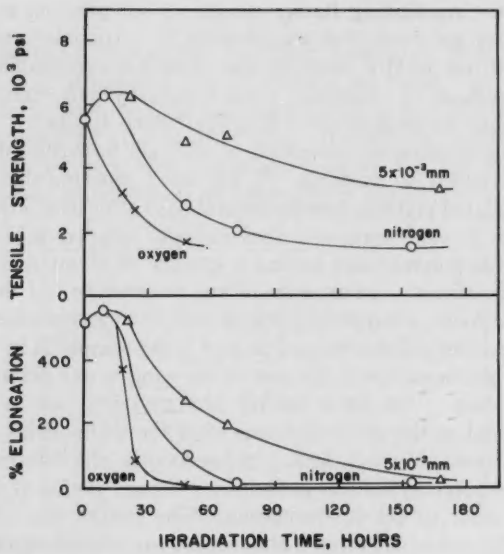

Fig. 1. Variation of the tensile strength and ultimate elongation of polyethylene film irradiated in oxygen, nitrogen, and a vacuum of 5×10^{-3} mm. with ultraviolet light from the G30T8 lamps.

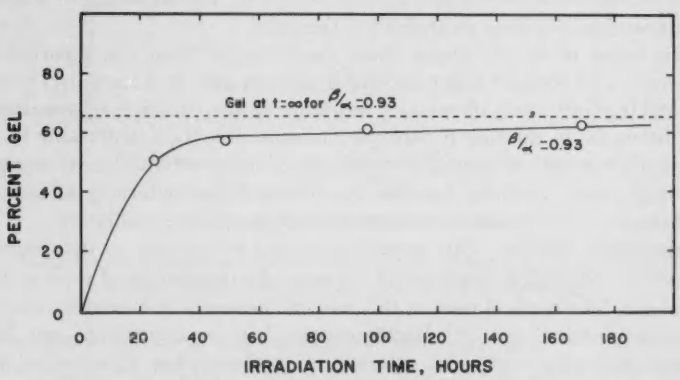

Fig. 2. Gel formation in polyethylene film irradiated in a vacuum of 5×10^{-3} mm. after a five-day delay between irradiation and gel determination.

and fibers since fibers are more highly oriented than films. This higher degree of orientation gives the fiber a tensile strength that is an order of magnitude greater than the film and an elongation that is an order of magnitude lower. However, it was found that the polyethylene fibers decay at essentially the same rate as polyethylene film irradiated under the same conditions.

Scission-to-Crosslinking Ratio. In one of our previous articles[2] it was reported that gel formation experiments in ultraviolet-irradiated polyethylene did not yield a value of the scission-to-crosslinking ratio, β/α, after the methods of Charlesby,[4] and Charlesby and Pinner.[5] Electron spin resonance investigations[6-9] of polyethylene irradiated with ionizing radiations have given an indication of why gel formation data have not previously yielded to analysis. It has been reported that free radicals exist in irradiated polyethylene for several days after irradiation. Lawton, Balwit, and Powell[6] suggested that radicals trapped in the crystalline portion of the polymer and having a lifetime of about five days are the crosslinking radicals. An experiment was designed to test this conclusion. In this experiment, a sample of 1-mil polyethylene was irradiated for 24 hr., and gel formation was determined on part of the sample 24 hr. after irradiation, while gel formation in the rest of the sample was determined 5 days after irradiation. The latter sample produced 58% gel as compared to 40% gel found in the determinations after the 24-hr. delay. No further gelation occurred after five days. Subsequently, the determination of gel formation in polyethylene has included an "aging" period of five days after irradiation prior to gel determination. The results thus obtained have yielded a very consistent value of the scission-to-crosslinking ratio.

Gel formation data for polyethylene irradiated in a vacuum of 5×10^{-2} mm. are plotted in Figure 2. An analysis of the data gives a value $\beta/\alpha = 0.93$. The solid curve shown in Figure 2 is the theoretical gel formation curve for this value of β/α and a value of 0.61 hr. for the incipient gelation time, also obtained from an analysis of the data.

This value of β/α is about three times larger than was reported by Charlesby and Pinner[5] using ionizing radiation and by Charlesby, Grace, and Pilkington[10] using ultraviolet radiation in the presence of sensitizers. The difference in the case of ionizing radiation may be attributable to the nature of the reactions caused by radiations of such vastly different energies. One might also conclude that the use of sensitizers materially affects the mechanisms which produce crosslinks during ultraviolet irradiation.

Orientation Studies. An investigation has been made to determine if ultraviolet irradiation appreciably changes the orientation of a polyethylene fiber. The method used in this part of the study is that described by Andrews[11] and Gurnee.[12] Highly oriented polymeric fibers are birefringent and will produce an interference pattern when illuminated with polarized light incident at right angles to the axis of the fiber. The degree of orientation of a fiber can be related to its birefringence. The birefringence of polyethylene fibers has been examined with a polarizing microscope, the 453.8 mμ line of mercury, isolated with an interference filter, being used as the monochromatic light source. The interference pattern was examined after irradiation with 3000 joules/cm.^{2} of ultraviolet light and was found to be identical to the pattern of the unirradiated sample. There was thus no detectable change in the orientation of the fiber.

Nylon

Tensile Properties. Nylon film has been irradiated with ultraviolet light from the G30T8 lamps in vacua of 5×10^{-2} and 1×10^{-6} mm. The rate of deterioration was the same in both cases and was the same as was previously reported at 5×10^{-3} mm. In addition, nylon fiber has been irradiated in nitrogen with ultraviolet light at 244, 314, and 369 mμ. The results of those measurements are presented in Figure 3.

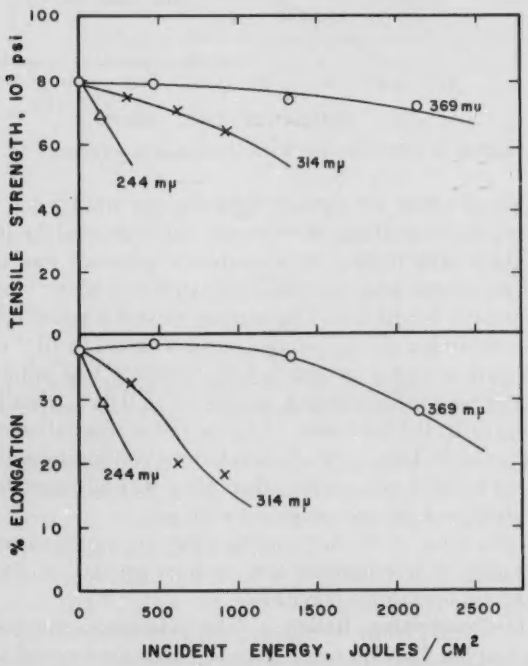

Fig. 3. Variation of the tensile strength and ultimate elongation of nylon fibers irradiated in nitrogen with ultraviolet light at 244, 314, and 369 mμ.

Comparative Effects of Oxygen and Nitrogen. It has been shown fairly conclusively that the hydrogen-containing polymers deteriorate more rapidly when irradiated in oxygen than they do when irradiated in a vacuum. It has also been shown that they deteriorate more rapidly when irradiated in nitrogen than they do when irradiated in a vacuum, but not as fast as when irradiated in oxygen. The question arises as to whether the small amounts of oxygen in the nitrogen can be the cause of the effect previously attributed to pressure.[3] One experiment was described in a previous paper[2] that indicated that the effect attributed to pressure could not have been entirely caused by trace amounts of oxygen. To further test this conclusion, the following experiment has been run. Three dif-

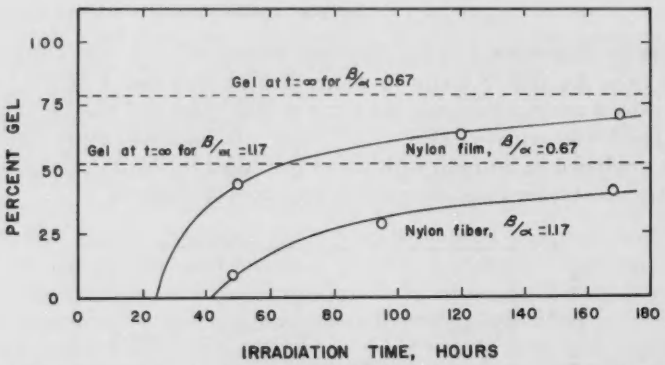

Fig. 4. Gel formation in nylon film and fibers irradiated in a vacuum of 5×10^{-2} mm.

ferent samples of nylon were given the following irradiation treatments. (*1*) A sample tube containing one sample was evacuated to 10^{-3} mm. or less, after which pure oxygen at atmospheric pressure was admitted to the tube. The sample tube was then evacuated to 2×10^{-1} mm., and the film was irradiated for 12 hr. This sample yielded a gel of 6.5%. (*2*) A sample tube containing another sample was evacuated to 10^{-3} mm. or less, after which tank nitrogen at atmospheric pressure was admitted to the tube. The oxygen in this nitrogen was less than 0.01%, that is, less than the total oxygen in the first test. After a 12-hr. irradiation, this sample yielded a gel of only 1.8%. (*3*) A sample tube containing a third sample was evacuated to 10^{-3} mm. or less, then filled with nitrogen to 10^{-1} mm. A 12-hr. irradiation of this sample gave 14.5% gel.

These results tend to further confirm that both oxygen and pressure cause higher rates of deterioration in ultraviolet irradiation of thin films or fibers of hydrogen-containing polymers.

Scission-to-Crosslinking Ratios. The scission-to-crosslinking ratio, β/α, for both nylon film and nylon fiber has been determined for a variety of irradiation conditions. The data for the film irradiated at 5×10^{-2} and 1×10^{-6} mm. give $\beta/\alpha = 0.60$, the same as was previously reported at 5×10^{-3} mm. Nylon fiber irradiated at 5×10^{-2} mm. has a considerably higher ratio, $\beta/\alpha = 1.17$. The experimental data for film and fiber are presented in Figure 4. Again, the solid lines are theoretical curves.

Mylar and Dacron

Tensile Properties. Mylar film was irradiated in oxygen at atmospheric pressure and in vacua of 5×10^{-2} and 1×10^{-6} mm. Hg with the G30T8 lamps. Fibers of Dacron have also been irradiated at 5×10^{-2} mm. Hg. The tensile properties of the irradiated film are plotted in Figure 5. It is seen that the variation of the tensile properties is essentially the same at 5×10^{-2} mm. as at $1 + 10^{-6}$ mm. Irradiation in oxygen causes a more rapid deterioration. The Dacron fibers seem to withstand ultraviolet

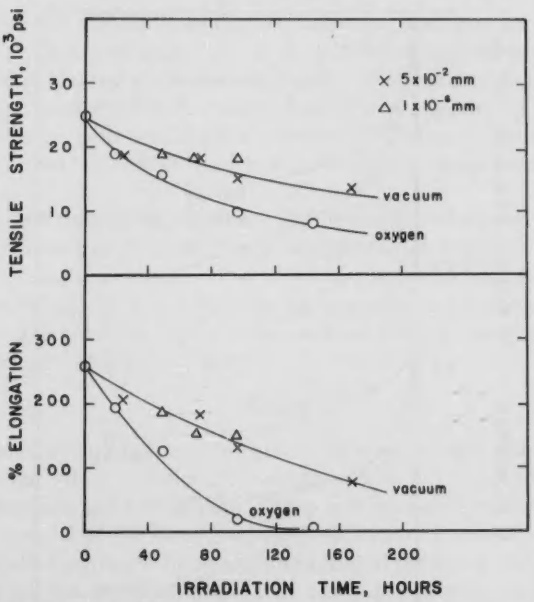

Fig. 5. Variation of the tensile strength and ultimate elongation of Mylar irradiated in oxygen and *in vacuo* with ultraviolet light from the G30T8 lamps.

irradiation somewhat better than Mylar film under the same irradiation conditions. For instance, after 168 hr. of irradiation at 5×10^{-2} mm. the tensile strength of Dacron fibers falls about 29% while the tensile strength of Mylar film falls about 45%.

Dacron fibers, 4.4 den., have been irradiated with ultraviolet light in the three wavelength bands at 244, 314, and 369 mμ. The results of tensile tests of the irradiated samples are given in Figure 6. These data show a wavelength dependence that is different from that found for most polymers in that there seems to be less deterioration of Dacron caused by the 244 mμ ultraviolet light than is caused by 314 mμ ultraviolet; although there is less deterioration in Dacron caused by 369 mμ ultraviolet than for either of the other two wavelengths. This wavelength dependence of Dacron is somewhat unusual, in that a similar dependence was not noted for Mylar film; however, the observed difference probably has a ready explanation.

There is a sharp increase in ultraviolet absorption by Mylar at about 310 mμ in going from longer to shorter wavelengths. Thus it might be expected that Mylar would furnish its own protection in the short wavelength regions and that the deterioration caused by 244 mμ ultraviolet would be less than that at 314 mμ. The fact that this was not observed in Mylar is probably attributable to the thinness of the film tested (only 0.25 mil). The Dacron fibers, however, have a diameter a little greater than

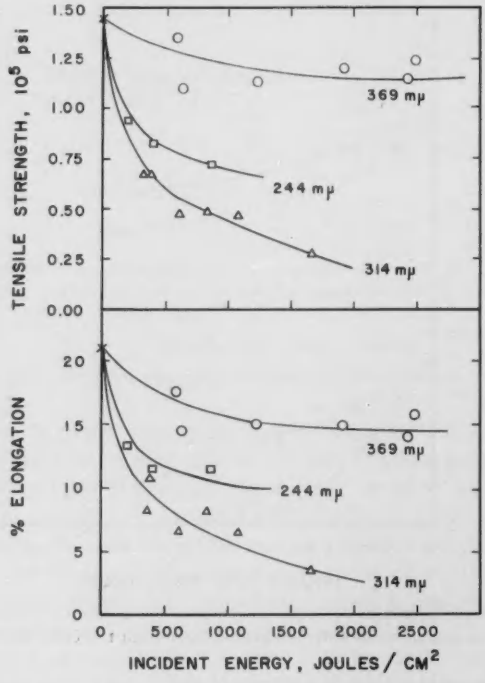

Fig. 6. Variation of the tensile strength and ultimate elongation of Dacron fiber irradiated in nitrogen with ultraviolet at 244, 314, and 369 mμ.

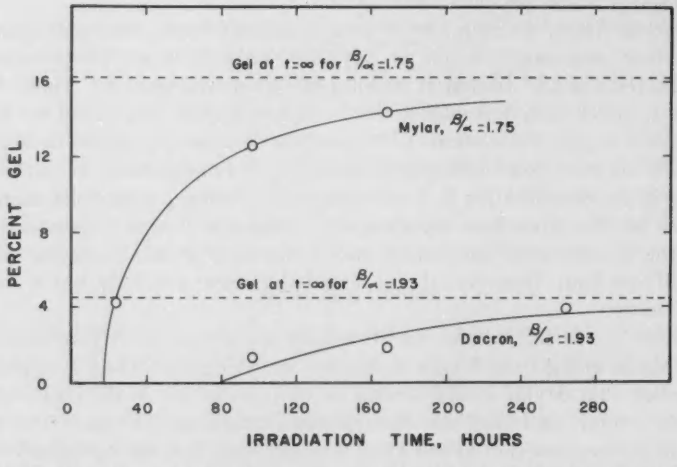

Fig. 7. Gel formation in Mylar film and Dacron fiber irradiated with ultraviolet light in a vacuum of 5×10^{-2} mm.

1.0 mil, and the surface shielding at short wavelengths should be more noticeable. Thus, one might expect the smaller rate of deterioration that was noticed in Dacron at short wavelengths. Surface shielding would also explain the observation that Dacron deteriorated less rapidly than Mylar when they were both irradiated with the G30T8 lamps, since the ultraviolet light from the G30T8 lamp is almost all short wavelength radiation (254.7 mμ).

Scission-to-Crosslinking Ratios. Gel formation data of Mylar and Dacron irradiated at 5×10^{-2} mm. are plotted in Figure 7. The solid curves are theoretical curves. Gel formation in Mylar yielded a scission-to-crosslinking ratio $\beta/\alpha = 1.75$ while gel formation in Dacron gives $\beta/\alpha = 1.93$. The β/α value for Mylar is the same as was previously reported for Mylar irradiated at 5×10^{-3} mm.

Teflon

Teflon was previously found to deteriorate more rapidly when irradiated *in vacuo* than when irradiated in nitrogen. In a further study of the effects of pressure and atmosphere, Teflon film has been irradiated in vacua of 5×10^{-2} and 1×10^{-6} mm., and in atmospheres of oxygen and nitrogen with the G30T8 lamps. The tensile properties of the film irradiated in both conditions of vacuum deterioration at the same rate as was previously reported for Teflon irradiated at 5×10^{-3} mm. Deterioration in oxygen was found to be greater than in nitrogen but less than *in vacuo*. The

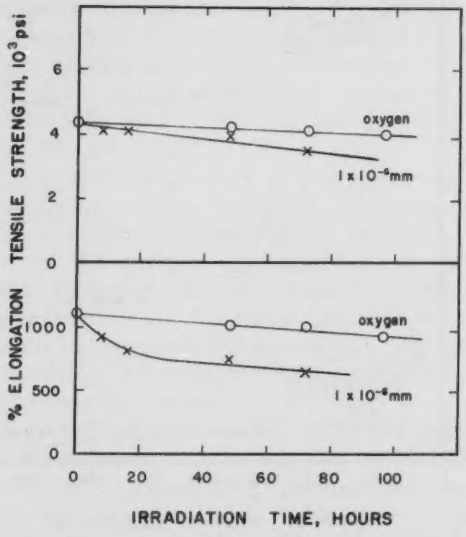

Fig. 8. Variation of the tensile strength and ultimate elongation of Teflon film irradiated in oxygen and in a vacuum of 1×10^{-6} mm. with ultraviolet light from the G30T8 lamps.

changes in tensile properties for Teflon film irradiated at 1×10^{-6} mm. and in oxygen are shown in Figure 8.

Teflon fibers have been irradiated *in vacuo*, and in oxygen and nitrogen. The fibers deteriorated at essentially the same rate as the film irradiated under the same conditions. The fibers show the same environmental effect in that they deteriorate more rapidly when irradiated *in vacuo* than when irradiated in either nitrogen or oxygen, but deteriorate more rapidly in oxygen than in nitrogen.

HT-1, Experimental Fiber

HT-1 is an experimental fiber noted for its stability at high temperatures. Very little is known about the composition of this polymer except that it is described by the manufacturer, du Pont, as an aromatic polyamide. It has no known solvents that do not cause degradation.

The tensile properties of this material have been determined after various irradiations with 244, 314, 340, and 369 mμ ultraviolet light and with visible light at 437 mμ in an atmosphere of nitrogen. The data for the tensile strength and elongation are plotted in Figure 9. HT-1 deteriorates more rapidly when irradiated with 244 mμ ultraviolet than when irradiated at 314 mμ; however, it deteriorates more rapidly when irradiated with 369

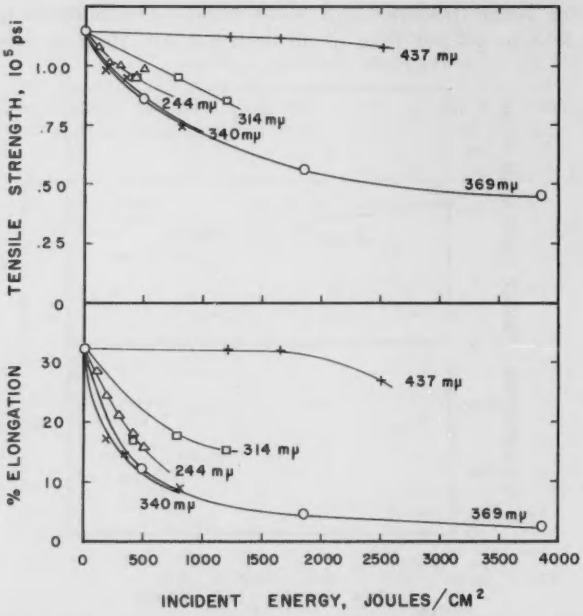

Fig. 9. Variation in the tensile strength and ultimate elongation of HT-1 irradiated in nitrogen with ultraviolet light at 244, 314, 340, and 369 mμ and with visible light at 437 mμ.

mμ ultraviolet light than it does at either of the other wavelengths. Because of this unusual wavelength dependence, the irradiations at 340 and 437 mμ were made to further confirm and to clarify the effect. It is seen that the deterioration caused by 340 mμ ultraviolet light is essentially the same as that caused by 369 mμ ultraviolet light. The visible light is virtually ineffective, although some deterioration is seen at long irradiation times. The explanation for the high deterioration at 369 mμ is not known at present. The energy absorption characteristics of the polymer fibers as a function of wavelength have not been determined, but one would suspect a Mylarlike absorption curtain somewhere between 315 and 340 mμ. Such an absorption could be due to the aromatic rings that the polymer is said to contain or possible due to an intentionally added protective agent.

HT-1 has been irradiated *in vacuo* and in oxygen as well as in nitrogen with the G30T8 lamps. These environmental conditions have little if any effect on the rate of deterioration of this polymer.

DISCUSSION AND CONCLUSIONS

In the previous articles in this series it was shown that polyethylene, nylon, Acrilan, and Mylar deteriorate more rapidly when irradiated with ultraviolet light in nitrogen than when irradiated *in vacuo*. This result is further substantiated by the work reported here. The hypothesis that was proposed to explain the greater stability of the hydrogen-containing polymers during vacuum irradiation (a hypothesis based on the mobility of hydrogen radicals in the polymer and the effect of pressure on the ability of these radicals to escape from the polymer) is still thought to be a reasonable explanation of the crosslinking and chain-scission mechanisms which lead to the observed results. The reverse effect of vacuum on the rate of deterioration of ultraviolet-irradiated Teflon has also been further substantiated, but is still unexplained.

The higher rate of deterioration of all of these polymers when irradiated in oxygen as compared to nitrogen irradiation is expected on the basis of results of other investigators using ionizing radiation. There is no reason to think that the effect of oxygen during ultraviolet irradiation needs a different explanation than that proposed to explain the same observation during irradiation with ionizing radiations.

Fibers deteriorate at essentially the same rate as films under the same experimental conditions. The orientation of a polyethylene fiber seems to be unaffected by ultraviolet irradiation.

The results of gel formation studies in polyethylene tend to verify the suggestions of Lawton, Balwit, and Powell[6] that crosslinking radicals are trapped in the crystalline portion of the polymer and remain there for several days. However, the scission-to-crosslinking ratio for ultraviolet-irradiated polyethylene is about three times higher than has been previously reported for polyethylene irradiated with ionizing radiation and for polyethylene irradiated with ultraviolet light in the presence of sensitizers.

This would indicate that different crosslinking or chain-scission mechanisms may be predominant under the different irradiation conditions.

References

1. Stephenson, C. V., B. C. Moses, and W. S. Wilcox, *J. Polymer Sci.*, **55,** 451 (1961).
2. Stephenson, C. V., B. C. Moses, R. E. Burks, Jr., W. C. Coburn, Jr., and W. S. Wilcox, *J. Polymer Sci.*, **55,** 465 (1961).
3. Stephenson, C. V., J. C. Lacey, Jr., and W. S. Wilcox, *J. Polymer Sci.*, **55,** 477 (1961).
4. Charlesby, A., *J. Polymer Sci.*, **11,** 513 (1953).
5. Charlesby, A., and S. H. Pinner, *Proc. Roy. Soc.* (*London*), **249A,** 367 (1959).
6. Lawton, E. J., J. S. Balwit, and R. S. Powell, *J. Chem. Phys.*, **33,** 395, 405 (1960).
7. Loy, B. R., *J. Polymer Sci.*, **44,** 341 (1960).
8. Charlesby, A., D. Libby, and M. G. Ormerod, *Proc. Roy. Soc.* (*London*), **262A,** 207 (1961).
9. Ohnishi, S., *Bull. Chem. Soc. Japan*, **35,** 254 (1962).
10. Charlesby, A., C. S. Grace, and F. B. Pilkington, *Proc. Roy. Soc.* (*London*), **268A,** 205 (1962).
11. Andrews, R. D., *J. Appl. Phys.*, **25,** 1223 (1954).
12. Gurnee, E. F., *J. Appl. Phys.*, **25,** 1232 (1954).

Résumé

Au cours de l'irradiation U.V. les polyéthylène, nylon, mylar, teflon et dacron se sont détériorés plus vite par irradiation dans l'oxygène que par irradiation dans l'azote. La détérioration par irradiation dans le vide est moins rapide qu'en présence d'oxygène ou d'azote pour tous ces polymères, excepté pour le teflon où elle est plus rapide. Des effets du milieu n'ont pas été mis en évidence pendant l'irradiation du HT-1. Pour le polyéthylène irradié à l'U.V., on a déterminé un rapport scission-pontage de 0.93.

Zusammenfassung

Polyäthylen, Nylon, Mylar, Teflon und Dacron zeigten alle bei Ultraviolettbestrahlung unter Sauerstoff eine raschere Qualitätsverminderung als unter Stickstoff. Die Qualitätsabnahme während einer Vakuumbestrahlung ist bei allen erwähnten Polymeren, mit Ausnahme von Teflon, wo sie schneller ist, langsamer als bei Sauerstoff- oder Stickstoffbestrahlung. Keine Milieueinflüsse waren bei der Bestrahlung von HT-1 zu erkennen. Für ultraviolettbestrahltes Polyäthylen wurde das Verhältnis von Spaltung zu Vernetzung zu 0,93 bestimmt.

Received September 19, 1962

Manuscripts should be submitted to one of the members of the Editorial Board or to the Editorial Office, c/o H. Mark, Polytechnic Institute of Brooklyn, 333 Jay Street, Brooklyn 1, New York. Those in Europe should be submitted to Professor G. Smets, University of Louvain, Louvain, Belgium, and those in the United Kingdom to Sir Harry W. Melville, Department of Scientific and Industrial Research, 5–11 Regent Street, London, S. W. 1, England. Address all other correspondence to Interscience Publishers, a Division of John Wiley & Sons, Inc., 605 Third Avenue, New York 16, New York.

A LEADING SCIENTIFIC JOURNAL
OF INTERNATIONAL REPUTATION

DIE MAKROMOLEKULARE CHEMIE

Editors

Professor Dr. phil. HERMANN STAUDINGER, Freiburg
Dr. Ing. e. h., Dr. rer. nat. h.c., Dr.(C) h.c., Dr. chem. h.c., Dr. sc. techn. h.c., Dr. h. c.

and

Professor Dr. phil. WERNER KERN, Mainz
Director, Institute of Organic Chemistry, Mainz

Advisory Board

H. BATZER, Stuttgart · H. BREDERECK, Stuttgart · J. W. BREITENBACH, Wien · S. CLAESSON, Uppsala · A. DOBRY, Paris · H. VON EULER, Stockholm · A. FREY-WYSSLING, Zürich · K. HAMANN, Stuttgart · K. H. HELLWEGE, Darmstadt · F. A. HENGLEIN, Karlsruhe · H. HOPFF, Zürich · E. HUSEMANN, Freiburg i.Br. · B. JIRGENSONS, Houston · O. KRATKY, Graz · W. KUHN, Basel · G. NATTA, Milano · F. PATAT, München · A. PETERLIN, Durham · CH. SADRON, Strasbourg · I. SAKURADA, Kyoto · G. SCHRAMM, Tübingen · G. V. SCHULZ, Mainz · R. SIGNER, Bern · G. J. SMETS, Louvain · H. A. STUART, Mainz · H. ZAHN, Aachen · K. ZIEGLER, Mülheim/Ruhr

Editorial Office: Dr. I. ROTHE

'Die Makromolekulare Chemie' is a leading scientific publication of international importance which deals with the various fields of macromolecular chemistry. The latest experimental results covering the complete range of macromolecular chemistry are reported, including contributions from organic, physical, physiological and technical chemistry in addition to the physics section so long as they contribute significantly to the further development of our knowledge regarding the structure and properties of macromolecular substances. This Journal is of special interest for research workers at universities, students and those engaged in industry and also to doctors and biologists. The papers which originate from various countries are published in German, English or French with the summary in two of the other languages. The editors, Professor HERMANN STAUDINGER, Nobel Prize Laureate in Chemistry and Professor WERNER KERN and the Advisory Board ensure that 'Die Makromolekulare Chemie' maintains its international scientific importance. The Journal appears in 10–12 volumes every year. Price per volume sfr 39.- (DM 36.-).

HÜTHIG UND WEPF VERLAG
BASEL (Switzerland)
Eisengasse 5—Cable: Hüthigwepf